



HAL
open science

Spatial and temporal patterns in diatom-prokaryote associations in the Southern Ocean

Yan Liu

► **To cite this version:**

Yan Liu. Spatial and temporal patterns in diatom-prokaryote associations in the Southern Ocean. Ecosystems. Sorbonne Université, 2019. English. NNT : 2019SORUS213 . tel-03139883

HAL Id: tel-03139883

<https://theses.hal.science/tel-03139883>

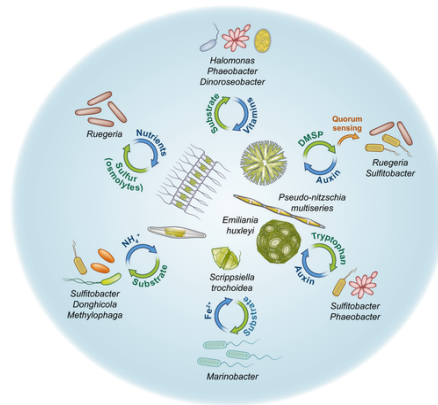
Submitted on 12 Feb 2021

HAL is a multi-disciplinary open access archive for the deposit and dissemination of scientific research documents, whether they are published or not. The documents may come from teaching and research institutions in France or abroad, or from public or private research centers.

L'archive ouverte pluridisciplinaire **HAL**, est destinée au dépôt et à la diffusion de documents scientifiques de niveau recherche, publiés ou non, émanant des établissements d'enseignement et de recherche français ou étrangers, des laboratoires publics ou privés.

Sorbonne Université
Ecole Doctorale des Sciences de l'Environnement d'Ile-de-France
Laboratoire d'océanographie microbienne – UMR 7621
Observatoire Océanologique de Banyuls-sur-mer

Spatial and temporal patterns in diatom-prokaryote associations in the Southern Ocean



Par **Yan LIU**

Soutenu le 20 septembre 2019
à Banyuls-sur-Mer

Devant un jury composé de :

Dr. Josep Gasol	ICM, Barcelona, Spain	Rapporteur
Professeur Sébastien Monchy	ULCO, LOG, Wimereux, France	Rapporteur
Dr. Dominique Lamy	Sorbonne Université, BOREA, Paris, France	Invité
Dr. Emma Rochelle-Newall	IRD, iEES-Paris, Paris, France	Présidente
Dr. Ingrid Obernosterer	CNRS, LOMIC, Banyuls-sur-Mer	Directeur de thèse

ACKNOWLEDGEMENTS

These three years in France have been a great life experience. I met amazing friends, participated interesting festivals, had delicious food and wine, travelled countries and did a lot of science. I could not enjoy the past three years without many people's help.

Many thanks to Ingrid, for offering me the opportunity of studying abroad. Thanks for your patience and encouragements. This PhD would not have been possible without your unfailing guidance. I would have been lost in the ocean without your knowledge of microbial ecology and I would not have successfully finished the work aboard without your support.

Many thanks to Stéphane, for your valuable suggestions in data analysis and for providing the beautiful maps in this thesis. Thanks for sharing your crucial expertise in biogeochemical cycles of the Kerguelen plateau. Thanks also for your fantastic Christmas dinner.

Special thanks to Lorenzo. Thank you for being so nice, thoughtful and funny. Thanks for your delicious Italian food and mango juice, for your invitation of New Year celebration, for your support and for sharing your feelings with me.

Pavla, Coco and Laurie, my dear best friends! Thanks for your company in the past three year, for helping me survive far away from home, for your understanding and support, for taking me as your family. Good luck with your writing and defence. I will be here for you.

Many thanks to Eva and Sara, for the fun lunch breaks, for the valuable advice for study and life, for your great Spanish dishes and wonderful wine tasting. Many thanks to Nyree, for your patience and expertise in the lab. Thanks for sharing your knowledge of bioinformatics that helped me a lot. Many thanks to Patricia, for your expertise in DOM and efficient correcting of the third chapter. I had a good time during our skype meeting. Thanks to Sheree, for helping me in bioinformatics and for sending me Hazel's photo. She is very adorable.

Special thanks to Angel, for your company in our office, for your assistance on data analysis and for the supportive friendship and valuable conversations. Many thanks to Jingguang and Justine, for your caring and support, for making our office better and better. Thanks to Laëtitia and Stefan, for sharing your experience of life and study. Thanks to all LOMIC members, past and present, for your support and creating a nice place for research.

Many thanks to Captain as well as the crew aboard. Thanks to the caterers for keeping us productive and well-fed through the long voyages. Thanks to Meng and Yiwu for your magic medicine. I would have always been seasick without your help. Thanks also for sharing your knowledge of oceanography. Thanks to all participants for sharing your research during science meeting aboard.

Thanks to the teachers and students in summer courses of oceanography and statistics. Thanks for your patience and support. I really learned a lot and enjoyed the classes.

Thanks to China Scholarship Council, for funding me this 3-year study.

Finally, many thanks to my family and my friends in China. Thanks to my parents for their support and understanding. To my friends for alleviating my homesickness. Special thanks to my little brother for taking care of our parents.

Résumé

L'interaction entre les micro-organismes a un impact profond sur les cycles biogéochimiques dans l'océan. La matière organique dissoute (MOD) représente l'un des liens les plus importants entre le phytoplancton et les procaryotes hétérotrophes. Dans cette thèse, nous avons étudié, sur différentes échelles spatio-temporelles, les associations entre la composition de la communauté des procaryotes et les assemblages de diatomées ou les caractéristiques de la MOD dans l'océan Austral. Une région particulièrement intéressante est située dans au voisinage des îles Kerguelen où la fertilisation naturelle du fer produit des efflorescences massives dominées par les diatomées. Nous avons abordé trois questions : (1) La composition des communautés diatomées peut-elle expliquer la biogéographie des procaryotes dans les régions de l'océan Austral (Chapitre 1)? (2) Comment la succession saisonnière de procaryotes est-elle affectée par les efflorescences consécutives du printemps et de l'été dans une région naturellement fertilisée en fer de l'océan Austral (Chapitre 2)? (3) Comment les procaryotes et la MOD sont-ils associés dans les régions où l'apport en fer est contrasté (Chapitre 3)? Pour répondre à ces questions, des échantillons prélevés lors de campagnes océanographiques ou par un échantillonneur autonome déployé pendant 4 mois dans l'océan Austral (projets SOCLIM et HEOBI) ont été analysés. La composition des communautés procaryotes et de diatomées a été examinée respectivement par le séquençage à haut débit et par des observations microscopiques. La composition moléculaire de la MOD a été étudiée par la spectrométrie de masse de résonance cyclotron de transformation de fourrier (FT-ICR MS).

Dans le Chapitre 1, nous décrivons des assemblages distincts de diatomées et des communautés procaryotes dans les eaux de surface des principales régions de l'océan Austral au printemps. Les changements de la composition des procaryotes étaient significativement corrélés avec ceux des diatomées. En revanche, les changements de la composition des procaryotes n'étaient pas liés à la distance géographique et ni aux paramètres environnementaux lorsque l'effet des diatomées était pris en compte. Ces résultats révèlent que le patron spatial dans la structure des communautés procaryotes est étroitement associé aux changements dans les assemblages de diatomées, plutôt qu'à la distance géographique et aux conditions environnementales. Nos résultats illustrent le rôle potentiel des diatomées sur la diversité

microbienne dans les eaux de surface de l'océan Austral.

Le Chapitre 2 présente une description détaillée de la succession saisonnière des communautés procaryotes dites « libre » (fraction de taille $< 0.8 \mu\text{m}$) et des procaryotes attachées aux particules (fraction de taille $> 0.8 \mu\text{m}$) dans des eaux naturellement fertilisées en fer au large des îles Kerguelen (Océan Austral). Nous avons observé des patrons variables dans la réponse des taxons procaryotes aux efflorescences consécutives printanières et estivales, chacune composée d'assemblages de diatomées distincts. À l'aide d'une analyse en réseau, nous avons identifié deux groupes de diatomées représentatifs de l'efflorescence printanière et estivale, respectivement, qui avaient des patrons de corrélation opposés avec les taxons procaryotes. Les caractéristiques écologiques potentielles des principaux taxons, indépendamment ou associées à des diatomées spécifiques, dans cette région naturellement fertilisée du fer de fer de l'océan Austral sont discutées.

Dans le Chapitre 3, nous présentons la composition des communautés procaryotes totales et actives et leurs associations aux caractéristiques de la MOD dans les eaux de surface de l'océan Austral pendant l'été. Nous avons étudié des sites localisés dans des eaux productives, naturellement fertilisées en fer au-dessus du plateau de Kerguelen et dans les eaux peu productives au large du plateau. Les corrélations entre la MOD et les communautés procaryotes étaient globalement plus fortes aux sites au-dessus du plateau de Kerguelen que dans les eaux hauturiers. Au-dessus du plateau, les patrons des associations entre MOD et la communauté procaryotes totale étaient différents de ceux des procaryotes actifs. Les composés contenant de l'azote avaient des contributions plus élevées aux associations positives entre la MOD et les procaryotes actifs qu'à celles entre MOD et procaryotes totaux. Les principaux groupes procaryotes actifs qui ont fortement corrélié avec la MOD étaient qualitativement semblables à tous les sites, mais quantitativement plus élevés sur le plateau de Kerguelen. Ces résultats nous mènent à conclure que la MOD d'origine phytoplanctonique influence la composition des communautés procaryotes dans les eaux de surface de l'océan Austral.

Summary

The interplay among microbes profoundly impacts biogeochemical cycles in the ocean. Dissolved organic matter (DOM) represents one of the most important links between phytoplankton and heterotrophic prokaryotes. In this thesis, we investigated the associations between prokaryotic community composition and either diatom assemblages or DOM characteristics on spatio-temporal scales in the Southern Ocean. A region of particular interest is located in the vicinity of Kerguelen Island where natural iron fertilization sustains massive diatom-dominated spring phytoplankton blooms. We addressed three questions: (1) Can diatom community composition explain biogeographic patterns of prokaryotes across Southern Ocean provinces (Chapter 1)? (2) How is the seasonal succession of prokaryotes affected by consecutive spring and summer blooms in a naturally iron-fertilized region of the Southern Ocean (Chapter 2)? (3) How are prokaryotes and DOM associated in regions with contrasting iron supply (Chapter 3)? To answer these questions, samples collected during oceanographic cruises or by a remote access sampler deployed for 4 months in the Southern Ocean (SOCLIM and HEOBI projects) were analysed. The composition of the prokaryotic and diatom communities was examined by High-Throughput-Sequencing and microscopic observations, respectively. The molecular composition of DOM was investigated via Fourier transform ion cyclotron resonance mass spectrometry (FT-ICR MS).

In Chapter 1, we report distinct diatom assemblages and prokaryotic communities in surface waters of major Southern Ocean provinces in spring. The compositional changes of prokaryotes were significantly correlated with those of diatoms. In contrast, spatial changes in the prokaryotic community composition were not related to geographic distance and to environmental parameters when the effect of diatoms was accounted for. These results reveal that the spatial pattern in the community structure of prokaryotes is tightly associated with changes in the diatom assemblages, rather than to geographic distance and environmental conditions. Our results illustrate the potential role of diatoms in shaping microbial diversity in surface waters of the Southern Ocean.

Chapter 2 provides a detailed description of the seasonal succession of the free-living (< 0.8

μm fraction) and the particle-attached ($> 0.8 \mu\text{m}$ fraction) prokaryotic communities in the naturally iron-fertilized waters off Kerguelen Island (Southern Ocean). We observed variable patterns in the response of prokaryotic taxa to the spring and summer blooms, each composed of distinct diatom assemblages. Using network analysis, we identified two groups of diatoms representative of the spring and summer bloom, respectively, that had opposite correlation patterns with prokaryotic taxa. The potential ecological features of key taxa, independent of or associated to specific diatoms, in this naturally iron fertilized region of the Southern Ocean are discussed.

In Chapter 3, we present the composition of total and active prokaryotic communities and their associations to DOM characteristics in surface waters of the Southern Ocean during summer. We investigated sites located in the productive naturally iron-fertilized waters above the Kerguelen plateau and in low productive off-plateau waters. The DOM-prokaryote correlations were overall stronger at sites located above the Kerguelen plateau than in offshore waters. Above the plateau, patterns of associations between DOM and the total prokaryotic community were different to those of the active prokaryotes. Nitrogen containing compounds had higher contributions to the positive associations between DOM and the active prokaryotes than to those between DOM and total prokaryotes. The key active prokaryotic groups that strongly correlated with DOM were qualitatively similar at all sites, but quantitatively higher on the plateau. These results let us conclude that DOM from phytoplankton origin shape prokaryotic community composition in surface waters of the Southern Ocean.

Table of contents

Introduction

1 Hydrodynamics of the Southern Ocean.....	1
1.1 Biophysical zonation of the Southern Ocean.....	1
1.2 Water masses and circulation of the Southern Ocean.....	2
1.3 Upwelling of the Southern Ocean.....	3
2 Southern Ocean -- the largest high-nutrient low-chlorophyll region.....	4
3 Dissolved organic matter and the Southern Ocean.....	6
3.1 Bulk classification and molecular characterization of marine DOM.....	6
3.2 Marine DOM in carbon cycle.....	7
3.3 DOM release by phytoplankton and prokaryotes.....	9
3.4 Southern Ocean -- the lowest DOC concentration region.....	10
4 Microbial activity in association with phytoplankton in the Southern Ocean.....	11
4.1 Microbial diversity of the Southern Ocean.....	11
4.2 Ecological adaptation of microbes in the Southern Ocean.....	20
4.3 Microbial associations in the Southern Ocean.....	21
4.4 Complex microbial associations in the field.....	22
5 Objectives of the thesis and organization of the manuscript.....	24

Methodology

1 Raw data processing.....	29
2 Diversity analysis.....	29
2.1 Alpha-diversity.....	30
2.2 Beta-diversity.....	31
3 Statistical analyses for microbial associations.....	31
3.1 Data transformation.....	32
3.2 Similarity/ distance and regression measures for correlation analysis.....	33
3.2.1 (Dis)similarity/distance-based approach.....	33
3.2.2 Regression-based approach.....	34

3.3 Data visualization.....	35
4 Statistical analyses for prokaryote-DOM associations.....	39
Chapter 1	39
Chapter 1 Supplementary material.....	57
Chapter 2	63
Chapter 2 Supplementary material.....	99
Chapter 3	105
Chapter 3 Supplementary material.....	133
General discussion and perspectives	137
1 Summary and general discussion.....	139
1.1 Microbial diversity in naturally iron-fertilized and the HNLC waters.....	140
1.2 Life strategies of diverse prokaryotes in the naturally Fe-fertilized region.....	143
1.3 A possible scenario of microbial associations over time in a naturally iron-fertilized region.....	146
2 Perspectives	148
References	151
 Appendices	
Appendix 1 Microbial diversity and activity in the Southern Ocean (Table 2 of the Introduction).....	185
Appendix 2 Master thesis--Prokaryotic diversity and activity in contrasting productivity regimes in late summer in the Kerguelen region	191

List of Figures and Tables

Introduction

Figure 1 Schematic of the Southern Ocean Meridional Overturning Circulation	2
Figure 2 Average nitrate concentrations and Chlorophyll concentrations.....	6
Figure 3 Schematic depiction of the biological carbon pump (BCP), the microbial loop (ML) and the microbial carbon pump (MCP).....	8
Figure 4 Observations of DOC in the central Atlantic, central Pacific, and eastern Indian Ocean, with all lines connected via the Antarctic circumpolar currents.....	10
Figure 5 Antarctica and the Southern Ocean.....	12
Figure 6 Tight associations between microalgae and bacteria.....	23
Figure 7 Map of sampling sites related to the thesis.....	25
Table 1 Molecular composition of dissolved organic matter (DOM) in the surface and the deep ocean.....	7
Table 2 Microbial diversity and activity in the Southern Ocean.....	185

Methodology

Figure 1 Correlation visualization via heatmap	35
Figure 2 Network visualization.....	36
Figure 3 Flowchart of microbial associations analysis (Chapter 1 and 2)	37
Figure 4 Flowchart of prokaryote-DOM association analysis (Chapter 3).....	38
Table 1 Major steps in data processing.....	29

Chapter 1

Figure 1 Map of the study region of the SOCLIM cruise.....	45
Figure 2 Clustering of stations based on Bray–Curtis dissimilarity of the diatom community composition and relative abundances of diatom species.....	46
Figure 3 Nonmetric multidimensional scaling (NMDS) of total (DNA) and active (RNA) prokaryotic communities based on Bray–Curtis dissimilarity.....	47
Figure 4 Relationship between changes in the community composition of diatoms and of total prokaryotes for the Southern Ocean stations.....	47

Figure 5 Heatmap of correlations between dominant diatom species and prokaryotic OTUs from total communities based on Pearson correlations.....	49
Table 1 Brief description of the study sites.....	44
Table 2 Partial Mantel test for prokaryotic and diatom community composition and geographic distance (a) and combined environmental parameters (b)	48

Chapter 2

Figure 1 Map of the study site (A3) above the Kerguelen Plateau.....	70
Figure 2 The (a) deployment and the (b) full view of McLane Remote Access Sampler.....	71
Figure 3 Temporal changes of environmental parameters.....	78
Figure 4 Diatom community composition as determined by microscopic observations.....	79
Figure 5 Relative abundance of ASVs (illustrated in the circles) and the Bray-Curtis similarity between pairwise comparisons of controls, HgCl ₂ and glutaraldehyde fixed samples.....	80
Figure 6 Nonmetric multidimensional scaling (nMDS) of free-living and particle-attached prokaryotic communities based on Bray-Curtis dissimilarity.....	82
Figure 7 Composition of (a) free-living and (b) particle-attached prokaryotic communities at the order level.....	83
Figure 8 Heatmap of abundant prokaryotic ASVs of the free-living community.....	85
Figure 9 Heatmap of abundant prokaryotic ASVs of the particle-attached community.....	86
Figure 10 Shannon index of prokaryotic communities.....	87
Figure 11 Network between dominant diatoms, free-living and particle-attached prokaryotes.....	89
Table 1 Overview of the samples collected by the RAS for microbial diversity analyses.....	73

Chapter 3

Figure 1 Map of the study region.....	112
Figure 2 Van Krevelen diagram of total DOM formulae of all samples pooled.....	120
Figure 3 Relative contribution of each DOM group to the total DOM data set at each site.....	121
Figure 4 Contribution of formula classes at each site.....	122
Figure 5 Principal component analysis of DOM composition.....	123
Figure 6 Dendrograms of (a) total and (b) active prokaryotic communities based on Bray–Curtis dissimilarity.....	123
Figure 7 Heatmaps of dominant prokaryotic ASVs that account for ≥ 1 % in at least one sample of total (DNA) prokaryotic community.....	125
Figure 8 Heatmaps of dominant prokaryotic ASVs that account for ≥ 1 % in at least one sample of active (RNA) prokaryotic community.....	126

Figure 9 Van Krevelen diagrams showing the correlation of molecular formulae with the canonical axis associating DOM composition with DNA/ RNA-based prokaryotic community composition.....	127
Figure 10 Number of positive correlations with the canonical axis associating (a) total or (b) active prokaryotic community composition and DOM molecular formulae containing nitrogen (N)	129
Figure 11 Number of strong positive correlations (Spearman, $r \geq 0.7$) with the canonical axis associating active prokaryotic groups (Order level) with molecular formulae.....	130
Table 1 Environmental and biological parameters of the stations sampled during the HEOBI cruise.....	118

General discussion and perspectives

Figure 1 Alpha-diversity of free-living prokaryotic communities from three chapters according to sampling dates	141
Figure 2 The number of positive correlations between active prokaryotes and DOM on and off the Kerguelen plateau.....	142
Figure 3 Seasonal patterns of SAR11 and SUP05 based on relative abundance.....	143
Figure 4 Seasonal patterns of Polaribacter and Nitrospiraceae based on relative abundance..	144
Figure 5 Seasonal patterns of Amylibacter and Aurantivirga based on relative abundance...	145
Figure 6 A possible scenario of microbial associations over time in a naturally iron-fertilized region	147

INTRODUCTION



Yan Liu

Introduction

1 Hydrodynamics of the Southern Ocean

The Southern Ocean comprises the southernmost waters of the world ocean, characterised as an oceanographically complex and biogeochemically important area. It plays a vital role in the global climate variability and changes, and the cycling of carbon, oxygen, and nutrients in the oceans, mainly based on its importance in the global ocean circulation and water mass formation, inter basin connections, and air-sea exchanges of heat, freshwater and tracer gases (Sarmiento et al., 2004; Le Quéré et al., 2007; Delworth et al., 2010). The Southern Ocean accounts for ~30% of global ocean uptake of CO₂, although it represents ~10% of the total surface area of the global ocean.

1.1 Biophysical zonation of the Southern Ocean

Southern Ocean is a key player in the global ocean circulation and biogeochemical cycles as a water mass crossroads (Sloyan and Rintoul, 2001; Sarmiento et al., 2004; Lumpkin and Speer, 2007). The Antarctic Circumpolar Current (ACC) is a critical component of the global ocean circulation (Orsi et al., 1995). It divides the Southern Ocean into three major zones (Fig. 1) (Gent, 2016): the Subantarctic Zone (SAZ), the Polar Frontal Zone (PFZ) and the Antarctic Zone (AAZ), separated by several fronts including the Subtropical Front (STF), the Subantarctic Front (SAF) and the Polar Front (PF) from north to south (Whitworth, 1980; Sokolov and Rintoul, 2002). The definition of zones is based on the changing balance of the contributions of salinity and temperature to the stratification (Pollard et al., 2002).

The northernmost front is the STF, also called Subtropical Convergence (~40-45°S, (Deacon, 1933)), which separates the SAZ from the warmer and saltier subtropical water (Sokolov and Rintoul, 2002). Across the STF, the temperature decreases at 150m depth from >12 to <10°C (Sokolov and Rintoul, 2002). The STF will be used as the northernmost boundary (~40°S) of the Southern Ocean in this thesis. The SAF is identified by the vertical changes of salinity with the lowest amount in the south of the SAF surface water (Pollard et al., 2002). Across the SAF, temperature drops to 2-4°C (Sokolov and Rintoul, 2002). The SAF is also the north boundary of the PFZ, where the warmer SAZ and the colder AAZ waters continuously mix. The PF marks the southern boundary of the PFZ with a temperature decrease of ~1-1.5°C (Moore et al., 1999).

Introduction

The coldest water ($< 2^{\circ}\text{C}$) constitutes the AAZ as the major zone in the Southern Ocean (Sokolov and Rintoul, 2002).

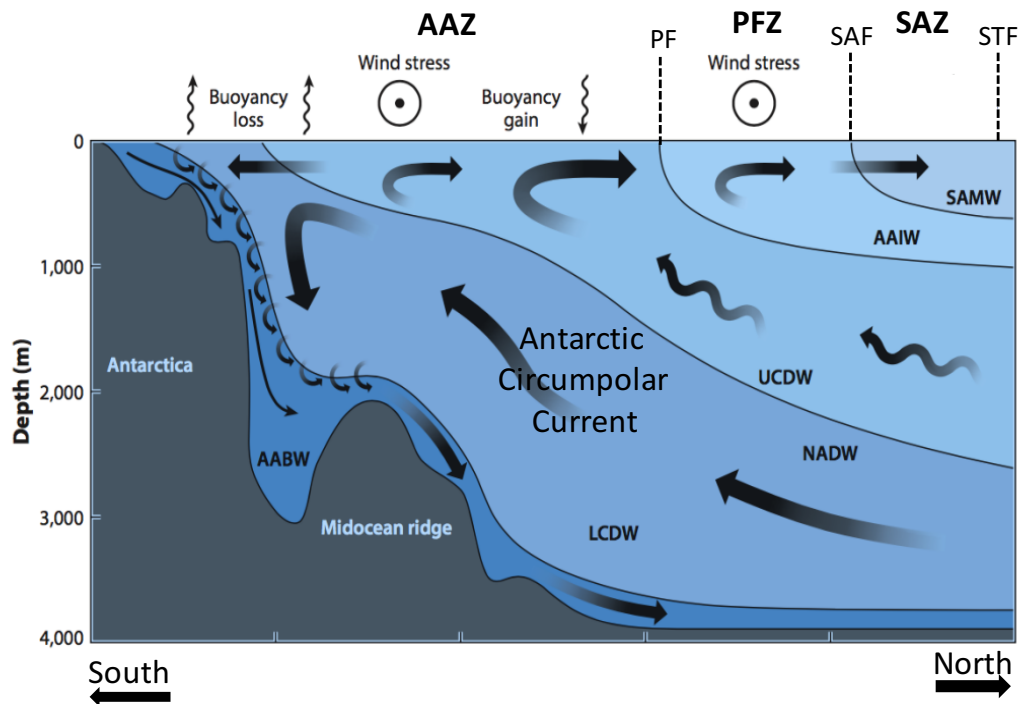


Fig. 1 Schematic of the Southern Ocean Meridional Overturning Circulation (MOC), the locations of ocean fronts and water masses, and atmospheric forcing and fluxes. Abbreviations: AABW, Antarctic Bottom Water; AAIW, Antarctic Intermediate Water; AAZ, Antarctic Zone; LCDW, Lower Circumpolar Deep Water; NADW, North Atlantic Deep Water; PF, Polar Front; PFZ, Polar Front Zone; SAF, Subantarctic Front; SAMW, Subantarctic Mode Water; SAZ, Subantarctic Zone; STF, Subtropical Front; UCDW, Upper Circumpolar Deep Water (adapted from Gent, 2016).

1.2 Water masses and circulation of the Southern Ocean

Water masses are the phenomenological expression of large-scale ocean dynamical processes, which transport both energy (in the form of heat) and matter (solids, dissolved substances and gases) around the globe, and have been the foundation to characterize and understand the large-scale circulation structures in the ocean (Ludicone et al., 2011). Three fronts separate distinct water mass regimes of the Southern Ocean from north to south: Subantarctic Mode Water (SAMW), Antarctic Intermediate Water (AAIW), Upper Circumpolar Deep Water (UCDW),

Introduction

North Atlantic Deep Water (NADW), Lower Circumpolar Deep Water (LCDW), Antarctic Bottom Water (AABW) (Fig. 1).

SAMW is beneath the surface of the SAZ and produces large property gradients in terms of temperature and salinity (Orsi et al., 1995). AAIW corresponds to the area of the PFZ. It upwells to feed northward transport near the surface via westerly wind (Speer et al., 2000). In the AAZ, south of the PF, water transition is mainly driven by wind and buoyancy, resulting the divergence of surface currents (Fig. 1). UCDW is characterized by high nutrient concentrations (Orsi et al., 1995). The upwelling of UCDW induces the interactions with the upper water and atmosphere (Speer et al., 2000). LCDW hosts high salinities, originating as sinking NADW (Whitworth and Nowlin, 1987). It moves southwards to form dense and cold AABW. The newly formed AABW sinks rapidly and form an abyssal layer beneath the entire Southern Ocean (Orsi et al., 1999). AABW contributes a major part of the world ocean, while the formation of AABW only occurs in the Weddell and Ross seas.

1.3 Upwelling of the Southern Ocean

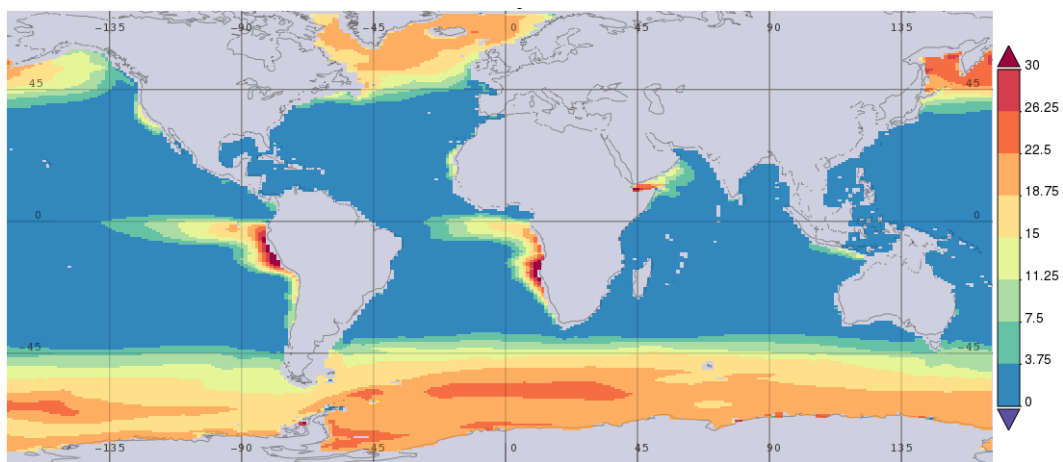
Upwelling is a wind-driven phenomenon in oceanography, which transfer the dense, cooler and usually nutrient-rich water towards the ocean surface. It is a return path of down-welling and a key part of the Meridional Overturning Circulation (MOC) (Marshall and Speer, 2012). Extensive mixing through MOC takes place between the ocean basins, reducing differences between them and making the Earth's oceans a global system. Upwelling is driven by three main factors, namely winds, Coriolis effects and Ekman transport. The Southern Ocean hosts the strongest surface winds of any open ocean area. Upwelling here is largely driven by winds (Marshall and Speer, 2012). It takes nutrient-rich waters from UCDW across the PF and towards the PFZ. Here it sinks to form AAIW and then flows across the SAF and the SAZ towards the STF and the surface water. As a result, the upwelling of the deep water presents the complement of the surface water loss. In this process, some of the cold nutrient-rich water returns into the deep ocean interior and contributes to the formation of AABW (Abouchami et al., 2011).

Introduction

2 Southern Ocean -- the largest high-nutrient low-chlorophyll region

High-nutrient low-chlorophyll (HNLC) areas are well known as important regions characterized by low phytoplankton production but excess macronutrients conditions. The three major HNLC regions of the world oceans are the subarctic eastern Pacific, the east equatorial Pacific and the Southern Ocean (Falkowski et al., 1998). The Southern Ocean has the largest HNLC region of the global ocean, which shows the greatest potential to participate in the global carbon cycle and to regulate climate (Sarmiento et al., 1998; Marinov et al., 2006) (Fig. 2).

(a)



(b)

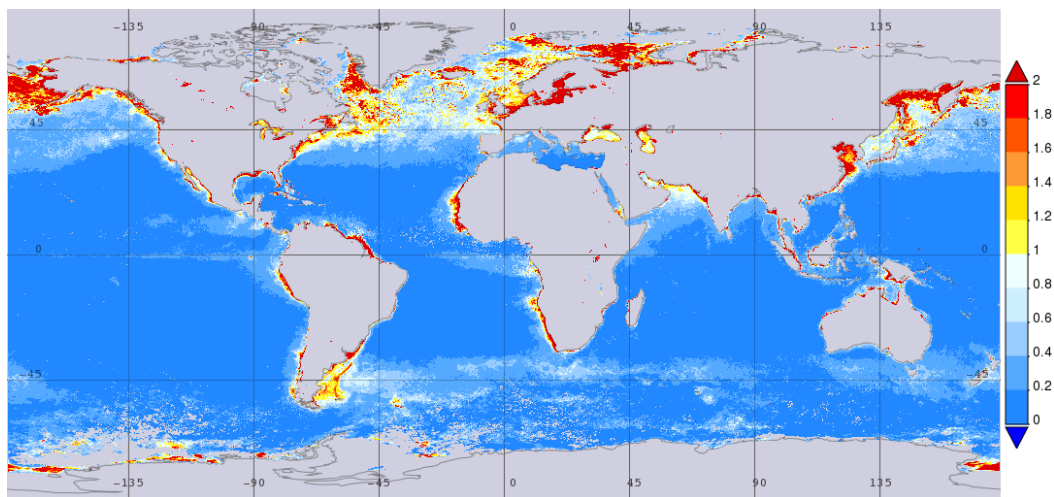


Fig. 2 (a) Average nitrate concentrations ($\mu\text{mol L}^{-1}$) in surface waters (data from Dec. 1997 to Dec. 2015); (b) Average Chlorophyll concentrations ($\mu\text{g L}^{-1}$) in surface waters (data from Dec. 1997 to Dec. 2018) (data downloaded from <https://giovanni.gsfc.nasa.gov/giovanni/>).

Introduction

The oceanic primary production plays a vital role in the global carbon cycle. About one third of organic carbon produced by marine phytoplankton are exported into the ocean interior (Falkowski et al., 1998). Photosynthesis is critically dependent on Chlorophyll concentrations. The mean concentration of Chlorophyll is $< 0.3\text{-}0.4 \mu\text{g L}^{-1}$ in most of the Southern Ocean, although it exceeds $1.0 \mu\text{g L}^{-1}$ during phytoplankton blooms and in coastal/shelf waters. (Moore and Abbott, 2000).

Iron has great importance in key metabolic processes in the ocean, in particular for photosynthesis and respiration and also nitrate reduction, and nitrogen fixation (Morel et al., 1991; Geider et al., 1993; La Roche et al., 1996; Falkowski et al., 1998). Southern Ocean surface waters contain extremely low iron (Fe) concentrations (Coale et al., 2004). In typical open ocean surface waters, the Fe concentration is $0.04\text{-}0.6 \text{ nM}$ (minimum concentrations in different Southern Ocean regions; Morre et al., 2003). The “Fe hypothesis” has been originally proposed by Martin (1990). It postulates that Fe addition to HNLC waters can increase phytoplankton productivity. In turn, it affects atmospheric carbon dioxide sequestration and carbon biogeochemistry. This hypothesis has been widely confirmed using short-term Fe-enrichment experiments (Boyd et al., 2000; Buesseler et al., 2004; Coale et al., 2004; Bakker et al., 2005; Croot et al., 2005; De Baar et al., 2005; Boyd et al., 2007) and long-term natural iron fertilization (Blain et al., 2007) in the Southern Ocean. Fe bioavailability also affects phytoplankton community (De Baar et al., 2005) and induces blooms around island systems in the Southern Ocean such as the Crozet Islands (Metzl et al., 1999; Sedwick et al., 2002), South Georgia (Moore and Abboot, 2002; Korb et al., 2004), Bouvet (Croot et al., 2004) and Kerguelen (Blain et al., 2001, 2002, 2007; Bucciarelli et al., 2001). Iron controls phytoplankton growth and communities, and further influences prokaryotic community composition (West et al., 2008; Landa et al., 2016; this thesis).

The source and the drivers of Fe distribution are aeolian dust, fluvial input, biological uptake, mixing with deeper waters and various processes occurring on the sea floor such as sediment resuspension and hydrothermal vents (Sander and Koschinsky, 2001; Ussher et al., 2004), of which the major source of Fe for the oceans is aeolian dust (Duce and Tindale., 1991). However, such atmospheric input has less influence on the Southern Ocean (Jickell et al., 2005). Horizontal advection or vertical mixing of deep iron-rich water are larger inputs than from the atmosphere (Blain et al., 2001; Planquette et al., 2007).

Introduction

3 Dissolved organic matter and the Southern Ocean

In the ocean, marine organic matter represents one of the largest bioreactive carbon reservoirs in the Earth biosphere (Hedges, 1992). The cycling of oceanic organic matter links the carbon exchanges between the atmosphere and the seafloor, in which dissolved organic matter (DOM) has great importance.

3.1 Bulk classification and molecular composition of marine DOM

Organic matter is present in a continuum of sizes, including a variety of living and non-living particles, gel-like structures and dissolved compounds. Generally, organic matter is composed of particulate organic matter (POM) and DOM. POM is a natural organic constituent of water in both living and non-living forms, that is retained on the filter of usually 0.2-0.7 μm pore size (Dittmar and Stubbins, 2014). DOM, the collection of compounds that contain reduced carbon, often bound to heteroatoms such as oxygen, nitrogen, phosphorus, and sulfur (Kujawinski, 2011), operationally defined as the fraction $< 0.2 \mu\text{m}$, comprises the majority ($> 95\%$) of the total organic matter (Williams, 1975). Marine DOM can be characterized by size, molecules of low molecular weight (LMW, $< 1000 \text{ Da}$) or high molecular weight (HMW, $> 1000 \text{ Da}$), or by reactivity (labile or refractory) (Christian and Anderson, 2002). It has been shown that LMW material comprises 65-80% of DOM (Carlson et al., 1985; Benner et al., 1992; Ogawa and Ogura, 1992). The carbon content of DOM amounts (DOC), on a global scale, to about 662 Gt C (Hansell et al., 2009), and it is thus similar to the amount of atmospheric CO_2 (750 Gt C) (Hansell et al., 2013). DOC has been classified into two major fractions with well-defined removal rates: labile DOC (LDOC; high removal rates; high turnover; no accumulation), represents a large flux of carbon in the ocean, but it constitutes a very small fraction ($< 1\%$) of the ocean DOC inventory, recalcitrant DOC (RDOC; a reservoir of organic carbon) contributing 94%, and the remaining 5% is classified as semi-labile DOC (Hansell et al., 2009; Hansell et al., 2013). The major source of DOC in the open ocean is primary production.

The molecular composition of DOM in the ocean is large unknown due to the limited suitable chromatographic techniques for the characterization of DOM. The most common classes of biochemicals identified contribute a trace amount ($\sim 10\%$) of total DOM (Table 1; Hansell and Carlson, 2002). Recent advanced techniques have improved our knowledge of

Introduction

molecular composition of DOM. For example, Fourier-transform ion cyclotron resonance mass spectrometry (FT-ICR MS), provides a massive amount of molecular formulas based on exact masses of DOM compounds (Kujawinski et al., 2002). Up to date, it is the only technique capable to resolve information on intact individual molecules of DOM (reviewed in Dittmar and Stubbins, 2014). Nuclear magnetic resonance (NMR) spectroscopy provides structural information of DOM (Mopper et al., 2007). It indicates a major contribution (~40% of DOC) of carbohydrates and amides in ultrafiltered DOM (reviewed in Dittmar and Stubbins, 2014).

Table 1 Molecular composition of dissolved organic matter (DOM) in the surface and the deep ocean (Hansell and Carlson, 2002).

	Surface ocean	Deep ocean
Total hydrolyzable neutral sugars (% DOC)	2-6	0.5-2.0
Total hydrolyzable amino acids (% DOC)	1-3	0.8-1.8
Total hydrolyzable amino sugars (% DOC)	0.4-0.6	0.04-0.07
Solvent extractable lipids (% DOC)	0.3-0.9	nd
Total (% DOC)	3.7-10.5	1.3-3.9
Total hydrolyzable amino acids (% DON)	6-12	4-9
Total hydrolyzable amino sugars (% DON)	0.8-1.7	0.2-0.4
Total (% DON)	6.8-13.7	4.2-9.4

Note: Total hydrolyzable yield of a specific class of biochemicals represent a sum of monomeric units that are separated by chromatography.

Nd, not determined.

3.2 Marine DOM in carbon cycle

Marine DOM participates mainly two processes during carbon cycling in the ocean (Fig. 3). At the surface layer of the oceans, DOM affects the penetration of light and exchange of gases, and participates in the carbon sinking flux as substrates of heterotrophic activity. 70% of total DOM are recycled by diverse heterotrophic prokaryotes in the microbial loop (ML; Azam et al., 1983), including nearly half of net primary production (Arnosti et al., 2011; Buchan et al., 2014). The fixed carbon derived by phytoplankton is for microbial respiration, transferred back into food web by zooplankton grazers, remineralized to inorganic carbon, and accumulated and transformed into RDOC as one path of carbon storage in microbial carbon pump (MCP; Jiao et al., 2010). The ML emphasizes the interactions between microbes and their physical and

Introduction

chemical surroundings (Azam et al., 1983; Azam, 1998), focusing on carbon cycling in the water column where prokaryotes, protozoa and viruses determine the fate of DOM, which points out that organic matter flux into prokaryotes is a major pathway of carbon flux. The MCP complements the biological carbon pump (BCP), which focuses on the capacity of the ocean to store atmospheric carbon dioxide (CO_2) during the long-term carbon storage (Jiao et al., 2010) (Fig. 3).

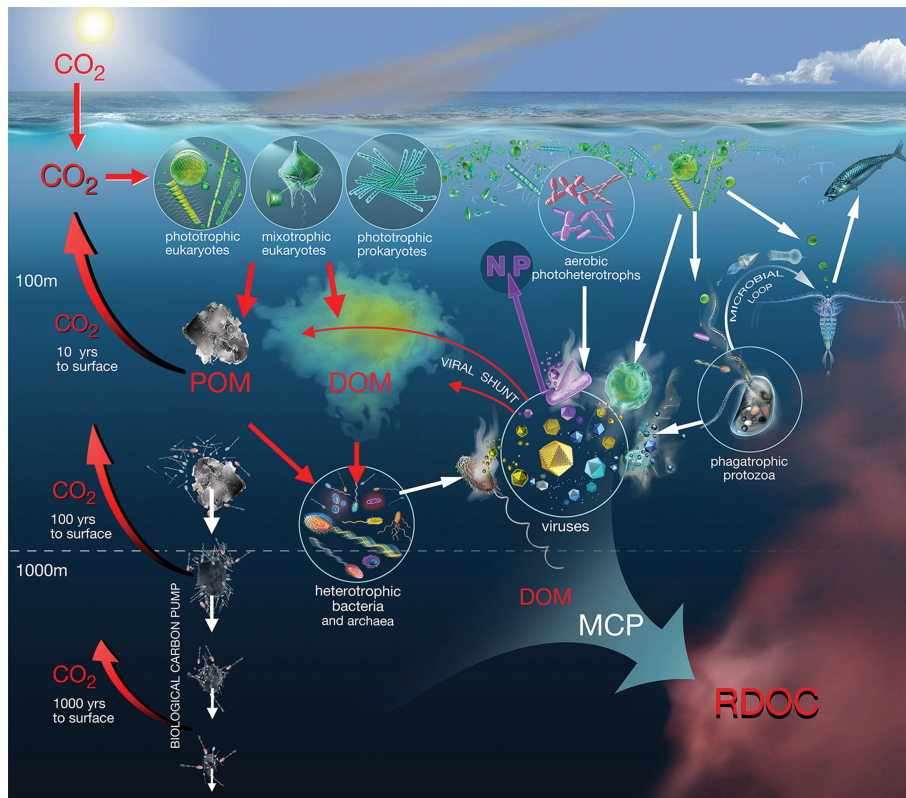


Fig. 3 Schematic depiction of the biological carbon pump (BCP), the microbial loop (ML) and the microbial carbon pump (MCP). The remineralization length scale in the left part of the figure shows the return of respired CO_2 back to the surface, from three depth zones (Zhang et al., 2018).

Over the past 100 years atmospheric CO_2 has increased due to anthropogenic activity. Such a change could profoundly affect the global carbon cycle. While a net oxidation of only 1% of the seawater organic matter pool in one year would produce a CO_2 flux larger than that coming annually from fossil fuel combustion (Hedges, 1997). That means although DOM is the largest ocean reservoir of reduced carbon, the oxidation of DOM (microbial respiration) should not be overlooked. A large part of overall microbial respiration in the ocean (50-90%) is attributable

Introduction

to heterotrophic prokaryotes (Robinson and Williams, 2005; Lefèvre et al., 2008; Obernosterer et al., 2008, 2010). Bacterial growth efficiencies (BGE, i.e. the fraction of organic carbon processed by heterotrophs that is incorporated into biomass), span over a large range (5-60%), but most BGEs reported for the marine environment are below 30% (Del Giorgio and Cole, 2000). The rates and efficiencies of organic matter transformation processes are key to understand to what extent heterotrophic microbes act as a source of CO₂ in the ocean.

3.3 DOM release by phytoplankton and prokaryotes

All marine organisms excrete DOM during growth and decay (Nagata, 2008). Most of the DOM is generally known as the product of decayed phytoplankton and consists of proteins (25-50%), lipids (5-25%) and carbohydrates (~ 40%) (Emerson and Hedges, 2008). DOM release by phytoplankton cells is a ubiquitous process via passive leakage and active exudation based on different mechanisms (Thornton, 2014). For example, passive diffusion, cell lysis by viral infections or senescence are passive loss; Resource acquisition, defence mechanisms and infochemicals are active exudation (Mykkestad, 2000; Thornton, 2014). In the oligotrophic ocean, cell lysis is a significant form of DOM release, which accounts for about 80% of total primary production (Agusti and Duarte, 2013). Autotrophic prokaryotes can produce large quantities of DOM, for example polysaccharides (reviewed in Kujawinski, 2011). Heterotrophic prokaryotes can also be sources of DOM. They can directly release DOM in the form of hydrolytic enzymes (Hansell and Carlson, 2002). The DOM molecules of prokaryotic origin are more resistant for other prokaryotes use than those of phytoplankton origin. During the remineralization of phytoplankton-derived DOM, prokaryotes appear to transform LMW to HMW DOM (Ogawa et al., 2001).

Introduction

3.4 Southern Ocean -- the lowest DOC concentration region

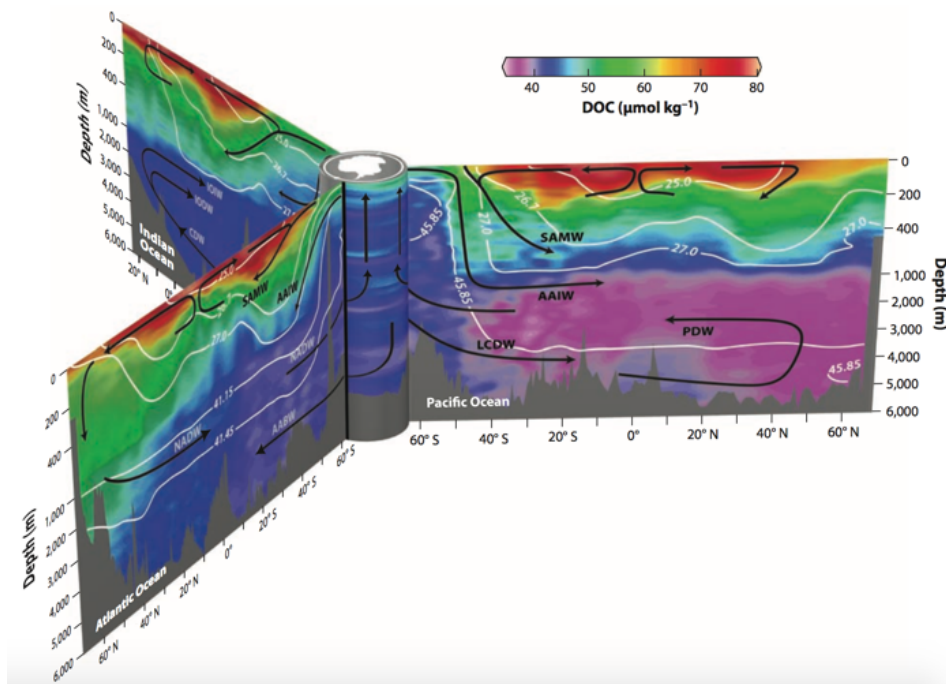


Fig. 4 Observations of DOC in the central Atlantic, central Pacific, and eastern Indian Ocean, with all lines connected via the Antarctic circumpolar currents (Hansell, 2013).

The Southern Ocean is a net sink for CO₂ and one of the main gateways for anthropogenic CO₂ into the ocean interior (Khatiwala et al., 2009). A particular characteristic of the Southern Ocean is that the concentrations of DOC in surface waters are the lowest in the global ocean (~40–50 μmol C L⁻¹) (Ogawa et al., 1999; Hansell, 2002; Hansell, 2013). This is due to the permanent upwelling of refractory organic matter from the deep ocean, and the low primary production limited by the micronutrient iron. The highest concentration of DOC in surface water of the Southern Ocean is 67 μM observed in Antarctic Circumpolar Current (ACC) zone (45°S–55°S), while it is lower in the Weddell Sea surface water (46.3 ± 3.3 μM; Lechtenfeld et al., 2014), which is much less than the global DOC concentrations in surface water (~70 μM) (Hansell et al., 2009). DOC concentrations of deep water from ACC, the Ross Sea and Weddell Sea water are similar (41.5–41.9 μM) (Hansell and Carlson, 1998).

Introduction

4 Microbial activity in association with phytoplankton in the Southern Ocean

The Southern Ocean represents a particular habitat for planktonic, autotrophic and heterotrophic microbes, with the special characteristics of the limited Fe supply. Prokaryotic heterotrophic activity responds strongly to phytoplankton growth. On the one hand, prokaryotic production increases significantly under Fe stimulation either by direct alleviation (Arrieta et al., 2004) or indirectly by enhanced phytoplankton growth and the subsequent increased supply of DOM (Olivier et al., 2004; Obernosterer et al., 2008). On the other hand, phytoplankton growth can be dependent on interactions with heterotrophic prokaryotes. For example, cobalamin produced only by bacteria and archaea limits phytoplankton activity together with Fe (Bertrand et al., 2015). Considering the critical Southern Ocean climate system and the importance of phytoplankton and heterotrophic communities in biogeochemical cycles (Falkowski et al., 2008), it is crucial to uncover the associations among them and decipher their potential roles in oceanic environment.

4.1 Microbial diversity of the Southern Ocean

Microbial diversity has been reported in nearly all regions of the Southern Ocean (Fig. 5) (Table 2 listed in Appendix 1) using various molecular approaches, from Fluorescence In Situ Hybridization (FISH), denaturing gradient gel electrophoresis (DGGE) to 454 pyrosequencing, Illumina sequencing and metagenomics. Shifts of microbial community composition generally occur depending on spatial and temporal changes, environmental selection, top-down or bottom-up controls, and the presence or absence of phytoplankton blooms. Certain trends in microbial composition are also apparent, in particular across a few transects (e.g., Straza et al., 2010; Wilkins et al., 2013). Alphaproteobacteria, Gammaproteobacteria and Bacteroidetes are the most abundant groups in the Southern Ocean with various frequencies in different regions (Simon et al., 1999; Gentile et al., 2006; West et al., 2008; Straza et al., 2010; Piquet et al., 2011; Ghiglione and Murray, 2012; Wilkins et al., 2013; Williams et al., 2013; Luria et al., 2014). Some specific groups, for example, SAR11 and Roseobacter-clade-affiliated (RCA) cluster, have been intensively studied. These groups have global distribution or high abundance in specific regions. To some extent, some of them are labelled as the settled assemblages according to their environmental or functional adaption. Based on the technological advances, metatranscriptomics and metaproteomics have been

Introduction

applied to establish the link between the function and taxonomy on a large scale (Williams et al., 2013; Williams et al., 2012).

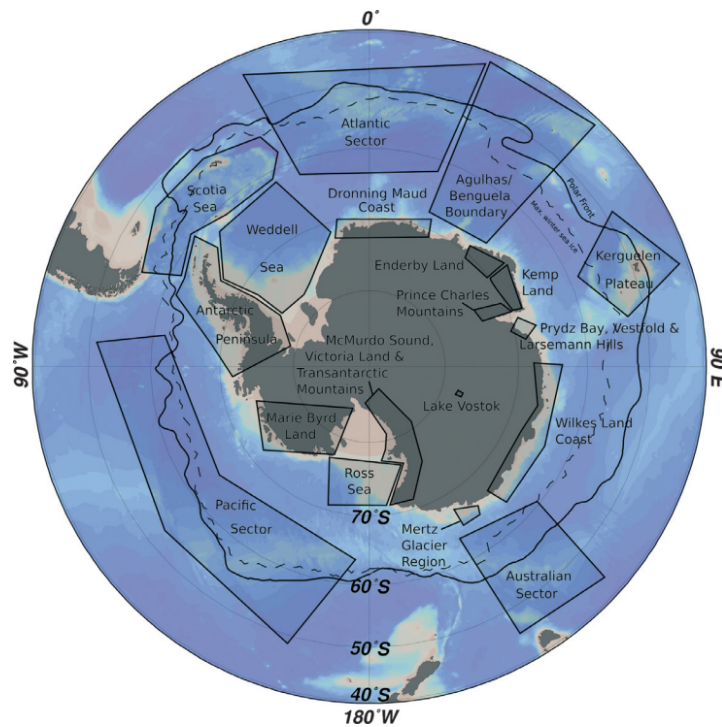


Fig. 5 Antarctica and the Southern Ocean. Polar Front (circumpolar full line); Maximum sea ice extent (circumpolar dotted line). Major regions of the Southern Ocean, including Agulhas/Benguela Boundary, Antarctic Peninsula, Australian Sector, Kerguelen Plateau, McMurdo Sound, Victoria Land, Transantarctic Mountains, Mertz Glacier Region, Pacific Sector, Ross Sea, Scotia Sea and Weddell Sea (Wilkins et al., 2013).

Alphaproteobacteria-SAR11

The SAR11 clade is the most abundant marine assemblage, contributing up to 25% of the total cell numbers in the global surface waters (Giovannoni, 2017). Since it was discovered in 1990 (Giovannoni et al., 1990) and cultured in 2002 (Rappé et al., 2002), this group of Alphaproteobacteria has been extensively studied. The biovolume of SAR11 cells has been estimated to be about $0.01 \mu\text{m}^3$, placing them among the smallest free-living cells (Rappé et al., 2002). Such small cell size suggests that the contribution of this group to marine biomass is less than their absolute numbers with overall 12% of the total prokaryotic biomass and 24-55% of total prokaryotic cells (Morris et al., 2002; Tada et al., 2013 in coldest regions), although the average biomass contribution of SAR11 is more than 20% in the Atlantic Ocean (Gasol and

Introduction

Kirchman, 2018). Another characteristic of the SAR11 clade is the streamlined genome which is one of the smallest (1.3 Mb) for any free-living organism and comparable with the genome size of symbionts or parasites (Giovannoni et al., 2005). The high surface area-to-volume ratio, small genome, dominant nutrient-uptake transporter gene, and complete biosynthetic pathways for amino acids reflect their preference of an oligotrophic strategy (Morris et al., 2002; Giovannoni et al., 2005; Sowell et al., 2009; Lauro et al., 2009).

Members of SAR11 showed high heterogeneity in distinct water columns from tropical to polar regions driven by latitude and temperature (Field et al., 1997; Carlson et al., 2009; Brown et al., 2012), while within the major surface-associated subgroups, SAR11 showed relative homogeneous diversity (García-Martínez and Rodríguez-Valera, 2000). SAR11 was consistent and abundant across surface samples in the Southern Ocean (Wilkins et al., 2013a; Luria et al., 2014) and especially in the temperate SAZ where the biomass was strongly correlated with temperature (Tada et al., 2013). A metagenomics survey investigated the biogeographic pattern of microbes in both sides of the PF, which has been suggested as a major biogeographical boundary in the distribution and abundance of microbial organisms (Selje et al., 2004; Abell and Bowman, 2005; Giebel et al. 2009; Weber and Deutsch, 2010). SAR11 was on average more abundant north of the PF and the highest contributor to the biogeographic partitioning of microbes in the Southern Ocean (Wilkins et al, 2013a; Wilkins et al., 2013). SAR11 also showed spatial separation with higher abundances in the western than in the eastern regions of the Scotia Sea (Topping et al., 2006), which suggests that SAR11 tends to be more abundant in less productive areas. Above the Kerguelen plateau, SAR11 was dominant in the HNLC region and less abundant during the decline of the phytoplankton bloom (West et al., 2008). In parallel, SAR11 showed low contributions to the bulk prokaryotic abundance and leucine incorporation during this late bloom stage. By contrast SAR11 was dominant at the onset and after the decline of the bloom at the same iron-fertilization region (Obenosterer et al., 2011; Dinasquet et al., 2019). A study conducted in the West Antarctic Peninsula (WAP) reported that SAR11 had high contribution in taking up LMW substrates and this group was less abundant in high chlorophyll *a* regions (Straza et al., 2010; Williams et al., 2012). The same results were also found in the Australian sector based on metagenomics and metaproteomics (Williams et al., 2013a). A negative correlation between SAR11 and phytoplankton blooms was previously observed in a seasonal study in the coastal Antarctic Peninsula and in Kerguelen Island waters (Ghiglione and Murray, 2012). This is consistent with an experimental study that showed SAR11 was rapidly outcompeted by other taxa in the presence of diatom-derived DOM (Landa

Introduction

et al., 2018). SAR11 has been consistently detected at high abundances from both spatial and temporal studies in the surface of the Southern Ocean. The highly homogeneous distribution might be because the taxa have similar ecological features (ecotypes) (García-Martínez and Rodríguez-Valera, 2000). However, sub-groups of SAR11 showed different dynamics over a 5-month time series study at a sub-tropical coastal station (Needham et al., 2017).

Alphaproteobacteria-Roseobacter clade

The Roseobacter clade, one of the most important groups in surface water samples (Buchan et al., 2005; Luria et al., 2014), showed the highest abundance in the Southern Ocean from a global study (Selje et al., 2004), particularly in the coldest regions (based on 16S rRNA data; Giebel et al., 2009). This clade was more active than SAR11 in the PF and SAZ, although it was numerically less abundant (Tada et al., 2013). This low abundance and high productivity trend is consistent with a previous study that showed Roseobacter was under-represented in abundance relative to the uptake of LMW substrates *in situ* (Alonso-Sáez and Gasol, 2007). The first genome of Roseobacter is from the species *Silicibacter pomeroyi* with a much larger genome (4.5 Mb) compared with SAR11 (1.3 Mb) (Moran et al., 2004; Giovannoni et al., 2005). *S. pomeroyi* has the highest proportion of genes related to their ability to rapidly respond to surrounding conditions among Alphaproteobacteria, which suggests the Roseobacter group has a distinct non-oligotrophic trophic strategy (Moran et al., 2004). Members of the Roseobacter clade are metabolically versatile, targeting a wider range of substrates than SAR11, with the capability of aerobic anoxygenic phototrophy and degradation of dimethylsulfoniopropionate (DMSP) (Moran et al., 2003; Wagner-Döbler and Biebl, 2006; Moran et al., 2007; Brinkhoff et al., 2008). They were often found in close association with phytoplankton blooms and cultures with free-living, particle-attached or in commensal relationships (reviewed in Buchan et al., 2005; Pinhassi et al., 2004).

Roseobacter contributes to 10-30% of the total prokaryotes in the surface waters of the Southern Ocean (reviewed in Wilkins et al., 2013c). They were highly abundant in phytoplankton blooms on the Kerguelen plateau (West et al., 2008; Obernosterer et al., 2011) and in the Scotia Sea (Topping et al., 2006; Jamieson et al., 2012). While it had less contribution to the total prokaryotes in the Weddell Sea (< 20%; Selje et al., 2004). These results refer to their ability in degradation of phytoplankton-derived DOM. The gene-related functions showed a spatial pattern as well (Wilkins et al., 2013a). Roseobacter and other copiotrophs have a higher

Introduction

number of transporters than oligotrophic genomes south of the PF in the Australian sector where diatoms were detected as the dominant phytoplankton group (Trull et al., 2011), which is consistent with the higher nutrient availability (Lauro et al., 2009; Wilkins et al., 2013a). Interestingly, Roseobacter had positive correlations with particulate organic carbon (POC) and particulate organic nitrogen (PON) along transects in the Southern Ocean (Tada et al., 2013). Additionally, the Roseobacter-clade-affiliated (RCA) cluster belonging to the Roseobacter clade showed seasonal patterns with low abundance in winter and increased in summer and autumn in the coastal waters of Antarctic Peninsula and around the Kerguelen plateau (Giebel et al., 2009; Ghiglione and Murray, 2012). A metagenomics study in the waters off Antarctica also found that the RCA cluster was more abundant in summer than in winter, in which Sulfitobacter showed the highest abundance (Grzymski et al., 2012). The RCA cluster has similar uptake systems as SAR11 for labile nutrients, such as ATP-binding cassette (ABC) transporters and tripartite ATP-independent periplasmic (TRAP) transporters (Williams et al., 2012). This supports the findings around the Kerguelen plateau that RCA was not only dominant inside the bloom but also abundant and active outside the bloom (West et al., 2008). Recently, culture-based work found that Roseobacter was present across a range of diatom strains isolated and cultivation time suggested their versatile ability for the diverse diatom-DOM (Behringer et al., 2018).

Alphaproteobacteria-Roseobacter clade – Sulfitobacter

Sulfitobacter is a group of bacteria belonging to Roseobacter known for their capacity to use organic sulfur compounds, such as DMSP (Moran et al., 2007; Ankrah et al., 2014), usually released during the decay of phytoplankton blooms. Members of this group also have the ability to utilize various labile carbon sources, such as carbohydrates and amino acids, evidenced using an extinction-dilution culture method from a polynya, in the Amundsen Sea (Choi et al., 2016). This is consistent with a metaproteomic study revealing that Sulfitobacter has various ABC transporters that enable the uptake of labile substrates (Williams et al., 2013). The flexibility of substrate assimilation makes Sulfitobacter abundant in coastal Antarctic waters (Zeng et al., 2014). Lastly, it showed high relative abundance if grown on diatom-DOM in a continuous culture and dominated in the surface waters with artificial iron addition by a short-term iron fertilization experiment (Singh et al., 2015; Landa et al., 2018). Additionally, Sulfitobacter showed clearly seasonal variation around the Kerguelen Island with high abundance in spring and summer and low abundance in autumn and winter (Ghiglione and Murray, 2012).

Introduction

Alphaproteobacteria-SAR116

SAR116 is a group of ubiquitous marine bacteria and is considered a metabolic generalist in ocean nutrient cycling (Giovannoni and Rappé, 2000; Oh et al., 2010). SAR116 has higher abundance north of the PF and this group is a moderate contributor to the biogeographic partitioning of microbes in the Southern Ocean (Wilkins et al., 2013a). The first genome of SAR116, “*Candidatus Puniceispirillum marinum* IMCC1322”, reported that it carries functional genes for utilizing light, DMSP, CO, and C1 compounds in the surface ocean (Oh et al., 2010). SAR116 targets similar substrates as SAR11 using ABC and TRAP transporters (amino acids, taurine, dicarboxylates) (Williams et al., 2013) and has similar biogeographic distributions as SAR11 (Wilkins et al., 2013a). These results suggest that SAR116 and SAR11 could occupy similar ecological niches (Oh et al., 2010; Williams et al., 2012). An annual study has supported this idea by examining the co-occurrence and activity of these two groups in the coastal NW Mediterranean Sea (Lami et al., 2009). Using FISH, Topping et al. (2006) found SAR116 was relatively more abundant than SAR11 in more productive waters in the Scotia Sea along a shorter latitude range (52°S-64°S). By contrast, SAR116 was exclusively detected at a HNLC site using DNA clone libraries (West et al., 2008) and showed a slightly decrease with an artificial iron fertilization (Singh et al., 2015). These results are consistent with the characteristics of its genome with versatile repertoire of genes (Oh et al., 2010). Lately, SAR116 showed its planktonic preference, which was only detected up to a depth of 40m (Singh et al., 2015).

Bacteroidetes- Flavobacteriaceae

Members of Bacteroidetes are one of the most abundant groups in the ocean, representing 10-30% of the total bacterial cells in coastal waters (Kirchman et al., 2002; Alonso-Sáez and Gasol, 2007). Flavobacteriaceae Family is one of the most common groups in marine and polar ecosystems (Kirchman 2002; Kirchman et al., 2003; Abell and Bowman, 2005b; Murray and Grzyski, 2007) and it is associated to increased production at low temperatures (Tada et al., 2013). Flavobacteriaceae is a major clade of Bacteroidetes and plays an important role in degrading HMW DOM. Members of this group are particularly prevalent in particle-attached communities and abundant with phytoplankton-derived DOM supply (DeLong et al., 1993; Abell and Bowman, 2005a; West et al., 2008; Teeling et al., 2012). This suggests that members of Flavobacteriaceae may act as the primary degraders of primary production products. This

Introduction

assumption of Flavobacteriaceae as degraders of polymers has been recently confirmed by genomic analysis with a suite of genes related to peptidases, glycoside hydrolases, glycosyl transferases, adhesion proteins and gliding motility (Fernández-Gómez et al., 2013).

In the Southern Ocean, Flavobacteriaceae contributed the most to the total abundance of Bacteroidetes in the Australian waters (Williams et al., 2013), where this group was strongly positively correlated with chlorophyll *a* across a wide range of concentrations (0.14-12.1 µg L⁻¹). West et al. (2008) found that Flavobacteriaceae related to the AGG58 group was more abundant in a natural iron fertilized bloom station above the Kerguelen plateau as compared to the HNLC region. The biogeographic pattern of Flavobacteriaceae has been previously reported across a latitudinal transect (from 44.7°S to 63.5°S) in the Southern Ocean (Abell and Bowman, 2005b). The abundance of Flavobacteriaceae was significantly higher south of the PF than north of it, using real-time PCR, DGGE analysis and metagenomes (Abell and Bowman, 2005b; Wilkins et al., 2013a). This may be because of the higher rates of primary productivity in the south and the role of the Flavobacteriaceae as primary degraders of HMW DOM.

Bacteroidetes- Flavobacteriaceae- Polaribacter

The Polaribacter species were initially isolated from polar sea ice (Gosink et al., 1998). To date, 20 described species with validly published names have been identified in various habitats (LPSN <http://www.bacterio.net/polaribacter.html>). Polaribacter is one of the major genera of Bacteroidetes found in the marine environment. Genome analysis of Polaribacter indicates its ability to associate with particles, degrade biopolymers, and sense and respond to light with proterorhodopsin gene (González et al., 2008).

In the Southern Ocean, members of Polaribacter were prevalent in coastal Antarctic marine bacterial communities (Ghiglione and Murray, 2012; Zeng et al., 2014). Polaribacter exhibits a clear biogeographic pattern. It was dominant in the colder water of the PFZ and AAZ compared with that in the SAZ (Abell and Bowman, 2005b), which is consistent with its psychrophilic characteristics. *Polaribacter irgensii*-related sequences were detected with high number in the Antarctic Peninsula (Murray and Grzymki, 2007), which were phylogenetically closest to prokaryotes from polar environments (Gosink et al., 1998; Brinkmeyer et al., 2003). A mesocosm study found diatom (*Nitzschia closterium*) derived DOM reduced the complexity of a flavobacterial community to few species in which Polaribacter was completely dominant,

Introduction

which suggests diatom-derived DOM has strong relationship with *Polaribacter* (Abell and Bowman, 2005a). A metagenomic study found that *Polaribacter* was positively correlated with chlorophyll *a* (Williams et al., 2013). Straza et al. (2010) previously found *Polaribacter* was highly active in the consumption of proteins over amino acids in the WAP, based on single-cell activity, which meets the general characteristics of Bacteroidetes as polymer degraders including proteins and polysaccharides (Fernández-Gómez et al., 2013). Above the Kerguelen plateau, a peak in *Polaribacter* abundances was detected during a spring bloom decay stage (Landa et al., 2016), consistent with their dominance in a metaproteome study conducted from the decay phase of an algal bloom in the North Sea (Teeling et al., 2012). In summer of the same region by an environmental study, *Polaribacter* was dominant in HNLC region off the Kerguelen plateau (West et al., 2008), while in the WAP it was dominant during phytoplankton blooms by both metagenomic and metaproteomic data (Grzymiski et al., 2012; Williams et al., 2012). By contrast, in winter of the Kerguelen Island, Landa et al. (2018) observed low abundance of *Polaribacter* in diatom-DOM cultures compared with controls without DOM supply. These results from different seasons and study regions suggest that seasonal variation of *Polaribacter* may follow seasonal cycles with the impact of phytoplankton-derived DOM, which differs in distinct regions of the Southern Ocean. *Polaribacter* was also dominant in the surface water in a polynya in the Amundsen Sea, where microbes were more active than their counterparts in open waters (Hollibaugh et al., 2007; Kim et al., 2014). This psychrophilic prokaryote was associated with high phytoplankton production (Kim et al., 2014) in this biologically productive regions. Similar to SAR116, *Polaribacter* showed a decrease in abundance following a short-term iron fertilization (Singh et al., 2015).

Bacteroidetes- Cryomorphaceae/AGG58

Members of the Family Cryomorphaceae are of the classical “Cytophaga-like” bacterial type (Bowman, 2014). In 16S rRNA gene clone data, this clade was originally designated as “AGG58 cluster” (DeLong et al., 1993) which represents a range of undescribed genus- and family-level entities (O’Sullivan et al., 2004; Abell and Bowman, 2005b; West et al., 2008). For clarity, Cryomorphaceae will be used in this thesis to represent this group of bacteria.

Cryomorphaceae was only detected in the PFZ and AAZ using DGGE rather in the SAZ (Abell and Bowman, 2005b) and outcompeted by *Polaribacter* with diatom (*Nitzschia closterium*) detritus addition (Abell and Bowman, 2005a). Cryomorphaceae was the most or

Introduction

the second most dominant group in the Order of Flavobacteriales in coastal waters of Antarctica (Murray and Grzyski, 2007; Zeng et al., 2014). During the declining phase of the phytoplankton bloom above the Kerguelen plateau Cryomorphaceae were dominant in the total bacterial abundance (~9%) with high production (~8%) using FISH (Obernosterer et al., 2011) and 16S rDNA clone libraries (West et al., 2008). Cryomorphaceae showed a slight increase from winter to summer by a seasonal study in both coastal waters of Kerguelen Island and Antarctic Peninsula (Ghiglione and Murray, 2012). The Bacteroidetes groups Cryomorphaceae and Polaribacter displayed similar seasonal patterns around the Kerguelen plateau (Obernosterer et al., 2011). Recently, however, Cryomorphaceae showed several functional features that differentiated it from other Bacteroidetes such as Polaribacter based on a genome study in the Amundsen Sea (Delmont et al., 2015). The Cryomorphaceae genome was enriched in genes with functions specifically related to outer membrane proteins and lipids which can facilitate inter cell interactions (Movva et al., 1980; Delmont et al., 2015).

Gammaproteobacteria-SAR86

The term SAR86 originated from 16S rRNA clone libraries belonging to Gammaproteobacteria from surface microbial communities (Britschgi and Giovannoni, 1991). It has been detected in the surface waters of the Southern Ocean (Abell and Bowman, 2005b; Topping et al., 2006; West et al., 2008; Obernosterer et al., 2011). It showed relatively higher contribution to the total bacteria in low primary production areas as compared to high primary production areas (Topping et al., 2006; Obernosterer et al., 2011). The genome analysis indicated that like SAR11, SAR86 exhibited metabolic streamlining, but was capable to degrade lipids and carbohydrates using TonB-dependent outer membrane receptors, but lacked pathways for amino-acid uptake (Dupont et al., 2012). Additionally, SAR86 coincided with SAR11 in an HNLC region using either FISH or 16S rRNA clone libraries (West et al., 2008; Obernosterer et al., 2011). The similar ecological preference and distinct carbon compound specialization suggests SAR86 and SAR11 may share the same ecological niches with minimum competition (Obernosterer et al., 2011; Dupont et al., 2012).

Gammaproteobacteria- Alteromonadales- Colwellia

Marine members of Alteromonadales include heterotrophs with broad substrate preferences and cold-adapted genera such as *Colwellia* recorded in the Southern Ocean seawater and sea-ice off

Introduction

Antarctica (Bowman et al., 1997; Piquet et al., 2011). Members of the *Colwellia* group are psychrophilic and are commonly found in polar ecosystems with the adaptation to cold environments by producing a source of cold-active extracellular enzymes at low temperatures (Méthé et al., 2005; Kim et al., 2018).

High *Colwellia* abundances were observed with diatom-DOM addition in mesocosms performed in the WAP and around the Kerguelen Island during winter and early spring (Luria et al., 2017; Landa et al., 2018). This is consistent with a metagenome study showing that *Colwellia* can degrade small aromatic compounds, which provides an ecological advantage to this group (Hu et al., 2017). While in summer of two consecutive years in the WAP, *Colwellia* dominated in the low productive summer and it was replaced by more diverse groups in the summer with high productivity (Fuentes et al., 2019). A similar study conducted in the Arctic summer also found a *Colwellia* related operational taxonomy unit (OTU) was either positively or negatively impacted by diatom DOM addition (Dadaglio et al., 2018). These results suggest that *Colwellia* are metabolic versatile and tend to outcompete other bacterial groups at low temperature.

4.2 Ecological adaptation of microbes in the Southern Ocean

In the cold waters of the Southern Ocean, it is crucial for microbes to adapt to the cold environment. The cold adaptation has been indicated by few studies (Dunker et al., 2002; Grzymiski et al., 2006). *Polaribacter* is a proteorhodopsin-containing bacterial group and can form gas vesicles which help the cold adaptation (Staley and Gosink, 1999). The mechanisms that lead to the adaptation of SAR11 in cold waters are not well understood, but are probably a consequence of gene related functions. SAR11 is also proteorhodopsin-containing which might be a partial reason for its characteristics of widespread occurrence (Giovannoni et al., 2005; Gasol and Kirchman, 2018). Williams et al. (2012) detected in their metaproteomic data proteorhodopsin even at low light intensity during Antarctic winter waters. Additionally, the highly present genes related to energy production and conversion in polar genomes of SAR11 induces their adaptability to cold environments in which some subgroups showed preference in polar waters (Brown et al., 2012).

Introduction

In terms of the nutrient and organic carbon acquisition, generally, in the surface waters of the Southern Ocean, Bacteroidetes groups, particularly Flavobacteriaceae thrive with increasing concentrations of Chlorophyll *a* (Williams et al., 2013a) and breaks down complex organic matter of phytoplankton cells and phytoplankton-derived detrital particles using extracellular enzymes (Teeling et al., 2012). Subsequently, Alphaproteobacteria and Gammaproteobacteria start being dominant and harbour the genetic potential to utilize labile (small) organic substrates (Wilkins et al., 2013a; Williams et al., 2013). For example, Flavobacteriaceae perform a potentially important function in nitrogen cycling in the Southern Ocean by generating ammonia from organic nitrogen (Williams et al., 2013). This by-product could be scavenged by other marine microorganisms, especially if we consider that certain marine Flavobacteriaceae have been shown to be unable to utilize ammonia as a nitrogen source (Suzuki et al., 2001). In the coastal waters of the WAP with substantial warming in recent decades, flavobacterial activity increased with several folds higher nitrate and ammonia uptake rates during high Chlorophyll *a* conditions at night time (Alcamán-Arias et al., 2018). Bacteroidetes and Gammaproteobacteria have dominant TonB-transporters (TBDT) proteins detected in their membrane off the Antarctic Peninsula in summer (Williams et al., 2012). Flavobacteriaceae contain TBDT and biopolymer-degrading enzymes which can help them to utilize storage polysaccharides from algae as substrates with their inferred lifestyle in cold marine waters (Williams et al., 2013; Xing et al., 2015). Gliding motility proteins were detected in Flavobacteriaceae, which allows the exploration of solid surfaces of phytoplankton or other particles (McBride, 2001). *Polaribacter* also contains TBDT, but cannot utilize some algal exudates such as taurine, polyamines and glycolate that Rhodobacterales has the ability to target (Buchan et al., 2005; González et al., 2008). ATP-binding transporters and ABC transporters were detected related to SAR11, specificity for amino acids, while Flavobacteriaceae was related to TBDT and low numbers of genes involved in the uptake of LMW compounds (Williams et al., 2013). Furthermore, Cryomorphaceae can potentially synthesize oligosaccharides which could protect them from host-derived antimicrobial compounds (Silipo and Molinaro, 2010; Delmont et al., 2015).

4.3 Microbial associations in the Southern Ocean

Phytoplankton and heterotrophic prokaryotes are major components of the global biogeochemical cycles and are known to interact in very complex ways (Azam and Malfatti,

Introduction

2007; Amin et al., 2012). These components are closely interrelated continuously. The utilization of phytoplankton-derived DOM by heterotrophic prokaryotes is a major carbon-flow pathway, in turn, heterotrophic prokaryotes provide inorganic nutrients for phytoplankton. Therefore, the phytoplankton-prokaryotes interactions impact the overall patterns of carbon flux and nutrients cycling.

The mechanisms behind the interactions investigated by culture work are manifold, for example, mutualism, antagonism and competition (reviewed in Amin et al., 2012; Cirri and Pohnert, 2019), which helps to understand how phytoplankton and prokaryotes affect their encounters and decipher their implication in oceanic nutrient fluxes (Fig. 6). For example, *Sulfitobacter* species promoted the cell division of *Pseudo-nitzschia multiseries* via signal molecules indole-3-acetic acid and tryptophan which are part of a complex exchange of nutrients, including diatom-excreted organosulfur molecules and bacterial-excreted ammonia (Amin et al., 2015). In return, *Sulfitobacter* heme transporter was downregulated during the co-culture with *Pseudo-nitzschia multiseries* (Hogle et al., 2016). A few interactions have also been studied in the Southern Ocean. In coastal McMurdo Sound, bacteria and diatoms showed a mutualistic relationship. *Fragilariopsis* contributed the most to the total abundance of diatoms, relied on cobalamin produced solely by bacteria and archaea, while bacterial growth fueled on organic matter derived from diatoms (Bertrand et al., 2015). In the same study the competition between *Methylophaga* and diatoms for the acquisition of cobalamin was shown. Bacteria could also stimulate diatom growth and influence the primary production of the Southern Ocean. In Australian sector, Hassler et al. (2011) found that exopolysaccharide (EPS), produced by a bacterial isolate (*Pseudoalteromonas* sp.) can enhance the bioavailability and solubility of iron by binding together, and further impact iron uptake of diatoms (*Chaetoceros* sp. and *Phaeocystis* sp.).

4.4 Complex microbial associations in the field

The culture-based work aforementioned, however, focused on one phytoplankton-prokaryote interaction, or one specific phytoplankton and surrounding prokaryotic groups, at a time (e.g., Amin et al., 2015; Segev et al., 2016). In the ocean, microbes form complex ecological webs in which natural microbes are often taxonomically highly complex and can encompass hundreds of different species. It is impractical to examine the interaction of each pairwise phytoplankton

Introduction

and prokaryote, since most of the species are not cultivated in the laboratory (~ 95% of species present in a given sample) (Staley and Konopka, 1985), which is probably because of the missed coexistence with partner species in pure cultures (Vartoukian et al., 2010; Stewart, 2012).

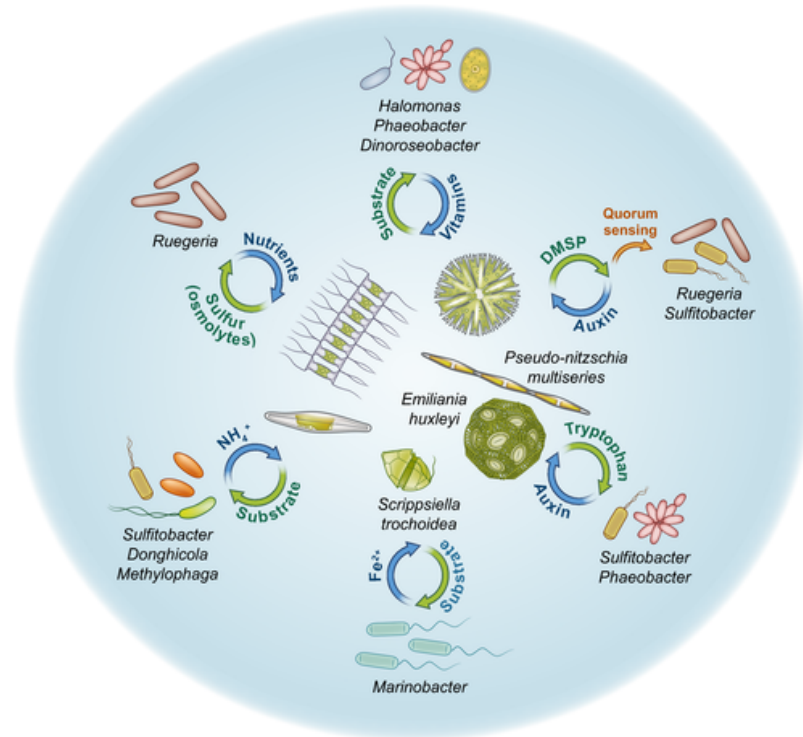


Fig. 6 Tight associations between microalgae and bacteria (mostly Proteobacteria, as highlighted in Amin et al., 2012) have resulted in the evolution of a complex network of cross-kingdom interactions and a fine specialisation of different organisms (Cirri and Pohnert, 2019).

Along with the advanced techniques for rapidly generating large data sets, the complex microbial associations have been studied with increased interest (Chaffron et al., 2010; Lima-Mendez et al., 2015; Needham and Fuhrman, 2016). For example, a global study of environmental microbes observed co-occurrence relations via the network approach (more details in the Methodology section), which makes the detection and the investigation of various types of interactions possible, although in a putative way (Chaffron et al., 2010). In their study, they confirmed previously known microbial associations and predicted the majority of associations that have not been recognized before. Therefore, through the co-occurrence relationships, one can interpret the possible ecological meaning behind and explore specific hypotheses related to observed associations in the laboratory (Orphan, 2009). In addition, the

Introduction

discovery of *in situ* associations was also performed between prokaryotes and DOM, which deciphers the complex microbial and molecular information, and provides insight on opening the “black box” on both sides in various ecosystems (Osterholz et al., 2016).

5 Objectives of the thesis and organization of the manuscript

The findings summarised above shed light on the importance of microbes, DOM and interrelated relationships in biogeochemical cycles, although the diverse microbes and microbial associations on spatiotemporal scale are largely unexplored in the Southern Ocean. The objective of this thesis is to investigate the composition of microbial communities and the associations among them on spatial and temporal scales, and to uncover the connections between prokaryotes and DOM in distinct environmental areas in the Southern Ocean.

All data related to this thesis was obtained via two cruises conducted in the Southern Ocean (Fig. 7).

The study of spatial microbial associations is presented in the first chapter of this manuscript. The aim is to investigate whether diatom community composition can explain biogeographic patterns of prokaryotes (SOCLIM project; Oct. 2016). This part of work was published in *Environmental Microbiology*.

The study of temporal microbial associations is presented in the second chapter of this manuscript. The aim is to discover seasonal successions of microbes and the putative microbial behaviour in two consecutive bloom events over a 4-month sampling period (SOCLIM project; Oct. 2016 - Feb. 2017).

Introduction

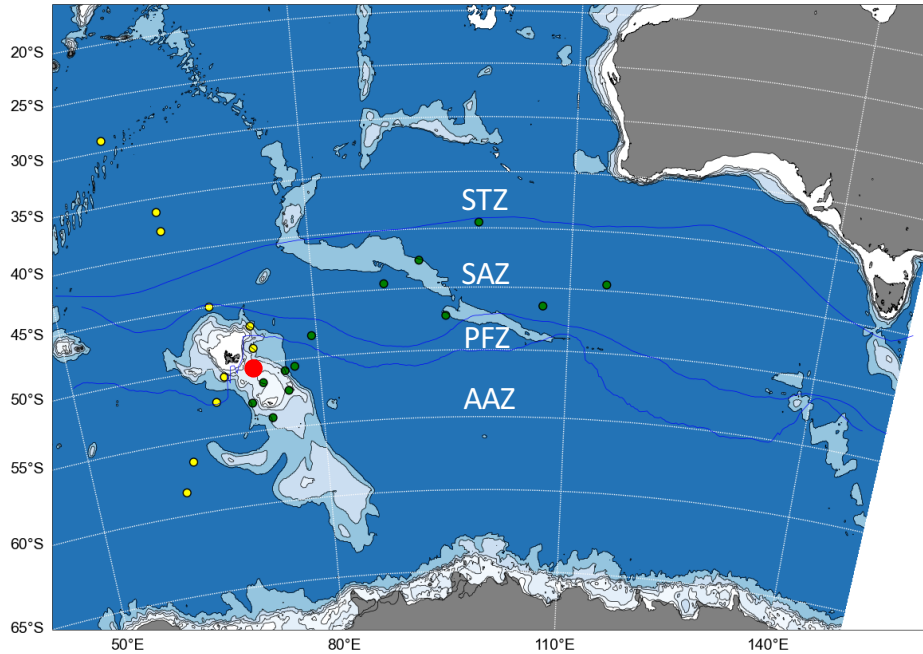


Fig. 7 Map of sampling sites related to the thesis. Yellow and green dots represent samples collected via SOCLIM and HEOBI cruises respectively. The red dot denotes the seasonal site (A3) conducted during SOCLIM cruise. STZ, Subtropical Zone; SAZ, Subantarctic Zone; PFZ, Polar Front Zone; AAZ, Antarctic Zone.

The study of prokaryote-DOM associations is presented in the third chapter of this manuscript. The aim is to integrate the microbial and molecular information and decipher the associations between DOM and prokaryotes in two contrasting ecosystems around the Kerguelen plateau (HEOBI project; Jan. -Feb. 2016).

An additional study of prokaryotic diversity and activity in contrasting regimes is also included in this manuscript and is presented in Appendix 2. This study was conducted through the MOBYDICK project (<https://mobydick.mio.osupytheas.fr>) in late austral summer (Feb.-Mar. 2018). One aim of this project is to investigate the composition of prokaryotic communities at sites with different levels of productivity. This part of the work is related to a Master thesis project. I co-supervised the master student (Alejandra Elisa Hernández Magaña) with the lab work and the bioinformatics

METHODOLOGY



Yan Liu

Methodology

1 Raw data processing

Since the time of sample collection was separated, two independent series of Illumina MiSeq runs were performed for prokaryotic diversity samples of the three chapters. One for Chapter 1 and 3 and one for Chapter 2. Two different pipelines were used for processing raw data, given the rapid updates of bioinformatic tools. Usearch pipeline (Edgar, 2013) was performed for the data set of Chapter 1 and DADA2 pipeline (Callahan et al., 2016) was performed for the data sets from Chapter 2 and 3. Usearch generates a traditional operational taxonomic unit (OTU) table, which combines grouped sequencing reads clustered with a customary dis/similarity value. DADA2 generates an amplicon sequence variant (ASV) table, which includes sequences with single-nucleotide difference over the sequenced gene region. The major steps of these two pipelines are described in Table 1. DADA2 uses an error model to estimate error rates from the data set after quality filtering (Step 3). This error model identifies the mismatches between sequences (e.g., A- >C), which is not included in Usearch pipeline.

Table 1 Major steps in raw data processing

	Usearch	DADA2
Step 1	Merge forward and reverse reads	Inspect read quality profiles
Step 2	Trim forward and reverse primers and quality filtering	Trim forward and reverse primers and quality filtering
Step 3	Dereplicate sequences	Learn error rates
Step 4	Cluster sequences into OTUs	Dereplicate sequences
Step 5	Denoise and remove chimeras	Merge paired reads
Step 6	Generate a count table	Construct a sequence table
Step 7	Assign taxonomy to OTUs	Remove chimeras
Step 8		Assign taxonomy to ASVs

2 Diversity analysis

Diversity is one of the most important concepts in ecology. From the aspect of ecological communities, diversity analysis has crucial importance in studies relative to species composition. Species diversity indices can be used to compare sampling sites from different ecosystems or successive observations from the same community.

Methodology

2.1 Alpha-diversity

Alpha-diversity represents the diversity within a given habitat or ecosystem (community). It is generally used to compute the diversity for each sampling site separately.

Richness

Richness refers to the number of different species/OTUs/ASVs present at one site. Sites with more species are considered richer. Observed richness simply counts the number of species observed once in a sample, which typically underestimate and strongly depend on sampling effort and sample completeness. Chao (1987) proposed Chao1 index which estimates the species richness including observed and undetected species by assuming that the number of observations for a species has a Poisson distribution. This index has been widely used for investigating alpha-diversity.

Evenness

Evenness (Hill, 1973) examines how homogeneous or even a community or ecosystem is in terms of the abundance of its species. A community in which all species are equally common is considered even and has a high degree of evenness. In this thesis, the evenness index was calculated using the formula:

$$E = \frac{H}{\log S}$$

where H is the Shannon index (see below) and S is the total number of species (i.e., richness).

Shannon index

The Shannon index (Margalef, 1958) is commonly used to characterize species diversity in a community. It incorporates both richness and evenness in its valuation. In this thesis, it is calculated by the formula below via phyloseq package (McMurdie and Holmes, 2013) in R:

$$H = - \sum_{i=1}^n p_i \ln p_i$$

Methodology

where n is the total number of species, p_i is the proportion of species i relative to the total number of species. $\ln p_i$ is the natural logarithm of this proportion p_i .

2.2 Beta-diversity

Beta-diversity is the diversity between samples or communities. For multivariate data sets that contain multiple sites, beta-diversity is commonly used for the comparison between each pair of sites. In this thesis, Bray-Curtis dissimilarity was used to evaluate beta-diversity.

Bray-Curtis dissimilarity

The Bray-Curtis dissimilarity (Bray and Curtis, 1957) is a common measure of compositional data in biodiversity based on counts at each site. This measure treats differences between high and low variable values equally. It is calculated by the formula below:

$$BC_d = \frac{\sum_{k=1}^n |y_{i,k} - y_{j,k}|}{\sum_{k=1}^n (y_{i,k} + y_{j,k})}$$

where k is the species. n is the total number of species. i and j are two different samples. $y_{i,k}$ and $y_{j,k}$ are the abundances of species k in sample i and j respectively.

3 Statistical analyses for microbial associations

A crucial need performing microbial association analysis is to integrate two or more data sets that are measured on the same samples. The integrative biology approach allows us to incorporate multiple types of data, characterized by many variables with less samples or observations. In this thesis, we focused on the integration of two types of data matrices that are measured on the same samples.

Methodology

Correlation analysis starts from a transformed abundance matrix, e.g., prokaryotic taxa data across different samples, locations or time points. Pairwise scores between taxa are then compute using a suitable similarity or distance measure. Variable pairs with P values below the threshold are visualized as a heatmap or network. Several key steps relative to correlation analysis in this manuscript are listed below (Legendre and Legendre, 2012; Buttigieg and Ramette, 2014).

3.1 Data transformation

Logarithmic transformation

Logarithmic transformation can reduce the range of a data set. The relative change of a variable, whose values are expressed as an exponent with respect to some base, is emphasised over its absolute change. Common bases are 2 (the binary logarithm), the natural logarithm, and 10. Logarithmic transformation can help linearize variables using appropriate bases.

Species profile transformation

This is a method of data standardisation that is often used prior to analysis. Data transformed in this way are called compositional data. This kind of data are commonly used to interpret ecological meaning behind, for example, the spatial distributions or temporal changes of microbial communities. Relative abundances can be transformed into percentages by multiplying 100. The formula is following:

$$y'_{ij} = \frac{y_{ij}}{y_{i+}}$$

where i is the sampling site, j is the species. y_{ij} is the abundance of species j at sampling site i . y_{i+} is the total abundance of all species at sampling site i .

Methodology

Hellinger transformation

Hellinger transformation is particularly suited to species abundance data. It gives low weights to variables with low counts and many zeros. The resulting value of this transformation is identical to the squared relative abundance data (see the formula below). Hellinger transformation is closely related to several (dis)similarity and distance measures, which is often preferable to be applied prior to analyses such as principal component analysis (PCA) or redundant analysis (RDA) (Legendre and Legendre, 2012).

$$y'_{ij} = \sqrt{\frac{y_{ij}}{y_{i+}}}$$

where i is the sampling site, j is the species. y_{ij} is the abundance of species j at sampling site i . y_{i+} is the total abundance of all species at sampling site i .

Z-scoring transformation

This method of data standardisation aims to create unit-free transformed variables with means and standard deviations. The mean of each variable is subtracted from the original values and the difference divided by the variable's standard deviation (see formula below). This transformation is used for standardisation of environmental variables in this thesis.

$$Z = \frac{x_i - \mu}{s}$$

where x_i is one original value of the variable x . μ is the mean of the variable x . s is the standard deviation of the variable x .

3.2 (Dis)similarity/ distance and regression measures for correlation analysis

3.2.1 (Dis)similarity/distance-based approach

Methodology

Spearman's rho

Spearman's rho (Kendall, 1943) uses ranks rather than the original variable values to measure correlation. Ranks of variables either go up or down across samples in a monotonic way, but not necessarily in a linear fashion. Spearman's rho considers how strongly the rankings between two variables disagree. The larger the disagreement the lower the rho value. This measure is suitable for raw or standardized abundance data and any monotonically related variables.

In this thesis, Spearman correlation and extended local similarity analysis (eLSA) were used for the study relative to temporal microbial dynamics and associations (Chapter 2; see Fig. 3 below). The eLSA pipeline integrates data normalization, statistical correlation calculation, statistical significance evaluation, and the network construction steps. It can integrate two data sets and detect similarity between shifted abundance profiles and is therefore frequently used to build association networks from time series data. To set threshold on similarity scores, most authors use a permutation test. The LSA score and Spearman's rho were both constraints for selection of statistically significant correlations (Ruan et al., 2006; Xia et al., 2013).

3.2.2 Regression-based approach

Sparse partial least squares regression

Partial least squares (PLS) regression (Wold, 1996; Wold et al., 2001) is a multivariate methodology which integrates two separate data matrices (X and Y) and calculate the correlations among variables. Unlike principal component analysis (PCA) which maximizes the variance in a single data set, PLS maximizes the covariance between two data sets by seeking for linear combinations of the variables from both sets. Sparse partial least squares (sPLS) is an advanced version of PLS. It aims at combining selection and modelling in a one-step procedure. This approach has been validated by a series of real biological data sets (Lê Cao et al., 2008). It provides variable selection to facilitate the interpretation of results. Two deflation steps are proposed to handle either a regression or a canonical framework of the biological study. If Y is deflated in an asymmetric way, variables in X can explain the Y variables (regression model). If Y is deflated in a symmetric way (canonical model), the aim is

Methodology

to model the relationships between the X and Y variables, and hence highlight interactions between the two sets of variables. SPLS was applied in correlation analysis of Chapter 1 (see Fig. 3 below).

3.3 Data visualization

Heatmap

Heatmap, also called ‘Clustered correlation’ or ‘Clustered Image Maps (CIM)’ was first introduced by Weinstein et al. (1994, 1997). This type of representation is based on a hierarchical clustering simultaneously operating on the rows and columns of a real-values similarity matrix. Each entry of the matrix is coloured on the basis of its value by a 2-dimensional coloured image. The rows and columns are reordered according to the hierarchical clustering (Fig. 1). The similarity matrix represented by the heatmap is the same as in the relevance network (see Fig. 2 below).

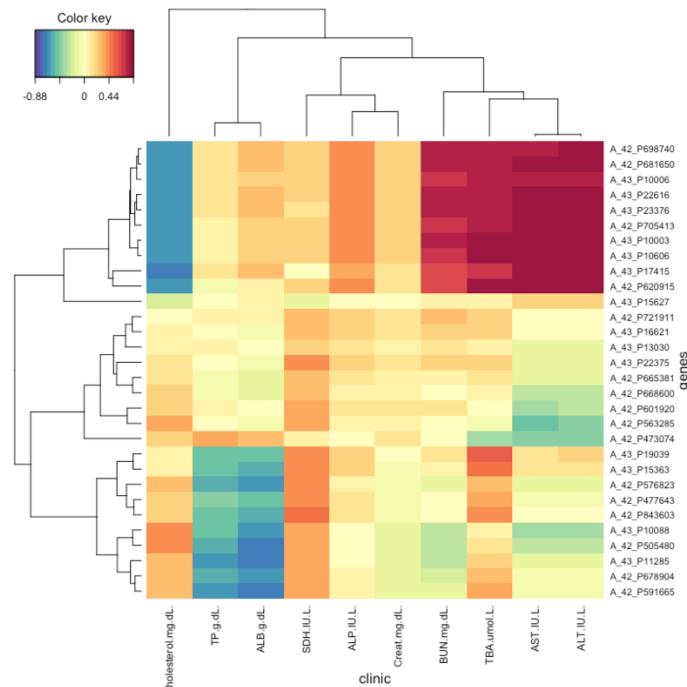


Fig. 1 Correlation visualization via heatmap. An example from a case study of mixOmics package in R.

Methodology

Network

The goal of network is to identify combination of microorganisms or genes that show significant co-presence or mutual exclusion patterns across samples and to combine them into a network (Faust and Raes, 2012). The essence of network and heatmap is identical, while the advantage of the network is that time delayed correlations can be visualized by special symbols, such as arrows. The network below shows the possible correlations among organisms (Fig. 2).

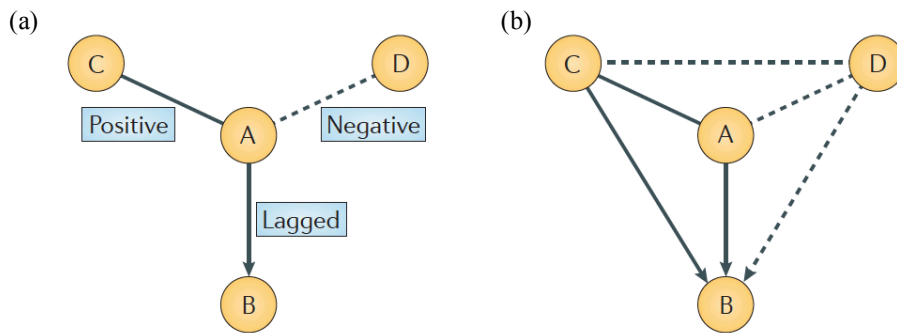


Fig. 2 (a) A ‘hub-and-spoke’ network showing how organisms B, C and D correlate with organism A (which is the hub of the network). Positive correlations are represented as solid lines, negative correlations as dashed lines and lagged associations as lines with arrows, pointing from the leading towards the lagging organism; (b) A network showing all of the correlations between all pairs of organisms (A–D), using the solid, dashed and arrow lines defined in panel (a). In addition to what is shown in panel (a), this also shows organism B with a lagged positive correlation to organism C and a lagged negative correlation to organism D, and organism C with a negative correlation to organism D (Fuhrman et al., 2015)

In this thesis, the spatial and seasonal microbial associations (Chapters 1 and 2) were carried out using some of these tools above. An integrated flowchart is showed below (Fig. 3).

Methodology

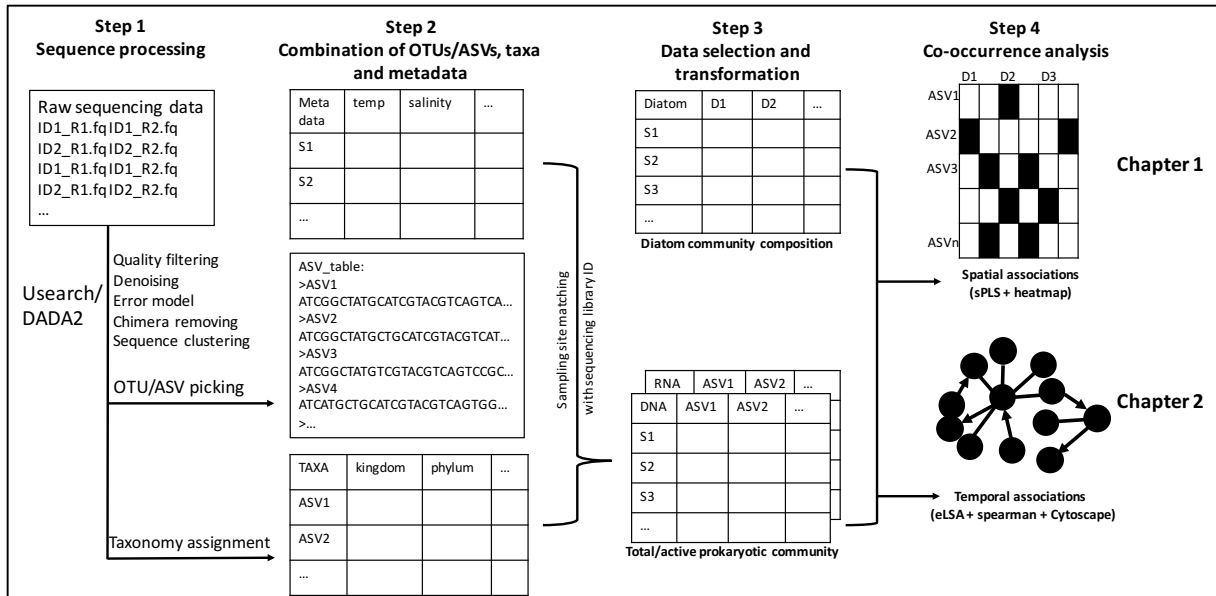


Fig. 3 Flowchart of microbial association analysis (Chapter 1 and 2).

4 Statistical analyses for prokaryote-DOM associations

To investigate the composition of prokaryotic community and of the DOM formulae, and their associations, a series of statistical analyses were applied in Chapter 3 (Fig. 4).

Principal component analysis

Principal component analysis (PCA) is an ordination technique. It produces a set of uncorrelated (orthogonal) axes to summarise the variance of a data set in a low-dimensional space. It provides an overview of linear relationships between samples and species. One of the most important advantages of PCA is, if a data set contains many variables and relatively few samples, it can help collapse these many variables into a few principal components (PCs), which maximizes the variance in the data set.

Principal coordinates analysis

Principal coordinates analysis (PCoA, also known as metric multidimensional scaling) summarises and attempts to represent inter-object (dis)similarity in a low-dimensional space (Gower, 1966). Rather than using raw data, PCoA takes a (dis)similarity matrix as input. As PCA, PCoA also produces a set of uncorrelated axes to summarise the variability in a data set.

Methodology

Each axis has an eigenvalue whose magnitude indicates the amount of variation captured in that axis. The proportion of a given eigenvalue to the sum of all eigenvalues reveals the relative 'importance' of each axis. Each sample has a 'score' along each axis. The sample scores provide the sample coordinates in the ordination plot.

Canonical correlation analysis

Canonical correlation analysis (CCorA) is suitable to examine linear relationships between two data sets. Unlike canonical correspondence analysis (CCA) and redundant analysis (RDA), CCorA is a symmetrical canonical analysis. It means one can correlate two data sets when it is unclear what are response and explanatory variables. It attempts to find axes of maximum linear correlation between two corresponding data matrices.

In this thesis, the combined analysis of compositional prokaryotic species and DOM compounds data (Chapter 3) were carried out using PCoA and CCorA. An integrated flowchart is showed below (Fig. 4).

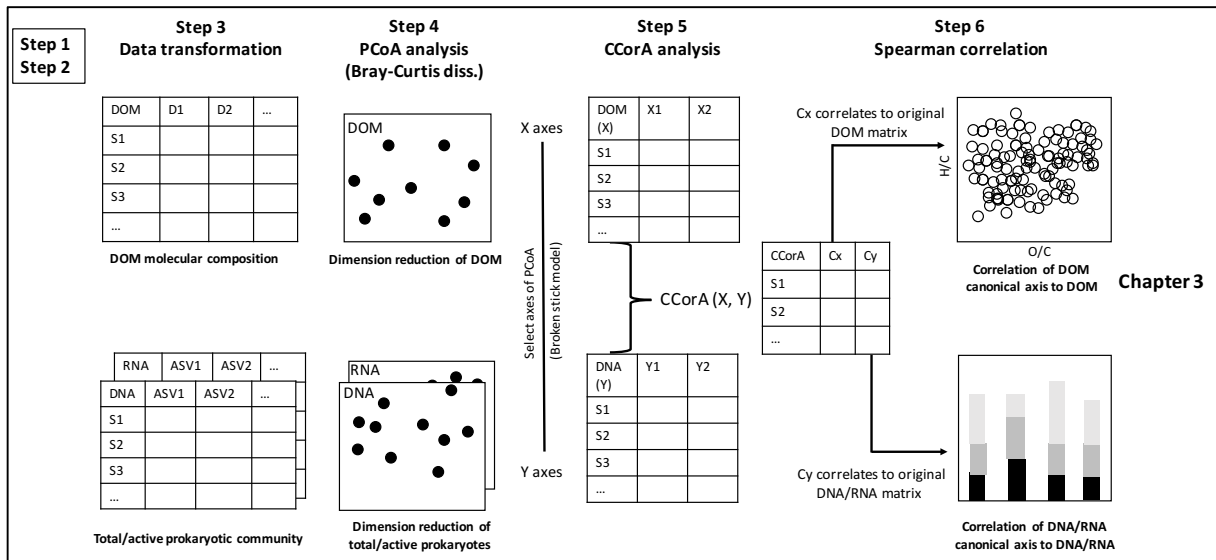


Fig. 4 Flowchart of prokaryote-DOM association analysis (Chapter 3). Steps 1 and 2 were processed the same as Fig. 3.

CHAPTER ONE

Spatial distribution of prokaryotes and their associations with diatoms



Preface

This thesis chapter is part of the Southern Ocean and Climate Project (SOCLIM, PI Stéphane Blain). I performed all molecular analyses, including the extraction of DNA and RNA, and the 16S rRNA gene amplification. I also carried out all bioinformatic procedures, and the statistical analyses to establish links between prokaryotic communities and diatoms. My work was carried out on seawater samples collected by Pavla Debeljak (LOMIC) during an oceanographic cruise in October 2016 aboard the French *R/V Marion Dufresne*. The diatom assemblages were described by Mathieu Rembauville (LOMIC). Contextual data were provided by different persons from the LOMIC: Philippe Catala (microbial abundance by flow cytometry), Olivier Crispi (inorganic nutrients) and Jocelyne Caparros (dissolved organic carbon).

Diatoms shape the biogeography of heterotrophic prokaryotes in early spring in the Southern Ocean

Yan Liu ¹, Pavla Debeljak ^{1,2},
Mathieu Rembauville,¹ Stéphane Blain¹ and
Ingrid Obernosterer ^{1*}

¹Sorbonne Université, CNRS, Laboratoire
d'Océanographie Microbienne (LOMIC), 66650
Banyuls-sur-Mer, France.

²Department of Limnology and Bio-Oceanography,
University of Vienna, 1090 Vienna, Austria.

Summary

The interplay among microorganisms profoundly impacts biogeochemical cycles in the ocean. Culture-based work has illustrated the diversity of diatom–prokaryote interactions, but the question of whether these associations can affect the spatial distribution of microbial communities is open. Here, we investigated the relationship between assemblages of diatoms and of heterotrophic prokaryotes in surface waters of the Indian sector of the Southern Ocean in early spring. The community composition of diatoms and that of total and active prokaryotes were different among the major ocean zones investigated. We found significant relationships between compositional changes of diatoms and of prokaryotes. In contrast, spatial changes in the prokaryotic community composition were not related to geographic distance and to environmental parameters when the effect of diatoms was accounted for. Diatoms explained 30% of the variance in both the total and the active prokaryotic community composition in early spring in the Southern Ocean. Using co-occurrence analyses, we identified a large number of highly significant correlations between abundant diatom species and prokaryotic taxa. Our results show that key diatom species of the Southern Ocean are each associated with a distinct prokaryotic community, suggesting that diatom assemblages contribute to shaping the habitat type for heterotrophic prokaryotes.

Introduction

Marine autotrophic and heterotrophic microbes are tightly coupled on spatial and temporal scales. The production and remineralization of dissolved organic matter (DOM) is a basic interaction that mediates the fluxes of large quantities of carbon and energy between these components of the microbial community (Ducklow *et al.*, 2006). Roughly half of recent primary production is taken up by heterotrophic microbes, resulting in a respiration that is several-fold higher than the annual increase in atmospheric carbon dioxide (CO₂) of 4 Gt (Ciais *et al.*, 2014). Diatoms are ubiquitous phototrophic microbes known to produce large quantities of DOM (Biddanda and Benner, 1997; Mykkestad, 2000). This group is abundant at high latitudes and dominates phytoplankton blooms in the nutrient-rich, cold surface waters of the Southern Ocean (Smetacek *et al.*, 2004; Assmy *et al.*, 2013; Quéguiner, 2013; Malviya *et al.*, 2016), thereby influencing the dynamics of heterotrophic microbes.

Phytoplankton blooms markedly affect the prokaryotic community composition (see reviews by Buchan *et al.*, 2014; Bunse and Pinhassi, 2017). The successional shifts were linked to the temporal modifications in the quantity and quality of the phytoplankton-derived DOM providing new niches for either opportunistic prokaryotic taxa or those adapted in the preferential utilization of the compounds released (Rinta-Kanto *et al.*, 2012; Sarmiento and Gasol, 2012; Teeling *et al.*, 2012; Li *et al.*, 2018). Using the exudate of a common diatom species as a growth substrate in an experimental approach and *in situ* observations allowed to establish a link between substrate preferences of several prokaryotic taxa and their presence during spring phytoplankton blooms in the Southern Ocean (Landa *et al.*, 2016). The reported co-occurrence patterns between eukaryotic and prokaryotic taxa extend the potential importance of biotic interactions to larger temporal and spatial scales (Gilbert *et al.*, 2012; Lima-Mendez *et al.*, 2015; Milici *et al.*, 2016; Needham and Fuhrman, 2016; Zhou *et al.*, 2018). These networks could in part be driven by the exchange of a suite of metabolites, discovered in experimental studies using model organisms.

The interplay between autotrophic and heterotrophic microbes could be governed by mechanisms that are

Received 30 October, 2018; revised 21 February, 2019; accepted 3 March, 2019. *For correspondence. E-mail ingrid.obernosterer@obs-banyuls.fr; Tel: (+33) 468887353; Fax: (+33) 04 68 88 73 98.

species-specific (Amin *et al.*, 2012). The production of compounds of the vitamin B group, such as B1 by *Marinomonas* sp. SBI22 (Paerl *et al.*, 2017), B2 (Johnson *et al.*, 2016) and B12 by *Ruegeria pomeroyi* DSS-3 (Durham *et al.*, 2015) was shown to support the growth of the phototrophs *Ostreococcus lucimarinus* and *Thalassiosira pseudonana*, respectively. The exchange of nitrogen and carbon governs certain associations between the nitrogen-fixing cyanobacterium UCYN-A and the unicellular algae *Braarudosphaera bigelowii* (Thompson *et al.*, 2012; Zehr, 2015). The production of siderophores by *Marinobacter* sp. DG879 that help acquire iron could promote interactions with phytoplankton, such as the dinoflagellate *Scrippsiella trochoidea* (Amin *et al.*, 2009). Diatom cell division was recently shown to be regulated by the excretion of hormones released by prokaryotes based on the co-cultured *Pseudo-nitzschia multiseriis* with *Sulfitobacter* sp. SA11 and *Thalassiosira pseudonana* with *Croceibacter atlanticus* (Amin *et al.*, 2015; van Tol *et al.*, 2017). These findings in combination with the observed co-occurrence of microbial taxa (Gilbert *et al.*, 2012; Lima-Mendez *et al.*, 2015; Milici *et al.*, 2016; Needham and Fuhrman, 2016; Zhou *et al.*, 2018) raise the question of whether interactions have the potential to drive biogeographic patterns of microbial communities in the aquatic environment.

The objective of the present study was to investigate the association between diatom assemblages and the prokaryotic community composition on a spatial scale. We specifically asked the question of whether diatom community composition can explain biogeographic patterns of prokaryotes. Both the total and potentially active prokaryotic community was considered with the aim to identify differences in their respective associations with diatoms. We explored this question in surface waters of the Indian sector of the Southern Ocean in early spring, when diatoms are the major contributor to phytoplankton biomass. We concurrently tested for the possible effects of geographic distance and environmental parameters, key factors identified in previous biogeographic studies of prokaryotic communities (see review by Hanson *et al.*, 2012).

Results

Environmental context

Our study was conducted over a large spatial distance (≈ 3000 km) in the Indian sector of the Southern Ocean, covering four oceanic zones, the subtropical zone (STZ), the subantarctic zone (SAZ), the polar front zone (PFZ) and the Antarctic zone (AAZ) (Table 1; Fig. 1). Gradients in environmental parameters, determined in seawater collected at 10 m, were particularly pronounced between the STZ and the SAZ, while overall minor variations within

Table 1. Brief description of the study sites.

Station	Date	Lat/Long	Temp (°C)	ΣN (μM)	PO_4^{3-} (μM)	Si(OH) ₄ (μM)	DOC (μM)	Chl a ($\mu g L^{-1}$)	PA ($\times 10^8 L^{-1}$)	Synecho ($\times 10^4 L^{-1}$)	PicoNano ($\times 10^6 L^{-1}$)	Diatoms ($\times 10^4 L^{-1}$)	Dinoflag ($\times 10^4 L^{-1}$)
Subtropical Zone													
O22	08 October 16	29.00°S 58.93°E	20.09	0.04	0.04	1.75	76	0.06	5.51	170.0	1.13	0.24	1.96
O24	10 October 16	38.00°S 63.65°E	14.60	2.91	0.21	2.37	62	0.29	7.64	3160.0	12.07	14.75	3.55
Subantarctic Zone													
O25	12 October 16	45.00°S 67.77°E	7.61	19.06	1.25	2.03	51	0.42	5.05	902.0	9.65	63.20	1.55
Polar Front Zone													
O12	25 October 16	47.00°S 72.22°E	4.60	25.42	1.68	7.72	50	0.39	6.02	134.0	4.79	14.52	3.44
TNS6	15 October 16	48.78°S 72.28°E	2.92	26.51	1.93	13.93	52	1.02	3.94	57.4	3.86	64.40	11.40
BDT	17 October 16	49.50°S 69.21°E	2.94	26.30	1.81	14.29	68	n.a.	4.46	47.7	6.74	1.51	0.19
Antarctic zone													
A3-1	18 October 16	50.63°S 72.06°E	2.19	28.21	1.85	19.48	52	1.44	3.66	19.5	2.88	150.70	5.40
A3-2	24 October 16	50.63°S 72.06°E	2.06	28.11	1.84	19.85	51	1.64	4.88	17.6	1.59	138.30	4.50
KER	18 October 16	50.68°S 68.38°E	2.38	28.23	1.97	18.41	51	0.32	2.89	15.6	5.37	13.52	3.88
FS	19 October 16	52.50°S 67.00°E	2.00	29.36	1.96	21.90	52	0.28	2.81	9.4	5.23	10.07	2.15
O11	20 October 16	56.50°S 63.00°E	1.00	29.90	2.01	30.95	46	0.27	2.30	3.4	4.00	13.72	1.62
SI	21 October 16	58.50°S 61.50°E	-1.12	29.27	1.87	35.89	48	0.22	1.88	b.d.	2.23	13.36	3.10

All values are from 10 m depth. ΣN = nitrate + nitrite; DOC, dissolved organic carbon; Chl a, chlorophyll a; PA, prokaryotic abundance; Synecho, Synchococcus; Pico-Nano, Pico-Nanophytoplankton; Dinoflag, Dinoflagellates; n.a., data not available; b.d., below detection. Salinity and concentrations of dissolved oxygen are provided in Supporting Information Table S1.

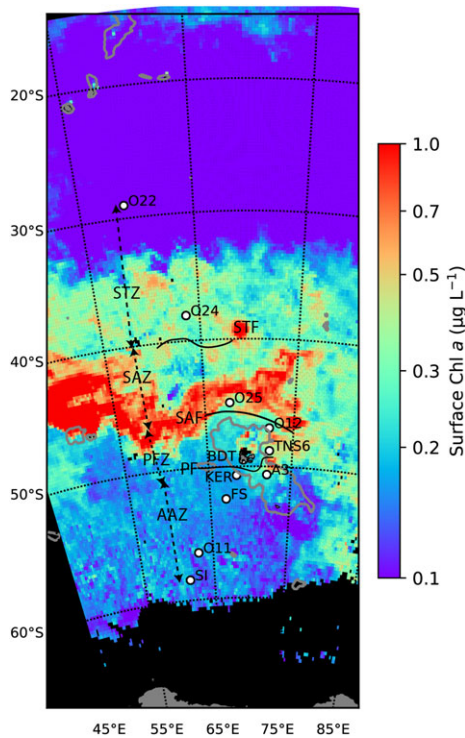


Fig. 1. Map of the study region of the Southern Ocean and Climate (SOCLIM) cruise (October 2016) with stations sampled for the present study indicated by white dots. Surface chlorophyll *a* is derived from ocean colour satellite images (COPERNICUS-GLOBECOLOR, October 2016, resolution 25 km). Dotted and full lines indicate ocean zones and fronts, respectively. STZ, Subtropical Zone; STF, Subtropical Front; SAZ, Subantarctic Zone; SAF, Subantarctic Front; PFZ, Polar Front Zone; PF, Polar Front; AAZ, Antarctic Zone.

surface waters of the PFZ and AAZ were detectable (see Supporting Information Table S1 for dissolved oxygen and salinity). Temperature decreased from 20.09°C in the STZ to −1.12°C at the southernmost station SI. Concentrations of DOC dropped from roughly 70 µM in the subtropical zone to 50 µM within and south of the SAZ. An opposite trend was observed for the major inorganic nutrients nitrate and nitrite, phosphate and silicic acid. Abundances of heterotrophic prokaryotes decreased by a factor of 3 from the STZ to the southernmost stations O11 and SI. The coastal site BDT (1 nautical mile from shore, 50 m overall depth) within a bay of Kerguelen Island was characterized by higher DOC concentrations and lower *Synechococcus* abundances, and much lower diatom abundances as compared to the stations located within the PFZ. Concentrations of chlorophyll *a* had no pronounced N to S gradient and highest concentrations were detectable above the Kerguelen plateau (stations A3-1 and A3-2), paralleled by the highest diatom abundances. Diatoms dominated in terms of abundance over dinoflagellates at all sampling sites except at station O22 in the STZ. Diatom carbon biomass accounted for 2%–14% of total phytoplankton biomass in

subtropical waters, while its contribution was on average 59% for all other stations (Rembauville *et al.*, 2017).

Diatom community composition

The composition of the diatom community, determined by microscopic observations, was significantly different among the four ocean zones (ANOSIM, $R = 0.78$, $P < 0.01$) based on Bray–Curtis dissimilarity. Samples originating from the SAZ (O25), the PFZ (O12 and TNS6) and the AAZ (A3, O11, KER, FS and SI) formed one main cluster, and samples originating from the STZ (O22 and O24) formed an independent branch, including the coastal site BDT (Fig. 2). Within the main group, separate clusters for the samples from the SAZ, the PFZ, station A3, located above the Kerguelen plateau, and the stations south of Kerguelen Island were detectable. Major diatoms in the STZ were small centric spp. (19%–67% of total diatom abundance), corresponding to an assemblage of diatoms <25 µm that could not be determined to the species level, and *Pseudonitzschia* spp. (8%–59%), while in the SAZ *Chaetoceros radicans* (51%) and *Chaetoceros socialis* (18%) dominated. In the PFZ *Thalassionema nitzschioides* (~32%), small centric spp. (9%–38%), *Fragilariopsis kerguelensis* (7%–22%) and *Eucampia antarctica* (2%–16%) were the main contributors to the diatom community (Fig. 2). These diatoms contributed also substantially to the community at station A3. However, the dominant species at this site was *Chaetoceros curvisetus*, accounting for 53% of total diatom abundance, followed by *Thalassionema nitzschioides* (22%–28%). In surface waters south of Kerguelen Island (O11, KER, FS and SI), *Fragilariopsis kerguelensis* contributed between 15% and 37% of total diatom abundance. *Pseudonitzschia* spp. (2%–31%), small centric spp. (3%–21%), *Chaetoceros curvisetus* (3%–18%), and *Thalassionema nitzschioides* (2%–10%) accounted for overall lower and more variable fractions of diatom abundance at these sites.

Composition of total and active prokaryotic communities

From the 12 stations, each sampled in biological triplicates, we obtained 36 subsamples for the total (DNA) and 36 subsamples for the active (RNA) prokaryotic community. From the total of 72 subsamples, we obtained 1326 operational taxonomic units (OTUs) defined at 97% similarity based on the 16S rRNA gene amplicon sequencing targeted on the V4–V5 region. A large number of OTUs (1217) were shared among the DNA and RNA data sets, with 1320 and 1323 OTUs obtained from the DNA and RNA samples, respectively. Unshared OTUs were not abundant in either the DNA or the RNA data set. nMDS ordination analysis showed that prokaryotic communities were significantly different among ocean zones (ANOSIM, $R = 0.69$, $P < 0.01$; Fig. 3). The three biological replicates

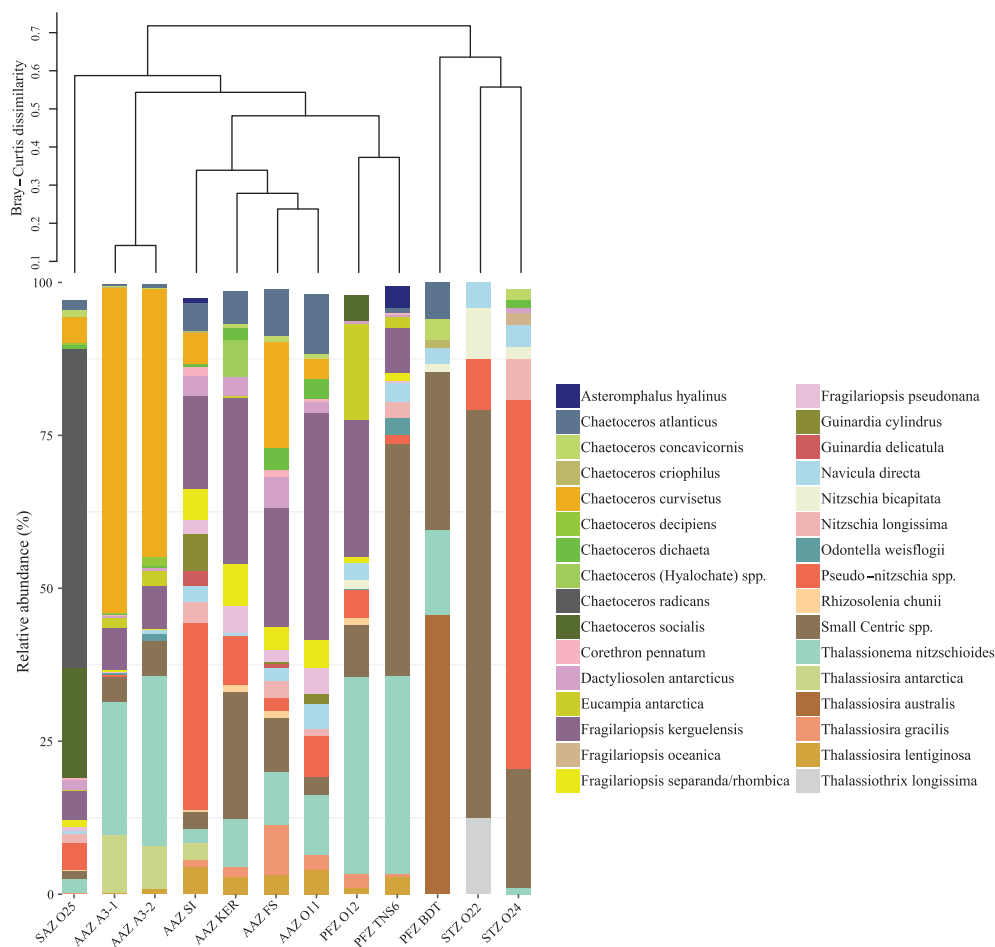


Fig. 2. Clustering of stations based on Bray–Curtis dissimilarity of the diatom community composition and relative abundances of diatom species. Diatom species with a relative abundance $\geq 1\%$ in at least one station are shown. Samples from the four ocean zones were significantly different (ANOSIM, $R = 0.78$, $P < 0.01$). STZ, Subtropical Zone; SAZ, Subantarctic Zone; PFZ, Polar Front Zone; AAZ, Antarctic Zone. Note: colour codes and associated names are ordered from top to bottom of each panel.

analysed from each station closely clustered together, illustrating the high replicability among samples for both DNA and RNA (Supporting Information Fig. S1). For the subsequent illustrations and analyses, the biological triplicates were pooled separately for the DNA and RNA data sets and the mean relative abundance was calculated for each OTU.

According to OTU abundances, sample assemblages were dominated by Alphaproteobacteria (DNA 42% of the sequences of all samples pooled, RNA 38%), Bacteroidetes (DNA 28%, RNA 34%), Gammaproteobacteria (DNA 18%, RNA 16%) and Cyanobacteria (DNA 9%, RNA 8%), with SAR11, Flavobacteria, Thiomicrospirales and Synechococcales as major sub-taxa respectively (Supporting Information Fig. S2). Deltaproteobacteria and Archaea were not abundant in surface waters (each $< 0.6\%$ of sequences pooled from all sites). Dominant OTUs (i.e. $\geq 1\%$ of the sequences in at least one sample) represented similar proportions of the total (DNA) and active (RNA) communities at a given site (Supporting

Information Fig. S2). For clarity, the following brief description is focused on DNA data. Within Alphaproteobacteria, SAR11 was the most abundant taxon, with two distinct OTUs belonging to SAR11 Ia being abundant (2%–16% of the sequences at a given site) either in the STZ or in the AAZ. Sphingomonadales were present in almost all samples. Within Gammaproteobacteria, one OTU belonging to Thiomicrospirales had high relative abundances in the SAZ, PFZ (except for BDT) and AAZ (3%–9%), and groups such as SAR86, Pseudomonadales and Alteromonadales revealed abundances $< 2\%$. Within Flavobacteria, two OTUs belonging to the NS2b marine group were abundant in the SAZ, PFZ (except for BDT) and AAZ (3%–12%), with highest relative abundances at station SI. Marine group NS9 was present with relatively high abundance at station A3-2 ($\sim 4\%$). SAR324 marine group belonging to Deltaproteobacteria represented 1%–2% of the reads at the AAZ stations, except for A3-2. Cyanobacteria had high abundances in the STZ and at station BDT,

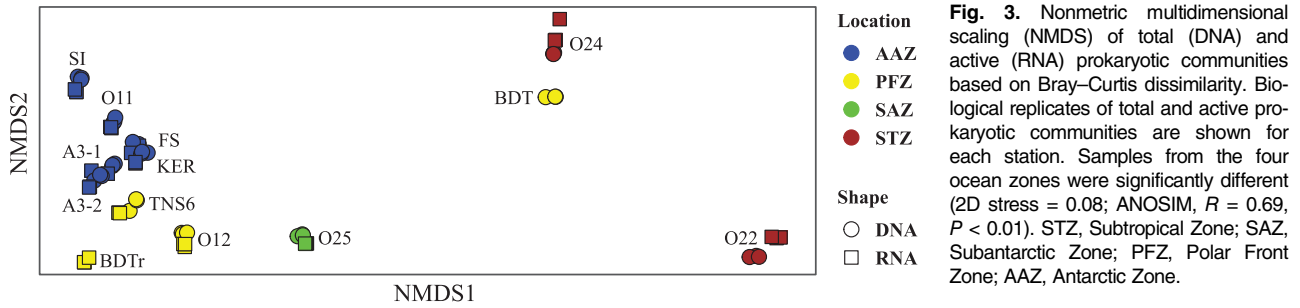


Fig. 3. Nonmetric multidimensional scaling (NMDS) of total (DNA) and active (RNA) prokaryotic communities based on Bray–Curtis dissimilarity. Biological replicates of total and active prokaryotic communities are shown for each station. Samples from the four ocean zones were significantly different (2D stress = 0.08; ANOSIM, $R = 0.69$, $P < 0.01$). STZ, Subtropical Zone; SAZ, Subantarctic Zone; PFZ, Polar Front Zone; AAZ, Antarctic Zone.

represented by *Synechococcus* and *Prochlorococcus*. Archaeal Thaumarchaeota varied between 0.5% and 1% at stations KER, FS, A3-1 and A3-2.

Linking prokaryotic and diatom community composition

To explore the question of whether prokaryotic community composition was linked to the diatom assemblages, we calculated the dissimilarity for each pair of samples of both prokaryotic and diatom communities. Based on the Mantel test, we observed significant relationships between changes in the diatom assemblages and in the total (DNA) (Fig. 4; $R = 0.55$; $P < 0.01$) and active (RNA; Supporting Information Fig. S3; $R = 0.55$; $P < 0.01$) prokaryotic communities for the Southern Ocean samples (SAZ, PFZ and AAZ; excluding BDT). This illustrates that the dissimilarity in the composition of each the total and active prokaryotic community increases with an increasing dissimilarity of the diatom assemblages. Significant relationships were also obtained for the entire data set, including the two stations in the STZ and station BDT (Supporting Information Fig. S4; $R = 0.78$, $P < 0.01$). We then tested the potential influence of geographic distance and environmental parameters. Geographic distance was not correlated to the changes in prokaryotic community composition (Mantel test, $P > 0.05$),

as shown by the lack of any significant distance decay relationship (Supporting Information Fig. S5). To determine the potential influence of environmental parameters, we performed a canonical correspondence analysis. For the Southern Ocean, temperature explained in part the separate clustering of the SAZ sample (Supporting Information Fig. S6; ANOVA, $P < 0.05$). For the entire data set, temperature, salinity and DOC explained the separate clustering of the samples from the STZ (Supporting Information Fig. S6; ANOVA, $P < 0.05$). We then applied the partial Mantel test to consider concurrently the influence of diatoms and geographic distance, and diatoms and environmental parameters on prokaryotic community composition (Table 2). Diatoms explained significantly the variance of the prokaryotic community composition, whereas geographic distance or environmental variables alone could not when the effect of diatoms on prokaryotic communities was controlled for (Table 2; overall $P < 0.05$). In addition, within the AAZ, the relationship between prokaryotic communities and geographic distance was not significant with and without controlling for the effect of diatoms ($P > 0.05$). Diatom community composition explained 30% of the variance in both the total and active Southern Ocean prokaryotic community composition. Including the two stations in the STZ and BDT, the respective variances explained 70%

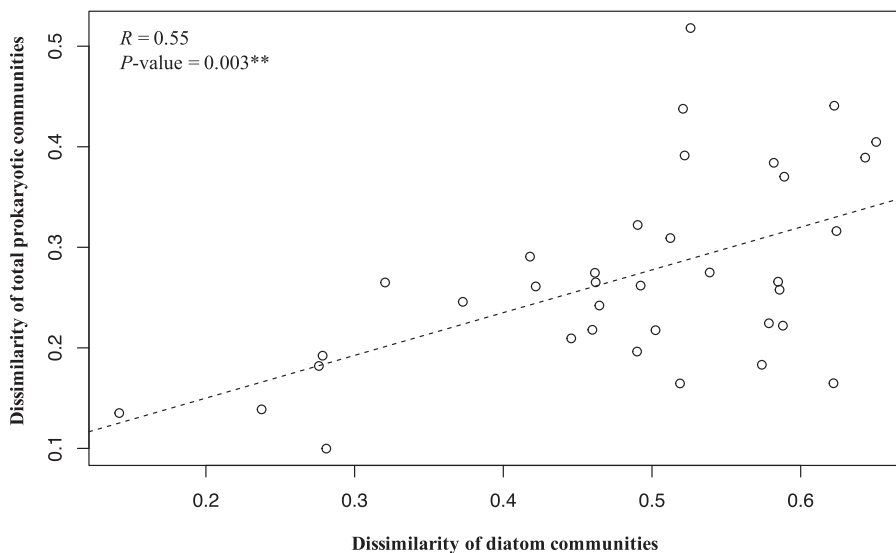


Fig. 4. Relationship between changes in the community composition of diatoms and of total prokaryotes for the Southern Ocean stations (SAZ, PFZ and AAZ excluding station BDT). Each point represents the Bray–Curtis dissimilarity between pairs of samples. The correlation coefficient was determined by the Mantel test. Dashed line denotes linear regression.

Table 2. Partial Mantel test for prokaryotic and diatom community composition and geographic distance (a) and combined environmental parameters (b) for Southern Ocean samples.

	Prokaryotes DNA	Diatoms		Prokaryotes RNA	Diatoms
(a)					
Diatoms	0.556**		Diatoms	0.551*	
Geographic distance	-0.089	0.167	Geographic distance	0.067	-0.105
(b)					
Diatoms	0.581**		Diatoms	0.540**	
Combined environmental parameters	-0.240	0.527**	Combined environmental parameters	-0.177	0.591**

The values shown in the tables are Rho values. Each value represents the correlation between two matrices while controlling for the effect of the third matrix.

** $P < 0.01$; * $P < 0.05$.

and 50% (Supporting Information Table S2). It was interesting to note that in contrast to prokaryotes, diatom community composition could be explained by the combined environmental parameters and in particular, salinity, dissolved oxygen, nitrate and nitrite (Supporting Information Table S2).

The potential relationships between dominant diatom species and prokaryotic OTUs were further investigated using co-occurrence analysis (Fig. 5). Diatom species and prokaryotic OTUs with $\geq 1\%$ relative abundance in at least one sample were considered. The correlation patterns were similar for total and active prokaryotic communities. The cluster analysis revealed several groups of diatoms, each associated with distinct prokaryotic assemblages. For the description of these groups, we focus on a few representative diatom species. *Fragilariopsis kerguelensis*, *Thalassionema nitzschooides* and *Chaetoceros curvisetus* were numerically abundant at several Southern Ocean sites (Fig. 2), and revealed strong positive correlations ($r \geq 0.6$) with distinct prokaryotic OTUs. *Fragilariopsis kerguelensis* was strongly positively correlated with several Flavobacteria OTUs belonging to groups NS5, NS9 and NS10. Positive correlations were also found with alphaproteobacterial OTUs belonging to the SAR11 I and SAR116 clades, and to Rhodobacterales, further with gammaproteobacterial OTUs belonging to Pseudomonadales, OM182 and SAR86, and to one OTU of the deltaproteobacterial SAR324 group. *Thalassionema nitzschooides* was positively correlated with Flavobacteria OTUs belonging to the NS4, NS7, NS9, *Polaribacter* and *Ulvibacter* groups, several Rhodobacterales OTUs as well as SAR11 lb. *Chaetoceros curvisetus*, a diatom that accounted for 53% of the diatom abundance at station A3 above the plateau revealed strong correlations with Flavobacteria OTUs exclusively belonging to the NS9 group, one OTU belonging to the gamma-proteobacterial Thiomicrospirales, and one OTU belonging to Thaumarchaeota. For comparison, *Chaetoceros radicans* and *Chaetoceros socialis*, dominant diatom species in the SAZ, revealed strong correlations to a distinct set of OTUs belonging to Flavobacteria groups NS2b, NS10 and NS4, to one OTU belonging each to Rhodobacterales, SAR11,

SAR86 and Thiomicrospirales. Small centric spp. and *Pseudo-nitzschia* spp., diatoms with overall higher relative abundances in subtropical waters were again associated with distinct OTUs belonging to all major groups. In addition, several strong ($r \geq 0.6$) positive correlations between Cyanobacterial OTUs and diatoms abundant in the STZ and at BDT were detectable.

Discussion

Contemporary environmental selection has widely been identified as one central mechanism for shaping the spatial distribution of heterotrophic microbes in the ocean (reviewed in Hanson *et al.*, 2012). Dispersal and drift are additional factors that were identified in biogeographic studies (Lindström and Langenheder, 2012; Wilkins *et al.*, 2013). In contrast, the potential influence of the community composition of microorganisms that can interact with heterotrophic microbes has only recently been taken into consideration in this context (Lima-Mendez *et al.*, 2015; Milici *et al.*, 2016; Zhou *et al.*, 2018). The present study reveals that the spatial pattern in the community structure of heterotrophic microbes in surface waters is tightly associated with changes in the diatom assemblages, rather than to geographic distance and environmental conditions. Our survey covers the major oceanographic zones of the Southern Ocean where diatoms are dominant components of the autotrophic community and our results illustrate their potential role in shaping microbial diversity in surface waters of this part of the ocean.

The key diatom species that we identified, based on their high relative abundances at several sites, could be indicative for two broad ecological niches in the Southern Ocean. *Fragilariopsis kerguelensis*, a chain forming, heavily silicified pennate diatom with overall low growth rates is typically associated with high-nutrient-low-chlorophyll (HNLC) systems (Smetacek *et al.*, 2004; Quéguiner, 2013). In contrast, small diatoms ($< 25 \mu\text{m}$), such as *Chaetoceros* spp., *Thalassionema nitzschooides* and *Thalassiosira* spp. are more lightly silicified and known to

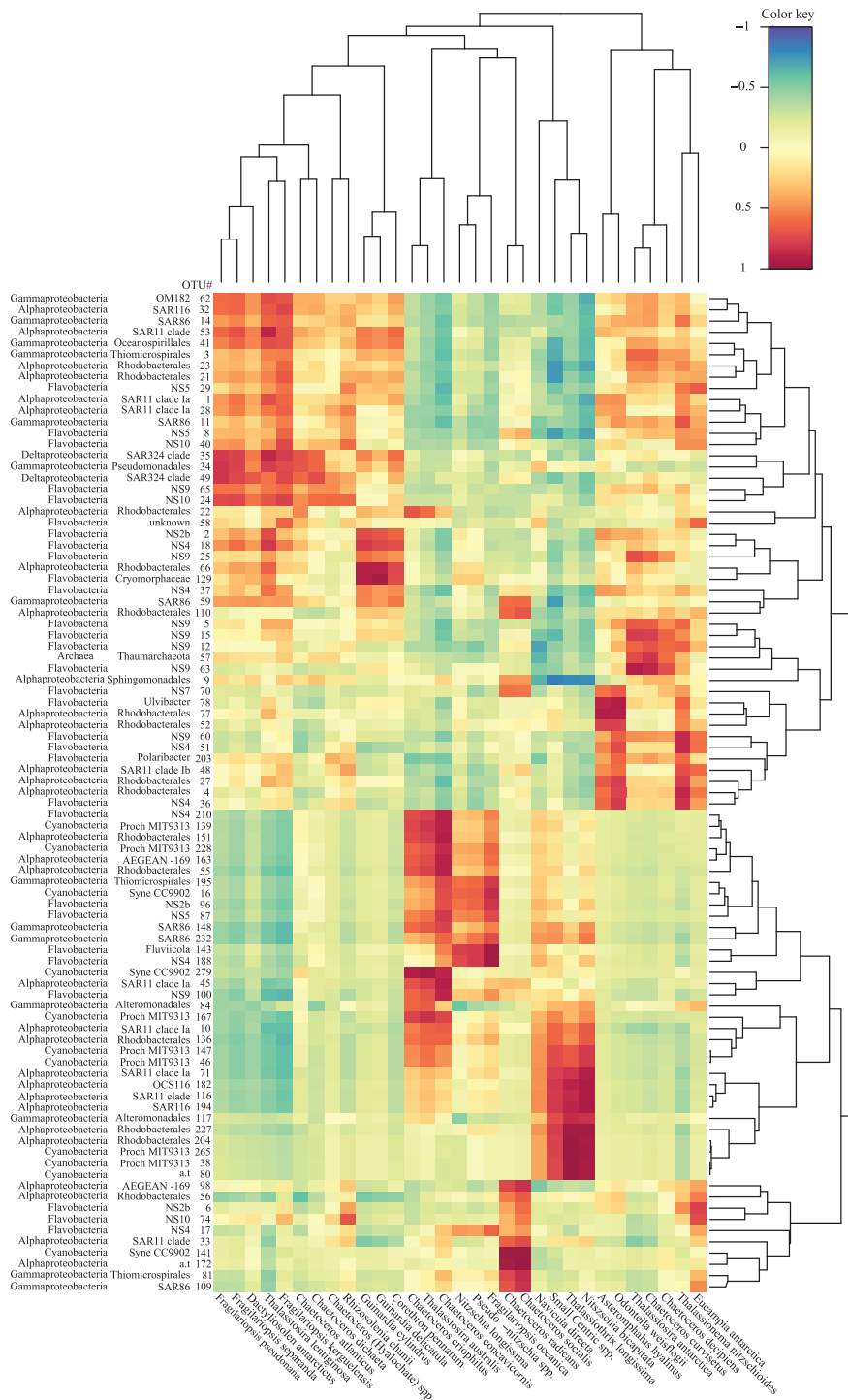


Fig. 5. Heatmap of correlations between dominant diatom species and prokaryotic OTUs from total communities based on Pearson correlations. Diatom species and prokaryotic OTUs with $\geq 1\%$ relative abundance in at least one sample are shown. Colour key: Red and blue colours represent positive and negative correlations, respectively. a.t. = ambiguous taxa.

develop rapidly under favourable conditions, such as in response to iron supply by natural fertilization in the region east of Kerguelen Island (Blain *et al.*, 2007; Lasbleiz *et al.*, 2016) or to mesoscale artificial iron additions (Assmy *et al.*, 2013). *Fragilariopsis kerguelensis* was associated to several OTUs of the SAR11 la and SAR116 clades and OTUs belonging to OM182 and SAR86, groups that were

previously characterized as oligotrophs to be adapted to conditions of low resource supply (Sowell *et al.*, 2009; Yooseph *et al.*, 2010; Swan *et al.*, 2013). Noticeably strong correlations were also found for deltaproteobacterial SAR324 OTUs. Members of this group are chemolithotrophic (Swan *et al.*, 2011; Sheik *et al.*, 2014) and thus likely better adapted to oligotrophic conditions. In contrast,

Thalassionema nitzschooides and *Chaetoceros curvisetus* had strong correlations with OTUs that were previously identified as rapid responders to phytoplankton blooms, as for example the flavobacterial OTUs *Polaribacter*, *Ulvibacter* and OTUs from the NS7 group (Buchan *et al.*, 2014). Among these, *Polaribacter* has frequently been observed in temperate (Teeling *et al.*, 2012; Klindworth *et al.*, 2014; Needham and Fuhrman, 2016) and polar regions under bloom conditions (Williams *et al.*, 2013; Delmont *et al.*, 2014; Luria *et al.*, 2016; Dadaglio *et al.*, 2018) and in response to labile organic matter supply (Dinasquet *et al.*, 2017; Luria *et al.*, 2017; Tada *et al.*, 2017). Similarly, *Rhodobacterales* had a higher number of strong positive correlations with *Thalassionema nitzschooides* and *Chaetoceros curvisetus* than with *Fragilariopsis kerguelensis*. The rapid response of the above mentioned OTUs to phytoplankton blooms has been attributed to their uptake capacities of specific phytoplankton-derived substrates, using functional profiling based on metatranscriptomics (Rinta-Kanto *et al.*, 2012; Teeling *et al.*, 2012; Beier *et al.*, 2015) and meta-proteomics (Li *et al.*, 2018).

We expected the composition of total and active prokaryotes to be different, but the spatial distribution and the co-occurrence patterns revealed to be highly similar between these communities. The use of RNA-based approaches to distinguish the active microbial community members from inactive or dormant ones is based on the relationship between cellular content of ribosomal RNA (rRNA) and metabolic activity (Kerkhof and Ward, 1993; Poulsen *et al.*, 1993). Several limitations were pointed out (Blazewicz *et al.*, 2013), including differences in the relationship between rRNA content and growth rate among taxa, and the possibly high rRNA content of dormant and inactive cells (Flårdh *et al.*, 1992; Fegatella *et al.*, 1998). Previous investigations in the study region have shown that bulk prokaryotic production and growth rates in early spring are substantially lower as compared to mid-summer, in particular at bloom sites (Christaki *et al.*, 2014). In contrast to the present study, total and active prokaryotic communities were different from each other in summer, both within the phytoplankton bloom above the Kerguelen plateau (Station A3) and in HNLC waters (West *et al.*, 2008). These observations suggest that while prokaryotes are stimulated by phytoplankton growth in early spring, our approach does not allow to differentiate the active community members from those potentially inactive or dormant (Lennon and Jones, 2011).

Our observation that key diatom species are each associated with several distinct prokaryotic taxa raises the question on the underlying mechanisms. While the exact processes are not tractable with the present data set, we provide a possible scenario. In contrast to heterotrophic prokaryotes, the spatial distribution of diatoms was significantly correlated to some environmental parameters. Because our study took

place in early spring when the effect of phytoplankton activity on inorganic nutrient drawdown is minor, this result suggests that environmental parameters are drivers of diatom assemblages and that diatoms may be setting the pace for the observed spatial changes in prokaryotic community composition. Previous field studies and satellite observations have indicated that the onset of spring phytoplankton blooms occurring in the region off Kerguelen Island can differ by several weeks (Sallée *et al.*, 2015). Considering each site independently, the varying contributions of the most abundant diatom species could represent different stages of the spring phytoplankton development at a given location with potential consequences on the prokaryotic community composition. The qualitative and quantitative differences in the DOM produced by the various diatoms are likely to present an important selection process (Landa *et al.*, 2016; Samento *et al.*, 2016).

The pronounced association between assemblages of diatoms and heterotrophic microbes observed in the present study could be driven by two particular features of the Southern Ocean that are the growth-limiting concentrations of bioavailable iron and organic carbon in surface waters. Iron availability controls autotrophic and heterotrophic metabolism, but the lack of bioavailable organic carbon represents an additional constraint for heterotrophic microbes (Church *et al.*, 2000; Obernosterer *et al.*, 2015). In early spring, autotrophic plankton outcompetes heterotrophs for access to iron (Fourquez *et al.*, 2015). Thus, diatom-derived organic matter is key in driving both heterotrophic microbial activity and diversity in this ocean region (Arrieta *et al.*, 2004; Obernosterer *et al.*, 2008; Landa *et al.*, 2016; Luria *et al.*, 2016). The spatial distribution of the diatom assemblages as observed in the present study in early spring likely reflects their respective ecological niches driven by the light-nutrient regime, including iron availability. Our results let us conclude that diatom assemblages shape the habitat type for heterotrophic microbes and thereby directly influence their community composition.

Experimental procedures

Study area and sampling strategy

The present study was performed during the Southern Ocean and Climate (SOCLIM) cruise (doi: 10.17600/16003300) aboard the *R/V Marion Dufresne* (08 October – 1 November 2016). The 12 stations sampled for the present study were located in four oceanographic zones, the subtropical zone (STZ), the subantarctic zone (SAZ), the polar front zone (PFZ) and the Antarctic zone (AAZ; Fig. 1; Table 1). In the AAZ, station A3, located above the Kerguelen plateau, was visited twice during the sampling period (stations A3-1 and A3-2). Station BDT (Baie de la Table) is a

coastal site (50 m overall depth) within a bay of Kerguelen Island. All environmental data and the samples for the diatom community composition were collected at 10 m with 12 l Niskin bottles mounted on a rosette equipped with a conductivity–temperature–depth (CTD, Seabird SBE9+) sensor. Seawater samples for microbial diversity analyses were taken from the underway seawater supply system that collected water at 5 m depth.

The sampling, storage and analyses of common environmental parameters were done according to previously described protocols. The major inorganic nutrients nitrite (NO_2^-), nitrate (NO_3^-), phosphate (PO_4^{3-}) and silicic acid ($\text{Si}(\text{OH})_4$) were determined using continuous flow analysis with a Skalar instrument (Aminot and K erouel, 2007; Blain *et al.*, 2014). Dissolved organic carbon (DOC) concentrations were determined by high-temperature oxidation on a Shimadzu TOC-VCP analyser (Benner and Strom, 1993; Obernosterer *et al.*, 2015). Concentrations of chlorophyll *a* (Chl *a*) were determined by High-Performance Liquid Chromatography (HPLC) analyses (Uitz *et al.*, 2009). The abundance of heterotrophic and autotrophic prokaryotes and pico- and nanoeukaryotes was done by flow cytometric analyses on a BD FACS Canto (Marie *et al.*, 2000; Obernosterer *et al.*, 2008). For the identification and enumeration of the diatom and dinoflagellate assemblages, 100 ml of seawater were fixed with Lugol solution (1% final concentration) and stored in the dark at 4 °C for 2 months. Observations were done in an Uterm ohl counting chamber (24 h, dark) using an inverted microscope with phase contrast (Olympus IX70) with 400× magnification as described in Rembauville *et al.* (2017).

For the analyses of the prokaryotic community composition, three 6 L biological replicates were collected at each site, filtered on 60 µm nylon screens, and then through 0.8 µm polycarbonate filters (47-mm diameter, Nuclepore, Whatman, Sigma Aldrich, St Louis, MO). Cells were then concentrated on 0.2 µm Sterivex filter units (Sterivex, Millipore, EMD, Billerica, MA) using a peristaltic pumping system (Masterflex L/S Easy-Load II). The Sterivex filter units were kept at –80°C until extraction.

DNA and RNA extraction and sequencing preparation

DNA and RNA were simultaneously extracted from one Sterivex filter unit using the AllPrep DNA /RNA kit (Qiagen, Hiden, Germany) with the following modifications. Filter units were thawed and closed with a sterile pipette tip end at the outflow. Lysis buffer was added (40 mM EDTA, 50 mM Tris, 0.75 M sucrose) and 3 freeze and thaw cycles were performed using liquid nitrogen and a water bath at 65°C. Lysozyme solution (0.2 mg ml⁻¹ final concentration) was added and filter units were placed on a

rotary mixer at 37°C for 45 min. Proteinase K (0.2 mg ml⁻¹ final concentration) and SDS (1% final concentration) were added and filter units were incubated at 55°C with gentle agitation every 10 min for 1 h. To protect the RNA, 10 µl of β-mercaptoethanol was added to 1 ml of RLT plus buffer provided by the kit. To each filter unit, 1550 µl RLT plus β-mercaptoethanol was added and inverted to mix. The lysate was recovered by using a sterile 5 ml syringe and loaded in three additions onto the DNA columns by centrifuging at 10 000g for 30 s. DNA and RNA purifications were performed following the manufacturer's guidelines (Qiagen, Germany) in which RNA was treated with DNase to avoid DNA contamination after the first wash step.

RNA was converted to cDNA using SuperScript III Reverse Transcriptase according to the manufacturer's instructions. Prior to reverse transcription, quality of RNA samples was examined by PCR test with general primer sets 341F (5'-CCTACGGGNGGCWGCAG) and 805R (5'-GACTACHVGGGTATCTAATCC) for the prokaryotic 16S rRNA gene, followed by the examination of amplification products on 1% agarose electrophoresis. Based on the results of the PCR test, DNase was performed once more on the RNA extracts of those samples with contaminating DNA left, to completely remove the residual DNA. DNA and cDNA were amplified and pooled as described in Parada *et al.* (2016) with a modification to the PCR amplification step. Briefly, the V4–V5 region of the 16S rRNA gene from DNA and cDNA samples was amplified with the primer sets 515F-Y (5'-GTGYCAGCMG CCGCGGTAA) and 926R (5'-CCGYCAATTYMTTTRAG TTT). Triplicate 10 µl reaction mixtures contained 2 µg DNA, 5 µl KAPA2G Fast HotStart ReadyMix, 0.2 µM forward primer and 0.2 µM reverse primer. Cycling reaction started with a 3 min heating step at 95°C followed by 22 cycles of 95°C for 45 s, 50°C for 45 s, 68°C for 90 s, and a final extension of 68°C for 5 min. The presence of amplification products was confirmed by 1% agarose electrophoresis and triplicate reactions were pooled. Each sample was added with unique paired barcodes. The Master 25 µl mixtures contained 1 µl PCR product, 12.5 µl KAPA2G Fast HotStart ReadyMix (Kapa Biosystems, Wilmington, MA), 0.5 µl barcode 1 and 0.5 µl barcode 2. The cycling program included a 30 s initial denaturation at 98°C followed by 8 cycles of 98°C for 10 s, 60°C for 20 s, 72°C for 30 s, and a final extension of 72°C for 2 min. About 3 µl PCR product was used to check for amplification on 1% agarose electrophoresis. The remaining 22 µl barcoded amplicon product was cleaned to remove unwanted dNTPs and primers by Exonuclease I and Shrimp Alkaline Phosphatase at 37°C, 30 min for treatment and 85°C, 15 min to inactivate. The concentration of double-stranded DNA was quantified by PicoGreen fluorescence assay (Life Technologies, Carlsbad, CA). After calculating the PCR product concentration of

each samples, they were pooled at equal concentrations manually. The pooled PCR amplicons were concentrated using Wizard SV gel and PCR clean-up system (Promega, Fitchburg, WI) according to the manufacturer's protocol. 16S rRNA gene amplicons were sequenced with Illumina MiSeq 2 × 300 bp chemistry on one flow-cell at Fasteris SA sequencing service (Switzerland). Mock community DNA (LGC standards, UK) was used as a standard for subsequent analyses and considered as a DNA sample for all treatments.

Data analysis

All samples from the same sequencing run have been demultiplexed by Fasteris SA and barcodes have been trimmed off. A total number of 4 150 902 sequences was obtained. Processing of sequences was performed using the Usearch pipeline (Edgar, 2013). Paired-end reads were merged using *fastq-mergepairs*. The positions of primers were checked using *search_oligodb* and *fastx_subsample* were used to subset a portion of all sequences to check (e.g. 5000 sequences). Primers were trimmed and merged reads in range of length from 336 to 486 were kept using *fastq-filter* based on maximum expected error (Needham and Fuhrman, 2016). In total, 2 000 219 sequences were kept after quality filtering. Data were denoised and chimera were identified and removed using *unoise3* with a *minsize* 10 according to mock community DNA (Edgar, 2016). During this step, singletons were discarded. Sequences were clustered using *usearch_global* and defined as OTUs at a 97% sequence similarity level. OTUs were assigned using *assign_taxonomy.py* against SILVA release 132 database (Quast et al., 2012). Sequences assigned to chloroplast were removed prior to subsequent analyses.

Statistical analyses

All statistical analyses were performed using R 3.4.2 version. The OTU and taxa tables were combined into one object using *phyloseq* R package.

Data were Hellinger transformed prior to the analyses based on Bray–Curtis dissimilarity (Legendre and Gallagher, 2001). Bray–Curtis dissimilarity matrices were generated via *vegdist()* function. Nonmetric dimensional scaling (NMDS) ordinations were generated based on Bray–Curtis dissimilarity using *monoMDS()* function in the package *Vegan* (Oksanen et al., 2015). Analysis of similarity (ANOSIM) was performed to test significant differences between sampling zones in microbial communities with R. Dendrograms were performed using *hclust()* with method 'average' in the *Vegan* package.

Mantel and partial Mantel tests were performed in *Vegan* using *mantel()* and *mantel.partial()* based on the Pearson correlation method. The linear model was applied

for the relationship between prokaryotic communities versus diatom communities in R. Geographical coordinates were transformed using the Haversine formula (Sinnott, 1984). Prior to correlation analysis, environmental variables were z-score transformed. The amount of variance in prokaryotic community composition explained by diatoms was estimated as the square of the correlation coefficient (Rho^2) based on partial Mantel test.

Sequences alignment was carried out using MAFFT algorithm web services by defaults (Kato et al., 2017). The phylogenetic tree was constructed using PhyML 3.0 online programs based on maximum likelihood method and 100 bootstraps with HKY85 substitution model (Guindon and Gascuel, 2003). The tree was visualized with SeaView version 4.7 and saved as rooted tree. Heat maps were generated using *heatmap3* package and rows were reordered corresponding to phylogenetic tree. The correlation heatmaps were generated using *spls()* and *cim()* in the *mixOmics* package with log-transformed data (Chun and Keleş, 2010; Rohart et al., 2017).

Canonical correspondence analysis was performed using *cca()* in *Vegan* package with z-score transformed data. The significance of environmental parameters was tested with an analysis of variance (ANOVA) using *Vegan* package in R.

Acknowledgements

We thank the captain and the crew of the *R/V Marion Dufresne* for their support aboard. We thank Olivier Crispi for sampling and analyses of inorganic nutrients, Jocelyne Caparros for the analyses of dissolved organic carbon and Philippe Catala for flow cytometry analyses. Chlorophyll a concentrations were determined by HPLC analyses at the SAPIGH analytical platform at IMEV, Villefranche-sur-Mer, by Josefina Ras and Celine Dimier. The detailed comments from two anonymous reviewers helped improve previous versions of the manuscript. The project SOCLIM (Southern Ocean and Climate) is supported by the Climate Initiative of the BNP Paribas Foundation, the French Polar Institute (Institut Polaire Emile Victor), and the French program LEFE-CYBER of the CNRS-INSU. This work is part of the PhD thesis of Y.L. supported by the China Scholarship Council (CSC; NO. 201606330072).

Conflict of interest

The authors declare no conflict of interest.

Accession numbers

Demultiplexed sequence files are available in NCBI under accession number PRJNA494099.

References

- Amin, S.A., Green, D.H., Hart, M.C., Kupper, F.C., Sunda, W. G., and Carrano, C.J. (2009) Photolysis of iron-siderophore chelates promotes bacterial–algal mutualism. *Proc Natl Acad Sci USA* **106**: 17071–17076.
- Amin, S.A., Parker, M.S., and Armbrust, E.V. (2012) Interactions between diatoms and bacteria. *Microbiol Mol Biol Rev* **76**: 667–684.
- Amin, S.A., Hmelo, L.R., van Tol, H.M., Durham, B.P., Carlson, L.T., Heal, K.R., *et al.* (2015) Interaction and signalling between a cosmopolitan phytoplankton and associated bacteria. *Nature* **522**: 98–101.
- Aminot, A., and Kérouel, R. (2007) *Dosage automatique des nutriments dans les eaux marines: méthodes en flux continu*. Versailles, France: Editions Quae.
- Arrieta, J.M., Weinbauer, M.G., Lute, C., and Herndl, G.J. (2004) Response of bacterioplankton to iron fertilization in the Southern Ocean. *Limnol Oceanogr* **49**: 799–808.
- Assmy, P., Smetacek, V., Montresor, M., Klaas, C., Henjes, J., Strass, V.H., *et al.* (2013) Thick-shelled, grazer-protected diatoms decouple ocean carbon and silicon cycles in the iron-limited Antarctic circumpolar current. *Proc Natl Acad Sci USA* **110**: 20633–20638.
- Beier, S., Rivers, A.R., Moran, M.A., and Obernosterer, I. (2015) The transcriptional response of prokaryotes to phytoplankton-derived dissolved organic matter in seawater: the response of prokaryotes to DOM in seawater. *Environ Microbiol* **17**: 3466–3480.
- Benner, R., and Strom, M. (1993) A critical evaluation of the analytical blank associated with DOC measurements by high-temperature catalytic oxidation. *Marine Chemistry* **41**: 153–160.
- Biddanda, B., and Benner, R. (1997) Major contribution from mesopelagic plankton to heterotrophic metabolism in the upper ocean. *Deep Sea Res I Oceanogr Res Pap* **14**: 2069–2085.
- Blain, S., Quéguiner, B., Armand, L., Belviso, S., Bombled, B., Bopp, L., *et al.* (2007) Effect of natural iron fertilization on carbon sequestration in the Southern Ocean. *Nature* **446**: 1070–1074.
- Blain, S., Capparos, J., Guéneuguès, A., Obernosterer, I., and Oriol, L. (2014) Distributions and stoichiometry of dissolved nitrogen and phosphorus in the iron fertilized region near Kerguelen (Southern Ocean). *Biogeosci Discuss* **11**: 9949–9977.
- Blazewicz, S.J., Barnard, R.L., Daly, R.A., and Firestone, M. K. (2013) Evaluating rRNA as an indicator of microbial activity in environmental communities: limitations and uses. *ISME J* **7**: 2061–2068.
- Buchan, A., LeClerc, G.R., Gulvik, C.A., and González, J.M. (2014) Master recyclers: features and functions of bacteria associated with phytoplankton blooms. *Nat Rev Microbiol* **12**: 686–698.
- Bunse, C., and Pinhassi, J. (2017) Marine bacterioplankton seasonal succession dynamics. *Trends Microbiol* **25**: 494–505.
- Christaki, U., Lefèvre, D., Georges, C., Colombet, J., Catala, P., Courties, C., *et al.* (2014) Microbial food web dynamics during spring phytoplankton blooms in the naturally iron-fertilized Kerguelen area (Southern Ocean). *Biogeosciences* **11**: 6739–6753.
- Chun, H., and Keleş, S. (2010) Sparse partial least squares regression for simultaneous dimension reduction and variable selection. *J Roy Stat Society: Series B (Stat Met)* **72**: 3–25.
- Church, M.J., Hutchins, D.A., and Ducklow, H.W. (2000) Limitation of bacterial growth by dissolved organic matter and iron in the Southern Ocean. *Appl Environ Microb* **66**: 455–466.
- Ciais, P., Sabine, C., Bala, G., Bopp, L., Brovkin, V., Canadell, J., *et al.* (2014) Carbon and other biogeochemical cycles. In *Climate Change 2013: The Physical Science Basis. Contribution of Working Group I to the Fifth Assessment Report of the Intergovernmental Panel on Climate Change*, Stocker, T.F., Qin, D., Plattner, G.-K., Tignor, M., Allen, S.K., Boschung, J., *et al.* (eds). Cambridge: Cambridge University Press, pp. 465–570.
- Dadaglio, L., Dinasquet, J., Obernosterer, I., and Joux, F. (2018) Differential responses of bacteria to diatom-derived dissolved organic matter in the Arctic Ocean. *Aquat Microb Ecol* **82**: 59–72.
- Delmont, T.O., Hammar, K.M., Ducklow, H.W., Yager, P.L., and Post, A.F. (2014) *Phaeocystis Antarctica* blooms strongly influence bacterial community structures in the Amundsen Sea polynya. *Front Microbiol* **5**: 646.
- Dinasquet, J., Richert, I., Logares, R., Yager, P., Bertilsson, S., and Riemann, L. (2017) Mixing of water masses caused by a drifting iceberg affects bacterial activity, community composition and substrate utilization capability in the Southern Ocean: iceberg influence on bacterioplankton. *Environ Microbiol* **19**: 2453–2467.
- Ducklow, H.W., Fraser, W., Karl, D.M., Quetin, L.B., Ross, R.M., Smith, R.C., *et al.* (2006) Water-column processes in the West Antarctic peninsula and the Ross Sea: interannual variations and foodweb structure. *Deep Sea Res Part 2 Top Stud Oceanogr* **53**: 834–852.
- Durham, B.P., Sharma, S., Luo, H., Smith, C.B., Amin, S.A., Bender, S.J., *et al.* (2015) Cryptic carbon and sulfur cycling between surface ocean plankton. *Proc Natl Acad Sci USA* **112**: 453–457.
- Edgar, R.C. (2013) UPARSE: highly accurate OTU sequences from microbial amplicon reads. *Nat Methods* **10**: 996–998.
- Edgar, R.C. (2016) UNOISE2: improved error-correction for Illumina 16S and ITS amplicon sequencing. *BioRxiv* **1**: 081257.
- Fegatella, F., Lim, J., Kjelleberg, S., and Cavicchioli, R. (1998) Implications of rRNA operon copy number and ribosome content in the marine oligotrophic Ultramicrobacterium *Sphingomonas* sp. strain RB2256. *Appl Environ Microb* **64**: 6.
- Flårth, K., Cohen, P.S., and Kjelleberg, S. (1992) Ribosomes exist in large excess over the apparent demand for protein synthesis during carbon starvation in marine *Vibrio* sp. strain CCUG 15956. *J Bacteriol* **174**: 6780–6788.
- Fourquez, M., Obernosterer, I., Davies, D.M., Trull, T.W., and Blain, S. (2015) Microbial iron uptake in the naturally fertilized waters in the vicinity of the Kerguelen Islands: phytoplankton–bacteria interactions. *Biogeosciences* **12**: 1893–1906.
- Gilbert, J.A., Steele, J.A., Caporaso, J.G., Steinbrück, L., Reeder, J., Temperton, B., *et al.* (2012) Defining seasonal marine microbial community dynamics. *ISME J* **6**: 298–308.

- Guindon, S., and Gascuel, O. (2003) A simple, fast, and accurate algorithm to estimate large phylogenies by maximum likelihood. *Syst Biol* **52**: 696–704.
- Hanson, C.A., Fuhrman, J.A., Horner-Devine, M.C., and Martiny, J.B.H. (2012) Beyond biogeographic patterns: processes shaping the microbial landscape. *Nat Rev Microbiol* **10**: 497–506.
- Johnson, W.M., Kido Soule, M.C., and Kujawinski, E.B. (2016) Evidence for quorum sensing and differential metabolite production by a marine bacterium in response to DMSP. *ISME J* **10**: 2304–2316.
- Katoh, K., Rozewicki, J., and Yamada, K.D. (2017) MAFFT online service: multiple sequence alignment, interactive sequence choice and visualization. *Brief Bioinform*: bbx108.
- Kerkhof, L., and Ward, B.B. (1993) Comparison of nucleic acid hybridization and fluorometry for measurement of the relationship between RNA/DNA ratio and growth rate in a marine bacterium. *Appl Environ Microbiol* **59**: 7.
- Klindworth, A., Mann, A.J., Huang, S., Wichels, A., Quast, C., Waldmann, J., et al. (2014) Diversity and activity of marine bacterioplankton during a diatom bloom in the North Sea assessed by total RNA and pyrotag sequencing. *Mar Genomics* **18**: 185–192.
- Landa, M., Blain, S., Christaki, U., Monchy, S., and Obernosterer, I. (2016) Shifts in bacterial community composition associated with increased carbon cycling in a mosaic of phytoplankton blooms. *ISME J* **10**: 39–50.
- Lasbleiz, M., Leblanc, K., Armand, L.K., Christaki, U., Georges, C., Obernosterer, I., and Quéguiner, B. (2016) Composition of diatom communities and their contribution to plankton biomass in the naturally iron-fertilized region of Kerguelen in the Southern Ocean. *FEMS Microbiol Ecol* **92**: fiw171.
- Legendre, P., and Gallagher, E. (2001) Ecologically meaningful transformations for ordination of species data. *Oecologia* **129**: 271–280.
- Lennon, J.T., and Jones, S.E. (2011) Microbial seed banks: the ecological and evolutionary implications of dormancy. *Nat Rev Microbiol* **9**: 119–130.
- Li, D.-X., Zhang, H., Chen, X.-H., Xie, Z.-X., Zhang, Y., Zhang, S.-F., et al. (2018) Metaproteomics reveals major microbial players and their metabolic activities during the blooming period of a marine dinoflagellate *Prorocentrum donghaiense*: microbial metaproteome during a dinoflagellate bloom. *Environ Microbiol* **20**: 632–644.
- Lima-Mendez, G., Faust, K., Henry, N., Decelle, J., Colin, S., Carcillo, F., et al. (2015) Determinants of community structure in the global plankton interactome. *Science* **348**: 1262073.
- Lindström, E.S., and Langenheder, S. (2012) Local and regional factors influencing bacterial community assembly: bacterial community assembly. *Environ Microbiol Rep* **4**: 1–9.
- Luria, C.M., Amaral-Zettler, L.A., Ducklow, H.W., and Rich, J.J. (2016) Seasonal succession of free-living bacterial communities in coastal waters of the Western Antarctic Peninsula. *Front Microbiol* **7**: 1731.
- Luria, C.M., Amaral-Zettler, L.A., Ducklow, H.W., Repeta, D. J., Rhyne, A.L., and Rich, J.J. (2017) Seasonal shifts in bacterial community responses to phytoplankton-derived dissolved organic matter in the Western Antarctic Peninsula. *Front Microbiol* **8**: 2117.
- Malviya, S., Scalco, E., Audic, S., Vincent, F., Veluchamy, A., Poulain, J., et al. (2016) Insights into global diatom distribution and diversity in the world's ocean. *Proc Natl Acad Sci USA* **113**: E1516–E1525.
- Marie, D., Simon, N., Guillon, L., Partensky, F., and Vaultot, D. (2000) Flow cytometry analysis of marine picoplankton. In *Living Color: Protocols in Flow Cytometry and Cell Sorting*, Maggio, D. (ed). Berlin, Heidelberg: Springer, pp. 421–454.
- Milici, M., Deng, Z.-L., Tomasch, J., Decelle, J., Wos-Oxley, M. L., Wang, H., et al. (2016) Co-occurrence analysis of microbial taxa in the Atlantic Ocean reveals high connectivity in the free-living bacterioplankton. *Front Microbiol* **7**: 649.
- Mykkestad, S.M. (2000) Dissolved organic carbon from phytoplankton. In *Marine Chemistry*, Wangersky, P.J. (ed). Berlin, Heidelberg: Springer, pp. 111–148.
- Needham, D.M., and Fuhrman, J.A. (2016) Pronounced daily succession of phytoplankton, archaea and bacteria following a spring bloom. *Nat Microbiol* **1**: 16005.
- Obernosterer, I., Christaki, U., Lefèvre, D., Catala, P., Van Wambeke, F., and Lebaron, P. (2008) Rapid bacterial mineralization of organic carbon produced during a phytoplankton bloom induced by natural iron fertilization in the Southern Ocean. *Deep Sea Res 2 Top Stud Oceanogr* **55**: 777–789.
- Obernosterer, I., Fourquez, M., and Blain, S. (2015) Fe and C co-limitation of heterotrophic bacteria in the naturally fertilized region off the Kerguelen Islands. *Biogeosciences* **12**: 1983–1992.
- Oksanen, J., Blanchet, F.G., Kindt, R., Legendre, P., Minchin, P.R., O'Hara, R.B., et al. (2015) *vegan: community ecology package. R Package Version 2.3-0*. Vienna, Austria: R Foundation for Statistical Computing.
- Paerl, R.W., Bouget, F.-Y., Lozano, J.-C., Vergé, V., Schatt, P., Allen, E.E., et al. (2017) Use of plankton-derived vitamin B1 precursors, especially thiazole-related precursor, by key marine picoeukaryotic phytoplankton. *ISME J* **11**: 753–765.
- Parada, A.E., Needham, D.M., and Fuhrman, J.A. (2016) Every base matters: assessing small subunit rRNA primers for marine microbiomes with mock communities, time series and global field samples: primers for marine microbiome studies. *Environ Microbiol* **18**: 1403–1414.
- Poulsen, L.K., Ballard, G., and Stahl, D.A. (1993) Use of rRNA fluorescence in situ hybridization for measuring the activity of single cells in young and established biofilms. *Appl Environ Microb* **59**: 1354–1360.
- Quast, C., Pruesse, E., Yilmaz, P., Gerken, J., Schweer, T., Yarza, P., et al. (2012) The SILVA ribosomal RNA gene database project: improved data processing and web-based tools. *Nucleic Acids Res* **41**: D590–D596.
- Quéguiner, B. (2013) Iron fertilization and the structure of planktonic communities in high nutrient regions of the Southern Ocean. *Deep Sea Res 2 Top Stud Oceanogr* **90**: 43–54.
- Rembauville, M., Briggs, N., Ardyna, M., Uitz, J., Catala, P., Penkerch, C., et al. (2017) Plankton assemblage estimated with BGC-Argo floats in the Southern Ocean: implications for seasonal successions and particle export. *J Geophys Res: Oceans* **122**: 8278–8292.
- Rinta-Kanto, J.M., Sun, S., Sharma, S., Kiene, R.P., and Moran, M.A. (2012) Bacterial community transcription patterns during a marine phytoplankton bloom: phytoplankton bloom metatranscriptome. *Environ Microbiol* **14**: 228–239.

- Rohart, F., Gautier, B., Singh, A., and Lê Cao, K.-A. (2017) mixOmics: an R package for omics feature selection and multiple data integration. *PLOS Comput Biol* **13**: e1005752.
- Sallée, J.-B., Llorca, J., Tagliabue, A., and Lévy, M. (2015) Characterization of distinct bloom phenology regimes in the Southern Ocean. *ICES J Mar Sci* **72**: 1985–1998.
- Sarmiento, H., and Gasol, J.M. (2012) Use of phytoplankton-derived dissolved organic carbon by different types of bacterioplankton: use of phytoplankton-derived DOC by bacterioplankton. *Environ Microbiol* **14**: 2348–2360.
- Sarmiento, H., Morana, C., and Gasol, J.M. (2016) Bacterioplankton niche partitioning in the use of phytoplankton-derived dissolved organic carbon: quantity is more important than quality. *ISME J* **10**: 2582–2592.
- Sheik, C.S., Jain, S., and Dick, G.J. (2014) Metabolic flexibility of enigmatic SAR324 revealed through metagenomics and metatranscriptomics: disentangling the ecophysiological role of SAR324. *Environ Microbiol* **16**: 304–317.
- Sinnott, R.W. (1984) Virtues of the Haversine. *Sky Telesc* **68**: 158.
- Smetacek, V., Assmy, P., and Henjes, J. (2004) The role of grazing in structuring Southern Ocean pelagic ecosystems and biogeochemical cycles. *Antarct Sci* **16**: 541–558.
- Sowell, S.M., Wilhelm, L.J., Norbeck, A.D., Lipton, M.S., Nicora, C.D., Barofsky, D.F., *et al.* (2009) Transport functions dominate the SAR11 metaproteome at low-nutrient extremes in the Sargasso Sea. *ISME J* **3**: 93–105.
- Swan, B.K., Martinez-Garcia, M., Preston, C.M., Sczyrba, A., Woyke, T., Lamy, D., *et al.* (2011) Potential for chemolithoautotrophy among ubiquitous bacteria lineages in the Dark Ocean. *Science* **333**: 1296–1300.
- Swan, B.K., Tupper, B., Sczyrba, A., Lauro, F.M., Martinez-Garcia, M., Gonzalez, J.M., *et al.* (2013) Prevalent genome streamlining and latitudinal divergence of planktonic bacteria in the surface ocean. *Proc Natl Acad Sci USA* **110**: 11463–11468.
- Tada, Y., Nakaya, R., Goto, S., Yamashita, Y., and Suzuki, K. (2017) Distinct bacterial community and diversity shifts after phytoplankton-derived dissolved organic matter addition in a coastal environment. *J Exp Mar Biol Ecol* **495**: 119–128.
- Teeling, H., Fuchs, B.M., Becher, D., Klockow, C., Gardebrecht, A., Bennke, C.M., *et al.* (2012) Substrate-controlled succession of marine bacterioplankton populations induced by a phytoplankton bloom. *Science* **336**: 608–611.
- Thompson, A.W., Foster, R.A., Krupke, A., Carter, B.J., Musat, N., Vaulot, D., *et al.* (2012) Unicellular cyanobacterium symbiotic with a single-celled eukaryotic alga. *Science* **337**: 1546–1550.
- Uitz, J., Claustre, H., Griffiths, F.B., Ras, J., Garcia, N., and Sandroni, V. (2009) A phytoplankton class-specific primary production model applied to the Kerguelen Islands region (Southern Ocean). *Deep Sea Res Part 1 Oceanogr Res Pap* **56**: 541–560.
- van Tol, H.M., Amin, S.A., and Armbrust, E.V. (2017) Ubiquitous marine bacterium inhibits diatom cell division. *ISME J* **11**: 31–42.
- West, N.J., Obernosterer, I., Zemb, O., and Lebaron, P. (2008) Major differences of bacterial diversity and activity inside and outside of a natural iron-fertilized phytoplankton bloom in the Southern Ocean. *Environ Microbiol* **10**: 738–756.
- Wilkins, D., van Sebille, E., Rintoul, S.R., Lauro, F.M., and Cavicchioli, R. (2013) Advection shapes Southern Ocean microbial assemblages independent of distance and environment effects. *Nat Commun* **4**: 2457.
- Williams, T.J., Wilkins, D., Long, E., Evans, F., DeMaere, M. Z., Raftery, M.J., and Cavicchioli, R. (2013) The role of planktonic *Flavobacteria* in processing algal organic matter in coastal East Antarctica revealed using metagenomics and metaproteomics: Metaproteomics of marine Antarctic *Flavobacteria*. *Environ Microbiol* **15**: 1302–1317.
- Yooseph, S., Nealson, K.H., Rusch, D.B., McCrow, J.P., Dupont, C.L., Kim, M., *et al.* (2010) Genomic and functional adaptation in surface ocean planktonic prokaryotes. *Nature* **468**: 60–66.
- Zehr, J.P. (2015) How single cells work together. *Science* **349**: 1163–1164.
- Zhou, J., Song, X., Zhang, C.-Y., Chen, G.-F., Lao, Y.-M., Jin, H., and Cai, Z.-H. (2018) Distribution patterns of microbial community structure along a 7000-mile latitudinal transect from the Mediterranean Sea across the Atlantic Ocean to the Brazilian Coastal Sea. *Microbial Ecology* **76**: 592–609.

Supporting Information

Additional Supporting Information may be found in the online version of this article at the publisher's web-site:

Fig. S1. Dendrograms of total (a) and active (b) prokaryotic communities based on Bray–Curtis dissimilarity of biological triplicates. Triplicates were named with number of station followed by a, b and c.

Fig. S2. Heatmap and phylogenetic tree of dominant prokaryotic OTUs that account for $\geq 1\%$ in at least one sample of the total (a) or active (b) prokaryotic community. The taxonomy classification of each OTU was done according to their closest sequence match assigned by the SILVA database.

Colour key: dark red and light yellow colours represent high and low abundances, respectively. a.t = ambiguous taxa

Fig. S3. Relationship between changes in the community composition of diatoms and of active prokaryotes. Each point represents the Bray–Curtis dissimilarity between pairs of samples. The correlation coefficient was determined by the Mantel test. Dashed lines denote linear regressions for the Southern Ocean stations (SAZ, PFZ and AAZ excluding station BDT).

Fig. S4. Relationship between changes in prokaryotic and diatom communities. Each point represents the Bray–Curtis dissimilarity between pairs of samples. The correlation coefficients were determined by Mantel test. (a) Total prokaryotic communities. The full line denotes the linear regression across the entire transect (filled and empty circles combined). The dashed line denotes the linear regression across the Southern Ocean (SAZ, PFZ and AZ excluding sample BDT) regions (empty circles only). (b) Active prokaryotic communities. The full line denotes the linear regression across the entire transect (filled and empty squares combined). The dashed line denotes the linear regression across

the Southern Ocean (SAZ, PFZ and AZ excluding sample BDT) regions (empty squares only).

Fig. S5. Distance-decay curves of dissimilarity of the composition of the total prokaryotic communities. Each point represents the Bray–Curtis dissimilarity between pairs of samples. The correlation coefficients were determined by Mantel test. (a) Entire transect (b) Southern Ocean (SAZ, PFZ and AZ excluding sample BDT). Non-significant results were also obtained for the active prokaryotic communities (data not shown).

Fig. S6. Canonical correspondence analysis of prokaryotic community composition and environmental parameters for (a) the entire transect and (b) for the Southern

Ocean (SAZ, PFZ and AZ excluding sample BDT). Highly auto-correlated parameters are not shown (PO_4^{3-} with NO_3^- and dissolved oxygen with temperature). The significant parameters were temperature, salinity and DOC for the entire transect (a) and temperature for the Southern Ocean (b). Station BDT was not considered because chlorophyll *a* data was not available.

Table S1 Additional environmental variables of the study sites.

Table S2. Partial Mantel test for prokaryotic and diatom community composition and geographic distance (a) and environmental parameters (b) for the entire dataset and Southern Ocean samples.

Supplementary material

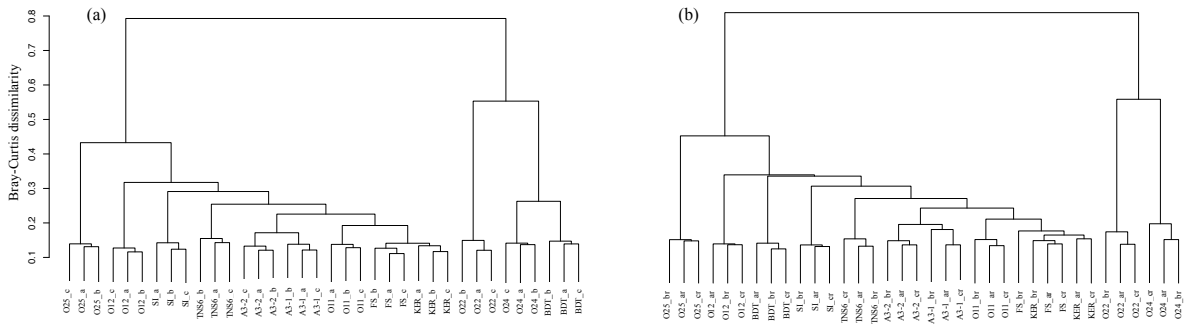
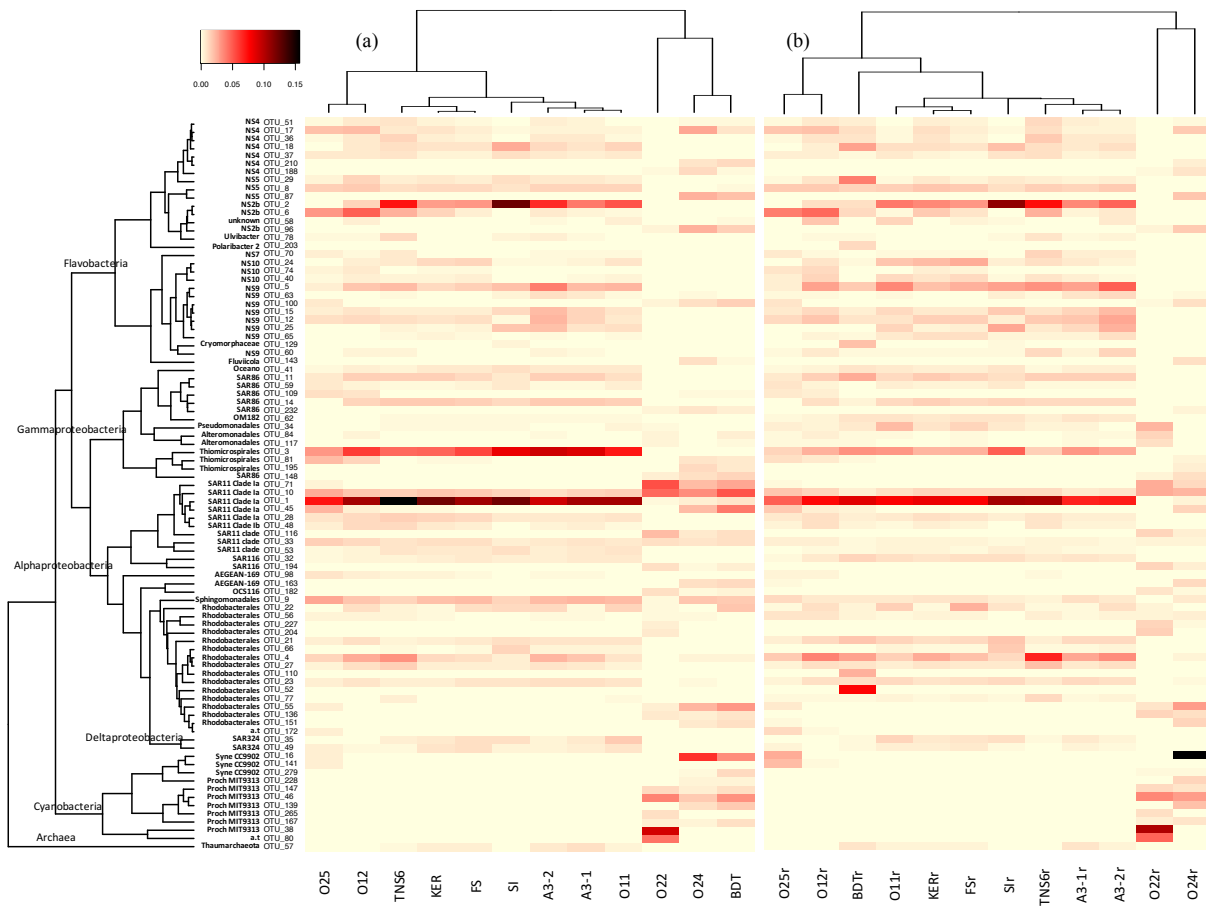


Fig. S1. Dendrograms of total (a) and active (b) prokaryotic communities based on Bray–Curtis dissimilarity of biological triplicates. Triplicates were named with number of station followed by a, b and c.



Chapter 1 Suppl.

Fig. S2. Heatmap and phylogenetic tree of dominant prokaryotic OTUs that account for $\geq 1\%$ in at least one sample of the total (a) or active (b) prokaryotic community. The taxonomy classification of each OTU was done according to their closest sequence match assigned by the SILVA database. Colour key: dark red and light yellow colours represent high and low abundances, respectively. a.t = ambiguous taxa

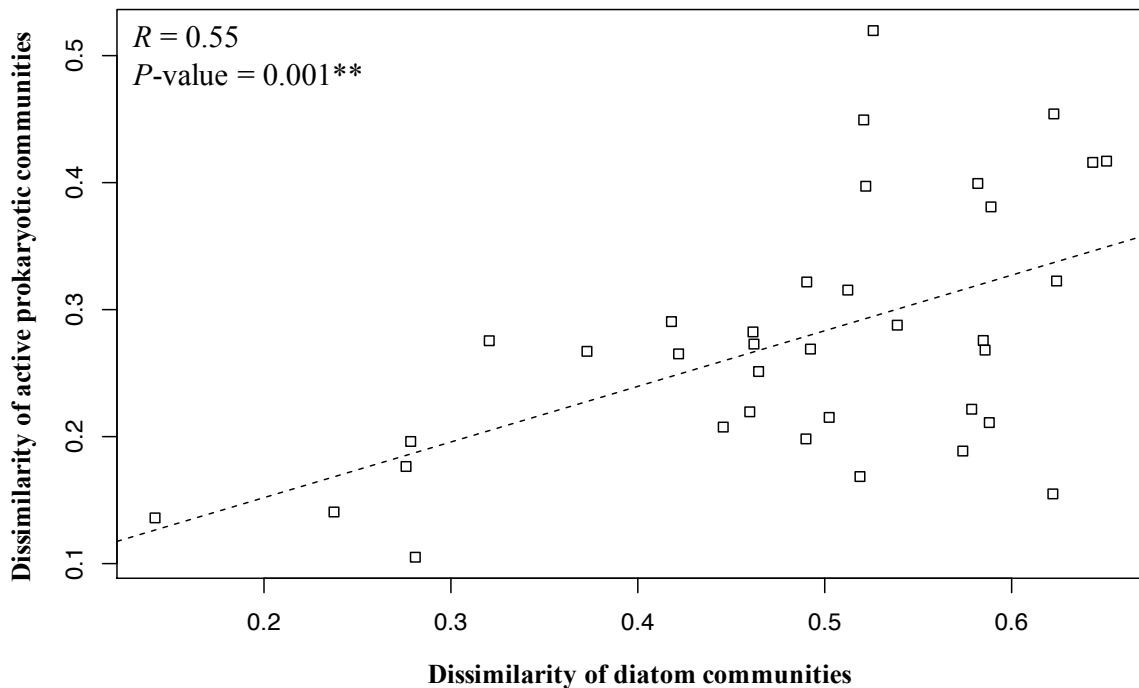


Fig. S3. Relationship between changes in the community composition of diatoms and of active prokaryotes. Each point represents the Bray–Curtis dissimilarity between pairs of samples. The correlation coefficient was determined by the Mantel test. Dashed lines denote linear regressions for the Southern Ocean stations (SAZ, PFZ and AAZ excluding station BDT).

Chapter 1 Suppl.

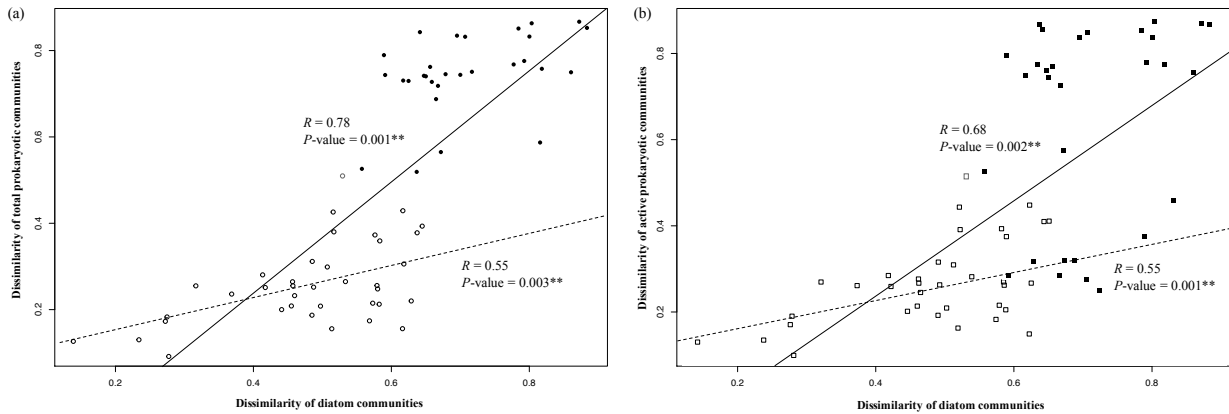


Fig. S4. Relationship between changes in prokaryotic and diatom communities. Each point represents the Bray–Curtis dissimilarity between pairs of samples. The correlation coefficients were determined by Mantel test. (a) Total prokaryotic communities. The full line denotes the linear regression across the entire transect (filled and empty circles combined). The dashed line denotes the linear regression across the Southern Ocean (SAZ, PFZ and AZ excluding sample BDT) regions (empty circles only). (b) Active prokaryotic communities. The full line denotes the linear regression across the entire transect (filled and empty squares combined). The dashed line denotes the linear regression across the Southern Ocean (SAZ, PFZ and AZ excluding sample BDT) regions (empty squares only).

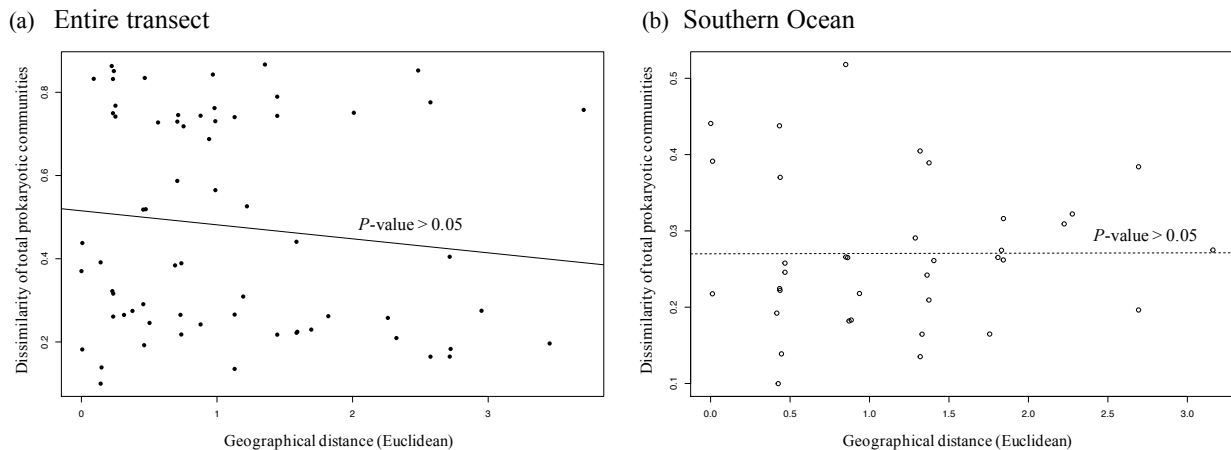


Fig. S5. Distance-decay curves of dissimilarity of the composition of the total prokaryotic communities. Each point represents the Bray–Curtis dissimilarity between pairs of samples. The correlation coefficients were determined by Mantel test. (a) Entire transect (b) Southern Ocean (SAZ, PFZ and AZ excluding sample BDT). Nonsignificant results were also obtained for the active prokaryotic communities (data not shown).

Chapter 1 Suppl.

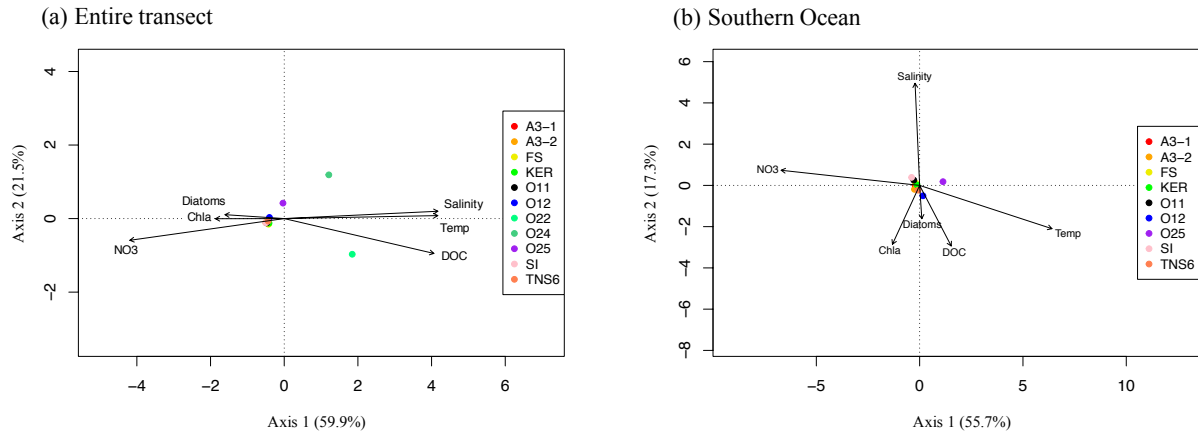


Fig. S6. Canonical correspondence analysis of prokaryotic community composition and environmental parameters for (a) the entire transect and (b) for the Southern Ocean (SAZ, PFZ and AZ excluding sample BDT). Highly auto-correlated parameters are not shown (PO_4^{3-} with NO_3^- and dissolved oxygen with temperature). The significant parameters were temperature, salinity and DOC for the entire transect (a) and temperature for the Southern Ocean (b). Station BDT was not considered because chlorophyll *a* data was not available.

Chapter 1 Suppl.

Table S1. Additional environmental variables of study sites

Station	Date	Lat/Long	Salinity	Oxygen (μM)
Subtropical Zone				
O22	08-Oct-16	29.00°S 58.93°E	35.71	235
O24	10-Oct-16	38.00°S 63.65°E	35.47	260
Subantarctic Front				
O25	12-Oct-16	45.00°S 67.77°E	33.94	304
Polar Front Zone				
O12	25-Oct-16	47.00°S 72.22°E	33.75	314
TNS6	15-Oct-16	48.78°S 72.28°E	33.85	275
Antarctic Zone				
BDT	17-Oct-16	49.50°S 69.21°E	33.51	337
A3-1	18-Oct-16	50.63°S 72.06°E	33.92	347
A3-2	24-Oct-16	50.63°S 72.06°E	33.92	344
KER	18-Oct-16	50.68°S 68.38°E	33.90	337
FS	19-Oct-16	52.50°S 67.00°E	33.94	337
O11	20-Oct-16	56.50°S 63.00°E	33.99	341
SI	21-Oct-16	58.50°S 61.50°E	33.87	358

Chapter 1 Suppl.

Table S2. Partial Mantel test for prokaryotic and diatom community composition and geographic distance (a) and environmental parameters (b) for the entire dataset and Southern Ocean samples.

(a)

	Entire dataset		Southern Ocean			Entire dataset		Southern Ocean	
	Prokaryotes DNA	Diatoms	Prokaryotes DNA	Diatoms		Prokaryotes RNA	Diatoms	Prokaryotes RNA	Diatoms
Diatoms	0.824**		0.556**		Diatoms	0.704**		0.551*	
Geographic distance	-0.423	0.438*	-0.089	0.167	Geographic distance	-0.238	0.270	0.067	-0.105

(b)

	Entire dataset		Southern Ocean			Entire dataset		Southern Ocean	
	Prokaryotes DNA	Diatoms	Prokaryotes DNA	Diatoms		Prokaryotes RNA	Diatoms	Prokaryotes RNA	Diatoms
Diatoms	0.854**		0.581**		Diatoms	0.738**		0.540**	
Combined environmental parameters	-0.569	0.569*	-0.240	0.527**	Combined environmental parameters	-0.414	0.414*	-0.177	0.591**
Temperature	-0.596	0.620**	0.003	0.389	Temperature	-0.439	0.472*	0.275	0.016
Salinity	-0.521	0.499*	-0.009	0.022	Salinity	-0.445	0.405*	-0.190	0.553*
Dissolved oxygen	-0.516	0.497*	-0.291	0.543**	Dissolved oxygen	-0.371	0.347*	-0.275	0.372
PO ₄ ³⁻	-0.555	0.584**	-0.442	0.356	PO ₄ ³⁻	-0.456	0.490*	-0.202	0.058
Si(OH) ₄	-0.380	0.544**	0.238	0.354	Si(OH) ₄	-0.036	0.354*	0.453*	-0.01
NO ₂ ⁻	-0.421	0.359	-0.435	0.460*	NO ₂ ⁻	-0.393	0.280	-0.301	0.622**
NO ₃ ⁻	-0.551	0.585**	-0.431	0.461*	NO ₃ ⁻	-0.441	0.484*	-0.158	0.170
DOC	-0.263	0.211	0.512	-0.154	DOC	-0.165	0.094	-0.026	0.547

The values shown in the tables are Rho values. Each value represents the correlation between two matrices while controlling for the effect of the third matrix.

** $p < 0.01$, * $p < 0.05$

CHAPTER TWO

Seasonal dynamics of prokaryotes and their associations with diatoms in the Southern Ocean



Preface

The work presented in this chapter is part of the Southern Ocean and Climate Project (SOCLIM, PI Stéphane Blain). I carried out the test series on the fixed seawater samples, I performed all molecular analyses, including the extraction of DNA and RNA, and the 16S rRNA gene amplification. I performed the bioinformatic procedures, and the network analyses to establish links between prokaryotic communities and diatoms. My work was carried out on seawater samples collected by a remote access sampler, an instrument that was developed, deployed and recovered by Stéphane Blain and Olivier Crispi. The diatom assemblages were described by Mathieu Rembauville (LOMIC). Olivier Crispi provided the inorganic nutrient analyses.

This work was presented during the IMBER meeting in Brest (June 2019) and it will be presented at the SAME meeting in Potsdam (Germany) in September (2019).

Chapter 2

Abstract

Iron-fertilized waters sustain annually occurring spring phytoplankton blooms over the Kerguelen plateau (Southern Ocean). Previous short-term observations have shown that these diatom-dominated blooms stimulate prokaryotic activity and shape community composition during the onset and declining stage. The investigation of the seasonal dynamics has thus far been hampered by the limited access to this remote site. We present here results of temporal changes in the prokaryotic community composition obtained by a remote access sampler deployed at an iron-fertilized site on the Kerguelen plateau. A total of 19 seawater samples were collected over 4 months at 5-11 days intervals in the surface mixed layer, covering the entire productive season. We observed two consecutive phytoplankton blooms, each composed of distinct diatom assemblages. Illumina sequencing of the 16S rRNA gene revealed pronounced seasonal patterns of the free-living ($< 0.8 \mu\text{m}$ fraction) and the particle-attached ($> 0.8 \mu\text{m}$ fraction) prokaryotic communities. Using network analysis, we identified two groups of diatoms representative of the spring and summer bloom, respectively, that had opposite correlation patterns with prokaryotic taxa. We discuss potential ecological features of key prokaryotic taxa, independent of or associated to diatoms, in a naturally iron fertilized region of the Southern Ocean.

Chapter 2

Introduction

Microbes in the surface waters of the ocean play key roles in global carbon and nutrient exchanges (see reviews Buchan et al., 2014; Seymour et al., 2017). Briefly, phytoplankton act as the major primary producers and support the marine food web, while prokaryotes consume organic matter produced by phytoplankton and remineralize a large portion back to CO₂. The relationship between phytoplankton and prokaryotes has been intensively explored in experimental studies and under bloom conditions, in particular to investigate the prokaryotic response to transient or continuous phytoplankton-derived DOM pulses (Pinhassi et al., 2004; Rieman et al., 2010; Sarmiento et al., 2016; Landa et al., 2016; Dadaglio et al., 2018). Phytoplankton blooms are worldwide phenomena and highly dynamic events that usually occur over a short time period because of the drawdown of nutrients, grazing or viral infections. They are often followed by secondary blooms of heterotrophic prokaryotes and shifts in the prokaryotic community composition over time (Teeling et al., 2012). Diatoms contribute 20-40% to global carbon fixation (Nelson et al., 1995; Mann, 1999; Armbrust, 2009), and many species were shown to interact with prokaryotes (Gärdes et al., 2011; Amin et al., 2012).

The *in situ* interactions between diatoms and prokaryotes under bloom conditions was mainly investigated in coastal systems. The most prominent prokaryotic affiliations are the Flavobacteriaceae, Gammaproteobacteria (e.g., SAR92 clade) and the alphaproteobacterial Roseobacter clade (Teeling et al., 2016). In addition, major phylogenetic groups showed different growth responses in the open ocean diatom dominated blooms, where gammaproteobacterial *Alteromonas* and Betaproteobacteria were strongly correlated with organic matter supply (Tada et al., 2011). Seasonal bacterial dynamics were also found associated with a spring diatom bloom, in which major changes of Flavobacteriales and Rhodobacterales were observed related to the amounts of transparent exopolymer particles (TEP) (Taylor et al., 2013). Most studies aiming to find the relationships between diatoms and prokaryotes take chlorophyll *a* as a proxy for the characteristic of blooms, which ignore that different diatoms, even closely related ones have various properties and associated with distinct prokaryotic phylotypes (Amin et al., 2012). Furthermore, different bloom types in terms of phytoplankton species have the ability to encourage the different responses by same prokaryotic groups (Fandino et al., 2005).

The time-series approach has been applied to evaluate the dynamics of microbial community composition and the associations with the surrounding environment over time (see review

Chapter 2

Fuhrman et al., 2015). Temporal prokaryotic community dynamics have been under intense scrutiny in coastal seawater (see review by Bunse and Pinhassi, 2017). Significant seasonal patterns of prokaryotic community composition during one year (Grzyski et al., 2012; Lindh et al., 2015) and recurrent patterns over multiple years have been studied (Gilbert et al., 2012; Chafee et al., 2017; Lambert et al., 2018). Although the temporal interactions between phytoplankton and prokaryotes have been recently studied in temperate regions (Gilbert et al., 2012; Needham and Fuhrman, 2016), microbial studies over few months in the open ocean are still limited due to logistic constraints in site access and support. The microbial communities in the Southern Ocean have been severely under-sampled compared with temperate oceans (Andersson et al., 2010; Lindh et al., 2015), even polar ecosystems (Grzyski et al., 2012; Ghiglione et al., 2012). Much less is known about the diatom-prokaryotes interactions.

The objective of the present study was to investigate the dynamics of microbial community composition and the temporal associations between diatom assemblages and the prokaryotes in the open ocean. We explored this question in the naturally iron-fertilized region off Kerguelen Island (Southern Ocean) utilizing a Remote Access Sampler.

Chapter 2

Material and methods

Study site and sampling strategy

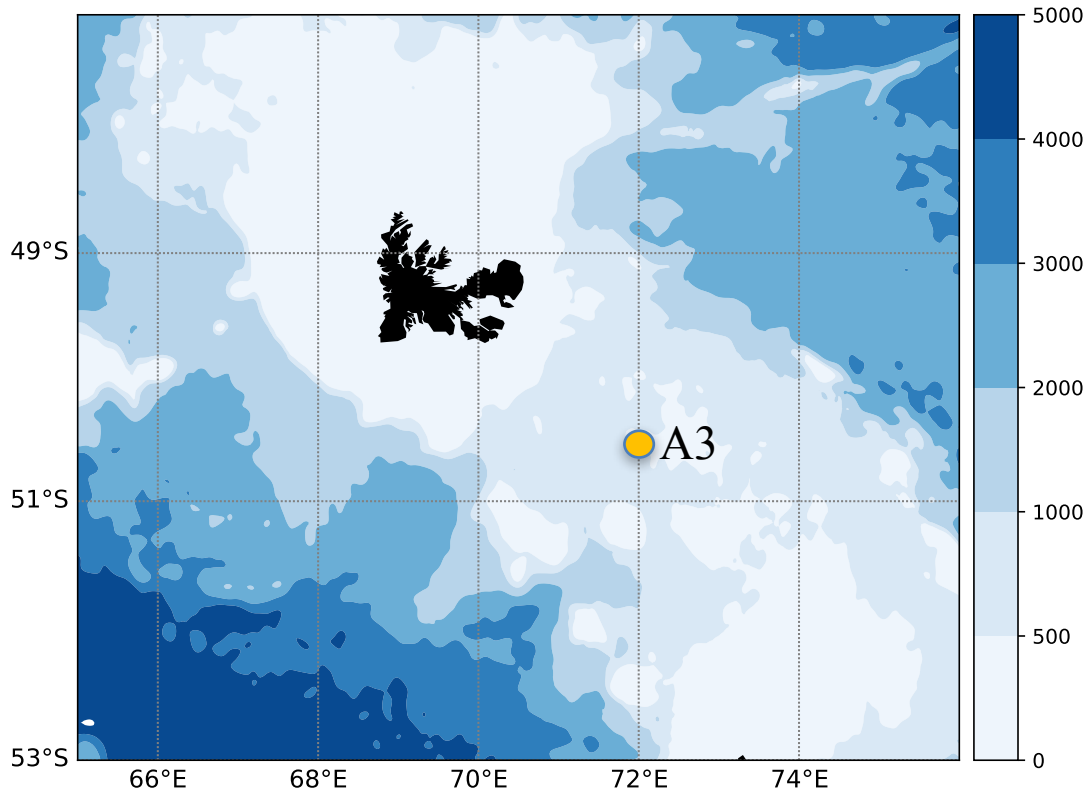
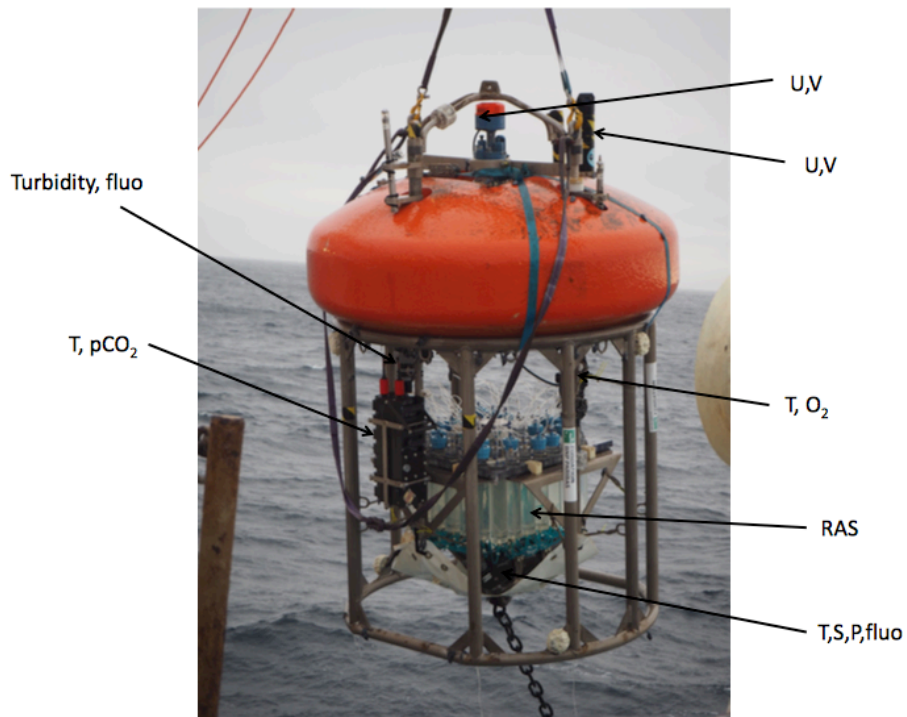


Fig. 1 Map of the study site (A3) above the Kerguelen plateau sampled via Remote Access Sampler (RAS) during the Southern Ocean and Climate (SOCLIM) cruise (October 2016 – April 2017). The bathymetry is from NOAA ETOPO1 at 1 degree resolution.

Chapter 2

(a)



(b)

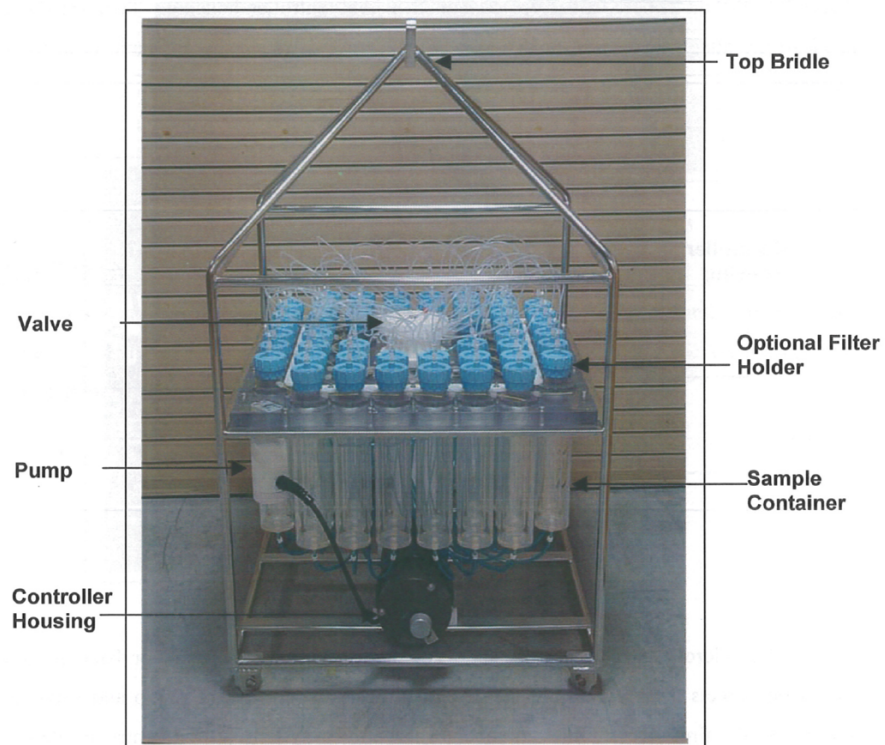


Fig. 2 The (a) deployment and the (b) full view of McLane Remote Access Sampler (RAS-500).

Chapter 2

Our study site is located in the Indian Sector of the Southern Ocean, above the Kerguelen plateau (50.63°S, 72.06°E; overall depth 527m) (Fig. 1). Seawater was collected with a Remote Access Sampler (RAS-500, Mac Lane) deployed from 25 October 2016 to 24 February 2017. The RAS was positioned at ~ 40m to allow sampling in the mixed layer throughout the season. The RAS can collect up to 48 seawater samples, each of 500 mL, in an autonomous manner, following a personalized pre-programmed schedule (Fig. 2). For the present study, 3 samples were collected at each time point (18 time points in total): 1 sample was pre-filtered through a 0.8 µm polycarbonate (PC) filter, and 2 samples remained unfiltered. The 0.8 µm-filtered samples served for inorganic nutrient analyses and the unfiltered samples were used for the determination of diatom and prokaryotic community composition (Table 1). Fixatives were added to the sample bags prior to deployment. Mercuric chloride (HgCl₂, 1% final conc.) was used as fixative for the 0.8 µm-filtered samples and for one of the unfiltered samples, and glutaraldehyde (25% final conc.) was used as fixative for the other unfiltered sample (Table 1). Following the 4-months deployment, the seawater of each sample bag was recovered in 500 mL PC carboys for transport to the home laboratory. An additional sample was taken on 6 April 2017 during the voyage of the recovery of the RAS. The seawater was collected at about 5m depth using the underway water supply system and fixed with glutaraldehyde until return to the home lab.

The mooring of the RAS was equipped with sensors continuously recording conductivity, temperature, dissolved oxygen (CTD, Seabird SBE19+) and the partial pressure of CO₂ (Carioca). The concentration of inorganic nutrients (nitrate, nitrite, silicic acid and ammonium) was determined according to standard protocols (Blain et al., 2014). The identification, enumeration and biomass determination of the diatom and dinoflagellate assemblages were done on 200 mL of unfiltered seawater. Microscopic observations were carried out in an Utermöhl counting chamber (24 h, dark) using an inverted microscope with phase contrast (Olympus IX70) with 400× magnification as described in Rembauville et al. (2017). For microbial diversity analyses, 200 mL of seawater were sequentially filtered through 0.8 µm and 0.2 µm PC filters (Nuclepore). The filters were kept at -80°C until DNA extraction.

Chapter 2

Table 1. Overview of the samples collected by the RAS for microbial diversity analyses. Positive and negative symbols indicate whether results (16S rRNA sequences for prokaryotes and microscopic observations for diatoms) are available. Dates of samples used for network analysis are shown in bold.

Date	Sample fixation		
	Prokaryotes		Diatoms
	HgCl ₂	Glutaraldehyde	Glutaraldehyde
2016.10.25	+	+	+
2016.11.06	+	+	+
2016.11.11	+	-	-
2016.11.17	+	+	+
2016.11.22	+	-	-
2016.11.28	+	+	+
2016.12.03	+	-	-
2016.12.09	+	+	+
2016.12.14	+	-	-
2106.12.20	+	-	+
2016.12.25	+	-	-
2106.12.31	+	-	+
2017.01.05	+	-	-
2017.01.11	+	+	+
2017.01.22	+	+	+
2017.02.02	+	+	+
2017.02.13	+	+	+
2017.02.24	-	+	+
2017.04.06*	-	+	-

* Sample was collected from the underway water supply system during the recovery of the RAS.

Chapter 2

Effect of fixatives on DNA extraction and microbial diversity

To evaluate the potential effect of HgCl₂ and glutaraldehyde, used as fixatives in the RAS, on DNA extraction and microbial diversity analyses, we performed two tests series using seawater from the coastal Mediterranean Sea (Bay of Banyuls sur mer, France). The objective of the first series was to test whether sufficient amounts of DNA could be extracted from fixed and stored 200 mL samples. We therefore compared three DNA extraction kits (ZYMO fungal/ bacteria DNA miniprep kit, QIAGEN AllPrep DNA/ RNA kit, MoBio DNeasy PowerWater kit) (Table S2). Surface seawater was collected with three 2-L PC carboys, each containing 1 L. One liter of non-fixed seawater was treated with a standard protocol, thereafter referred to as control. 200 mL sub-samples (in 4 replicates) were immediately sequentially filtered through 0.8 µm and 0.2 µm filters and stored at -80°C. Seawater in the other two PC carboys were fixed either with HgCl₂ (1% final conc.) or glutaraldehyde (25% final conc.) and stored at 4°C in the dark for 4 months. The fixed samples were then filtered (200 mL, in 4 replicates) through 0.8 µm and 0.2 µm filters and stored at -80°C until DNA extraction. For each treatment (control, +HgCl₂, +glutaraldehyde) one filter was sacrificed for the DNA extraction with a given kit. After comparison of the results, the MoBio DNeasy PowerWater kit was chosen for further work (Table S2). For a first evaluation of the quality of the sequences, we only considered 3 samples (< 0.8 µm fraction of the control, +HgCl₂, +glutaraldehyde treatments). In the second test series, the same sampling, fixation and storage protocol was applied. However, using only one DNA extraction kit (MoBio DNeasy PowerWater kit) allowed us to obtain DNA and sequences from biological triplicates of each treatment.

DNA extraction and sequencing preparation

DNA was extracted from the 0.8 µm and 0.2 µm filters using the MoBio DNeasy PowerWater kit (Qiagen, Germany) following the manufacturer's guidelines with a few modifications. The filters were cut into small pieces with a sterile scalpel and then transferred to the 5 ml PowerWater DNA bead tube. The samples were heated at 65°C for 10min to aid the lysis of some organisms after adding solution PW1. The filters were placed on a vortex adapter at maximum speed for 10 min. According to the protocol, DNA extracts were obtained and ready for amplification. The V4-V5 region of the 16S rRNA gene from both fractions was amplified with the primer sets 515F-Y (5'-GTGYCAGCMGCCGCGGTAA) and 926-R (5'-CCGYCAATTYMTTTRAGTTT) as described in Parada et al. (2016) with a modification to

Chapter 2

the PCR amplification step. Triplicate 20 μ L reaction mixtures contained 2 μ g DNA, 5 μ l KAPA2G Fast HotStart ReadyMix, 0.2 μ M forward primer and 0.2 μ M reverse primer. Cycling reaction started with a 3 min heating step at 95°C followed by 30 cycles of 95°C for 45 s, 50°C for 45 s, 68°C for 90 s, and a final extension of 68°C for 5 min. The presence of amplification products was confirmed by 1% agarose electrophoresis and triplicate reactions were pooled. The pooled PCR amplicons were purified using Sephadex G-50 Superfine resin (GE Healthcare Bio-Sciences, USA) following the protocol. It aims to desalt the samples and eliminate unincorporated nucleotides and excess PCR primers. 16S rRNA gene amplicons were sequenced with Illumina MiSeq 2 \times 250 bp chemistry on one flow-cell at GeT-PlaGe platform (Toulouse, France). Mock community DNA (LGC standards, UK) was used as a standard for subsequent analyses and considered as a DNA sample for all treatments.

Data analysis

All samples from the sequencing run were demultiplexed by GeT-PlaGe and barcodes were trimmed off. Processing of sequences was performed using the DADA2 pipeline (version 1.10; Callahan et al., 2016) in R with following parameters: trimLeft=c(19,20), truncLen=c(240,200), maxN=0, maxEE=c(2,2), truncQ=2. Briefly, the pipeline combines the following steps: filtering and trimming, dereplication, sample inference, chimera identification, and merging of paired-end reads. It provides exact amplicon sequence variants (ASVs) from sequencing data with one nucleotide difference instead of building operational taxonomic units (OTUs) based on sequence similarity. ASVs were assigned against SILVA release 132 database (Quast et al., 2012). Singletons and sequences assigned to chloroplast and mitochondria were removed prior to subsequent analyses.

Statistical analyses

All statistical analyses were performed using R 3.4.2 version. The ASV and taxa tables were combined into one object using phyloseq R package (McMurdie and Holmes, 2013). Data were Hellinger transformed prior to the analyses based on Bray–Curtis dissimilarity (Legendre and Gallagher, 2001). Bray–Curtis dissimilarity matrices were generated via vegdist() function. For the comparison of prokaryotic ASVs and the similarity between different test treatments, pairwise RAS test sub-samples was combined and visualized by Anvi'o platform (Eren et al., 2015). Nonmetric dimensional scaling (NMDS) ordinations were generated based on Bray–

Chapter 2

Curtis dissimilarity using `monoMDS()` function in the package `Vegan` (Oksanen et al., 2015). Analysis of similarity (ANOSIM) was performed to test significant differences between fractions in microbial communities with R. Sequences alignment was carried out using MAFFT algorithm web services by defaults (Kato et al., 2017). The phylogenetic tree was constructed using PhyML 3.0 online programs based on maximum likelihood method and 100 bootstraps with HKY85 substitution model (Guindon and Gascuel, 2003). The tree was visualized with SeaView version 4.7 and saved as rooted tree. Heatmaps were generated using `heatmap3` package and rows were reordered corresponding to phylogenetic tree. The richness and Shannon indexes were examined using `estimate_richness()`, and evenness index was calculated by “Shannon/log(richness)”. Base package and the package `ggplot2` were used to plot graphs.

Network construction

Extended local similarity analysis (eLSA) was applied to determine the potential correlations between prokaryotic taxa and diatoms, with time being taken into consideration. Correlations of co-occurrence at each time point and correlations that may be lagged in time can be found using eLSA with the focus on the “coexistence” of microbial taxa (Ruan et al., 2006; Xia et al., 2011). For this analysis, 12 time points each separated by 11 days were used (Table 1). The prokaryotic ASVs and diatom species, each with relative abundances $\geq 1\%$ in at least one sample in each data set (diatom community composition, free-living prokaryotes and particle-attached prokaryotes) were included. Time delayed (D) positive and negative correlations with the setting of 0 to 2 units were examined, where 1 unit equals 11 days. Growth rates for prokaryotes range between 0.02-0.47 d^{-1} in early spring and summer at our study site (Obernosterer et al., 2008; Landa et al., 2016) and growth rates of major diatom species in the Southern Ocean vary between 0.24 to 0.62 d^{-1} (Timmermans et al., 2004).

Chapter 2

Results

Environmental context

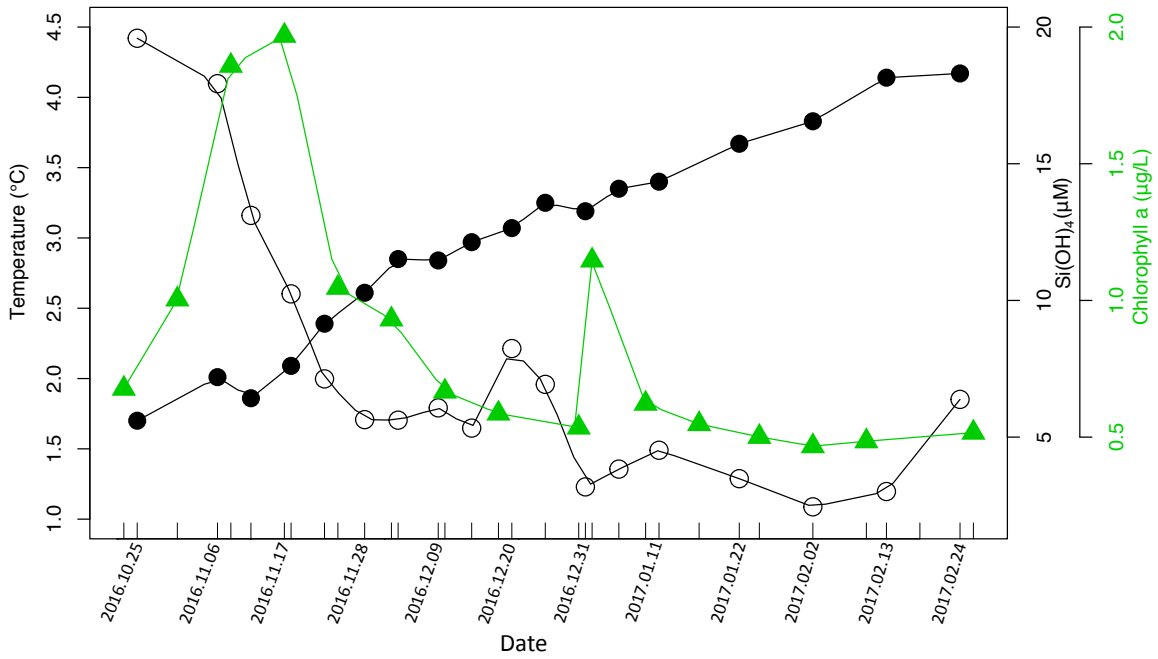
The combined data obtained by the sensors mounted on the mooring and from the analyses of seawater collected by the RAS provided detailed insights to seasonal changes of several environmental parameters (Fig. 3). The surface mixed layer was as deep as 150m in late October, it increased up to 100m during November and stayed at roughly 50m during the remaining observation period (S. Blain, personal communication). Temperature in the surface mixed layer was 1.7°C in late October and steadily increased to 4.2°C by February 24 (Fig. 3a). The concentration of silicic acid decreased from 20 μM to 6 μM during the first month of observation and a small increase (up to 8 μM) in silicic acid was detectable in late December. A drawdown of nitrate from 28 to 24 μM was observed over the first three weeks, and nitrate concentrations remained lower than this level throughout the season with a sharp decrease in early January (Fig. 3b). By contrast, ammonium concentrations increased from $< 0.5 \mu\text{M}$ to up to 2 μM in late December. Satellite images revealed two consecutive phytoplankton blooms, the first peaking in mid November and the second in early January. Bulk diatom biomass, based on the biovolumes determined for each diatom species, provided a similar seasonal picture (Fig. S1), indicating that diatoms were dominant contributors to both blooms.

Diatom community composition

A total of 38 diatom taxa, most of them at the species level, were identified by microscopic observations (Table S1), and 21 species had a relative abundance $\geq 1\%$ in at least one sample (Fig. 4). At the onset and during the first bloom, small centric diatoms such as *Chaetoceros* *Hyalochaete* (~50% of total diatom abundance), *Thalassionema nitzschioides* (~20%), *Thalassiosira antarctica* (~5%) and other small centrics (~5%) that could not be determined to the species level dominated. After the first bloom, *Pseudo-nitzschia* spp. increased in relative abundance and remained abundant until February 13 (range 6-43%). Major contributors to the second bloom were *Chaetoceros* *Hyalochaete* (~30%), *Pseudo-nitzschia* spp. (~35%), small centrics (~5%) and *Corethron inerme* (~5%). This latter diatom species further increased in abundance (up to 20 %) during the remaining season. Other diatom species that were more abundant during summer than spring were *Guinardia cylindrus* (1-14%), *Proboscia alata* (0.2-2%) and *Cylindrotheca closterium* (0.3-14%).

Chapter 2

(a)



(b)

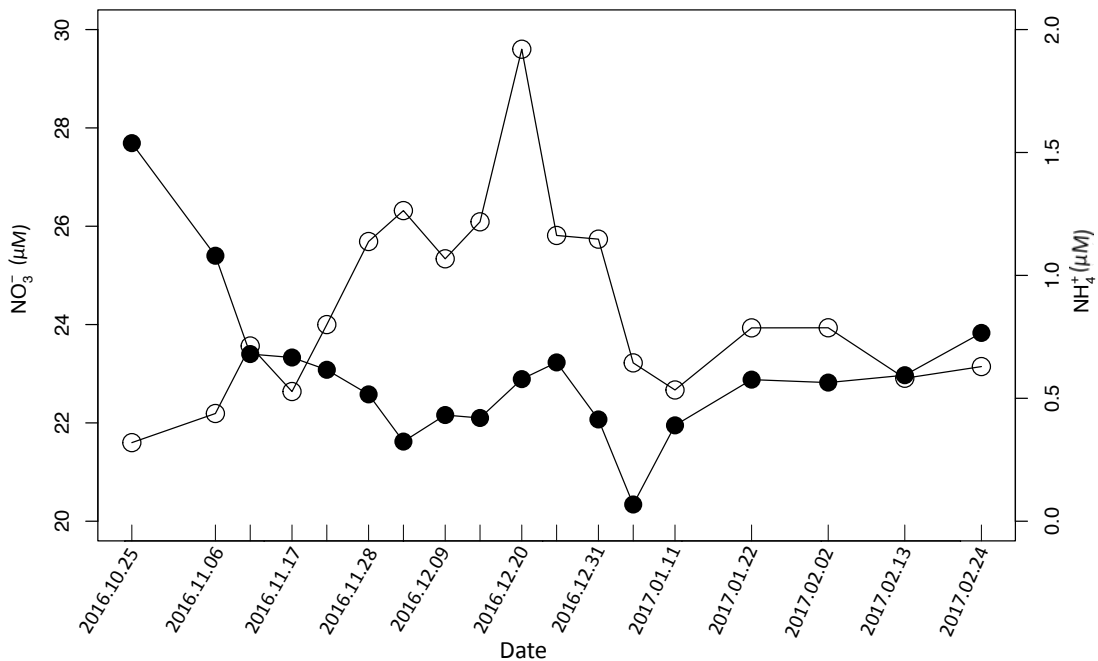


Fig. 3. Temporal changes of environmental parameters (a) temperature (full black symbols), silicic acid (Si(OH)₄) (open black symbols) and chlorophyll *a* (full green triangle) (b) nitrate (NO₃⁻) (full black symbols) and ammonium (NH₄⁺) (open black symbols). Chlorophyll *a* is derived from ocean color satellite images; the dates for chlorophyll *a* images are not identical to the sampling dates.

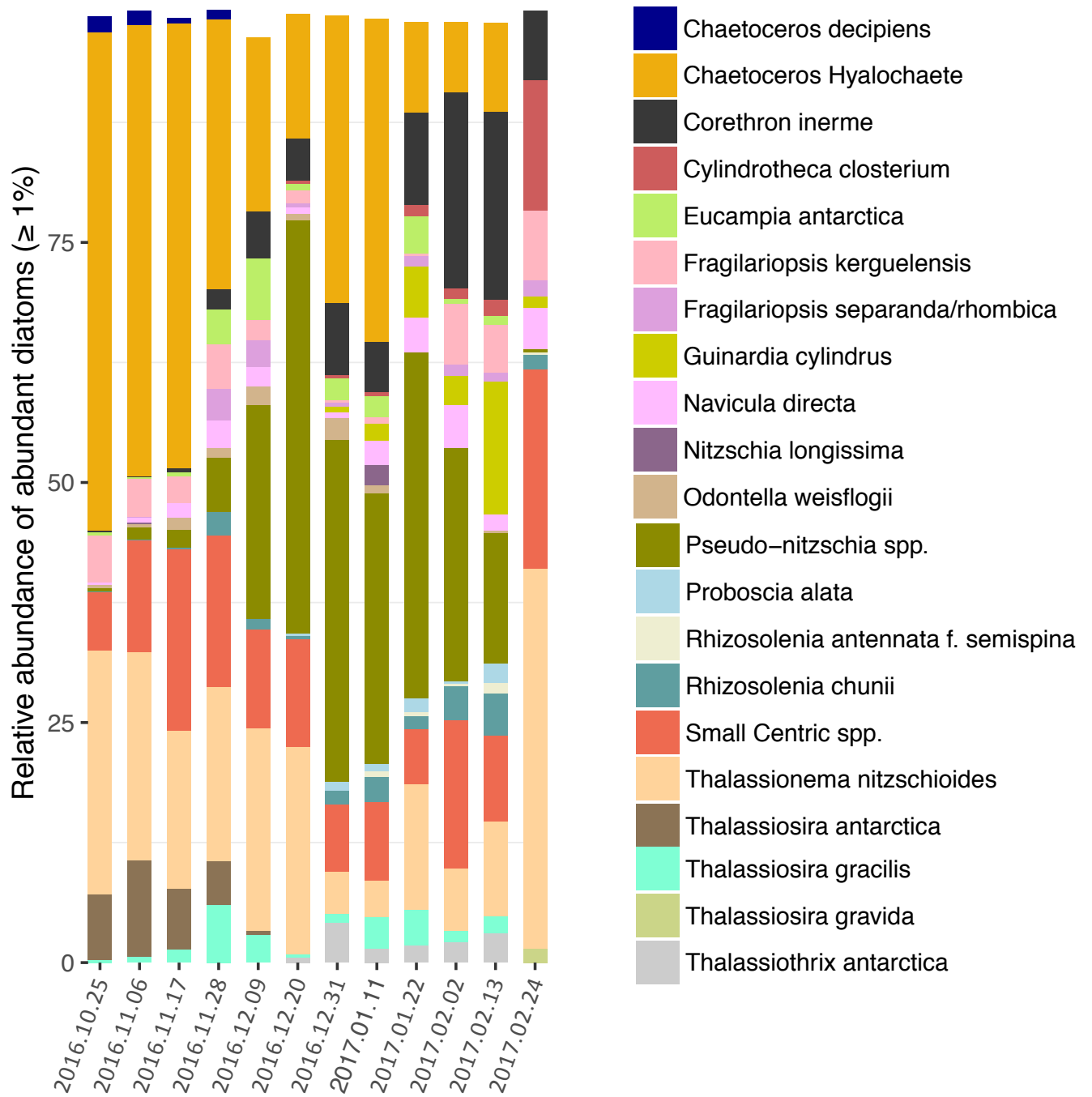


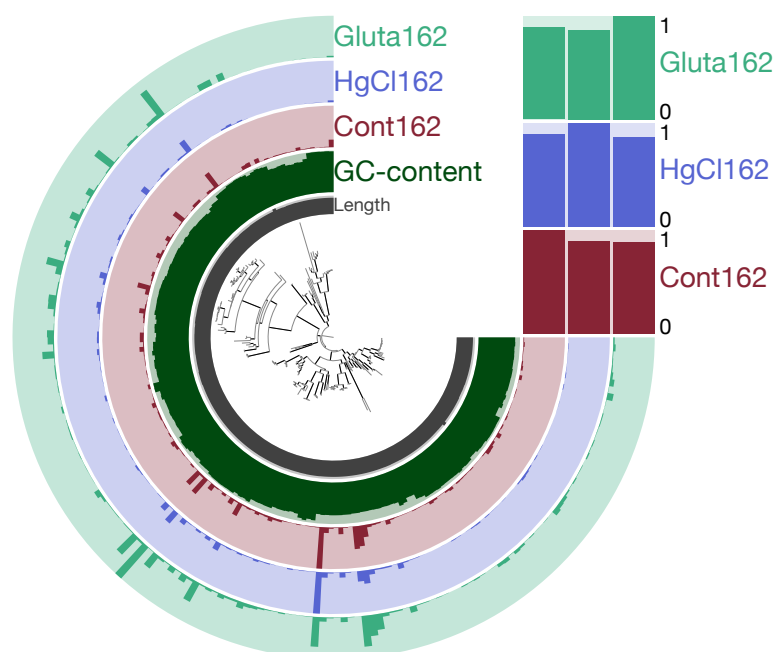
Fig. 4. Diatom community composition as determined by microscopic observations. Diatom taxa with a relative abundance $\geq 1\%$ are shown. The complete list of diatom species is provided in Table S1.

Chapter 2

Effect of fixatives on microbial diversity

Based on the concentration of DNA obtained by the different extraction kits tested (Table S2), we chose the MoBio DNeasy PowerWater kit for all further DNA extractions. From our first test series 3 samples were sequenced, one sample fixed with HgCl₂, one fixed with glutaraldehyde and one control. In a second test series, we sequenced 3 replicates of each, for both the free-living (< 0.8 μm fraction) and the particle-attached community (> 0.8 μm fraction). Because of the low number of sequences and sequencing contamination, 2 samples were removed from the second series, resulting in 3 and 16 samples in total. The rarefied number of sequences was 17 943 and 9 903 for the first and the second test series, respectively. The distribution of dominant prokaryotes (ASVs ≥ 1% in at least one sample) and the similarity between pairwise samples are shown in Fig. 5. Results from the first test revealed high similarity between the 3 samples (Fig. 5a). The results from the second test overall confirmed these results for the free-living fraction. By contrast, for the particle-attached fraction samples fixed by HgCl₂ had higher similarity with controls than samples fixed by glutaraldehyde (Fig. 5b). We therefore chose the samples fixed by HgCl₂, with the exception of 2 dates (2017.02.13 and 2017.02.24) for which only glutaraldehyde fixed samples were available (Table 1).

(a)



(b)

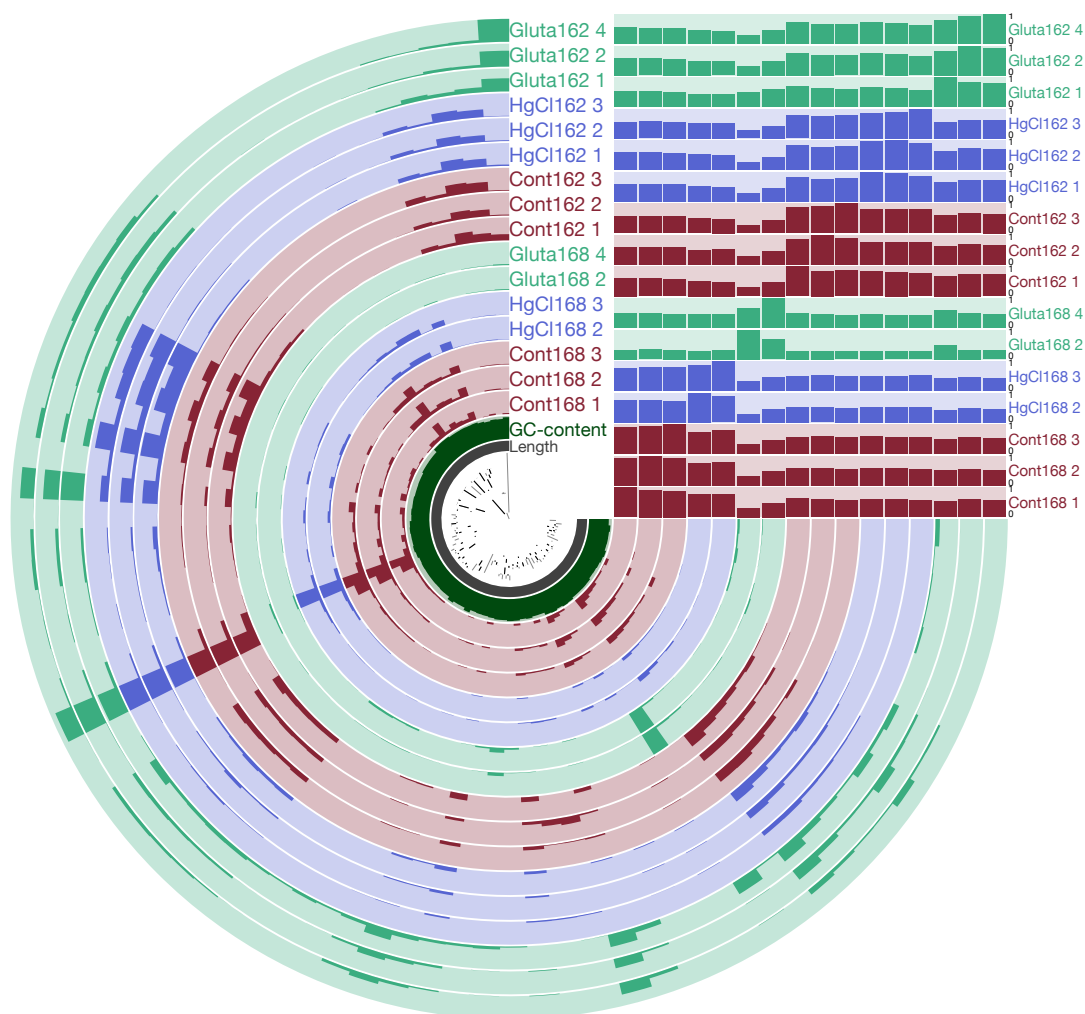


Fig. 5. Relative abundance of ASVs (illustrated in the circles) and the Bray-Curtis similarity between pairwise comparisons of controls, HgCl₂ and glutaraldehyde fixed samples (inserted histograms; similarity from 0-1). A phylogenetic tree according to the maximum likelihood is presented in the center. Results from the first and second test series are shown in panels (a) and (b), respectively. Cont162 and Cont168 refer to 16S rRNA gene sequences from the free-living and particle-attached prokaryotes of the control samples, respectively; Gluta162 and Gluta168 refer to 16S rRNA gene sequences from the free-living and particle-attached prokaryotes of the glutaraldehyde fixed samples, respectively; HgCl162 and HgCl168 refer to the 16S rRNA gene sequences from the free-living and particle-attached prokaryotes of the HgCl₂ fixed samples, respectively. Numbers following each sub-sample in the second test series (b) denote the replicate names.

Chapter 2

Composition of free-living and particle-attached prokaryotes

The number of sequences obtained for all samples varied between 14 749 - 52 581. After subsampling to the minimum number of sequences, we obtained a total of 792 ASVs. The number of ASVs per date varied between 92 and 194 in the free-living and between 103 and 240 in the particle-attached fraction. nMDS ordination analysis showed that community composition was significantly different between free-living and particle-attached prokaryotes (ANOSIM, $R=0.4839$, $P=0.001$) (Fig. 6) and that the communities of both fractions shifted over time.

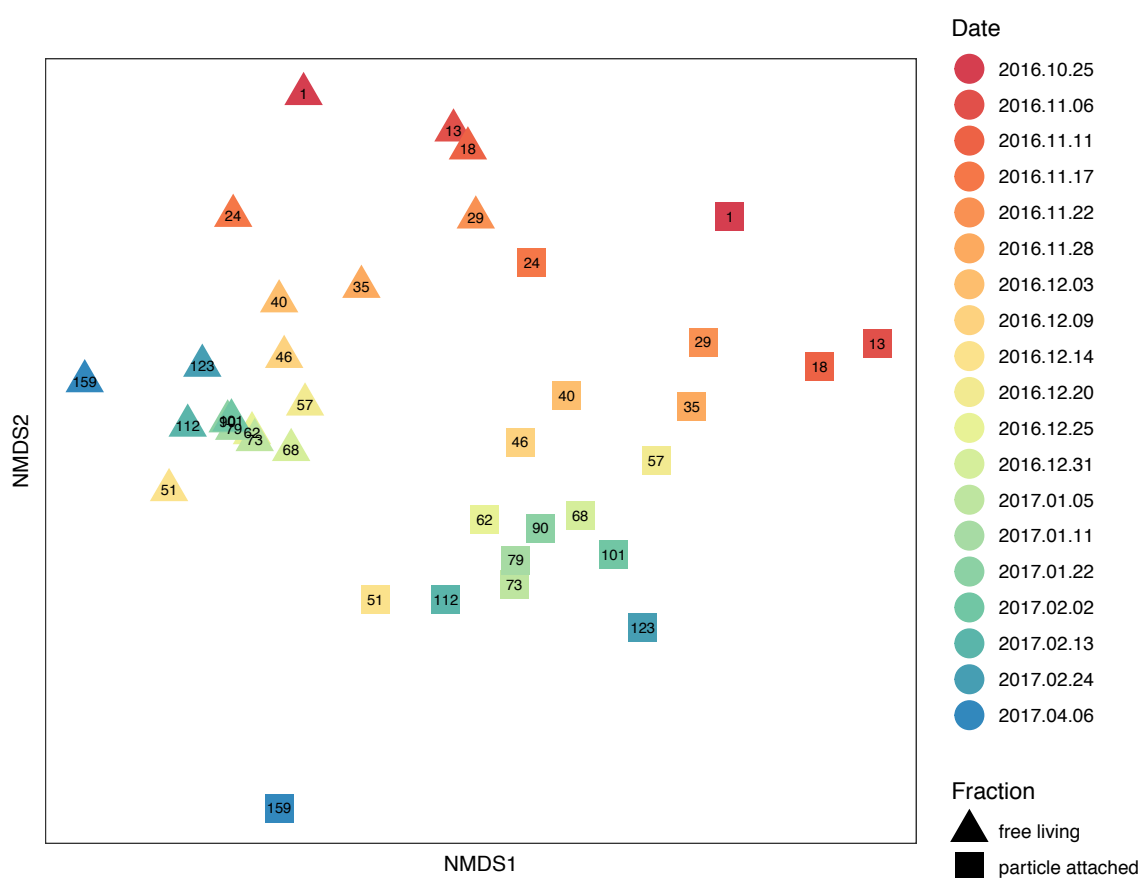


Fig. 6 Nonmetric multidimensional scaling (nMDS) of free-living and particle-attached prokaryotic communities based on Bray-Curtis dissimilarity. Triangle and square symbols denote free-living and particle-attached communities, respectively. The number in each symbol represents the elapsed in time (in days) from the first sampling date (1).

Chapter 2

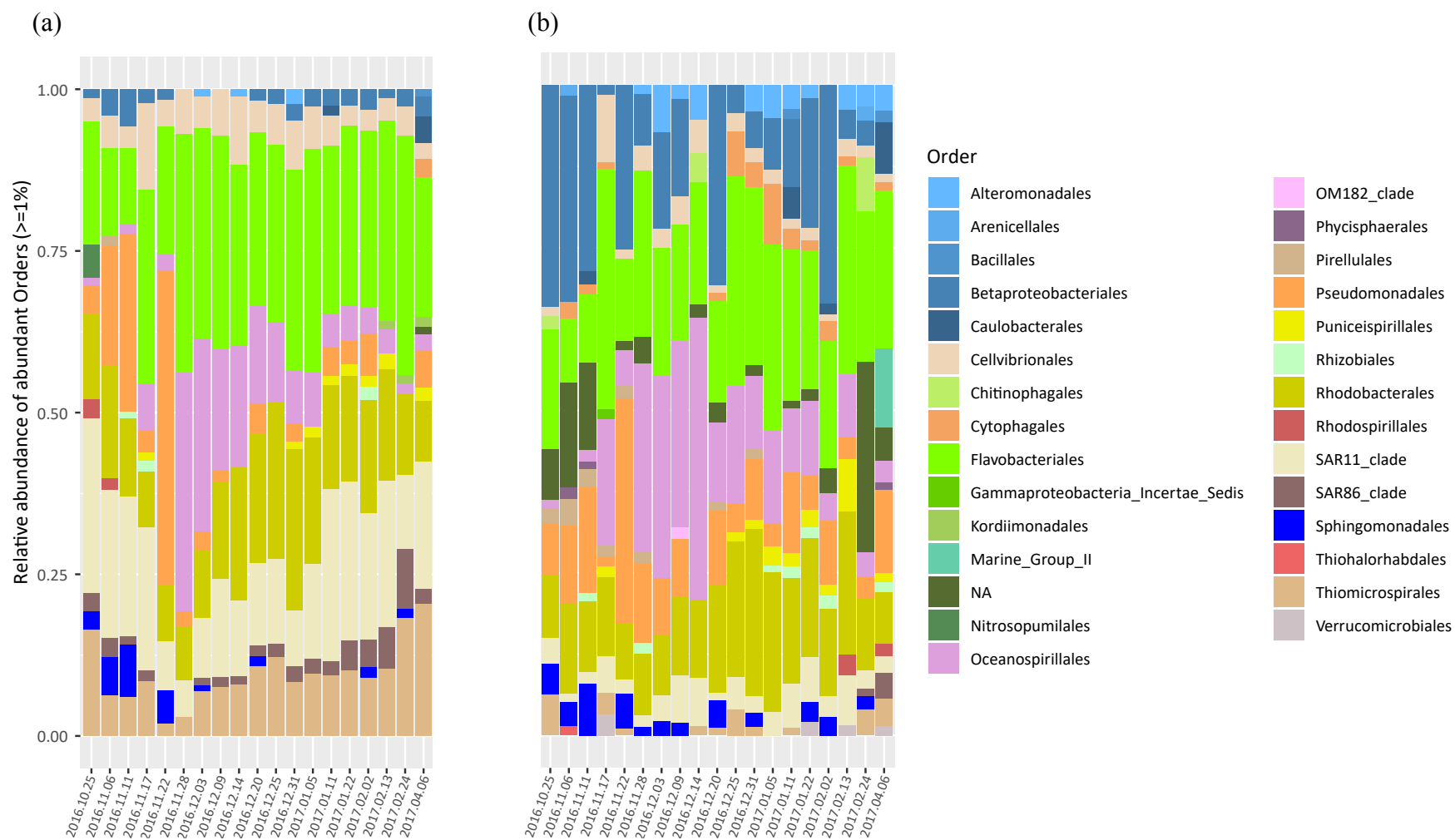


Fig. 7 Composition of (a) free-living and (b) particle-attached prokaryotic communities at the order level.

Chapter 2

Alphaproteobacteria, Bacteroidetes, Gammaproteobacteria and Archaea were abundant in both size-fractions and pronounced temporal changes at the Order level could be observed (Fig. 7). Higher relative abundances of SAR11, SAR86 and Thiomicrospirales were detected in the free-living fraction, while Betaproteobacteriales and Cytophagales had overall higher and more variable contributions to the total abundance in the particle-attached fraction. For the description of the seasonal dynamics of the prokaryotic communities at the ASV level, we focus in the following on the dominant ones (relative abundance $\geq 1\%$ in at least one sample), detected at the evenly spaced 12 time points and used for the network analysis. For free-living prokaryotes, Alphaproteobacterial SAR11, and the Rhodobacterales *Amylibacter* and *Planktomarina* were dominant ASVs (Fig. 8; all 19 samples shown in Fig. S2). One ASV belonging to the SAR11 clade Ia was abundant (6-16% of relative abundance) throughout the season, with the exception of one date, just after the first bloom (2%). One *Amylibacter* ASV and several *Planktomarina* ASVs, both belonging to Rhodobacterales, were abundant from the decline of the first bloom onwards. Gammaproteobacterial SUP05 contributed with 6-17% throughout the season, except for one date just after the first bloom (3%). One SAR92 ASV (up to 11%) and two ASVs belonging to Nitrincolaceae (together up to 36%) had high abundances after the first bloom decreasing towards the end of the season, when SAR86 ASVs increased in relative abundance. Bacteroidetes consisted almost exclusively of subgroup Flavobacteriales, and revealed a succession among different members. ASVs belonging to NS2b, NS4 and NS9 were the most abundant ones prior to the first bloom (together 13%) while *Aurantivirga*, *Polaribacter*, and *Ulvibacter* ASVs became dominant during the peak and decline of the first bloom. Cryomorphaceae ASVs were present during the different stages of second bloom and NS2b and *Formosa* ASVs increased towards the end of the season.

In the particle-attached fraction, a number of highly abundant ASVs belonged to Gammaproteobacteria (Fig. 9; all 19 samples shown in Fig. S3). One *Cupriavidus* ASV accounted for up to 31% of the total relative abundance at the onset of the first bloom and this ASV revealed an oscillating pattern throughout the season. One *Pseudomonas* ASV co-varied with *Cupriavidus*. One SAR92 ASV and two Nitrincolaceae ASVs had seasonal patterns similar to those in the free-living fraction. The SAR11, *Amylibacter* and *Planktomarina* ASVs determined for the free-living fraction were also present in the attached fraction, but their relative abundances were substantially lower ($< 5\%$). This was also the case for *Aurantivirga*, *Ulvibacter* and *Dokdonia* ASVs belonging to Flavobacteriales.

Chapter 2

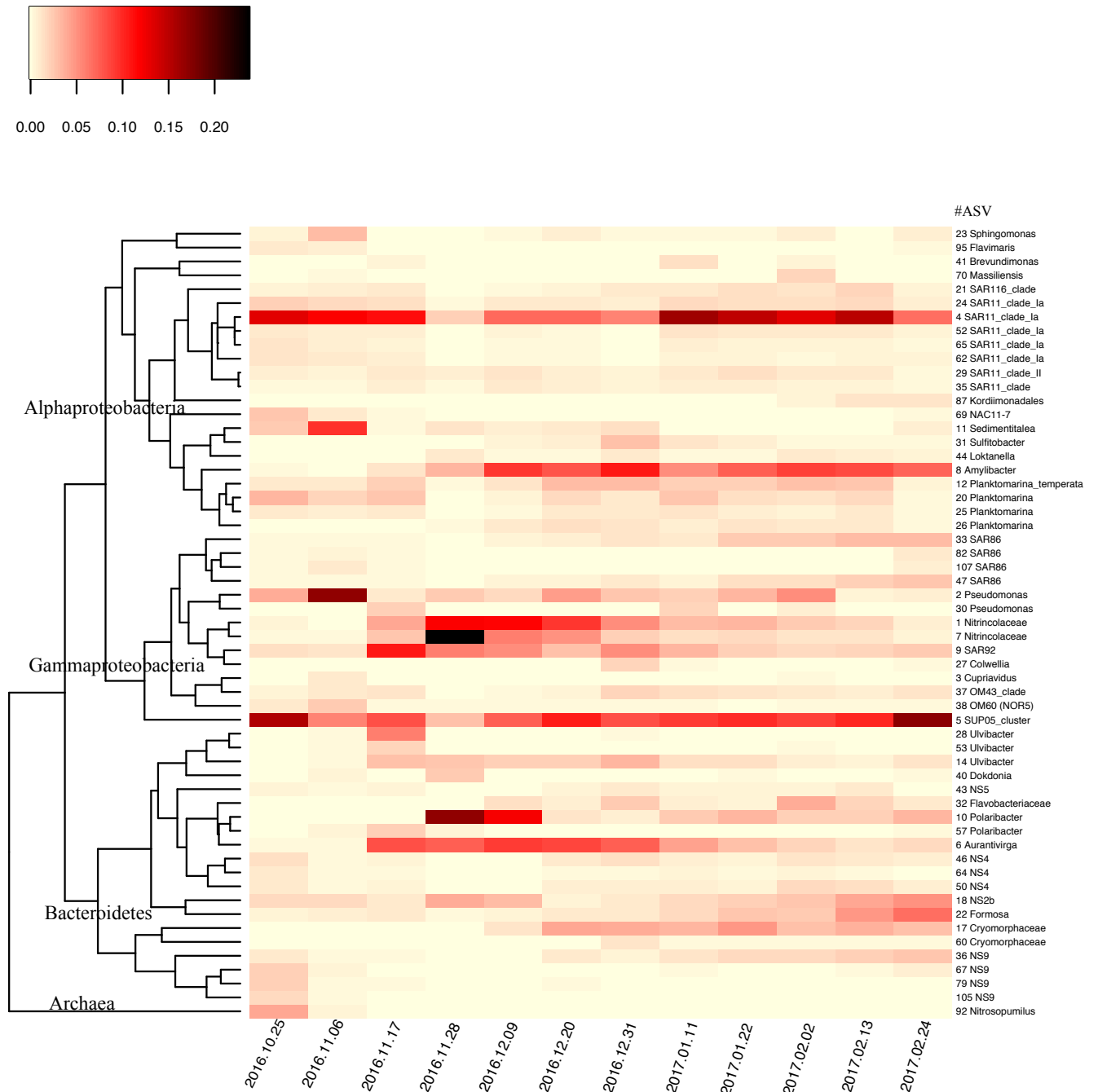


Fig. 8 Heatmap of abundant prokaryotic ASVs ($\geq 1\%$ of total relative abundance in at least one sampling date) of the free-living community. Results of 12 time points sampled at 11-day interval and used for the network analysis are shown.

Chapter 2

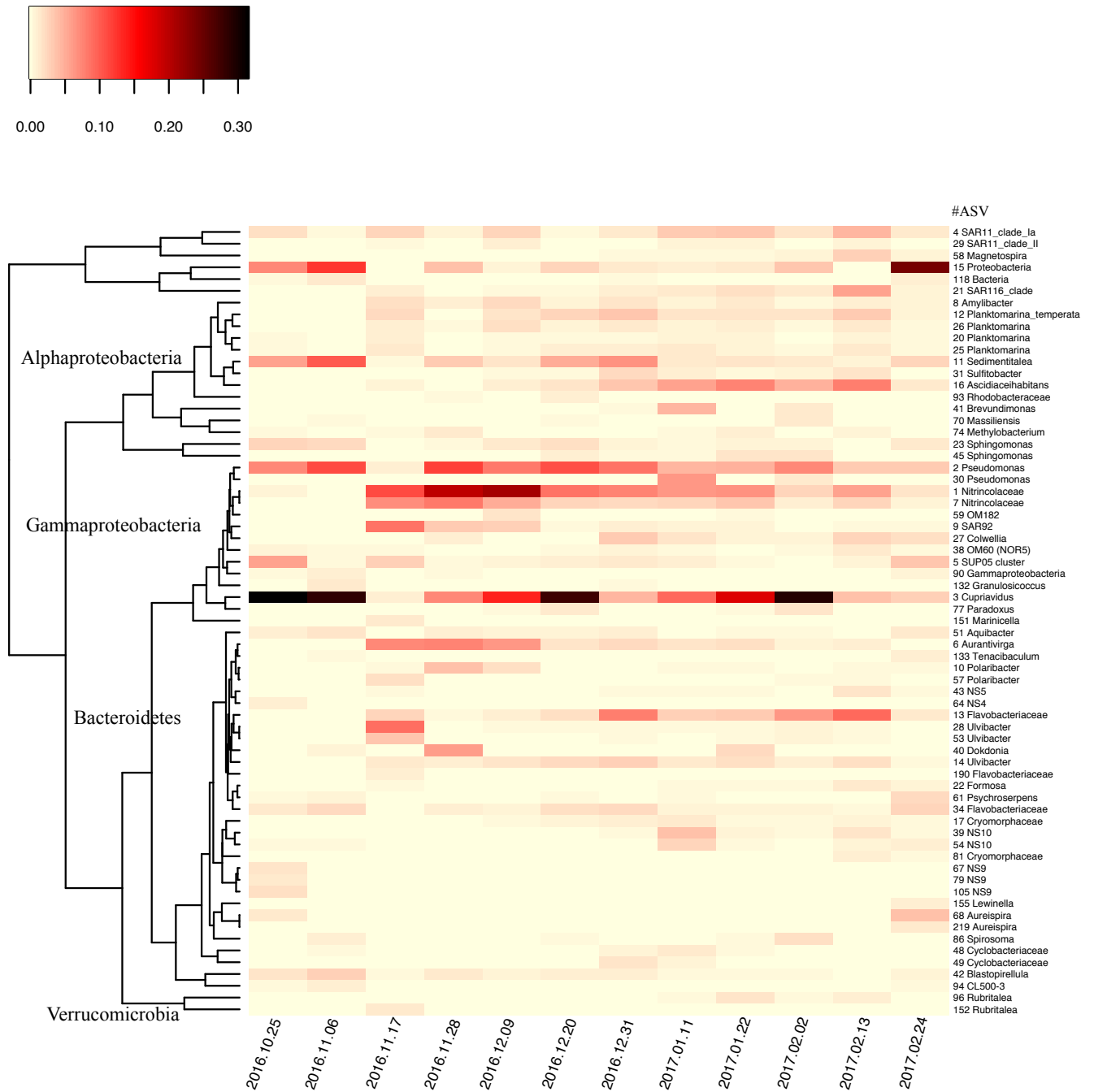


Fig. 9 Heatmap of abundant prokaryotic ASVs ($\geq 1\%$ of total relative abundance in at least one sampling date) of the particle-attached community. Results of 12 time points sampled at 11-day interval and used for the network analysis are shown.

Chapter 2

Prokaryotic Alpha-diversity

Prokaryotic diversity indices showed a distinct seasonal pattern, in the free-living and particle-attached communities (Fig. 10). The Shannon index, calculated with all ASVs, of the free-living community was highest prior to the first bloom and rapidly decreased during the decline of the bloom. Thereafter, this index steadily increased over time to reach a value in late summer similar to the one determined in early spring. The Shannon index of the particle-attached communities followed overall a similar temporal pattern, with the exception that the index was low prior to the first bloom. The Shannon diversity was similar for the two fractions at most time points, except for the two blooms. During the first and second bloom, the particle-attached community had respectively lower and higher Shannon diversity as compared to the free-living community. Richness and evenness revealed similar temporal trends in both fractions (Fig. S4).

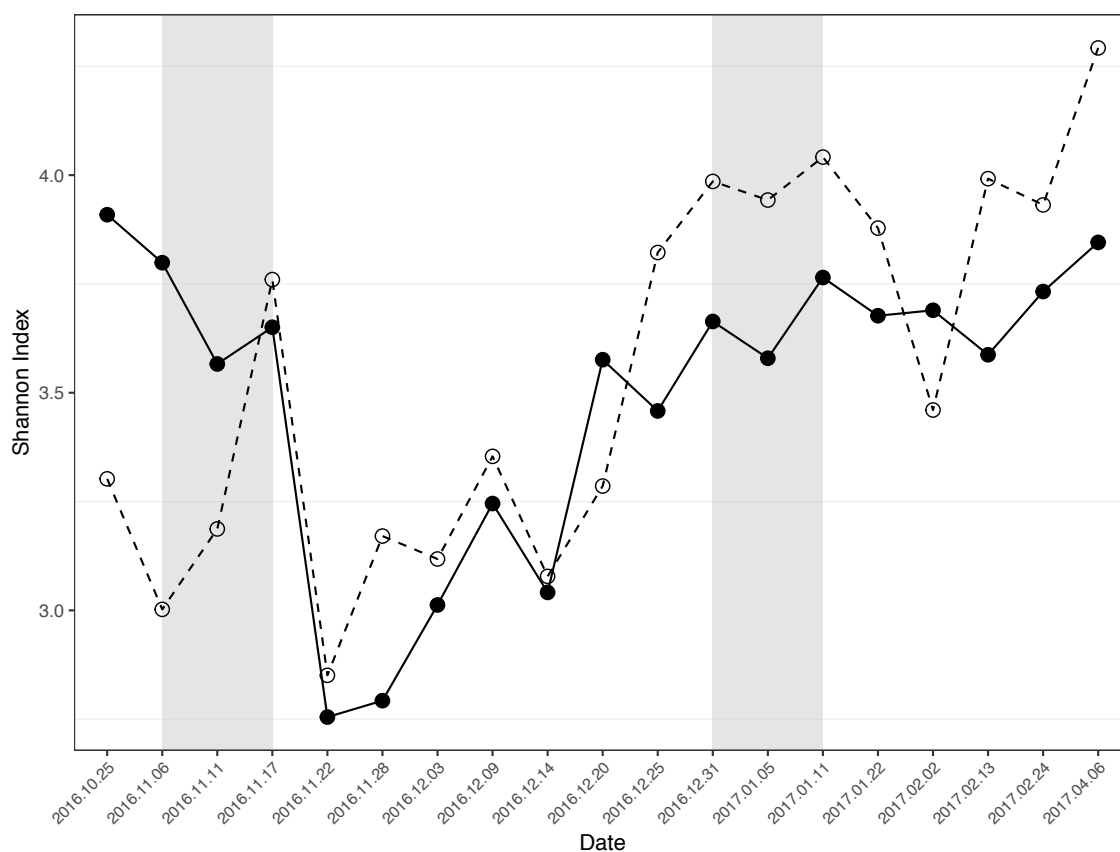


Fig. 10 Shannon index of prokaryotic communities. The solid and dashed lines represent the free-living and particle-attached fractions, respectively. Grey shades denote the time period of blooms.

Chapter 2

Associations between dominant prokaryotic taxa and diatom species

To investigate potential associations, we performed network analyses between diatoms and free-living and particle-attached prokaryotic taxa (each $\geq 1\%$ of total abundance in at least one sample), based on 12 equally distant time points (Fig. 11). The network shows all detected correlations with the minimum absolute Spearman's $r > 0.77$ ($P \leq 0.05$ and $Q \leq 0.05$). Our analysis revealed three groups of diatoms with different patterns. One group was composed of diatoms with higher relative abundances during the spring bloom, such as *Chaetoceros decipiens* and *Thalassiosira antarctica*, and these diatoms had overall only a few and mostly negative correlations with ASVs. Another group was composed of diatoms that were more abundant during summer, including the second bloom, and these diatoms had a large number of positive correlations with ASVs. Examples are *Guinardia cylindrus* and *Corethron inerme* that had the highest number of positive correlations (in total 15 and 11, respectively) with ASVs in the free-living and particle-attached fractions. *Thalassiothrix antarctica* had more correlations with attached prokaryotes (5) than with free-living ones (2). The third group of diatoms was abundant throughout the season and revealed only few (*Chaetoceros Hyalochaete*) or no correlations (*Thalassionema nitzschioides* and small centric spp.) with ASVs.

A subset of ASVs, comprised of 8 free-living and 7 particle-attached ASVs, revealed opposite correlations with the spring and summer diatom groups. The ASVs with opposite correlations belonged to Cryomorpaceae, Flavobacteriaceae, Rhodobacterales and the SAR86 clade. One Cryomorpaceae ASV and one Sulfitobacter ASV were present both in the free-living and particle-attached fractions. This Cryomorpaceae detected from both fractions correlated with the same diatom species, while the Sulfitobacter associated to different ones. Several ASVs in the free-living fraction had 1-2 week time-lagged positive associations with diatoms from the second bloom. Examples are ASVs belonging to SAR86, Kordiimonadales, Flavobacteriales NS9 and Formosa. On the contrary, correlations that indicated ASVs were ahead of time with respect to diatoms were more abundant in the particle-attached fraction. These time-delayed correlations were detectable for ASVs belonging to Cryomorpaceae, to Rhodobacterales Ascidiaceihabitans, Magnetospira and Sphingomona.

Chapter 2

Fig. 11 Network between dominant diatoms, free-living and particle-attached prokaryotes based on significant associations detected by both extended local similarity analysis (eLSA) and Spearman correlations with significance P-value ≤ 0.05 and Q-value ≤ 0.05 in each. Green, red and purple squares denote diatoms, free-living and particle-attached prokaryotic taxa, respectively. The solid and dashed lines represent positive and negative correlations, respectively. Lines with an arrow denote time-delayed correlations. Filled arrows indicate that the associated prokaryotic taxa are ahead of time with respect to diatoms ($D > 0$). Open arrows indicate that the associated prokaryotic taxa are behind with respect to diatoms ($D < 0$). Delta and diamond arrows indicate time-lagged correlations with a delay of 1 and 2, respectively. The number following each prokaryote specifies the ASVs. Abbreviations of diatoms are as follows: Chae_deci Chaetoceros decipiens, Chae_Hyal Chaetoceros Hyalochaete, Core_iner Corethron inerme, Cyli_clos Cyllindrotheca closterium, Euca_anta Eucampia antarctica, Frag_sepa Fragilariopsis separanda, Guin_cyli Guinardia cylindrus, Odon_weis Odontella weisflogii, Pseu_nitz Pseudo nitzschia, Prob_alat Proboscia alata, Rhiz_ante Rhizosolenia antennata, Rhiz_chunii Rhizosolenia chunii, Thal_anta Thalassiosira antarctica, Thal_grac Thalassiosira gracilis, Tham_nitz Thalassionema nitzschioides, Thax_anta Thalassiothrix antarctica. Abbreviations of prokaryotes are: Ascidi Ascidiaceihabitans, RhodoSedi Sedimentitalea, CytophaCyclo Cyclobacteriaceae, Sphing Sphingomonas, Plank Planktomarina, PlankTem Planktomarina temperata, SphingFlavimaris Sphingorhabdus flavimaris.

Chapter 2

Discussion

The temporal dynamics of microbial communities ranging from time scales of days to several years have opened the microbial “black box” by providing insights on the potential ecological niches of prokaryotic taxa in a wide range of aquatic environments (e.g., Fuhrman et al., 2006; Alonso-Sáez et al., 2008; Lamy et al. 2009; Gilbert et al., 2012; Lambert et al., 2018). On seasonal time scales, spring phytoplankton blooms were shown to be major drivers of compositional shifts (reviewed in Buchan et al., 2014; Bunse and Pinhassi, 2017), mainly driven by the release of DOM originating from phytoplankton (Teeling et al., 2016). Other types of interactions between autotrophs and heterotrophs (Amin et al., 2012) are likely to be enhanced during bloom events when activity and biomass are higher than during other periods of the year (Gasol and Kirchman, 2018). Temperate marine environments, where most of the seasonal studies were carried out, are characterized by a single, often diatom-dominated spring bloom, and the predominance of autotrophic dinoflagellates and small sized eukaryotes during the remaining season (e.g., Teeling et al., 2016). Our observations of the changes in microbial community composition during two consecutive spring and summer phytoplankton blooms, each dominated by diatoms and characterized by distinct assemblages, provide a novel perspective. We will discuss potential ecological features of key prokaryotic taxa, independent of or associated to diatoms, in a naturally iron fertilized region of the Southern Ocean.

The two phytoplankton blooms differ in several aspects, with consequences on the associated heterotrophic microbial communities. The spring bloom is initiated by the stratification of the water column, allowing phytoplankton to grow under favourable light conditions on the large winter stock of major inorganic nutrients and iron (Blain et al., 2007). This bloom started in early November and extended over roughly 1 month. It was dominated by small ($< 25 \mu\text{m}$), fast growing diatom species such as *Chaetoceros* spp., *Thalassionema nitzschioides*, *Thalassiosira* spp. and small centric spp.. The summer bloom was induced by a re-supply of silicic acid, most likely due to an entrainment of deeper water (Sallée et al., 2015). This bloom was overall shorter in duration (2 weeks) and had its peak in early January. Large ($> 25 \mu\text{m}$), slow growing diatoms, such as *Corethron inerme*, *Guinardia cylindrus*, *Thalassiothrix antarctica*, and *Rhizosolenia* spp. were major contributors to this bloom. Satellite-based Chl *a* concentrations indicate inter-annual variability in the magnitude of phytoplankton biomass accumulation and in the exact timing of the blooms (Fig. S5). In addition, 2 consecutive blooms are not detectable each year, but they appear to become more

Chapter 2

frequent over the past years. Previous investigations during the projects KEOPS1 (January-February 2006) and KEOPS2 (November 2011) have shown that heterotrophic prokaryotes markedly respond to phytoplankton blooms induced by natural iron fertilization in surface waters of the Kerguelen region. Prokaryotic heterotrophic production in surface waters at the same study site was 8-times higher during the spring phytoplankton bloom (November 2011; at $2 \mu\text{g Chl } a \text{ L}^{-1}$ in the surface mixed layer) as compared to surrounding HNLC waters (Christaki et al., 2014). A similar enhancement of prokaryotic production was observed also later in the season (January-February 2006) during the declining phase of the bloom (at 1.6 to $1 \mu\text{g Chl } a \text{ L}^{-1}$ in the surface mixed layer) (Obernosterer et al., 2008). The supply of phytoplankton-derived DOM is crucial for heterotrophic prokaryotes in these waters limited by the availability of labile organic carbon (Obernosterer et al., 2015). The trace metal iron represents an additional constraint. At the onset of spring, heterotrophic prokaryotes were shown to be outcompeted by small diatoms for the access to this trace element (Fourquez et al., 2015). C-limitation could render heterotrophic prokaryotes less competitive, an observation that is also reported for sub Antarctic waters (Fourquez et al., Submitted). In the presence of larger-sized autotrophs this competition is alleviated resulting in an enhanced iron uptake by prokaryotes (Fourquez et al., 2015). This latter scenario could be the case of the second bloom.

The prokaryotic community structure, as illustrated by the Shannon index, revealed overall high diversity during early spring, followed by a pronounced decrease during the decline of the bloom. This change in the community structure could also be seen in major modifications of the most abundant taxa, in particular in the free-living fraction. During the onset and peak of the spring bloom alphaproteobacterial ASVs belonging to SAR11 and Rhodobacterales Sedimentitalea, gammaproteobacterial ASVs belonging to the SUP05 cluster, *Pseudomonas*, and the Cellvibrionales SAR92 clade, and the Flavobacteriales ASVs *Ulvibacter* and *Aurantivirga* were among the most abundant taxa (Fig. 8). During the declining phase of the bloom, the communities were dominated by Oceanospirillales ASV Nitrincolaceae, Cellvibrionales ASV SAR92, and the Flavobacteriales ASVs *Polaribacter* and *Aurantivirga*. The most drastic changes were the rapid decrease in the relative abundance of SUP05 and SAR11 and the concurrent increase in the relative abundance of Nitrincolaceae, *Pseudomonas*, SAR92 (Cellvibrionales) and *Polaribacter* (Flavobacteriaceae).

The high contribution of SAR11 and SUP05, accounting together for 30% of total relative abundance in early spring, reflects their competitiveness under nutrient-poor conditions

Chapter 2

(Giovannoni, 2017; Swan et al., 2011; Rogge et al., 2017). Their oligotrophic-type life style rendered them key players in early spring, when both bioavailable iron and carbon were present at growth limiting concentrations (Obernosterer et al., 2015). SAR11 were reported to be the dominant contributors to prokaryotic biomass production, as determined by ^3H leucine and MICRO-CARD-FISH (Fourquez et al., 2016). By contrast, copiotrophs rapidly increased their contribution to the community during the decline of the bloom. The success of these latter taxa is likely due to their competitiveness in the utilization of phytoplankton-derived DOM under conditions when the access to iron is constrained. Using a gene-specific metatranscriptomics approach at the same study site in spring (November 2011), Flavobacteriaceae and Cellvibrionaceae contributed each 10-15% to total prokaryotic siderophore uptake gene expression, and the contribution of Nitrincolaceae (formerly Oceanospirillaceae) was about 5% (Debeljak et al., 2019). Pseudomonadaceae used a different mechanism, that is Fe^{3+} uptake by ABC transporters (Debeljak et al., 2019). In addition, all groups substantially contributed to the expression of genes coding for bacterioferritin, a compound with a regulatory function for the storage and release of intracellular iron (Marchetti et al., 2009; Botebol et al., 2015; Debeljak et al., 2019). Based on in situ MICRO-CARD-FISH and ^{55}Fe , Gammaproteobacteria and Bacterioidetes were the dominant contributors to iron uptake in spring (November 2011), with lower contributions by SAR11 (Fourquez et al., 2016). An efficient utilization or low requirements of iron by this streamlined bacterial group could explain its high relative abundance during the onset of the spring bloom. Taken together, these observations provide insights on the underlying metabolic capabilities that render these taxa competitive at the different bloom stages in spring.

One ASV belonging to the gammaproteobacterial SUP05 cluster was another key player of the free-living community. SUP05 was present throughout the season, but it had particularly high abundances prior to the start of the bloom, and in late summer. Representatives of the SUP05 cluster were shown to be abundant in Antarctic coastal waters (Arctic96BD-19 clade, Ghiglione and Murray, 2012; Grzyski et al., 2012) and south of the Polar Front (GSO-EOSA-1, Wilkins et al., 2013a). In the study region, one Arctic96BD-19 OTU accounted for about 10% to total clones at the same site as well as in HNLC waters (West et al., 2008). Metagenomic studies have indicated that this lineage has the potential to couple carbon fixation to the oxidation of reduced sulfur compounds, and also to utilize organic carbon (Swan et al., 2011). This potential mixotrophic life style could provide the SUP05 members with a competitive

Chapter 2

advantage. In the present study, the relative abundance pattern of SUP05 paralleled that of SAR11.

In contrast to spring, the bloom in summer had a more subtle effect on the prokaryotic community composition. During the second part of the season a number of ASVs that had low relative abundances in spring, increased in relative abundance and remained dominant. The most noticeable ASVs in the free-living fraction were Rhodobacterales ASVs *Amylibacter* and *Planktomarina*, Cellvibrionales ASV SAR92, and Flavobacterales ASVs *Aurantivirga* and Cryomorpaceae. The high relative abundances of *Planktomarina* (RCA cluster), *Amylibacter* (formerly NAC11-7 lineage), SAR92 and Cryomorpaceae ASVs are coherent with observations carried out at the same study site from January 19 to February 13 2005 (project KEOPS1). Based on clone libraries and the fingerprinting method single strand conformation polymorphism (SSCP), Operational taxonomic units (OTUs) related to NAC11-7, SAR92 and the clade AGG58, belonging to Cryomorpaceae, were significantly more abundant within the Kerguelen bloom as compared to HNLC waters (West et al., 2008). In addition, the three bacterial taxa contributed substantially to leucine incorporation, with SAR92 accounting for up to 40% of prokaryotic biomass production in the upper 120 m water column (Obenosterer et al., 2011). These combined observations, separated by 10 years, suggest that these prokaryotic taxa play a key role in the microbial cycling of phytoplankton-derived carbon in the Southern Ocean.

Only a few of the ASVs with high relative abundances in the free-living fraction were also abundant in the particle-attached fraction (Fig. 9). These included the Flavobacterales ASV *Aurantivirga*, the Oceanospirillales ASVs Nitrospiraceae, the Cellvibrionales ASV SAR92, the Pseudomonadales ASV *Pseudomonas* and the SUP05 cluster belonging to Thiomicrospirales. The ASV with the highest relative abundance in the particle-attached fraction was *Cupriavidus*, an ASV belonging to Burkholderiaceae. This ASV further revealed an oscillating pattern over time. Members of this family were shown to be abundant in Arctic sediments, with respectively low concentration of organic carbon and high concentrations of iron and manganese in pore waters (Algora et al., 2015). Burkholderiales (e.g., *Acidovorax* genus) are capable of oxidizing iron and manganese under aerobic conditions and to reduce these elements under anaerobic conditions (Carlson et al., 2013; Algora et al., 2015), scenario that are both possible within particles considered in this study. In addition, it has been shown that freshwater strains taxonomically close to *Cupriavidus necator* H16 produce the siderophore cupriachelin that is

Chapter 2

structurally similar to siderophores produced by oceanic bacteria (Kreutzer et al., 2012; Kreutzer and Nett, 2012). These findings hint to a potential role of this abundant ASV in the iron cycle in the particle-sphere. A genomic approach could help investigate this question in more detail.

Our network analysis provided insights to the question of whether the seasonal patterns observed for key prokaryotic taxa were driven by their associations to diatoms. Of the most abundant taxa during the first bloom, only 2 ASVs were highly correlated with one diatom. Nitrincolaceae ASVs (formerly Oceanospirillaceae) revealed strong positive correlations with a 3-week time-lag following *Thalassiosira antarctica*, an abundant diatom of the first bloom. This correlation was observed for 2 different ASVs in the free-living and particle-attached fractions. Could this association be related to the utilization of DOM from *Thalassiosira antarctica*? In an experimental study carried out at the same study site in spring (November 2011), OTUs belonging to Nitrincolaceae maintained similar abundances in chemostat cultures based on seawater alone or amended with the exudate of *Chaetoceros debilis* (Landa et al., 2018). This observation could either suggest that Nitrincolaceae do not specifically respond to diatom-derived DOM or point to selective differences in chemical characteristics of the exudates from these diatoms (Biddanda and Benner, 1997; Biersmith and Benner, 1998; Sarmiento et al., 2013). A recent study found that one genus (*Neptunomonas*) belonging to Nitrincolaceae had the highest number of connections with various small phytoplankton species in coastal seawaters of the Southern Ocean via network analysis (Fuentes et al., 2019), which indicates members of this family may be versatile degraders of phytoplankton-derived DOM. In addition, based on MICRO-CARD-FISH results from short-term (5h) phytoplankton-bacteria incubations, Sarmiento and Gasol (2012) have shown that gammaproteobacterial groups (e.g., *Alteromonas* and NOR5) had substantially lower contributions to the uptake of diatom-derived DOC (*Skeletonema costatum* and *Chaetoceros* sp.) as compared to Bacterioidetes. Together, these results suggest that the rapid increase of Nitrincolaceae is a response to the enhanced DOM supply rather than by the type of DOM (Sarmiento et al., 2016).

Among the abundant summer taxa, 3 ASVs belonging to Cryomorphaceae had strong correlations with several diatom species that are *Corethron inerme*, *Proboscia alata*, *Cylindrotheca closterium*, *Guinardia cylindrus*, *Pseudo-nitzschia*, and *Thalassiothrix antarctica*. Because of these multiple correlations, specific associations between these ASVs and one diatom species are unlikely. The Cryomorphaceae ASVs were abundant during the

Chapter 2

different phases of the second bloom, a finding also reported in other studies. For example, O'Sullivan et al. (2004) observed different groups of Cryomorpaceae (AGG58 clusters) present during different phytoplankton stages. Lucas et al. (2015) detected the fluctuating patterns of abundant Cryomorpaceae in each of two consecutive bloom events dominated by dinoflagellates and diatoms respectively. These observations suggest members of Cryomorpaceae may not be primary degraders of complex organic matter (Bowman, 2014), especially if we consider the low relative abundance of this group compared to other members of Bacteroidetes in the present and in previous studies (Lucas et al., 2015). In addition, Cryomorpaceae may harbor distinct ecological niches as compared with Polaribacter during phytoplankton bloom conditions in terms of algal polysaccharide degradation (Teeling et al., 2016). Polaribacter could degrade biopolymers and provide labile (small) organic substrates for Cryomorpaceae. This scenario could explain the successive pattern of Polaribacter and Cryomorpaceae observed in the present study. Further, Polaribacter was positively correlated with *Fragilariopsis separanda*, a diatom species that showed higher abundance prior to the summer bloom.

The highly abundant *Amylibacter* (formerly NAC11-7) had only one negative correlation with *Chaetoceros decipiens*, while other Rhodobacterales ASVs, each with lower relative abundances were positively associated with one or few specific diatoms. Particle-attached *Sulfitobacter* was positively correlated with large diatoms dominating the summer bloom such as *Corethron inerme*, *Thalassiothrix antarctica* and *Proboscia alata*. Other associations were *Planktomarina* (RCA cluster) with *Pseudo-nitzschia* spp. and *Loktanella* with *Rhizosolenia chunii*. Members of the Roseobacter-clade-affiliated (RCA) cluster commonly occur during phytoplankton bloom events (Teeling et al., 2012; Buchan et al., 2014; Klindworth et al., 2014; Teeling et al., 2016), an observation that was explained by the high functional diversity of this group (Brinkhoff et al., 2008; Newton et al., 2010; Luo and Moran, 2014). Furthermore, *Sulfitobacter*, *Loktanella* and *Planktomarina temperata* have all the potential for aerobic anoxygenic photosynthesis (AAnP) (Moran et al., 2007; Giebel et al., 2011; Boeuf et al., 2013; Giebel et al., 2013). Both dissolved organic matter (DOM) and light could stimulate the growth of AAnP bacteria (Suzuki and Béjà, 2007).

Our results provide support for the idea of functional diversity of Rhodobacterales, as illustrated by two examples. The association of *Sulfitobacter*-related taxa with diatom species

Chapter 2

has been explored in much detail (Moran et al., 2007; Landa et al., 2019). Sulfitobacter OTUs were more abundant in diatom-DOM amended cultures performed at the same study site (Landa et al., 2018), supporting the idea that members of this group can rapidly take advantage of the labile DOM provided by autotrophs. Sulfitobacter can also utilize dimethylsulfoniopropionate (DMSP) as a sole carbon source (Curson et al., 2008) released by phytoplankton (Simó, 2001). Sulfitobacter has the ability to synthesize indole-3-acetonitrile (IAA) that could stimulate the growth of diatom species (Amin et al., 2015), leading to potentially tight interactions with phytoplankton (Moran et al., 2007). A different ecology seems to hold for Amylibacter. In the study of Landa et al. (2018), NAC11-7 (now Amylibacter) performed better in seawater alone as compared to the DOM-amended treatment. A more streamlined genome, as shown for one cultivated representative, could render some Roseobacter members more adapted to oligotrophic conditions (Luo et al., 2014). Amylibacter could possess these features, leading to high competitiveness of this ASV, in a similar manner as SAR11, throughout a large part of the season and independent from DOM supplied by phytoplankton.

In summary, we observed different patterns in the prokaryotic response to two consecutive diatom blooms in the Southern Ocean. The spring bloom was dominated by small, fast-growing diatom cells that had only a few positive associations with prokaryotic taxa. The trace element iron, limiting for both autotrophic and heterotrophic microbes, could lead to a scenario where competition dominates the interactions. The higher number of positive associations during summer could be due to the slower growth of diatoms, and the partial alleviation of carbon limitation of prokaryotes, allowing the concurrent growth of autotrophic and heterotrophic microbes. This environmental context could be more favorable for interactions. Our study further suggests key players characterized by varying extents of dependency on phytoplankton blooms and its DOM supply. Taken together, our study showed the pronounced seasonal succession of diatoms and prokaryotes, and uncovered two distinct ecological niches for diatoms with specific prokaryotes associated.

Supplementary materials

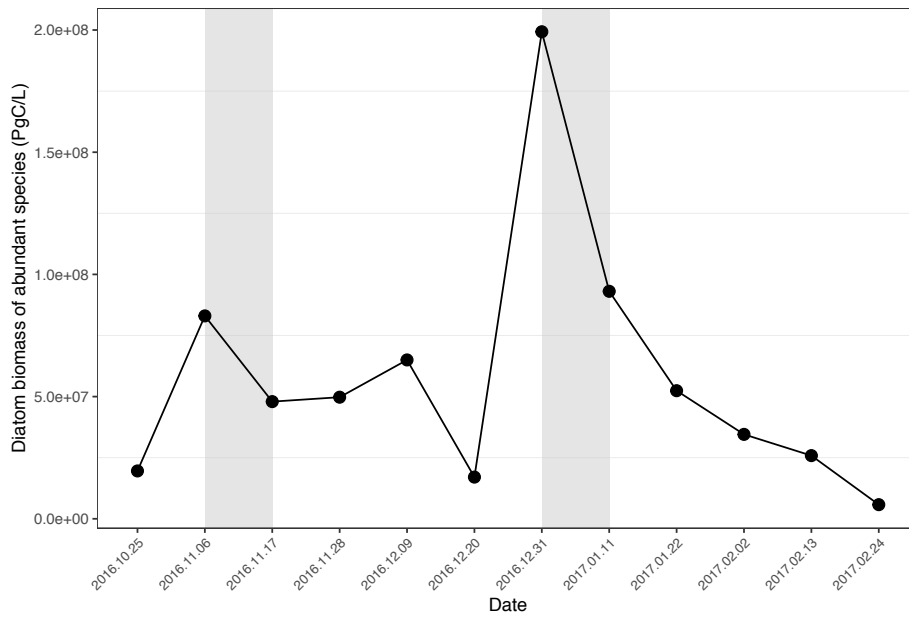


Fig. S1 Temporal changes of total diatom biomass estimated by average biovolume of each taxon. Biomass of the abundant diatom contributors ($\geq 1\%$ of total diatom abundance) is shown.

Chapter 2 Suppl.

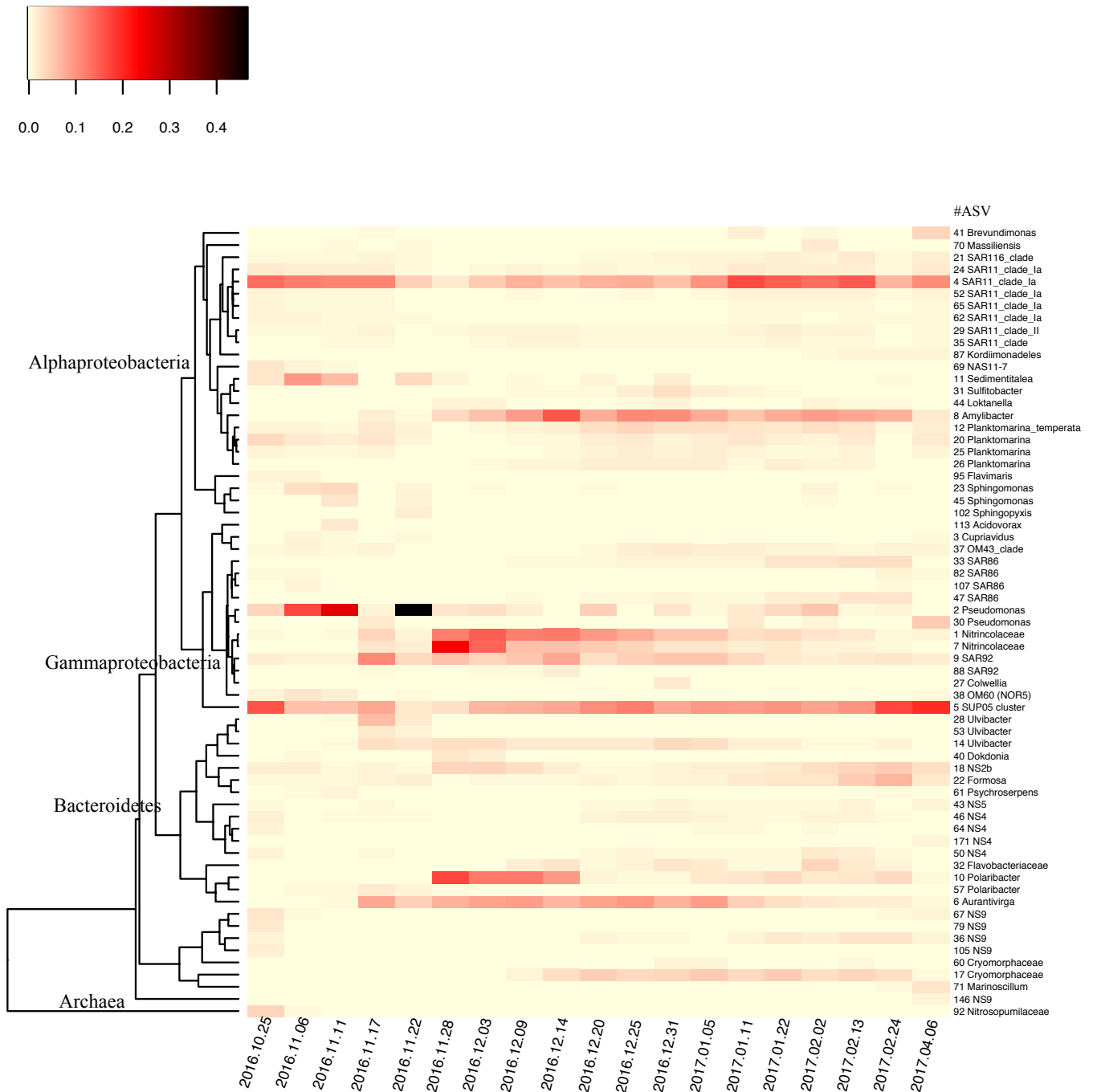


Fig. S2 Heatmap of dominant prokaryotic ASVs that account for $\geq 1\%$ of total relative abundance in at least one sampling date of the free-living community. Results of 19 time points are shown.

Chapter 2 Suppl.

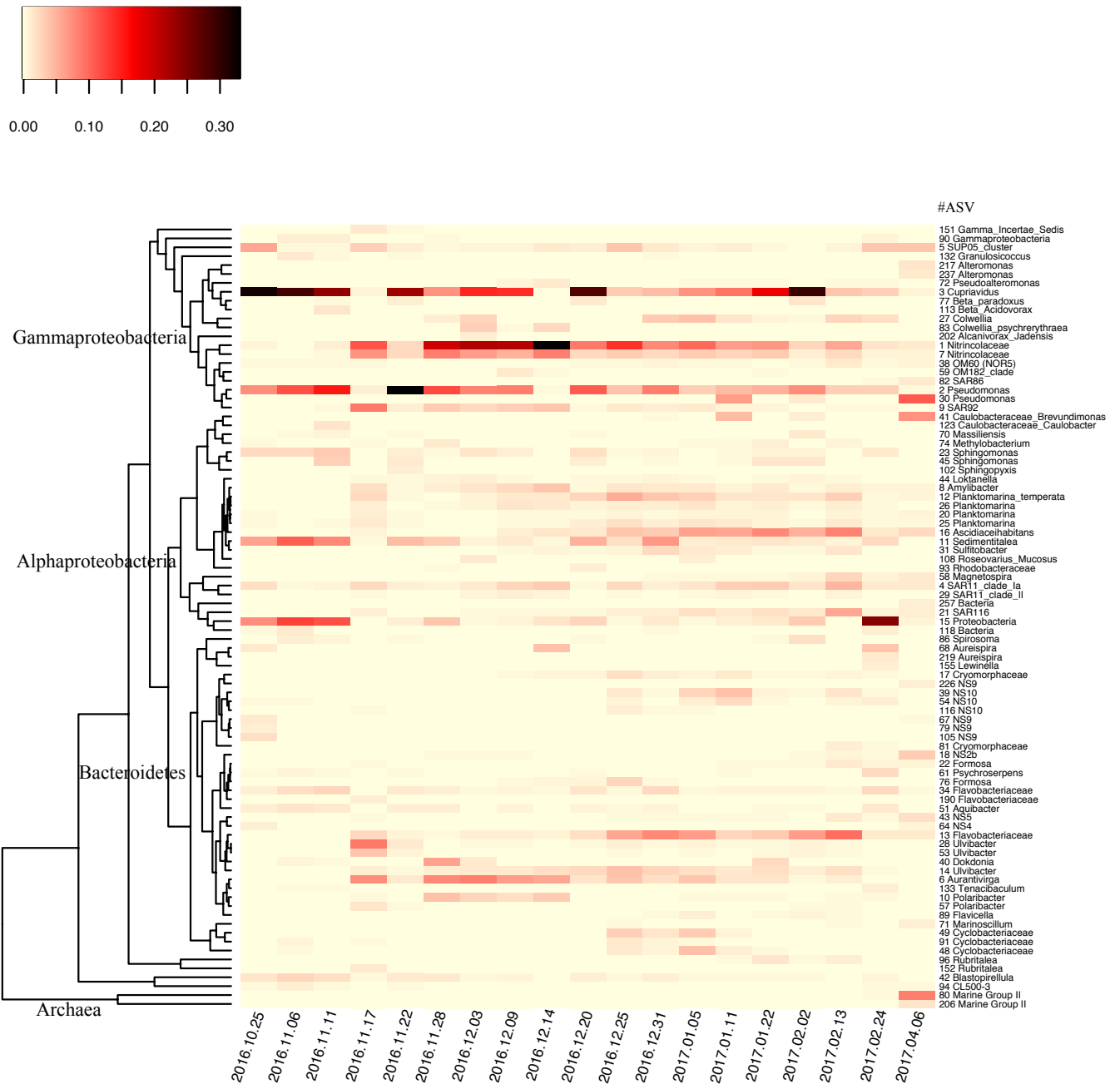
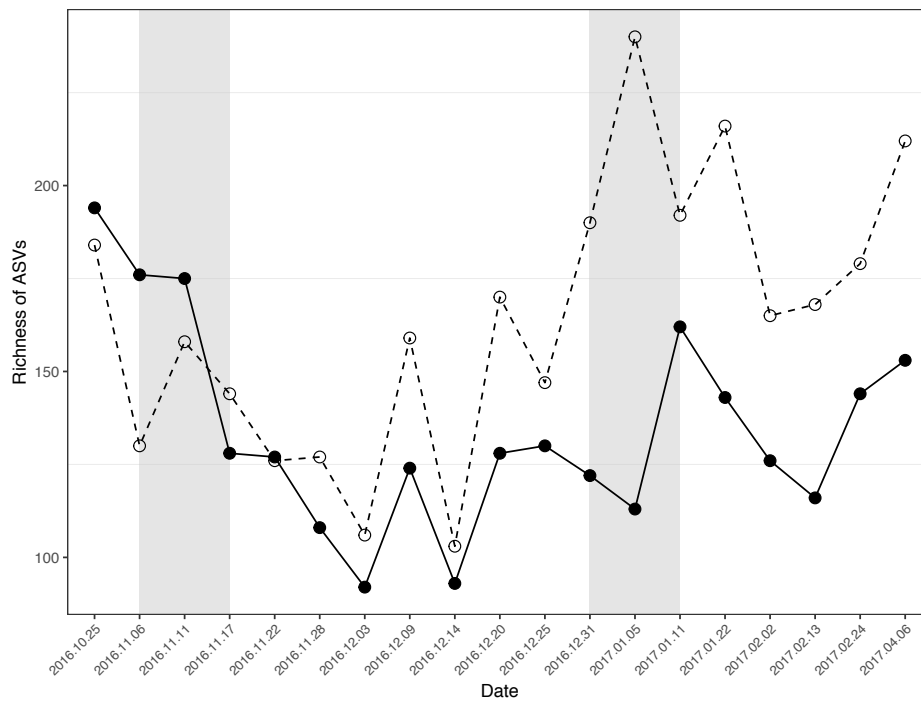


Fig. S3 Heatmap of dominant prokaryotic ASVs that account for $\geq 1\%$ of total relative abundance in at least one sampling date of the particle-attached community. Results of 19 time points are shown.

Chapter 2 Suppl.

(a)



(b)

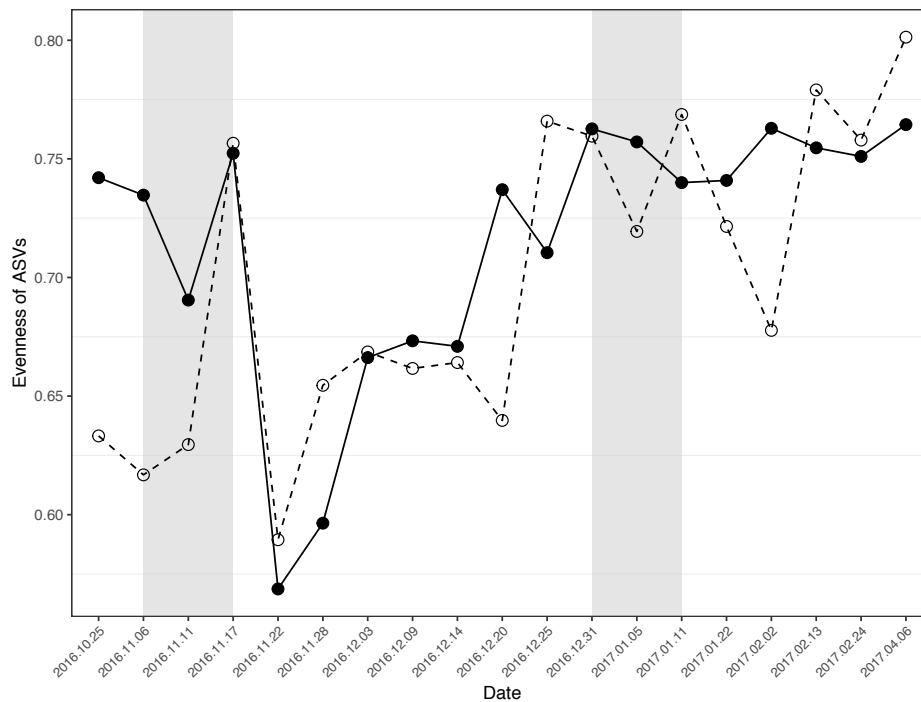


Fig. S4 Alpha-diversity indexes of prokaryotes (a) richness and (b) evenness. The solid and dashed lines represent free-living and particle-attached fraction respectively. Grey shades denote the time period of blooms.

Chapter 2 Suppl.

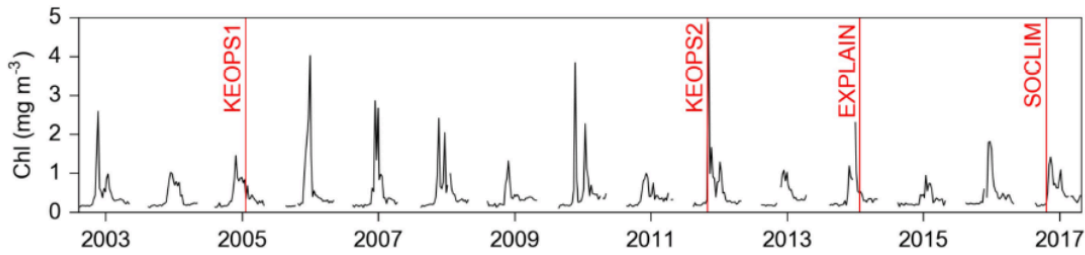


Fig. S5 Annual Chlorophyll *a* concentrations from satellite images (provided by Mathieu Rembauville). Red lines represent the sampling time of different cruises.

Table S1 Characteristics of diatoms (38 in total) observed in the present study.

Diatom taxon	Classification
<i>Actinocyclus curvatus</i>	Centric diatoms
<i>Asteromphalus hookeri</i>	Centric diatoms
<i>Chaetoceros atlanticus</i>	Centric diatoms
<i>Chaetoceros criophilus</i>	Centric diatoms
<i>Chaetoceros decipiens</i>	Centric diatom
<i>Chaetoceros dichaeata</i>	Centric diatoms
<i>Chaetoceros Hyalochaete</i>	Centric diatoms
<i>Corethron inerme</i>	Centric diatoms
<i>Corethron pennatum</i>	Centric diatoms
<i>Cylindrotheca closterium</i>	Pennate diatoms
<i>Dactyliosolen antarcticus</i>	Centric diatoms
<i>Eucampia antarctica</i>	Centric diatoms
<i>Fragilariopsis kerguelensis</i>	Pennate diatoms
<i>Fragilariopsis separanda/rhombica</i>	Pennate diatoms
<i>Fragilariopsis pseudonana</i>	Pennate diatoms
<i>Guinardia cylindrus</i>	Centric diatoms
<i>Manguinea fusiformis</i>	Pennate diatoms
<i>Membraneis challengerii</i>	Pennate diatoms
<i>Navicula directa</i>	Pennate diatoms
<i>Nitzschia bicapitata</i>	Pennate diatoms
<i>Nitzschia longissima</i>	Pennate diatoms
<i>Odontella weisflogii</i>	Centric diatoms
<i>Pseudo-nitzschia</i> spp.	Pennate diatoms
<i>Proboscia alata</i>	Centric diatoms
<i>Proboscia inermis</i>	Centric diatoms
<i>Rhizosolenia antennata</i> f. <i>semispina</i>	Centric diatoms
<i>Rhizosolenia chunii</i>	Centric diatoms
<i>Rhizosolenia polydactyla</i>	Centric diatoms

Chapter 2 Suppl.

Table S1 cont'd

Rhizosolenia simplex	Centric diatoms
Rhizosolenia styliformis	Centric diatoms
Small centric	Centric diatoms
Thalassionema nitzschioides var. lanceolata	Pennate diatoms
Thalassionema nitzschioides	Pennate diatoms
Thalassiosira antarctica	Centric diatoms
Thalassiosira gracilis	Centric diatoms
Thalassiosira gravida	Centric diatoms
Thalassiosira lentiginosa	Centric diatoms
Thalassiothrix antarctica	Pennate diatoms

Note: Classification information from this link https://keys.lucidcentral.org/keys/v3/australian-antarctic-division/antarctic_marine_diatoms.html

Table S2 Kits used for testing DNA extraction of 200 mL fixed seawater samples.

Test kit	Sample fixation				Control	
	HgCl ₂		Glutaraldehyde		Free-living	Particle-attached
	Free-living	Particle-attached	Free-living	Particle-attached		
	DNA concentration (ng μL^{-1})					
ZYMO	1.260	0.064	bd	0.019	nm	nm
QIAGEN	0.081	0.063	0.010	0.130	nm	nm
MoBio DNeasy Powerwater	0.328	0.267	0.387	0.156	0.463	0.429

Note: bd, below detection; nm, not measured.

CHAPTER THREE

Dissolved organic matter-prokaryote associations in contrasting Southern Ocean regions



Preface

This thesis chapter is part of the Heard Earth Ocean Biosphere Interactions Project (PI Mike Coffin, IMAS, Hobart, Australia). Within this collaborative project, I performed all molecular analyses, including the extraction of DNA and RNA, and the 16S rRNA gene amplification. I further carried out all bioinformatic procedures, and the statistical analyses to link DOM molecular formulae with prokaryotic communities. My work was carried out on seawater samples collected by Ingrid Obernosterer and Stéphane Blain during an oceanographic cruise from January to February 2016 aboard the Australian R/V Investigator. Patricia Medeiros (Univ. of Georgia, Athens, USA) performed all FT-ICR MS analyses. She provided a statistical analysis (PCA) of these results. She also helped improve previous versions of this chapter. Contextual data were provided by Philippe Catala (LOMIC, microbial abundance by flow cytometry), Jocelyne Caparros (LOMIC, dissolved organic carbon) and Bozena Wojtasiewicz and Tom Trull (UTAS-IMAS, Hobart, Australia, Chlorophyll *a* data).

Chapter 3

Abstract

We explored the associations between dissolved organic matter (DOM) and the total and active prokaryotic communities in surface waters of the Southern Ocean in summer. Fourier-transform ion cyclotron resonance mass spectrometry (FT-ICR MS) was used for the characterization of DOM and prokaryotic communities were described by Illumina sequencing of the 16S rRNA genes (DNA) and transcripts (RNA). The composition of DOM and of total and active prokaryotes revealed pronounced differences between sites located on the Kerguelen plateau (Antarctic Zone) and across a transect in Sub Antarctic waters. Correlations between DOM molecular formulae and prokaryotic communities were overall stronger for sites above than off the plateau. In Kerguelen plateau waters, the molecular formulae that were correlated with total prokaryotes showed the same correlation pattern as those associated with active prokaryotes. Molecular formulae containing nitrogen had a higher number of positive correlations on the plateau than that off the plateau. We further identified key taxa by focusing on strong positive correlations (Spearman, $r \geq 0.7$) between molecular formulae and prokaryotes. Active prokaryotic groups that strongly correlated with DOM were qualitatively similar in all samples, but quantitatively higher on the plateau. Members of Flavobacteriales were the main contributors to the total correlations, followed by Rhodobacterales and SAR11. Our results suggest that the composition of nitrogen-containing organic compounds shapes prokaryotic communities in Kerguelen surface waters in summer, most likely due to phytoplankton-derived DOM in this naturally iron-fertilized waters in the Southern Ocean.

Chapter 3

Introduction

Dissolved organic carbon (DOC) contributes a significant global reservoir of carbon (662 Gt C; Hansell et al., 2009), which is almost equal to atmospheric carbon dioxide (750 Gt C). Therefore, the production and the consumption of DOM significantly impact the ocean carbon cycle and climate. Autotrophs are the primary producers of marine dissolved organic matter (DOM). Part of the DOM can be consumed and remineralized by heterotrophic prokaryotes (Azam et al., 1983). The interaction between DOM and heterotrophic prokaryotes represents one of the fundamental relationships in the microbial loop, which strongly affects the carbon and nutrient cycling, and thereby regulates the productivity and stability of aquatic food webs (Kujawinski et al., 2011; Zhang et al., 2018).

DOM produced by autotrophs serves as growth substrate for prokaryotes by providing readily bioavailable substrates such as proteins (Carlson, 2002; Orsi et al., 2016), amino acid (Sarmiento et al., 2013) and polysaccharides (Biersmith and Benner, 1998; Biddanda and Benner, 1997). However, a large fraction of this biologically labile pool remains uncharacterized (Becker et al., 2014; Landa et al., 2014; Longnecker et al., 2015). Phytoplankton-derived DOM was shown to induce shifts in the composition of prokaryotic communities, both experimentally (Luria et al., 2014; Tada et al., 2017; Landa et al., 2018) or during phytoplankton blooms (reviewed by Buchan et al., 2014; Bunse and Pinhassi, 2017). The DOM-induced changes in prokaryotic community composition imply substrate preferences of prokaryotic taxa with varying metabolic capabilities (Cottrell and Kirchman, 2000; Alonso-Sáez and Gasol, 2007). In turn, DOM composition can be influenced by individual metabolic reactions catalyzed by prokaryotes (Alonso-Sáez et al., 2012) or be transformed by prokaryotic communities over time (Medeiros et al., 2017; Vorobev et al., 2018).

Understanding the relationships between DOM and prokaryotes needs the identification of molecular and biological composition of each of these components. DOM is a highly diverse mixture of compounds containing up to 20 000 molecular formulas in a single sample (Riedel and Dittmar, 2014). The characterization of DOM in high-resolution is achievable due to advanced techniques. Fourier-transform ion cyclotron resonance mass spectrometry (FT-ICR MS) was proposed nearly 20 years ago (Kujawinski et al., 2002). This approach identifies a large part of the DOM components (Seidel et al., 2014) which were uncharacterized by traditional chromatographic methods. It has been increasingly used to characterize DOM

Chapter 3

composition in diverse ecosystems, e.g., forest soils (Roth et al., 2015; Ide et al., 2017), lakes (Kellerman et al., 2014), rivers (Medeiros et al., 2015) and oceans (Hansman et al., 2015). Amplicon sequencing yields millions of reads for the identification of prokaryotes and is widely used for high-throughput assignments of prokaryotic taxonomy on a fine-scale phylogeny (Eren et al., 2015; Tikhonov et al., 2015; Callahan et al., 2016). The *in situ* associations between DOM and prokaryotes were recently investigated by combined multivariate statistics (Osterholz et al., 2016). Their study provided insight on the connections of molecular and biological information.

The objective of the present study was to investigate the associations between DOM and prokaryotes in different Southern Ocean provinces. Both the total and potentially active prokaryotic community was considered with the aim to identify differences in their respective associations with DOM.

Chapter 3

Material and Methods

Environmental context

The seawater samples were collected during the Heard Earth-Ocean-Biosphere-Interactions (HEOBI) cruise aboard the *R/V Investigator* between January 8th and February 26th 2016. A total of 13 stations were sampled for microbial parameters and 10 of them were additionally sampled for DOM-characterization (Fig. 1). These 10 sites were located in major Southern Ocean provinces. Four stations (UW-2, UW-3, UW-11 and UW-12) were located in the Subantarctic Zone (SAZ), 1 station (UW-4) was located in the Polar Front Zone (PFZ) and 5 stations were located in the Antarctic Zone (AAZ). All samples were collected at 5m depth using the underway seawater supply system. Seawater collection was done concurrently with CTD-deployments, whenever possible.

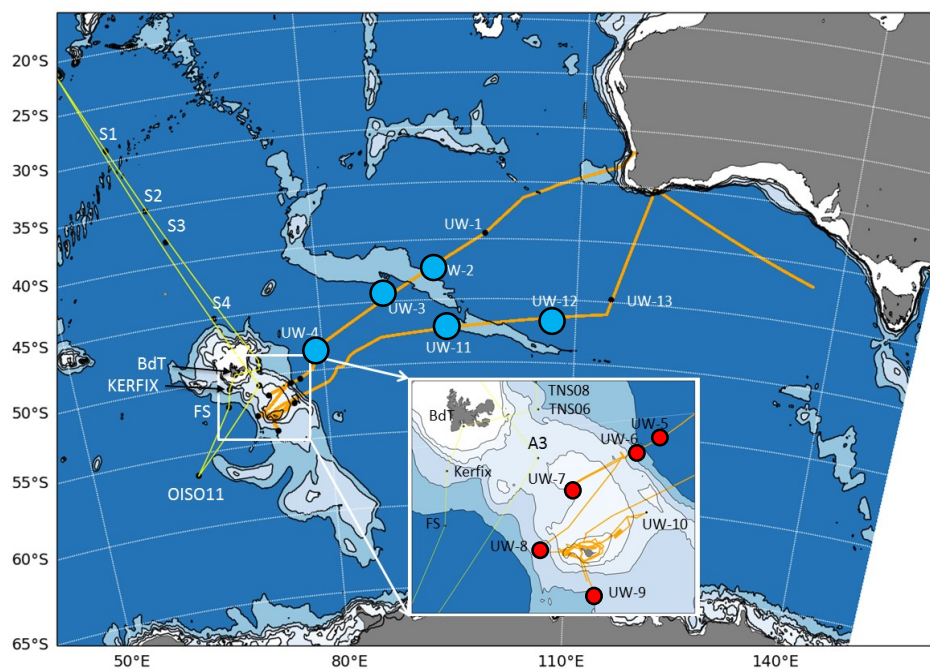


Fig. 1 Map of the cruise transect and study region of the Heard Earth-Ocean-Biosphere Interactions (HEOBI) cruise (January 8 to February 26 2016). Stations sampled for the present study are named UW-1 to UW-13. Stations highlighted by large colored dots were concurrently sampled for microbial parameters and DOM characteristics. Red and blue dots are samples considered in this chapter as “on” and “off” the Kerguelen plateau, respectively.

Chapter 3

DOM extraction and FT-ICR-MS analysis

Samples for DOM extraction were sequentially filtered through 0.8 μm (Polycarbonate Isopore filters, Nuclepore) and 0.2 μm (SuporPlus Membranes, Millipore). Solid-phase extraction was performed on PPL cartridges (Varian) (Agilent, Lake Forest, CA, USA) as described in Landa et al. (2014). Briefly, the $< 0.2 \mu\text{m}$ filtrate was acidified to pH 2 with 6N HCl, and 4L of the acidified filtrate was then passed over one pre-treated PPL cartridge (6 mL HPLC-grade methanol) at a flow rate of 3 mL min⁻¹. The PPL cartridge was then rinsed with 0.01 N HCl (36 mM) and air-dried. The PPL cartridges were placed in methanol-rinsed aluminium foil and stored at 4°C until further analyses. The extracted DOM was recovered by sequential elution with each 10 ml methanol (HPLC grade) into combusted 20 ml glass tubes at a flow rate of $< 2 \text{ ml min}^{-1}$. Elutes were dried in a Genevac Personal Evaporator (Genevac, Ipswich, UK) and then stored at -20°C in the dark until further analyses. We performed several blanks consisting of Milli-Q water that was acidified, passed through a PPL cartridge and further treated in the same manner as the seawater.

The molecular composition of the DOM extracts (200 mg C L⁻¹ in methanol) was analyzed on a 9.4 T Fourier transform-ion cyclotron resonance mass spectrometer (FT-ICR MS) with electrospray ionization (ESI; negative mode) at the National ICR Users' Facility at the National High Magnetic Field Laboratory (NHMFL, Florida State University, Tallahassee, FL). Sample processing was done as described in Vorobev et al. (2018) and Letourneau and Medeiros (2019). A total of 150 scans were accumulated for each sample. Each m/z spectrum was internally calibrated with respect to an abundant homologous alkylation series whose members differ in mass by integer multiples of 14.01565 Da (mass of a CH₂ unit) confirmed by isotopic fine structure (Savory et al., 2011), achieving a mass error of $< 0.4 \text{ ppm}$. Molecular formulae were assigned for masses in the range of 150 and 750 Da by applying the following restrictions: ¹²C₁₋₁₃₀ ¹H₁₋₂₀₀ O₁₋₁₅₀ ¹⁴N₀₋₄ S₀₋₂ P₀₋₁. Assignment of molecular formulae was performed by Kendrick mass defect analysis (Wu et al., 2004) with PetroOrg software (Corilo, 2015) and using the criteria described by Rossel et al. (2013). Only compounds with a signal-to-noise ratio of 6 or higher were used in the analysis to eliminate inter-sample variability based on peaks that were close to the limit of detection. The peak intensity of each molecular formula was normalized to the sum peak intensities of the total identified peaks in each sample. Repeated analysis of several of these samples revealed that differences in DOM composition due to instrument variability were substantially smaller than variability between samples.

Chapter 3

Microbial community characteristics

The abundance of heterotrophic and autotrophic prokaryotes and pico- and nanoeukaryotes was done by flow cytometric analyses on a BD FACS Canto (Marie et al., 2000; Obernosterer et al., 2008). Prokaryotic production was estimated by [³H]leucine incorporation applying the centrifugation method (Smith and Azam, 1992) as described in Obernosterer et al. (2008). Briefly, 1.5 mL samples were incubated with a mixture of [3,4,5-³H(N)] leucine (Perkin Elmer, 123.8 Ci mmol⁻¹; 7 nM final concentration) and nonradioactive leucine (13 nM final concentration). Controls were fixed with trichloroacetic acid (TCA; Sigma) at a final concentration of 5%. Samples were incubated for 2-3h in the dark at *in situ* temperature. Incubations were terminated with TCA (5% final concentration). The radioactivity incorporated into bacterial cells was measured aboard in a HIDEX scintillation counter.

Microbial community composition

For the analyses of the prokaryotic community composition, three 6 L biological replicates were collected at each site, filtered through 60 µm nylon screens, and then through 0.8 µm polycarbonate filters (47-mm diameter, Nuclepore, Whatman, Sigma Aldrich, St Louis, MO). Cells were then concentrated on 0.2 µm Sterivex filter units (Sterivex, Millipore, EMD, Billerica, MA) using a peristaltic pumping system (Masterflex L/S Easy-Load II). The Sterivex filter units were kept at -80°C until extraction.

DNA and RNA extraction and sequencing preparation

DNA and RNA were simultaneously extracted from one Sterivex filter unit using the AllPrep DNA/ RNA kit (Qiagen, Hilden, Germany) with the following modifications. Filter units were thawed and closed with a sterile pipette tip end at the outflow. Lysis buffer was added (40 mM EDTA, 50 mM Tris, 0.75 M sucrose) and 3 freeze and thaw cycles were performed using liquid nitrogen and a water bath at 65 °C. Lysozyme solution (0.2 mg ml⁻¹ final concentration) was added and filter units were placed on a rotary mixer at 37°C for 45 minutes. Proteinase K (0.2 mg ml⁻¹ final concentration) and SDS (1% final concentration) were added and filter units were incubated at 55 °C with gentle agitation every 10 minutes for 1 hour. To protect the RNA, 10 µl of β-mercaptoethanol was added to 1 ml of RLT plus buffer provided by the kit. To each filter unit, 1550 µl RLT plus-β-mercaptoethanol was added and inverted to mix. The lysate was

Chapter 3

recovered by using a sterile 5 ml syringe and loaded in three additions onto the DNA columns by centrifuging at 10,000 g for 30 seconds. DNA and RNA purification were performed following manufacturer's guidelines in which RNA was treated with DNase (Qiagen, Germany) to avoid DNA contamination after the first wash step.

RNA was converted to cDNA using SuperScript III Reverse Transcriptase according to the manufacturer's instructions. Prior to reverse transcription, quality of RNA samples was examined by PCR test with general primer sets 341F (5' - CCTACGGGNGGCWGCAG) and 805R (5'- GACTACHVGGGTATCTAATCC) for the prokaryotic 16S rRNA gene, followed by the examination of amplification products on 1% agarose electrophoresis. Residual DNA was removed from RNA samples by digestion with DNase. DNA and cDNA was amplified and pooled as described in Parada et al. (2016) with a modification to the PCR amplification step. Briefly, the V4 - V5 region of the 16S rRNA gene from DNA and cDNA samples was amplified with the primer sets 515F-Y (5' - GTGYCAGCMGCCGCGGTAA) and 926R (5' - CCGYCAATTYMTTTRAGTTT). Triplicate 10 µl reaction mixtures contained 2 µg DNA, 5 µl KAPA2G Fast HotStart ReadyMix, 0.2 µM forward primer and 0.2 µM reverse primer. Cycling reaction started with a 3min heating step at 95 °C followed by 22 cycles of 95 °C for 45 s, 50 °C for 45 s, 68 °C for 90 s, and a final extension of 68 °C for 5 min. The presence of amplification products was confirmed by 1 % agarose electrophoresis and triplicate reactions were pooled. Each sample were added with unique paired barcodes. The Master 25 µl mixtures contained 1 µl PCR product, 12.5 µl KAPA2G Fast HotStart ReadyMix (Kapa Biosystems, USA), 0.5 µl barcode 1 and 0.5 µl barcode 2. The cycling program included a 30 s initial denaturation at 98°C followed by 8 cycles of 98 °C for 10 s, 60 °C for 20 s, 72 °C for 30 s, and a final extension of 72 °C for 2 min. 3 µl PCR product were used to check for amplification on 1% agarose electrophoresis. The remaining 22 µl barcoded amplicon product was cleaned to remove unwanted dNTPs and primers by Exonuclease I and Shrimp Alkaline Phosphatase at 37 °C, 30 min for treatment and 85 °C, 15 min to inactivate. The concentration of double-stranded DNA was quantified by PicoGreen fluorescence assay (Life Technologies). After calculating the PCR product concentration of each samples, they were pooled at equal concentrations manually. The pooled PCR amplicons were concentrated using Wizard SV gel and PCR clean-up system (Promega, USA) according to the manufacturer's protocol. 16S rRNA gene amplicons were sequenced with Illumina MiSeq 2 x 300 bp chemistry on one flow-cell at Fasteris SA sequencing service (Switzerland). Mock community DNA (LGC standards,

Chapter 3

UK) was used as a standard for subsequent analyses and considered as a DNA sample for all treatments.

Data analysis of prokaryotes

All samples from the same sequencing run were demultiplexed by Fasteris SA and barcodes were trimmed off. A total number of 3 424 946 sequences was obtained. Processing of sequences was performed using the DADA2 pipeline (Callahan et al., 2016; version 1.10) in R with following parameters: trimLeft=c(19,20), truncLen=c(240,200), maxN=0, maxEE=c(2,2), truncQ=2. Briefly, the pipeline combines the following steps: filtering and trimming, dereplication, sample inference, chimera identification, and merging of paired-end reads (Callahan et al., 2016). It provides exact amplicon sequence variants (ASVs) from sequencing data with one nucleotide difference instead of building operational taxonomic units based on sequence similarity. ASVs were assigned against SILVA release 132 database (Quast et al., 2012). Sequences assigned to chloroplast and mitochondria were removed prior to subsequent analyses.

Statistical analyses

All statistical analyses were performed using R 3.4.2 version. The ASV and taxa tables were combined into one object using phyloseq R package (McMurdie and Holmes, 2013). DOM and DNA/RNA compositional data were obtained based on FT-ICR MS and Illumina sequencing, respectively. For the overview of the DOM data, van Krevelen diagrams and bar charts were generated by basic R functions and ggplot2 package. Principal component analysis (PCA; provided by Patricia Medeiros using Matlab) was used to compute the contributions of the formulae (loadings) to the variance of DOM data. Standard deviation (std) of the loadings of the PCA was calculated and the formulae with loadings larger than 1 std or smaller than -1 std were selected. Bar plots were made to show the distinct DOM compositions between on and off the plateau based on the subset of DOM shown each by the type of atoms (C, N, S). For the overview of the prokaryotic data, dendrograms were performed using hclust() with method “average” in the Vegan package (Oksanen et al., 2015). Bray-Curtis dissimilarity matrices were generated via vegdist() function. Data were Hellinger transformed prior to the analyses based on Bray-Curtis dissimilarity (Legendre and Gallagher, 2001). Bray-Curtis dissimilarity was calculated for DOM intensity formulae and DNA relative abundances using Vegan package.

Chapter 3

For the correlation analysis between DOM and prokaryotes, 10 samples with DOM assignment available were included, in which 5 (UW-5 to UW-9) were considered as samples on the plateau and 5 (UW-2 to UW-4 and UW-11 and UW-12) were considered as samples off the plateau. Thus, we obtained two sub data sets (i.e., one containing samples on the plateau and one containing samples off the plateau) for DOM, DNA and RNA community composition each. Principal coordinate analysis (PCoA) was used to summarize the variation in each sub data set based on the first few significant axes. These axes explained the high variance of each data set and were selected by a broken stick model. PCoA axis 1 (78.3% of the total variation) for DOM on the plateau and PCoA axes 1-2 (75.1-87.6% of the total variation) for other data sets on and off the plateau were kept. These selected subsets of principal coordinates were fed into a canonical correlation analysis (CCorA) using Vegan package. The correlations between DOM and DNA/RNA were computed in a symmetric way. The canonical variates which are scores of the samples on the canonical axes from each data set were extracted from corresponding canonical space and correlated back to the original data sets. Van Krevelen plots and barplots were used to visualize the correlations between DOM and DNA/RNA, respectively. Key prokaryotic groups were retrieved based on strong (Spearman, $r \geq 0.7$; $P \leq 0.05$) positive correlations.

Results and discussion

Environmental context

In surface waters (5m) temperature was highest in the STZ and varied between 8.8°C and 12.3°C at stations located in the SAZ. It decreased from 6.9°C in the PFZ to 5.9°C at the northernmost station in the AAZ and dropped to 2.6°C at the southernmost station (Table 1). Chlorophyll *a* showed the highest concentration at station (UW-7) in the AAZ within the available data. *Synechococcus* had highest abundance at the station in the STZ and overall decreased towards the south with much lower abundances at stations in the AAZ. A similar north to south gradient was also observed for prokaryotic abundance. Abundances of pico- and nano-eukaryotes were highest at a station in the SAZ. Pico-eukaryotes showed the lowest abundance at stations in the AAZ. Nano-eukaryotes had the moderate abundance at stations in the AAZ and lowest abundance at station in the SAZ.

Chapter 3

Table 1 Environmental and biological parameters of the stations sampled during the HEOBI cruise. Stations are listed according to zones. STZ-Subtropical zone, SAZ-Subantarctic Zone, PFZ-Polar Frontal Zone, AAZ-Antarctic Zone.

	Station	Date	Lat (°S) /Long(°E)	Temp (°C)	Chla ($\mu\text{g L}^{-1}$)*	DOC (μM)	Syne ($\times 10^2$ cells mL^{-1})	Pico-eukaryotes ($\times 10^3$ cells mL^{-1})	Nano-eukaryotes ($\times 10^3$ cells mL^{-1})	PA ($\times 10^5$ cells mL^{-1})	PHP (pmol L^{-1} h^{-1})
STZ	UW-1	12/01/2016	39.495/ 99.386	15.9	0.302	63	134.3	3.81	2.17	14	34
SAZ	UW-2	14/01/2016	42.668/ 92.476	12.1	NA	59	112	5.69	2.26	11.9	40
	UW-3	15/01/2016	44.511/ 88.297	10.1	NA	54	89.6	10.4	7.04	9.64	34
	UW-11	16/02/ 2016	47.27/ 95.439	8.8	NA	46	57.2	3.16	5.93	9.24	170
	UW-12	18/02/2016	46.48/ 106.9	10.1	NA	46	84.1	4.19	1.57	10.3	21
	UW-13	19/02/2016	44.506/ 114.246	12.3	NA	49	22.4	5.06	2.06	10.8	35
PFZ	UW-4	17/01/2016	48.278/ 79.371	6.9	0.644	49	9.8	4.98	6.91	7.05	35
AAZ	UW-5	19/01/2016	50.53/ 77.011	5.9	0.422	47	1.1	4.71	4.43	6.17	51
	UW-6	20/01/2016	50.788/ 75.786	3.1	0.521	43	0.131	0.0944	2.00	3.54	19
	UW-7	21/01/2016	51.506/ 73	4.1	1.315	47	0.026	0.176	3.78	4.10	47
	UW-8	23/01/2016	52.927/ 71.372	3.3	0.840	44	0.026	0.152	2.84	4.19	16
	UW-9	01/02/2016	54.17/ 73.658	2.6	0.336	NA	0.157	0.38	3.19	3.90	9
	UW-10	10/02/2016	52.298/ 76.004	2.96	NA	40	0.026	0.115	2.01	4.73	21

Chapter 3

Note: *Data from Wojtasiewicz et al. (Submitted).

NA, not available.

Syne - Synechococcus

PA - Prokaryotic abundance

PHP - Prokaryotic Heterotrophic Production

Chapter 3

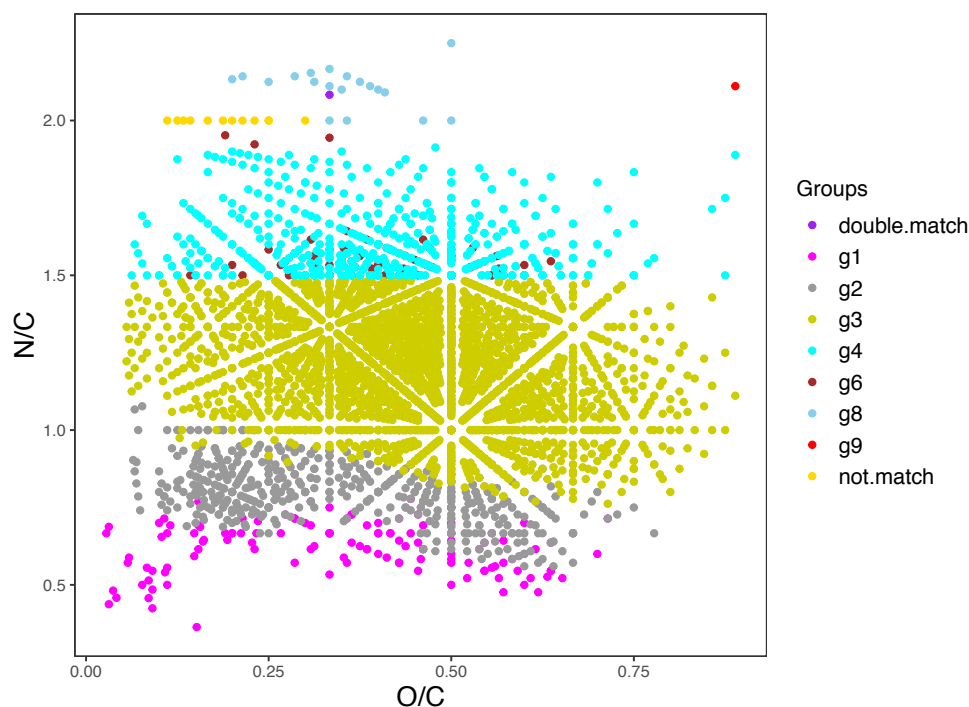


Fig. 2 Van Krevelen diagram of total DOM formulae of all samples pooled. The definition of DOM groups follows those described in Šantl-Temkiv et al. (2013) and modified by Seidel et al. (2014). The groups detected in the present study refer to Table 2.

Table 2 Definition of DOM groups. AImod – modified aromaticity index

Groups	Definition
g1	AImod > 0.66, polycyclic aromatics (PCAs)
g2	$0.5 < \text{AImod} \leq 0.66$, highly aromatic compounds
g3	$\text{AImod} \leq 0.5$ and $\text{H/C} < 1.5$, highly unsaturated compounds
g4	$1.5 \leq \text{H/C} < 2.0$ and $\text{N} = 0$, unsaturated aliphatic compounds with no N
g6	$1.5 \leq \text{H/C} < 2.0$ and $\text{N} > 0$, unsaturated aliphatic compounds containing N
g7	$\text{N} > 0$, compounds containing N
g8	$\text{S} > 0$, compounds containing S
g9	$\text{P} > 0$, compounds containing P
g10	$\text{N} > 0$ and $\text{S} > 0$, compounds containing N and S
double.match	compounds that are assigned to more than one group. In this study, it includes g7, g8 and g10
not.match	compounds that are not assigned to any group

Note: We did not detect g5 in our data. AImod determined according to Koch and Dittmar (2006, 2016).

Chapter 3

Molecular DOM composition

In total, we identified 4576 DOM molecular formulae via FT-ICR MS for the 10 samples. The ratio of intensity-weighted molecular mass to charge was in the range of 158 to 750 Da. All formulae were grouped and are visualized using a van Krevelen diagram based on O/C and H/C ratios (Kim et al., 2003; Seidel et al., 2014) (Fig. 2 and Table 2). Highly unsaturated compounds (g3) were the most numerous contributors to the total DOM molecules (min-max among stations 84.7-92.7 %) (Fig. 3) with a wide range of O/C (0.06-0.89) and H/C (0.76-1.48) ratios. Unsaturated aliphatic compounds (g4 and g6) that could potentially contain unsaturated fatty acids (Šantl-Temkiv et al., 2013) accounted for a lower fraction of the total DOM formulae (sum of g4 and g6 among stations 5.5-11.6%). A substantial fraction of the DOM compounds fell into the formula class of CHO in all samples (on average 83%), followed by CHON and minor contributions from CHOS (Fig. 4).

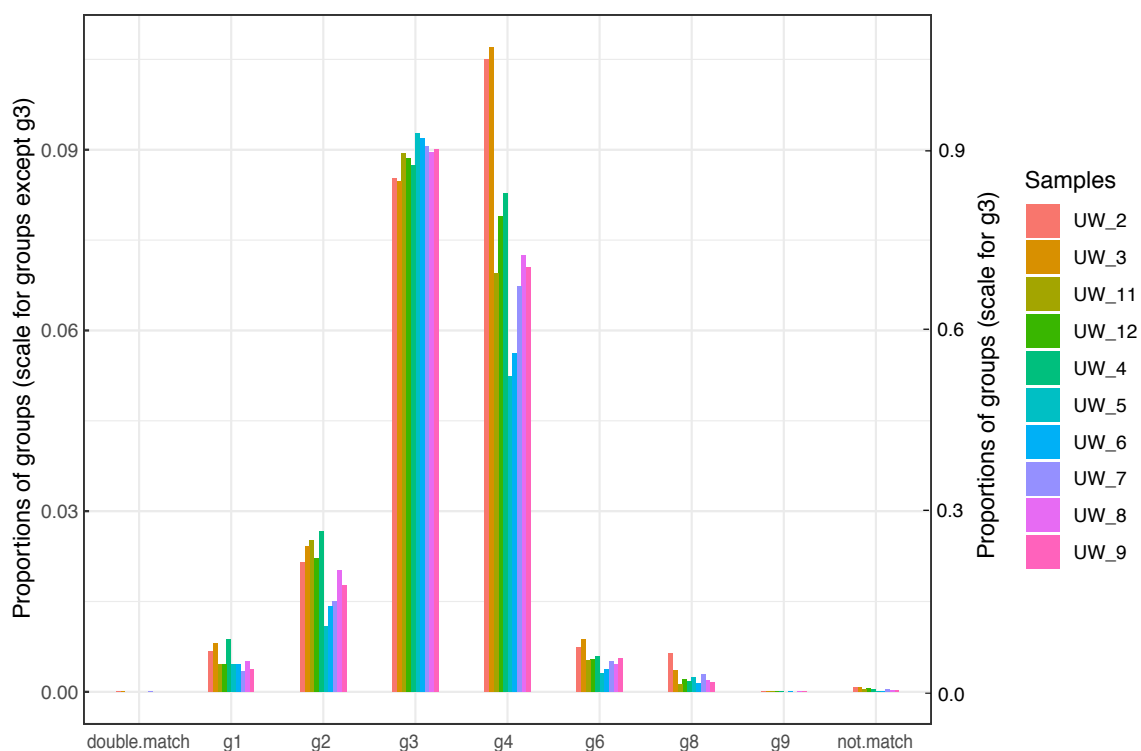


Fig. 3 Relative contribution of each DOM group to the total DOM data set at each site. Note different scales for g3 (right y-axis) and the other groups (left y-axis).

Chapter 3

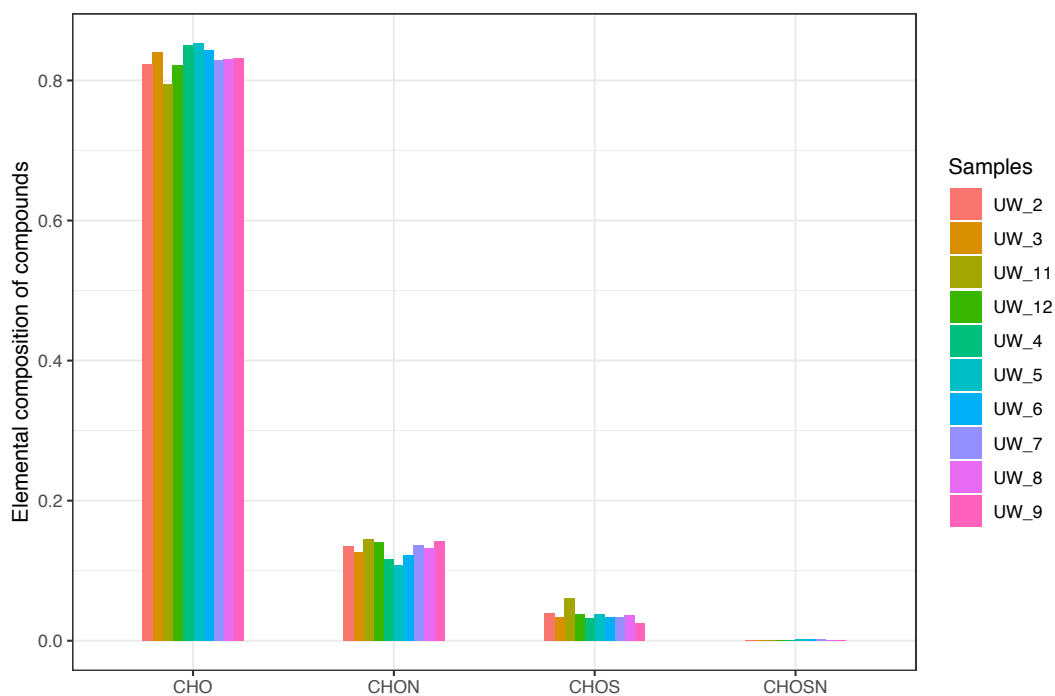


Fig. 4 Contribution of formula classes at each site. CHO-compounds containing C, H and O; CHON – compounds containing C, H, O and N; CHOS- compounds containing C, H, O and S, CHOSN - compounds containing C, H, O, S and N.

The highly similar patterns in DOM composition based on these general features revealed by FT-ICR MS is consistent with previous studies across large spatial scales and depth layers (e.g., Hansman et al., 2015). To investigate in more detail potential differences in DOM composition between samples, we employed principal component analysis (PCA) to the total DOM data set. Samples were clearly separated in two groups (Fig. 5a). One group corresponded to samples collected in the AAZ above the Kerguelen plateau (UW-5 to UW-9) and one group was composed of samples originating from the SAZ and the PFZ (UW-2 to UW-4 and UW-11 and UW-12). In the following, we grouped the seawater collected in the AAZ as samples collected on the Kerguelen plateau, and the seawater collected in the SAZ and PFZ as off-plateau samples based on the first component of PCA which contributed most of the variance of DOM data (24% to the total variance; Fig. 5a). Samples had a smaller range of the number of C atoms in molecule on the plateau (10-20) than that off the plateau (~6-40) (Fig. 5b). Samples on the plateau were enriched in compounds with various numbers of N atoms (Fig. 5c). They were also enriched with compounds containing one S atom, while samples off the plateau were relatively enriched with compounds with zero or two S atoms (Fig. 5d).

Chapter 3

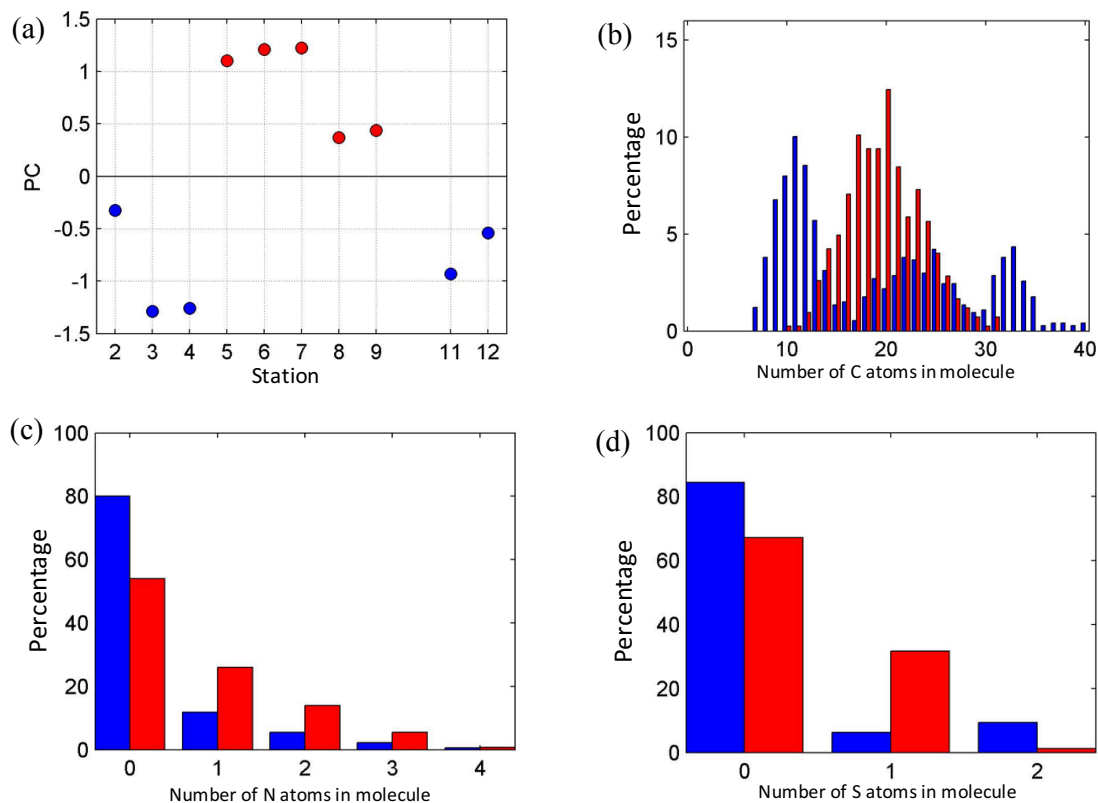


Fig. 5 (a) Principal component analysis of DOM composition. Scores of the first principal component are shown color coded. Red and blue dots represent samples on and off the plateau respectively. (b-d) The fraction of formulae with C, N and S for these formulae selected by PCA as enriched on (red) and off (blue) the plateau.

Composition of total and active prokaryotic communities

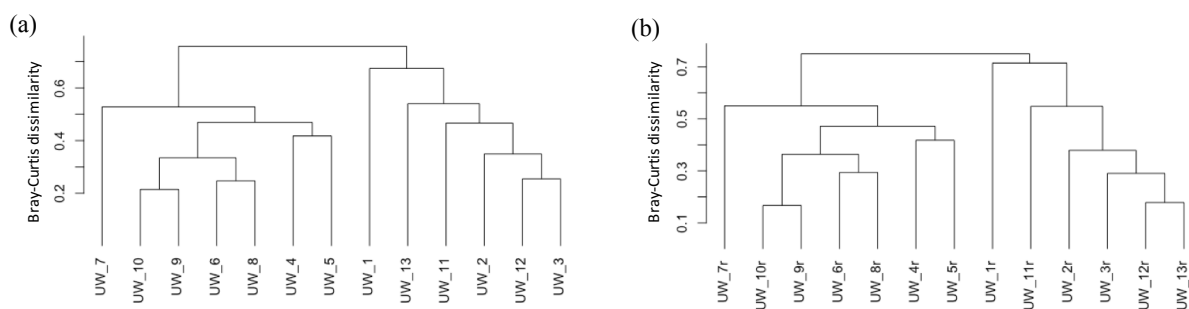


Fig. 6 Dendrograms of (a) total and (b) active prokaryotic communities based on Bray–Curtis dissimilarity.

From the 13 stations, we obtained a total of 36 and 34 subsamples including biological replicates for the total (DNA) and active (RNA) prokaryotic communities, respectively. The

Chapter 3

biological triplicates from each station were mostly clustered together (Fig. S1 and S2). One replicate of the total prokaryotic community of sample UW-8 and UW-11, and one replicate of the active prokaryotic community of sample UW-12 and UW-13 were removed because of their high dissimilarities. For the subsequent illustrations and analyses, the biological replicates were pooled separately for the DNA and RNA data sets and the mean relative abundance was calculated for each ASV. In total, we obtained 2 190 ASVs after removing singletons from the total data set. 723 ASVs were shared among the DNA and RNA data sets, with 1 323 and 1 590 ASVs obtained from DNA and RNA samples, respectively. The total and active prokaryotes revealed a similar clustering (Fig. 6). Similar to the pattern of the compositional DOM data, samples on and off the plateau were significantly different for both the total and active communities (ANOSIM R 0.77, P=0.002 for DNA; ANOSIM R 0.77, P=0.001 for RNA). Considering only 10 samples used for DOM analyses, samples on and off the plateau were also significantly different for both the total and active communities (ANOSIM R 0.90, P=0.004 for DNA; ANOSIM R 0.88, P=0.007 for RNA). In both cases, UW-4 was clustered with the on the plateau samples, in contrast to DOM composition (Fig. 6).

According to ASV abundance, sample assemblages were dominated by Bacteroidetes (DNA 44% of the sequences of all samples pooled, RNA 39%), Alphaproteobacteria (DNA 34%, RNA 38%) and Gammaproteobacteria (DNA 17%, RNA 17%), with Flavobacteriales (DNA 43%, RNA 38%), SAR11 (DNA 17%, RNA 13%)/ Rhodobacterales (DNA 13%, RNA 20%) and Cellvibrionales (DNA 4%, RNA 5%) as major sub-taxa respectively (Fig. 7; Fig. 8). Dominant ASVs (i.e., $\geq 1\%$ of the sequences in at least sample) represented similar proportions of the total (DNA) and active (RNA) communities at a given site. For clarity, the following brief description is focused on DNA data (Fig. 7) and major differences between DNA and RNA is also noted. Within Bacteroidetes, dominated by Flavobacteriaceae, genera *Polaribacter*, *Aurantivirga* and *Ulvibacter* were abundant on the plateau. NS2b was relatively abundant off the plateau. Formosa, NS4 and NS5 were widespread in both, samples on and off the plateau. Within Alphaproteobacteria, SAR11 was the most abundant taxon and was present in all sampling stations. SAR11 Ia contributed 13 % (RNA 15 %) of the total sequences. Interestingly, SAR11 IV was abundant off the plateau. *Planktomarina* belonging to Rhodobacterales was dominant in samples on the plateau. AEGEAN-169 marine group belonging to Rhodospirillales was only abundant off the plateau. Within Gammaproteobacteria, SAR92 and SUP05 were abundant on the plateau. Various ASVs of SAR86 were present on and off the plateau. In addition, *Synechococcus* was also observed off the plateau and was absent on the plateau.

Chapter 3

Members of NS10 marine group were abundant on the plateau of the RNA data set (Fig. 8), while they were absent in the DNA data set (Fig. 7).

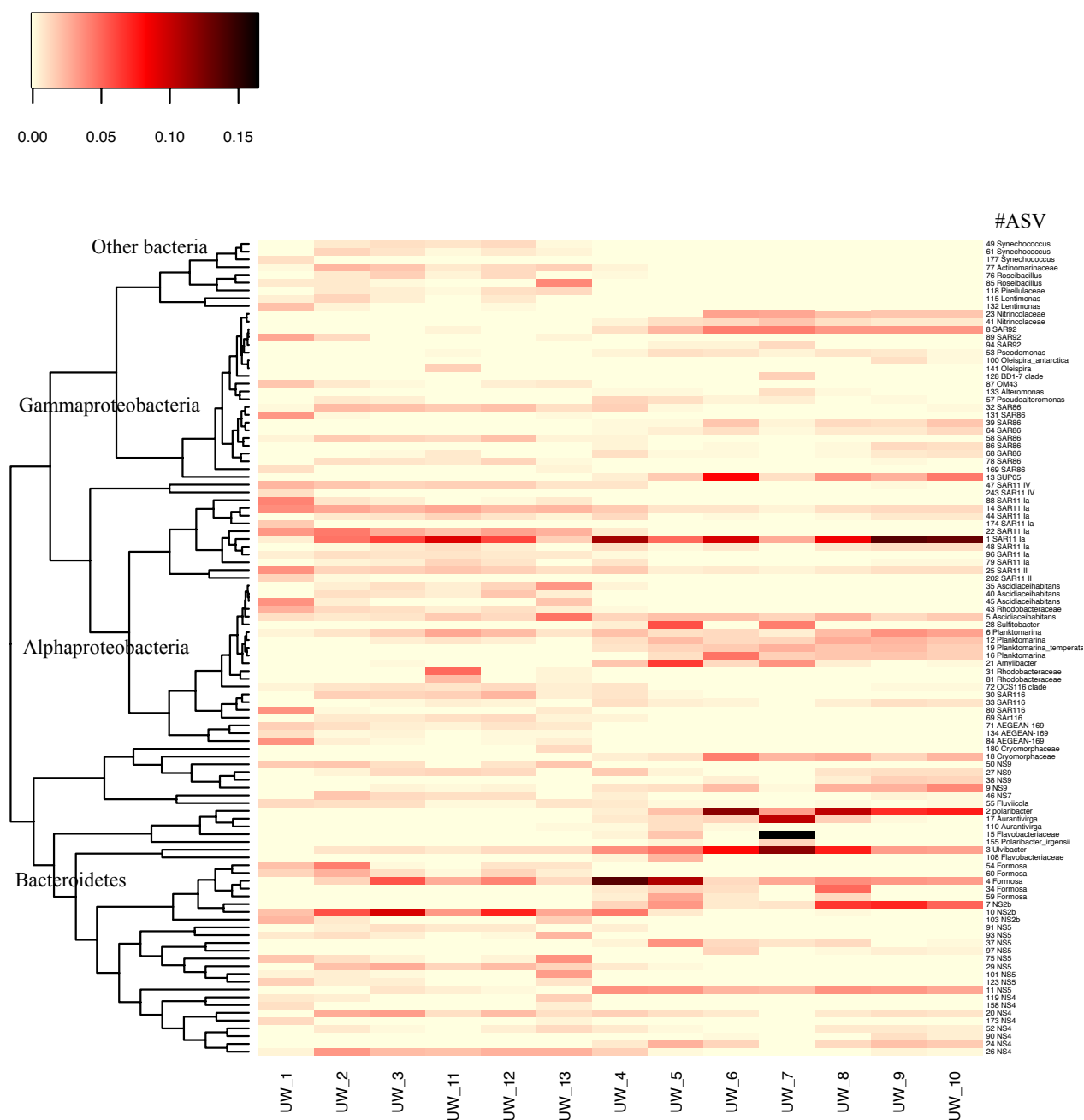


Fig. 7 Heatmaps of dominant prokaryotic ASVs that account for $\geq 1\%$ in at least one sample of total (DNA) prokaryotic community.

Chapter 3

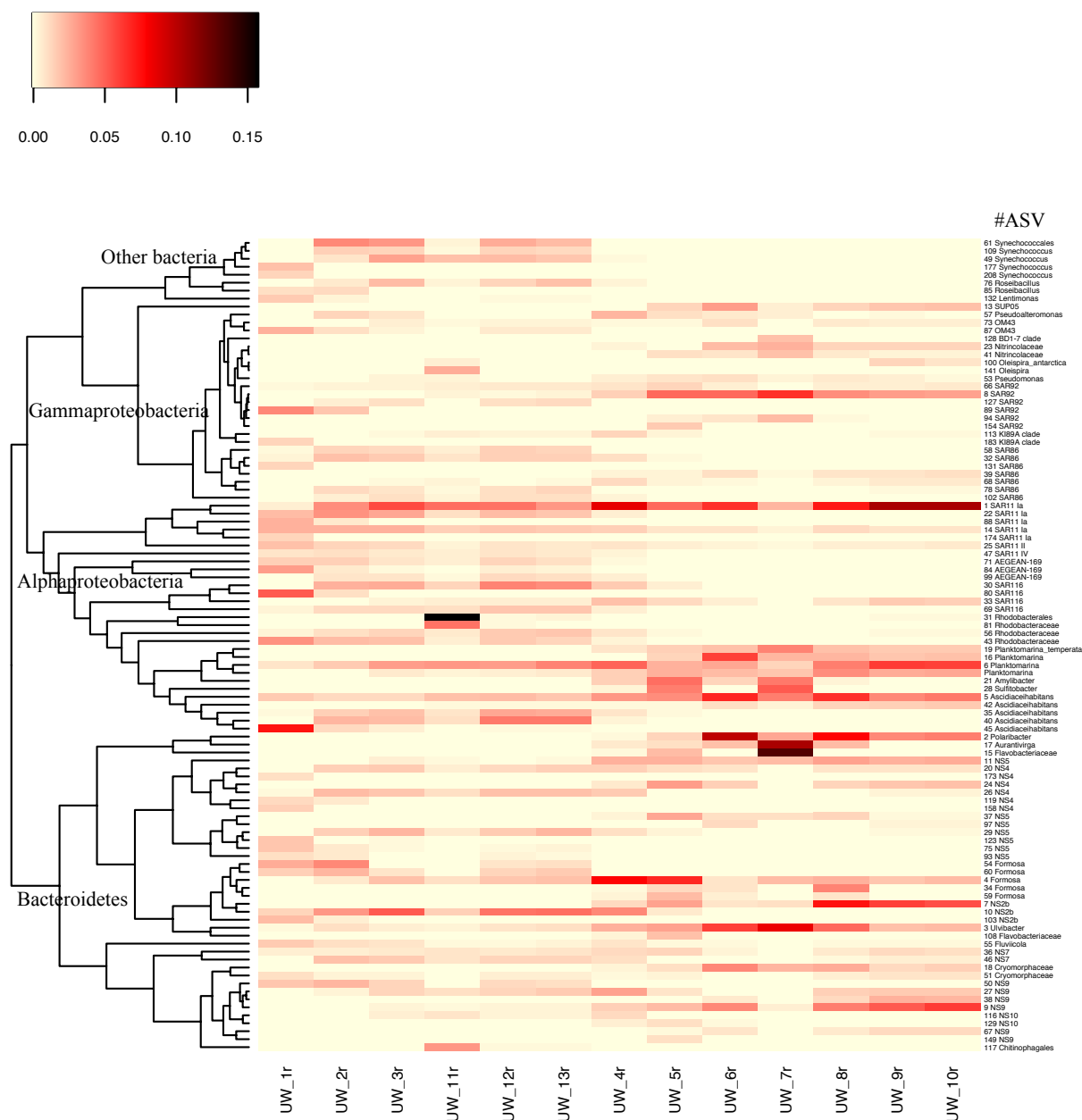


Fig. 8 Heatmaps of dominant prokaryotic ASVs that account for $\geq 1\%$ in at least one sample of active (RNA) prokaryotic community.

Linking DOM composition and prokaryotic communities

The correlations between DOM molecular formulae and prokaryotic ASVs were investigated by statistical analyses combining PCoA and CCorA and illustrated using van Krevelen diagrams according to O/C and H/C ratios (Osterholz et al., 2016). To reduce the influence of coincidence between molecules with the same O/C and H/C ratios, we highlighted the

Chapter 3

barycenter of each group of correlations (Fig. 9). The correlations on the plateau were overall stronger than those off the plateau for both total and active prokaryotic communities (Fig. 9). Similar DOM-prokaryote correlation patterns were found for total and active prokaryotic communities (Fig. 9a, c). Most of the molecular formulae with positive correlations with the total/active prokaryotic community have variable H/C and low-to-moderate O/C ratios, partially including the lipid-like and protein-like compounds, defined in g4 and g6 (Fig. 9a, c; Table 2; Wu et al., 2018). Slightly differences in the correlations between molecular formulae and total and active prokaryotic communities were observed off the plateau (Fig. 9b, d).

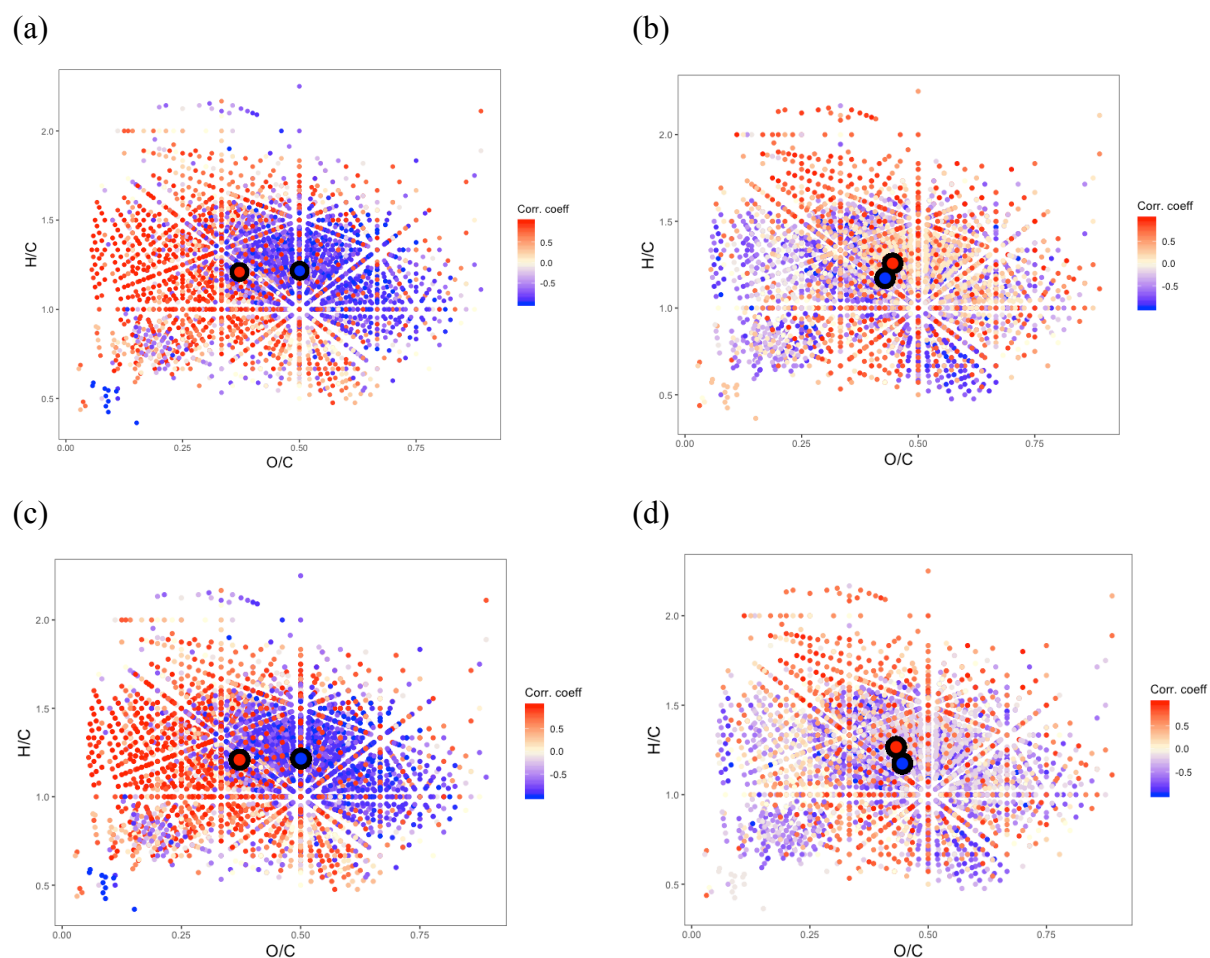


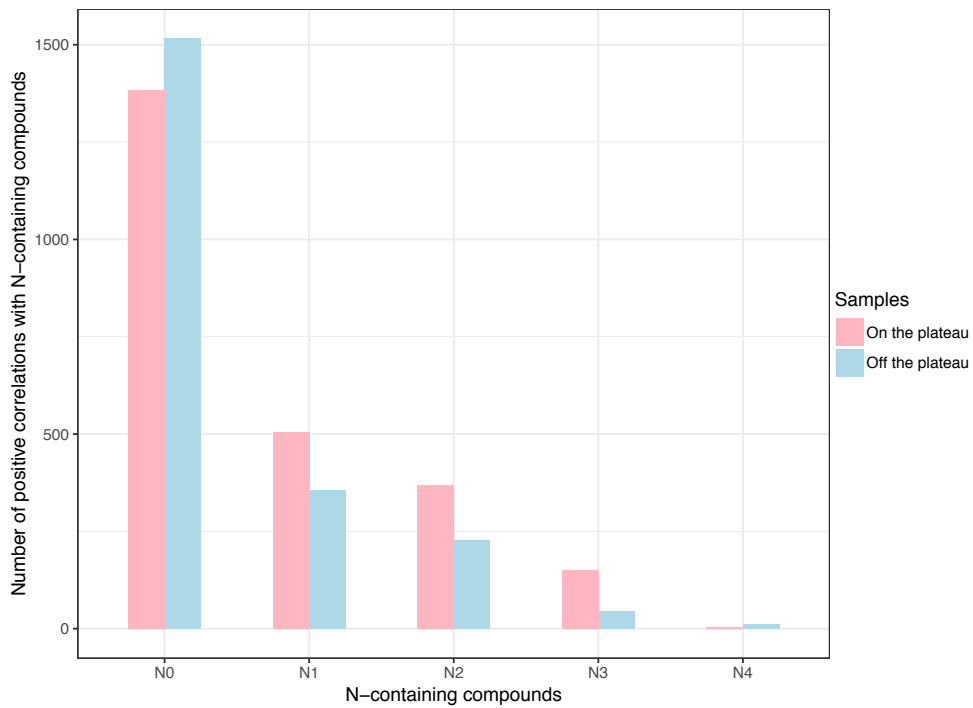
Fig. 9 Van Krevelen diagrams showing the correlations of molecular formulae (relative intensities) with the canonical axis associating DOM composition with DNA-based prokaryotic community composition (a) on the plateau and (b) off the plateau, and RNA-based prokaryotic community composition (c) on the plateau and (d) off the plateau. Large red and blue dots represent the barycenters of molecular formulae with positive and negative correlations, respectively.

Chapter 3

On the plateau, molecular formulae with positive correlations to the total/ active prokaryotic community showed higher N content than that off the plateau (Fig. S2). Further, the positive correlations between the N containing molecular formulae and the prokaryotic communities appear to be separated into three layers based on the N content (Fig. S2, N/C ratio). The number of positive correlations with N-containing molecular formulae confirmed the visual difference of DOM-prokaryote correlations on and off the plateau for both total and active prokaryotic communities (Fig. 10). In addition, off the plateau, a higher number of positive correlations with N-containing molecular formulae were observed for active prokaryotic community than that for total prokaryotic community. By contrast, the S-containing molecular formulae showed a more variable pattern (Fig. S3). This suggests that N-containing compounds such as peptides and lipids and prokaryotes are tightly linked. Nitrogen-rich compounds likely represent recently synthesized molecules (Benner, 2002; Kujawinski et al., 2011), and thereby present a bioavailable source for prokaryotes (Kaiser and Benner, 2008).

Chapter 3

(a)



(b)

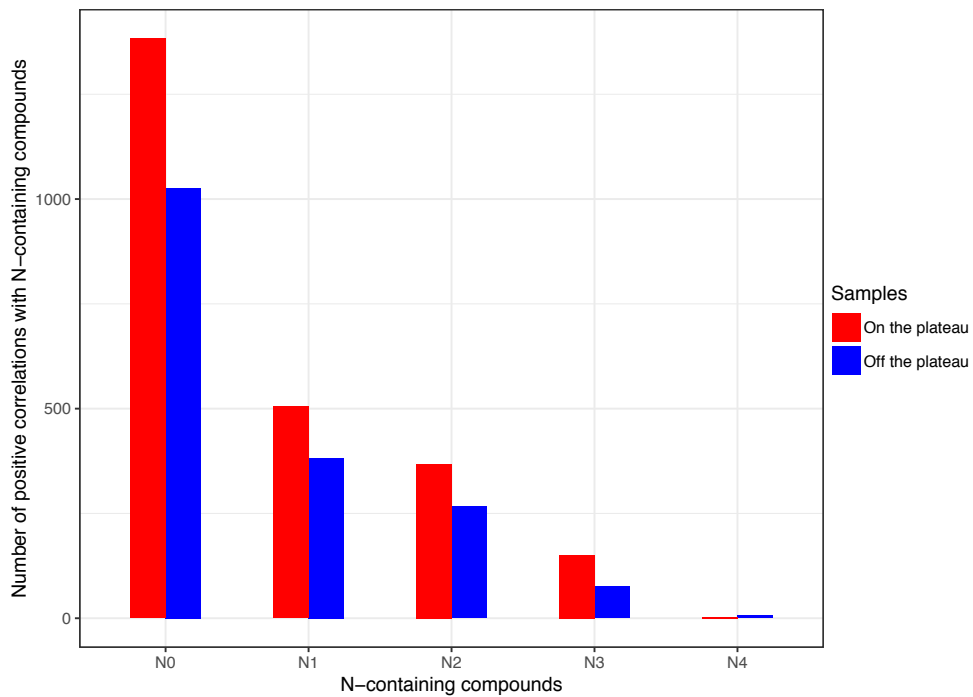


Fig. 10 Number of positive correlations with the canonical axis associating (a) total or (b) active prokaryotic community composition and DOM molecular formulae containing nitrogen (N). (a) Pink and light blue bars represent DNA-based correlations on and off the plateau, respectively. (b) Red and blue bars represent RNA-based correlations on and off the plateau, respectively.

Chapter 3

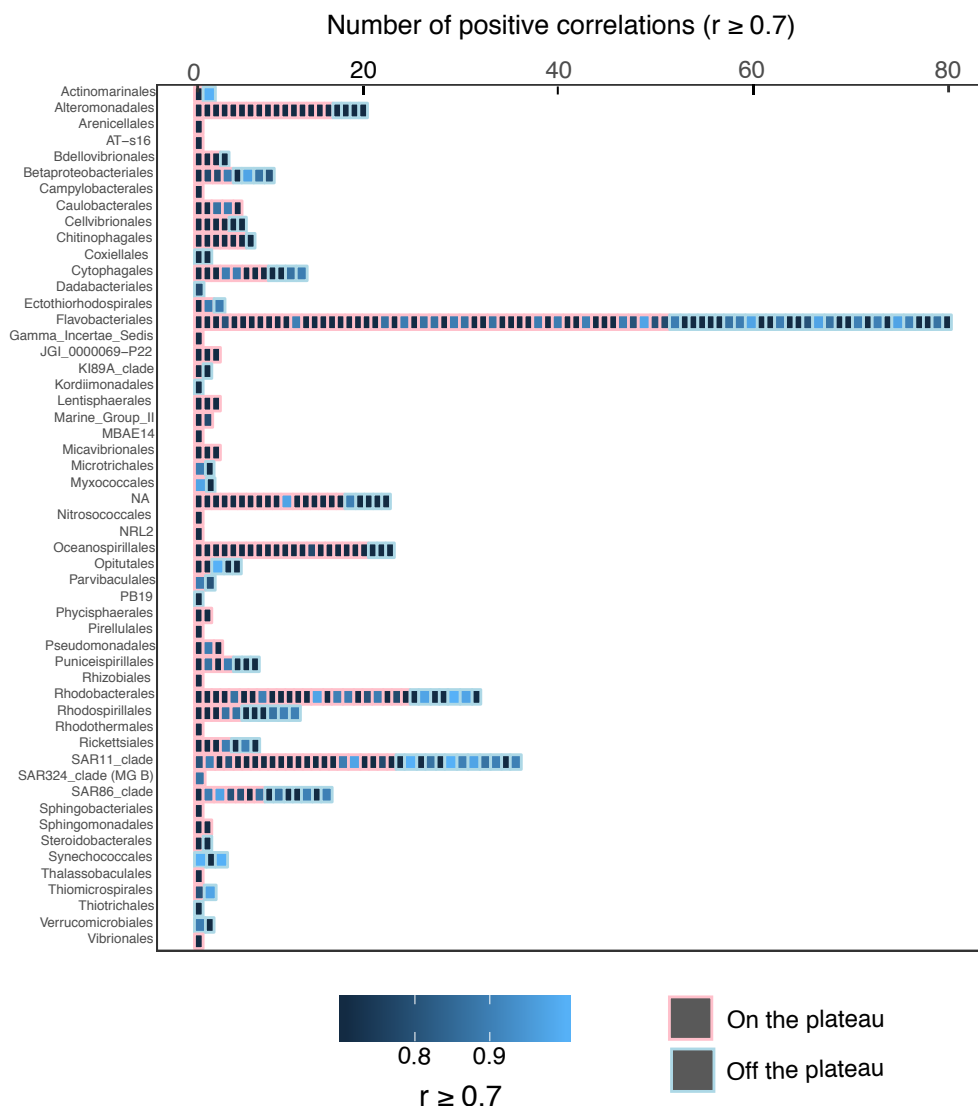


Fig. 11 Number of strong positive correlations (Spearman, $r \geq 0.7$) with the canonical axis associating active prokaryotic groups (Order level) with molecular formulae.

To identify the key prokaryotic contributors to the DOM-prokaryote relationships, we focused on strong positive correlations (Spearman, $r \geq 0.7$) between molecular formulae and active prokaryotic groups. Most prokaryotic groups were shared in samples on and off the plateau (Fig. 11). For most active prokaryotic groups, the number of correlations was overall higher on the plateau than that off the plateau. The highest number of correlations was associated with Flavobacteriales both on (51) and off (29) the plateau, followed by Rhodobacteriales (23 on plateau and 7 off plateau). SAR11 also showed high contributions to the total correlations both on (22) and off (12) the plateau. By contrast, for total prokaryotic groups, the number of correlations was overall lower on the plateau than that off the plateau. Flavobacteriales, Rhodobacteriales and SAR11 of the total community on the plateau had a

Chapter 3

much lower number of correlations (8, 3 and 6) than those of the active community (Fig. S4). The access to N-containing substrates is likely to be different among these prokaryotic groups. Members of Flavobacteriales were shown to be efficient in the utilization of polymeric N-containing compounds, such as proteins and chitin (Cottrell and Kirchman, 2000; Fourquez et al., 2016). In the present study, NS9 marine group affiliated with dissolved proteins accounted for high number of correlations (Fig. S5; Orsi et al., 2016). SAR11 is known for its efficient utilization of labile, low molecular weight molecules in a range of marine environments (Alonso-Sáez and Gasol, 2007; Laghdass et al., 2012; Fourquez et al., 2016). Based on a metaproteomic study, transporters and enzymes for taurine uptake and degradation were shown to be abundant in SAR11 (Williams et al., 2012). Alteromonadales and Oceanospirillales belonging to Gammaproteobacteria showed a higher number of correlations on the plateau than that off the plateau (Fig. 11). Mou et al. (2011) found that members of Oceanospirillales could degrade the polyamine putrescine which represents a source of labile nitrogen to prokaryotes (Mou et al., 2011). SAR86 had moderate numbers of correlations, which was also active in DON cycling, using amino acid and protein (Nikrad et al., 2014; Orsi et al., 2016). Members of Synechococcales were only present off the plateau and showed strong correlations (Fig. 8; Fig. 11), which reflects the characteristics of their genomes containing DON transporters (Palenik et al., 2003; Palenik et al., 2006; Carlson, 2002).

Supplementary material

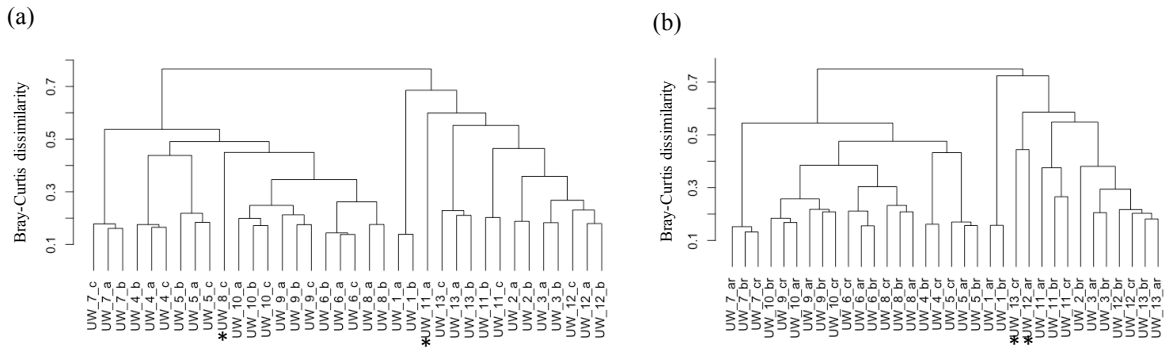
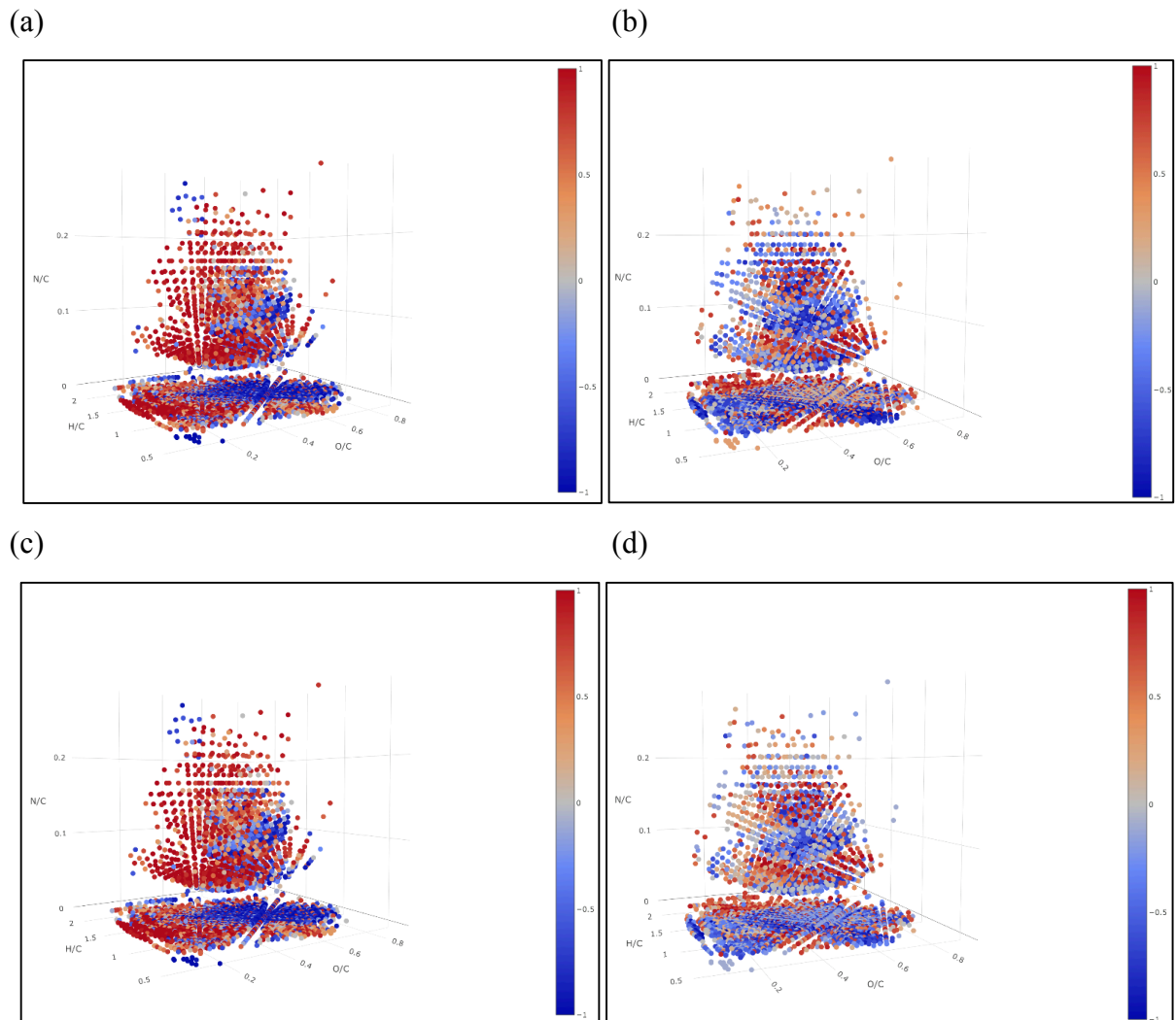


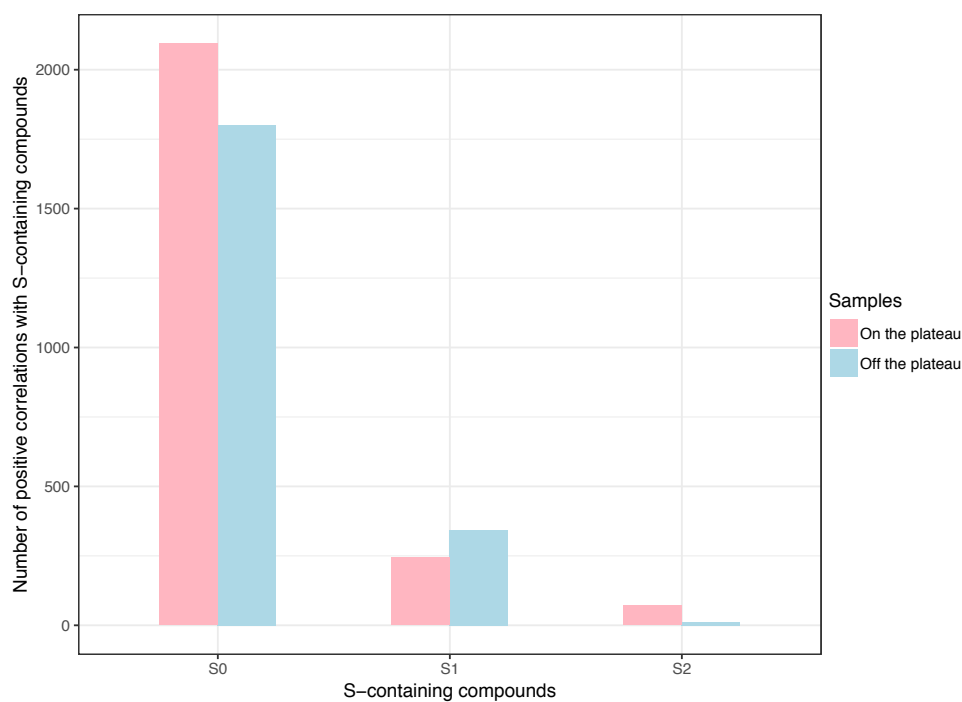
Fig. S1 Dendrograms of (a) total and (b) active prokaryotic communities based on Bray–Curtis dissimilarity of biological replicates. Replicates were named by the number of stations followed by a, b and c. *, samples were removed for further analyses.



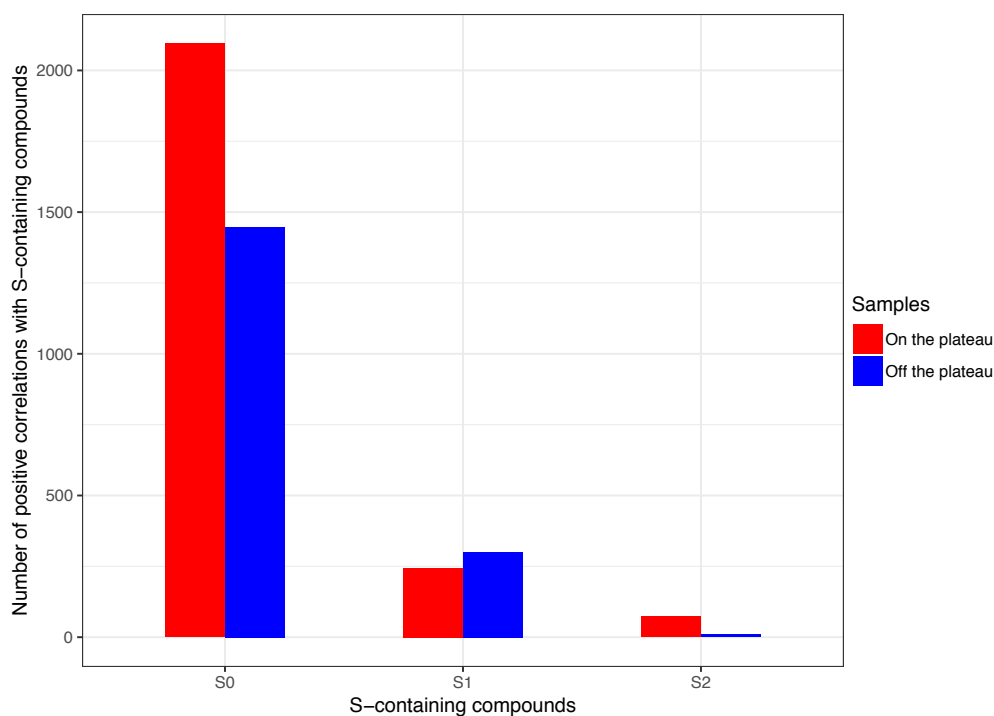
Chapter 3 Suppl.

Fig. S2 3D Van Krevelen diagrams illustrating the correlations of molecular formulae (relative intensities) with the canonical axis associating DOM composition with (a) total prokaryotic community composition on the plateau (b) total prokaryotic community composition off the plateau (c) active prokaryotic community composition on the plateau and (d) active prokaryotic community composition off the plateau.

(a)



(b)



Chapter 3 Suppl.

Fig. S3 Number of positive correlations with the canonical axis associating (a) total or (b) active prokaryotic community composition and DOM molecular formulae containing sulfur (S). (a) Pink and light blue bars represent DNA-based correlations on and off the plateau, respectively. (b) Red and blue bars represent RNA-based correlations on and off the plateau, respectively.

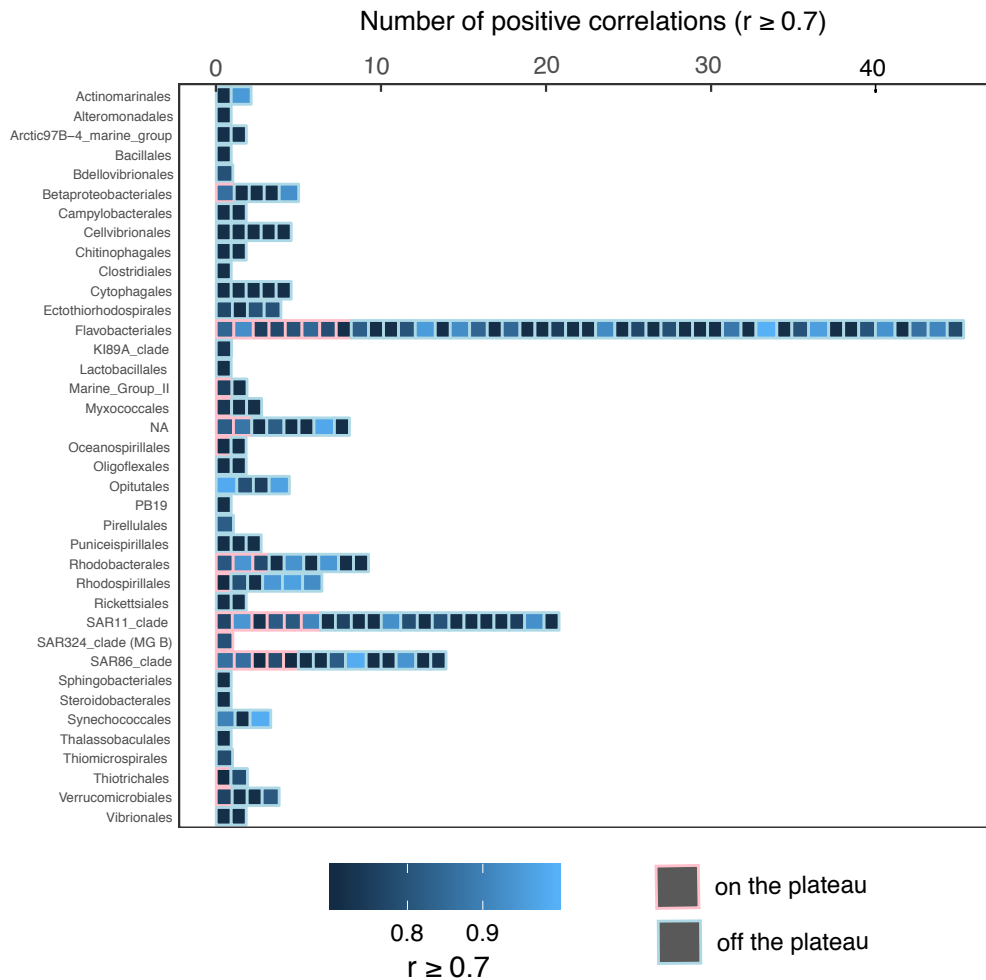


Fig. S4 Number of strong positive correlations (Spearman, $r \geq 0.7$) with the canonical axis associating total prokaryotic groups (Order level) with molecular formulae.

Chapter 3 Suppl.

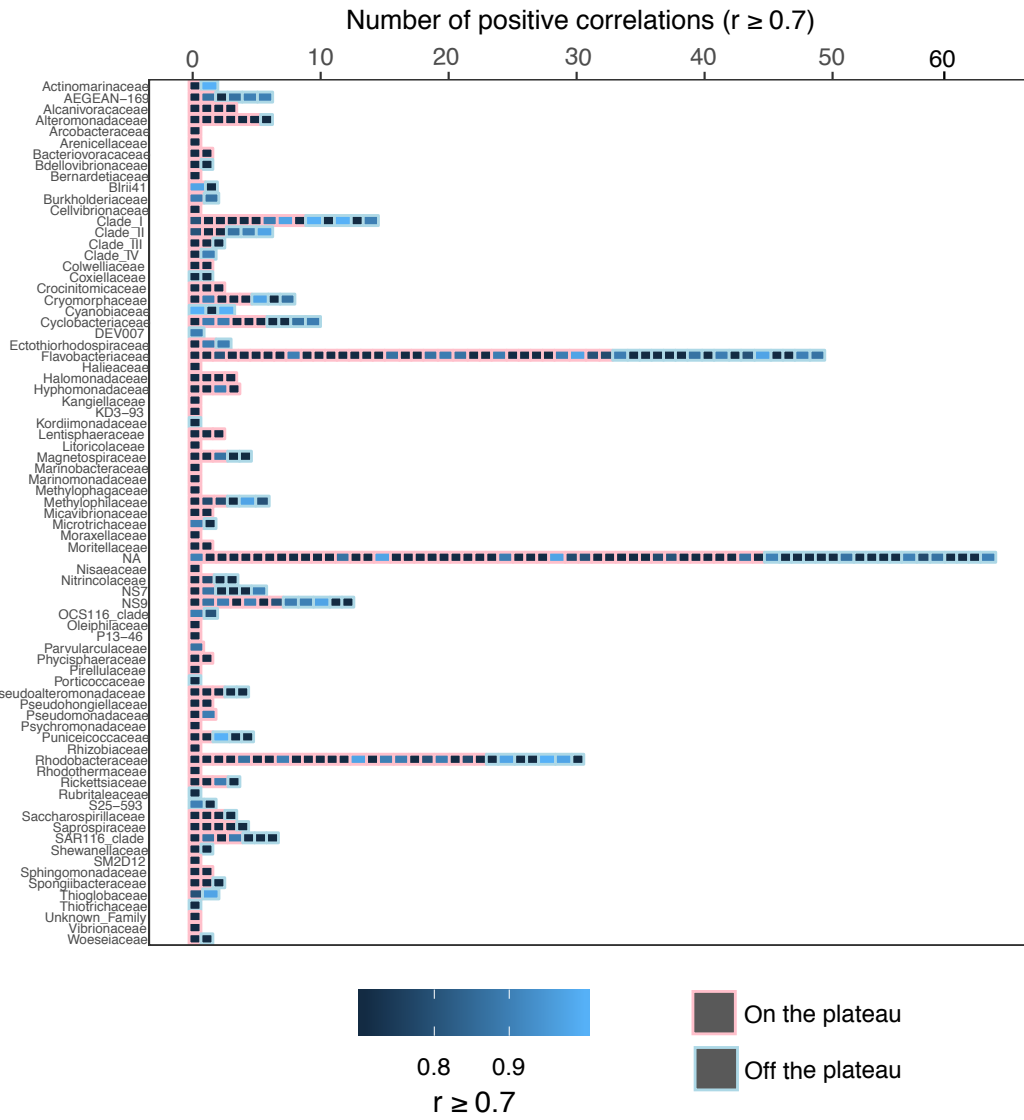


Fig. S5 Number of strong positive correlations (Spearman, $r \geq 0.7$) with the canonical axis associating active prokaryotic groups (Family level) with molecular formulae.

GENERAL DISCUSSION AND PERSPECTIVES



Olivier Crispi

General discussion and perspectives

1 Summary and general discussion

The present thesis investigates the link between heterotrophic prokaryotes, diatoms and dissolved organic matter in the Southern Ocean. An area of particular interest is the naturally iron fertilized region around Kerguelen Island in otherwise High-Nutrient-Low-Chlorophyll (HNLC) waters. Chapter 1 and Chapter 3 provide results on the associations between the diversity of prokaryotes and diatoms and between prokaryotes and Dissolved Organic Matter (DOM) on spatial scales. Chapter 2 focuses on the seasonal dynamics of prokaryote-diatom associations at one site located in iron-fertilized waters above the Kerguelen plateau covering the entire productive seasons.

In Chapter 1, the study was conducted over a large spatial distance with most samples collected in the Southern Ocean. In this study, the spatial distributions of diatoms and prokaryotes, and potential associations between them were investigated. Environmental parameters and geographic distance were additionally considered to identify what factors determine the biogeography of heterotrophic prokaryotes. Distinct compositions of diatom and prokaryotic communities were observed among major ocean zones. Diatoms could explain a large amount of variance of prokaryotic communities, which was not the case for environmental parameters or geographic distance. These results led us conclude that diatoms have a major influence on prokaryotic community composition in the Southern Ocean in early spring.

In Chapter 2, the study was conducted at a well-known site on the Kerguelen plateau during 4 months, to investigate the temporal dynamics of prokaryotes and diatoms, and the associations between them. We found pronounced temporal dynamics of prokaryotes and diatoms. During two consecutive bloom events, inverse correlation patterns were observed between prokaryotes with associated diatoms. Specific taxa were associated with each bloom and the ecology of these taxa was discussed in this chapter. In the discussion section below, a possible scenario of the microbial associations is provided.

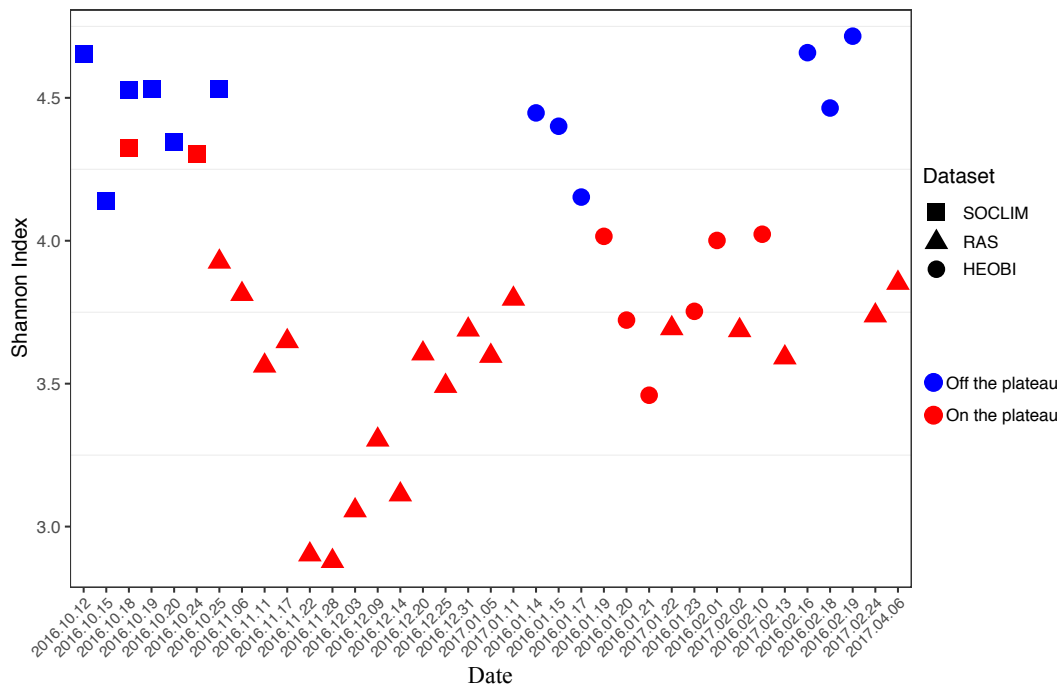
In Chapter 3, the study was conducted in surface Kerguelen plateau waters and HNLC sites, aiming to uncover the associations between prokaryotes and DOM in these two contrasting systems. Distinct compositions of prokaryotic communities and DOM were observed. DOM also showed different distributions on and off the plateau. Major associations between active

General discussion and perspectives

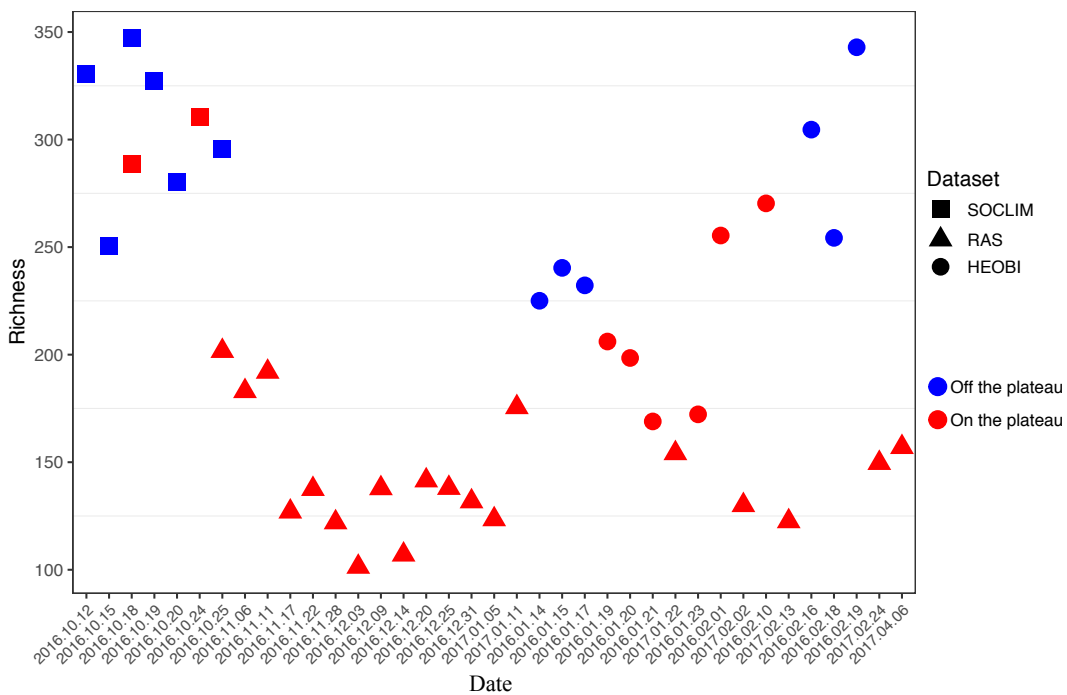
prokaryotes and N-related molecules were found on the plateau, which suggests prokaryotes actively respond to DOM in this iron fertilized region.

1.1 Microbial diversity in naturally iron-fertilized and HNLC Southern Ocean waters

(a)



(b)



General discussion and perspectives

(c)

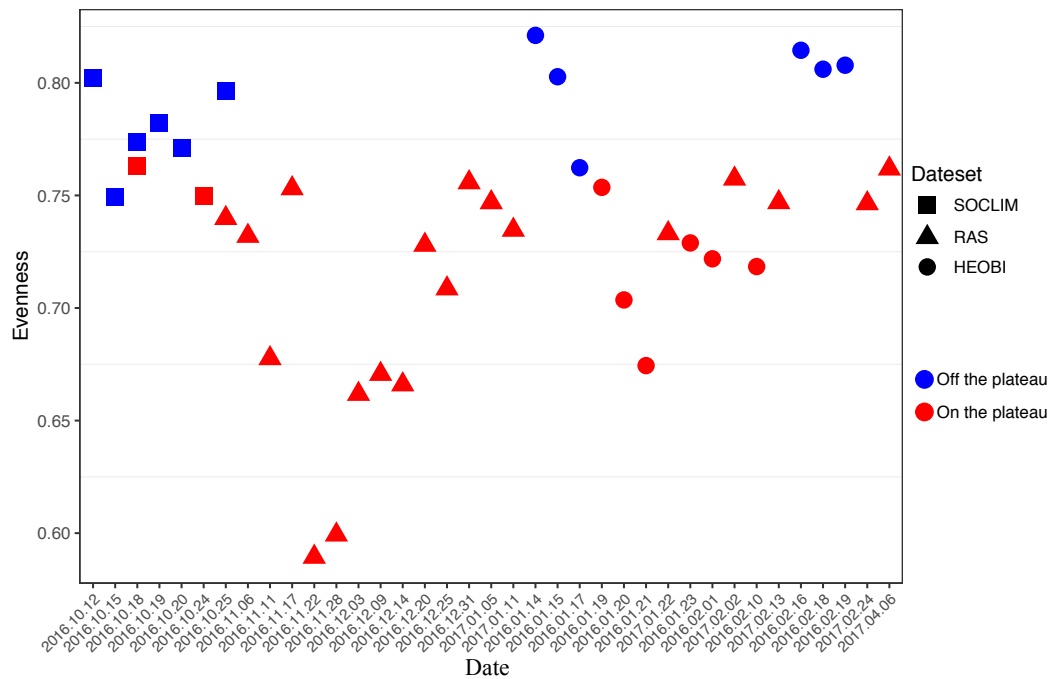


Fig. 1 Alpha-diversity of free-living prokaryotic communities from three chapters according to sampling dates. (a) Shannon index (b) Richness and (c) Evenness. The red and blue symbols denote samples collected on and off the Kerguelen plateau respectively. Squares, triangles and circles represent samples studied in Chapter 1 (SOCLIM), Chapter 2 (RAS) and Chapter 3 (HEOBI). Note dates in different years.

The results from the three chapters combined provide information on prokaryotic diversity in contrasted Southern Ocean regimes (Fig. 1). We found samples have overall higher diversity, as determined by the Shannon index, in HNLC waters as compared to those on the Kerguelen plateau (Fig. 1a). Similar patterns were also found in terms of richness and evenness (Fig. 1b, c). These results suggest that under higher organic carbon supply conditions a lower number of taxa accounted for the majority of total number of species abundance. This could reflect a competitive advantage of these groups.

General discussion and perspectives

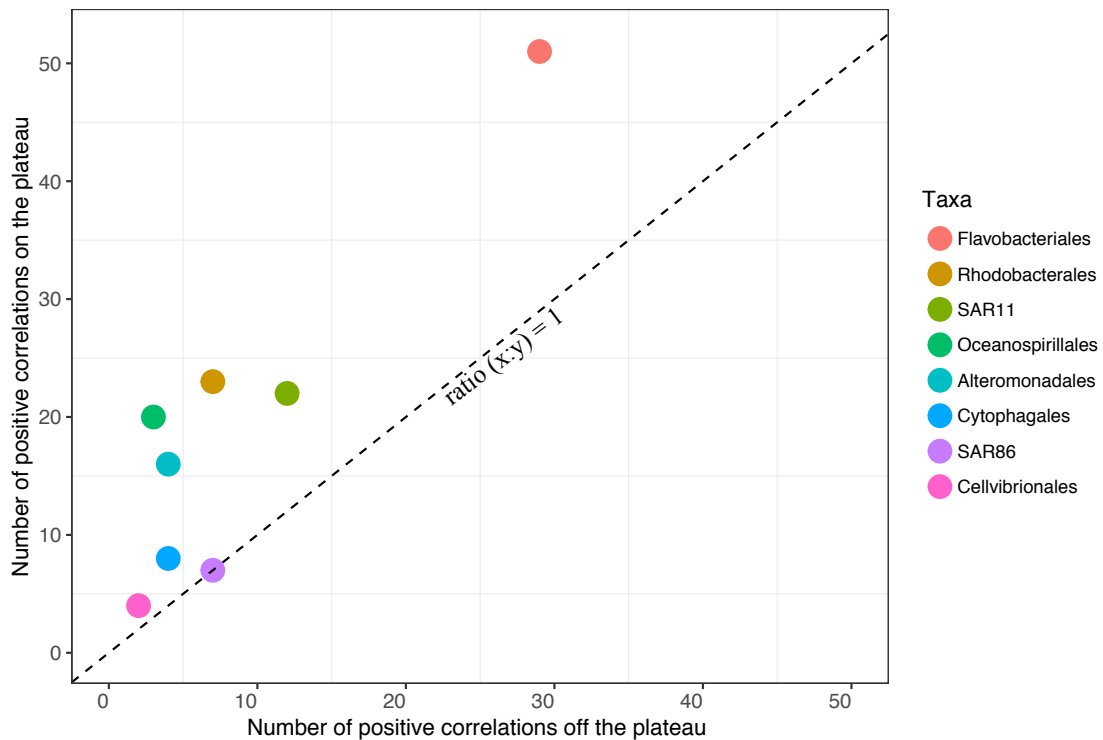


Fig. 2 The number of positive correlations between active prokaryotes and DOM on and off the Kerguelen plateau. Dashed line (ratio = 1) represents that taxa on this line has the same number of correlations on and off the plateau.

The diatom-prokaryote associations provided insight on the identification of the major prokaryotic groups that have potentially responded to the DOM released by diatoms. Strong positive correlations were detected between small diatoms and Flavobacteriales, Rhodobacterales and SAR11 (Chapter 1, Fig. 5). This finding was confirmed by the analysis of active prokaryote-DOM associations (Chapter 3). These prokaryotic groups were detected with a higher number of correlations with DOM compared to other prokaryotic groups on the plateau (Fig. 2), followed by Oceanospirillales and Alteromonadales. Interestingly, SAR11 was found in both iron fertilized and HNLC regions with a higher number of correlations with DOM detected on the plateau. This result provides a new perspective that contrasts with previous findings that SAR11 was more active in less productive areas. Nitrospiraceae was the dominant family in the Order of Oceanospirillales on the plateau (Chapter 3, Fig. 3b). Highly significant time-delayed associations between Nitrospiraceae and small diatoms were also detected in spring on the plateau in our seasonal study (Chapter 2, Fig. 10). These consistent results suggest that members of this group could rapidly respond to labile DOM. Alteromonadales showed the largest on-off plateau difference among all abundant prokaryotic groups (Fig. 2) in terms of the number of correlations, which corresponds well to a previous study in which *Alteromonas*

General discussion and perspectives

thrived in numbers in an incubation experiment containing *Chaetoceros* sp.-derived DOC (Sarmiento and Gasol, 2012).

1.2 Life strategies of diverse prokaryotes in the naturally Fe-fertilized region

According to the seasonal dynamics of prokaryotes, we observed several types of patterns based on highly abundant prokaryotes. This could reflect different life strategies of diverse prokaryotes in this naturally Fe-fertilized region.

Type I: The ubiquitous, streamlined, iron competitive prokaryotes (k-strategists)

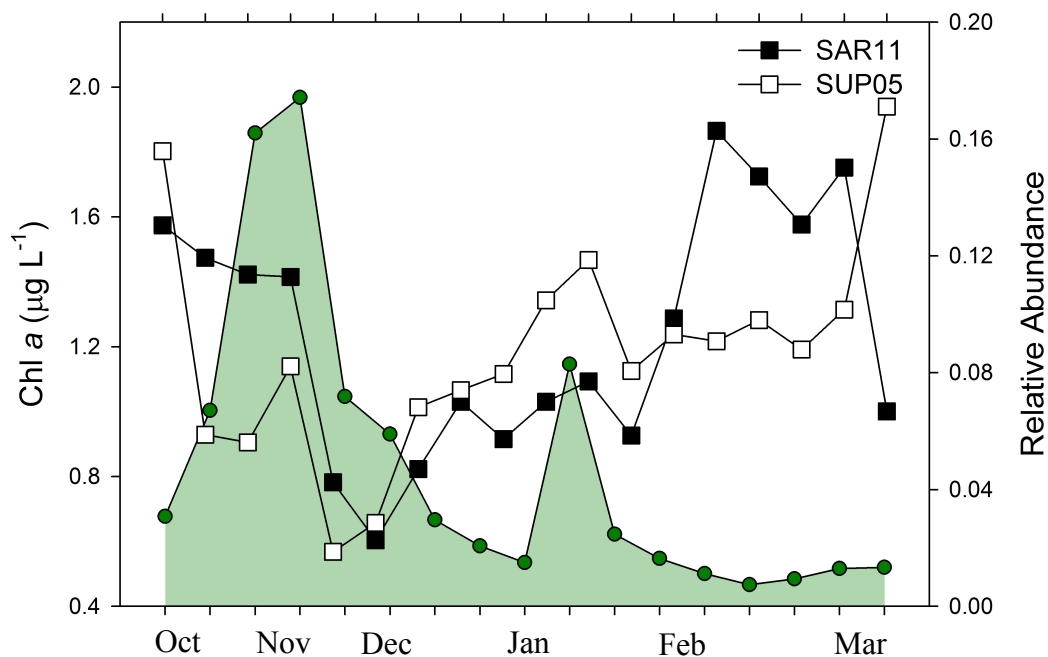


Fig. 3 Seasonal patterns of SAR11 and SUP05 based on relative abundance. Green shade denotes the concentration of Chlorophyll *a*.

SAR11 and SUP05 are omnipresent throughout the seasons (Fig. 3). At the onset of the spring bloom, they could compete with small, fast-growing diatoms for iron, while they were outcompeted by other copiotrophic prokaryotes during the late stage of this bloom. SAR11 is a well-known streamlined oligotrophic organism. SUP05 has been recently proposed as streamlined following the definition of streaming theory (Rogge et al., 2017). They can successfully grow in environments with low nutrient concentrations. Members of the SUP05 were also shown to be chemolithotrophic (Shah et al., 2017). In the first chapter, we also

General discussion and perspectives

observed the co-occurrence pattern of SAR11 and SUP05 in the HNLC region (off the plateau) (Chapter 1, Fig. S2), which suggests the co-occurrence of SAR11 and SUP05 could be a widespread pattern in different ocean systems, an idea also proposed by other studies (Rogge et al., 2017).

Type II: The primary colonizers in the spring bloom decay stage (r-strategists)

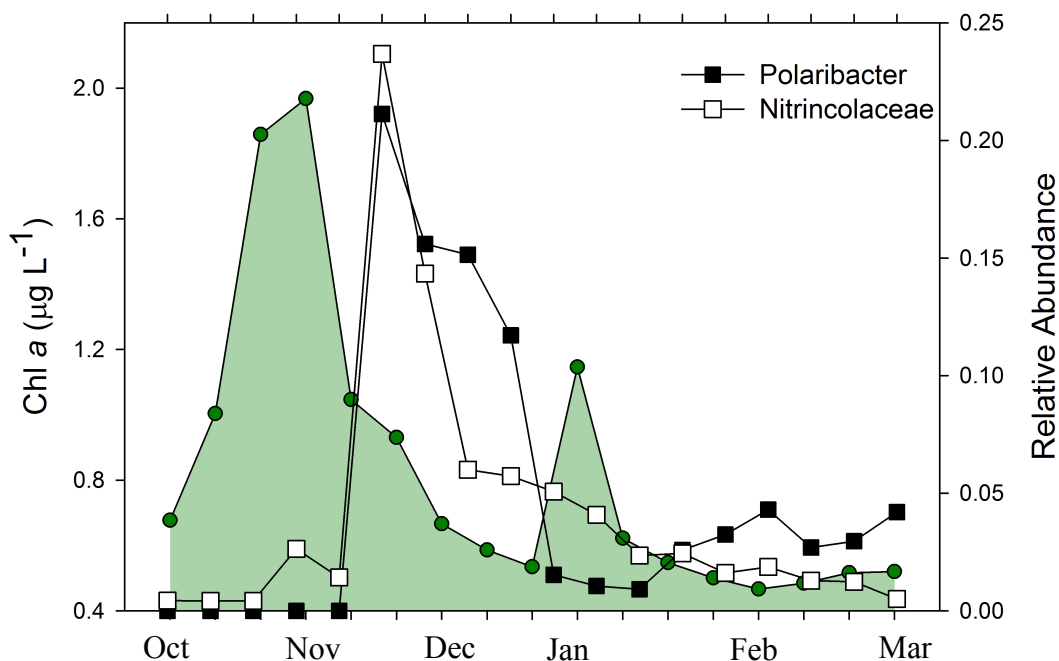


Fig. 4 Seasonal patterns of Polaribacter and Nitrincolaceae based on relative abundance. Green shade denotes the concentration of Chlorophyll *a*.

Polaribacter and Nitrincolaceae thrived in the late stage of the spring bloom and quickly decreased in abundance (Fig. 4). This suggests that both of them are possible utilizers of labile DOM in the post-spring bloom when the competition for Fe with small diatoms is reduced. Polaribacter is a metabolic versatile organism. It can utilize complex organic matter as primary degrader and was previously detected in a spring bloom decay stage (González et al., 2008; Landa et al., 2016). Given the similar seasonal pattern compared with Polaribacter, members of Nitrincolaceae could also be versatile. This idea was supported by a network analysis in which one genera of this group had a number of correlations with diverse small phytoplankton in the Southern Ocean (Fuentes et al., 2019). Additionally, both Polaribacter and Nitrincolaceae were almost absent in the summer bloom dominated by large diatoms, which suggests that members of the two groups have a specific ecological niche. It was interesting to note that these

General discussion and perspectives

two groups had discriminable associations with distinct diatom species in the same habitat (Chapter 2, Fig. 10).

Type III: Persistent response to moderate supply of phytoplankton DOM

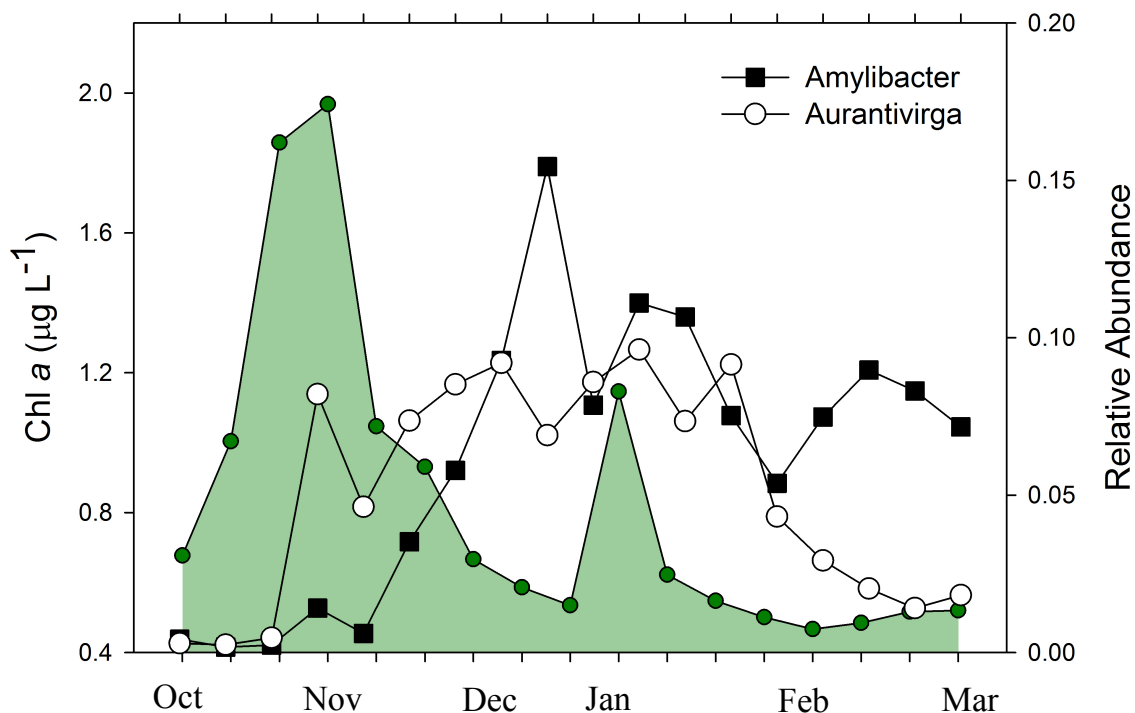


Fig. 5 Seasonal patterns of Amylibacter and Aurantivirga based on relative abundance. Green shade denotes the concentration of Chlorophyll *a*.

Amylibacter and Aurantivirga started being abundant at the very late stage of the spring bloom and dominated in the summer bloom (Fig. 5). This type of seasonal pattern, different from the two described above, could reflect a different life strategy. These taxa seem to be stimulated by the bloom, but they are not as competitive as type II taxa to grow on labile DOM. We hypothesize that the slower increase in relative abundance of type III prokaryotes could be due to their utilization of more complex DOM. Their co-occurrence could be explained by their respective substrate specificity. During summer, large, slow-growing diatoms provided a less competitive habitat for prokaryotes in which they could directly utilize labile DOM. The similar contributions of type I and type III prokaryotes to total abundance in summer suggest positive interactions to be more important than in spring.

General discussion and perspectives

1.3 A possible scenario of microbial associations over time in a naturally iron-fertilized region

According to the microbial seasonal dynamics and associations between diatoms and prokaryotes (Chapter 2, Fig. 8-10), we provided a possible scenario for the temporal changes of microbes in naturally iron fertilized systems. A conceptual scheme for this seasonal change in terms of bulk diatoms and zooplankton at the same study area has been proposed (Quéguiner, 2012). Here we introduce prokaryotes at a fine phylogenetic level to this scheme, aiming to provide a new perspective for future research (Fig. 6).

In early spring, the increase in available light and in the inorganic nutrients induces the development of small diatoms with high growth rates and light silicification (e.g., *Chaetoceros* sp.). These diatom assemblages are largely affected by iron availability. This group of diatoms provides an ecological niche in which only a small set of prokaryotes with strong competition for iron can rapidly grow (e.g., SAR11 and SUP05). The decrease of the spring bloom is likely due to the nutrient limitation and prokaryotic degradation (Quéguiner, 2012). In this stage, the drawdown of diatoms alleviates the iron competition and the accumulated organic matter benefits the rapid growth of copiotrophic prokaryotes (e.g., *Polaribacter*). In parallel, organic matter in the form of diatoms support the growth of zooplankton, therefore carbon biomass is transferred into higher trophic levels.

General discussion and perspectives

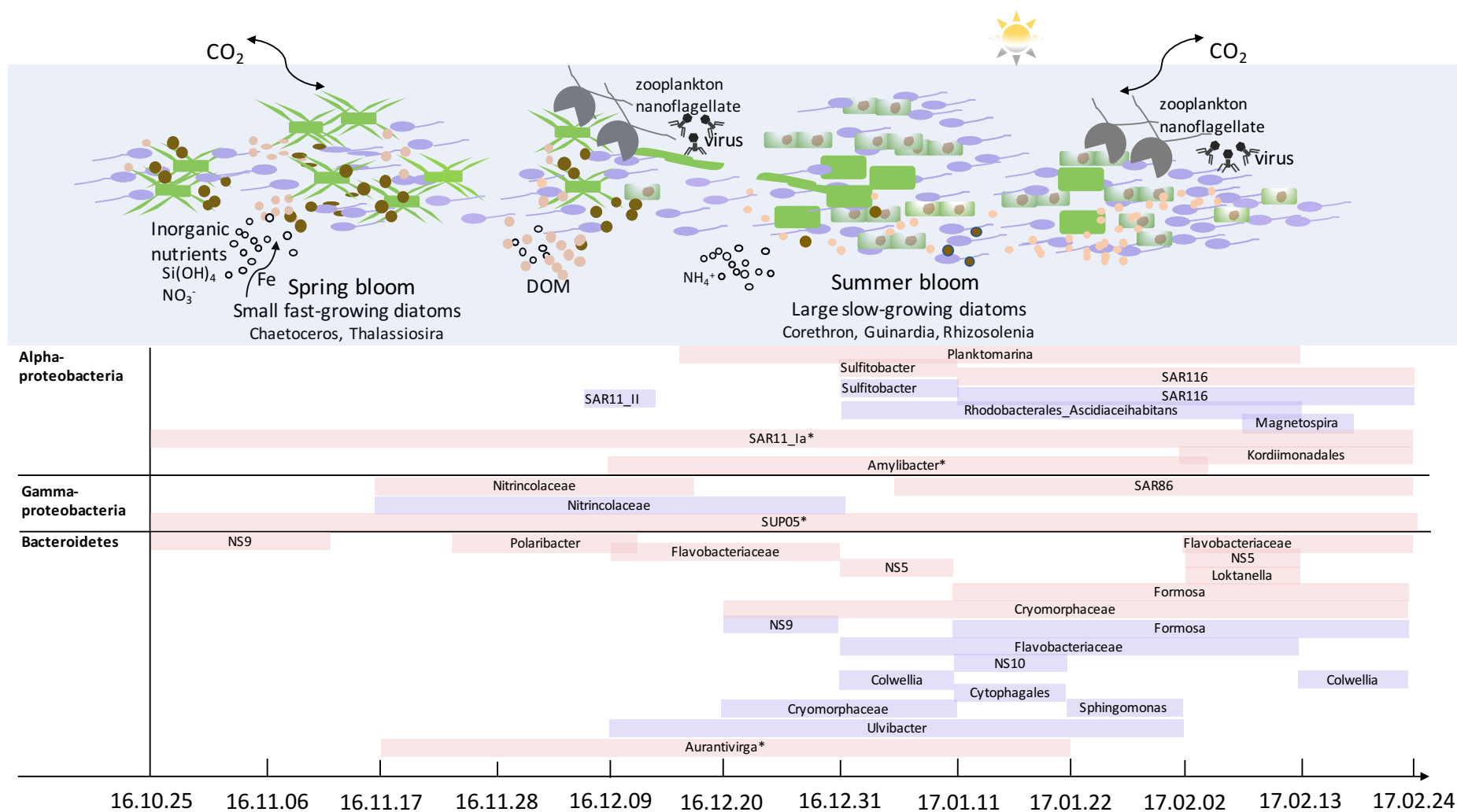


Fig. 6 A possible scenario of microbial associations over time in a naturally iron-fertilized region. Pink and purple shades represent free-living and particle-attached prokaryotes respectively. *, taxa were not detected in the association network (Chapter 2, Fig. 10)

General discussion and perspectives

In summer, diatoms are composed of large, slow-growing, heavily silicified species (e.g., *Corethron* sp.). These diatoms are less competitive for iron compared with those smaller ones (Fourquez et al., 2015). They provide a relatively relaxed ecological niche for the growth of diverse prokaryotes. On the one hand, larger diatoms exude organic compounds further away from the cell surface than smaller diatoms (i.e., phycosphere; Amin et al., 2012). The larger phycosphere impacts a higher number of prokaryotes and reduce the competition in terms of space. On the other hand, larger cells provide better loci for prokaryote attachment. For example, we detected a higher number of prokaryotes from particle-attached fraction in summer than in spring. In addition, zooplankton control is less important than in the first bloom, because of the defense mechanisms of highly silicified diatoms. This suggests that this group of diatoms is likely persistent over a long-time period, which benefits the long-term association between prokaryotes and diatoms (e.g., Cryomorphaceae).

2 Perspectives

We describe in this thesis results related to microbial diversity and dissolved organic matter in a naturally iron fertilized region and in surrounding HNLC waters in the Southern Ocean. We specifically answered several questions proposed in the general introduction. We will provide several insights for future research.

Microbial associations are the major drivers of the changing composition of prokaryotic communities, which needs more attention in future ecological studies. In Chapter 1, we found diatoms rather than environmental conditions or geographic distance to influence the biogeography of heterotrophic prokaryotes. This finding extends the traditional view that geography and inorganic nutrients are the major factors of shifts in prokaryotic community composition. The interactions among microbes impact the prokaryotic diversity and biogeographic patterns, and require future exploration in microbial ecology.

From the temporal dynamics of the seasonal study, we present several potential life strategies of a few prokaryotic groups (Fig. 3-5). Experimental co-culture work could help better understand the role of DOM supply. For example, one could search whether SAR11 and SUP05 co-exist in the lab using chemostats, which will be a challenge considering the difficulty

General discussion and perspectives

of SAR11 cultivation. Other temporal studies could also be explored to extend the prokaryotic groups using different life strategies.

Our work highlights a number of potential novel diatom-prokaryote associations, which all need to be confirmed in the laboratory. One of the most important role of *in situ* microbial association analysis is to predict the potential interaction between microbes. In Chapter 2, we detected the two blooms have specific prokaryotes associated with. However, the discovery of the underlying mechanism of each correlation requires culture work, integrating data on functional genes, transcripts and proteins. Further exploration of several questions is needed. For example, how *Corethron inerme* and *Sulfitobacter* are correlated together? Is this based on a “mutualistic” relationship in which both benefit from each other or on “commensalism” in which one benefits while the other is not affected? In addition, it would be also interesting to investigate the gene expression of one species in different habitats, since we found the same prokaryotic species (e.g., *Sulfitobacter* sp.) are associated with distinct diatoms.

Several prokaryotic groups actively respond to a subset of DOM molecules (Chapter 3). This preliminary result needs more detailed exploration with the advanced techniques in the future. For example, the current characterization of DOM compounds is based on molecular mass, although the resolution of DOM analysis is already improved by FT-ICR MS. Those compounds classified by molecular formulae are unambiguous, which actually refer to a mixture of isomers and not necessarily indicate the presence of a structural or functional group. Therefore, more advanced techniques are needed to reduce the ambiguity of DOM classification. On the prokaryote’s side, amplicon sequencing data are helpful for identifying the potential key groups responding to DOM. However, to answer the question of how and to what extent they respond to changing DOM, ‘Omics’ data, such as metatranscriptomics and metaproteomics are required.

REFERENCES

-A-

- Abell, G.C.J. and Bowman, J.P. (2005a) Colonization and community dynamics of class Flavobacteria on diatom detritus in experimental mesocosms based on Southern Ocean seawater. *FEMS Microbiology Ecology* **53**: 379–391.
- Abell, Guy C.J. and Bowman, J.P. (2005b) Ecological and biogeographic relationships of class Flavobacteria in the Southern Ocean. *FEMS Microbiology Ecology* **51**: 265–277.
- Abouchami, W., Galer, S.J.G., de Baar, H.J.W., Alderkamp, A.C., Middag, R., Laan, P., et al. (2011) Modulation of the Southern Ocean cadmium isotope signature by ocean circulation and primary productivity. *Earth and Planetary Science Letters* **305**: 83–91.
- Agustí, S., and Duarte, C. M. (2013) Phytoplankton lysis predicts dissolved organic carbon release in marine plankton communities. *Biogeosciences* **10**: 1259-1264.
- Alcamán-Arias, M.E., Farías, L., Verdugo, J., Alarcón-Schumacher, T., and Díez, B. (2018) Microbial activity during a coastal phytoplankton bloom on the Western Antarctic Peninsula in late summer. *FEMS Microbiology Letters* **365**: fny090.
- Algora, C., Vasileiadis, S., Wasmund, K., Trevisan, M., Krüger, M., Puglisi, E., and Adrian, L. (2015) Manganese and iron as structuring parameters of microbial communities in Arctic marine sediments from the Baffin Bay. *FEMS Microbiology Ecology* **91**: no. 6.
- Alonso-Sáez, L. and Gasol, J.M. (2007) Seasonal variations in the contributions of different bacterial groups to the uptake of Low-Molecular-Weight compounds in northwestern Mediterranean coastal waters. *Applied and Environmental Microbiology* **73**: 3528–3535.
- Alonso-Sáez, L., Sánchez, O., and Gasol, J.M. (2012) Bacterial uptake of low molecular weight organics in the subtropical Atlantic: Are major phylogenetic groups functionally different? *Limnology and Oceanography* **57**: 798–808.
- Alonso-Sáez, L., Sánchez, O., Gasol, J.M., Balagué, V., and Pedrós-Alio, C. (2008) Winter-to-summer changes in the composition and single-cell activity of near-surface Arctic prokaryotes. *Environmental Microbiology* **10**: 2444–2454.
- Amin, S.A., Green, D.H., Hart, M.C., Kupper, F.C., Sunda, W.G., and Carrano, C.J. (2009) Photolysis of iron-siderophore chelates promotes bacterial-algal mutualism. *Proceedings of the National Academy of Sciences* **106**: 17071–17076.
- Amin, S.A., Hmelo, L.R., van Tol, H.M., Durham, B.P., Carlson, L.T., Heal, K.R., et al. (2015) Interaction and signalling between a cosmopolitan phytoplankton and associated bacteria. *Nature* **522**: 98–101.

- Amin, S.A., Parker, M.S., and Armbrust, E.V. (2012) Interactions between Diatoms and Bacteria. *Microbiology and Molecular Biology Reviews* **76**: 667–684.
- Andersson, A.F., Riemann, L., and Bertilsson, S. (2010) Pyrosequencing reveals contrasting seasonal dynamics of taxa within Baltic Sea bacterioplankton communities. *The ISME Journal* **4**: 171–181.
- Ankrah, N.Y.D., Lane, T., Budinoff, C.R., Hadden, M.K., and Buchan, A. (2014) Draft Genome Sequence of *Sulfitobacter* sp. CB2047, a Member of the Roseobacter Clade of Marine Bacteria, Isolated from an *Emiliania huxleyi* Bloom. *Genome Announcements* **2**: e01125-14.
- Armbrust, E.V. (2009) The life of diatoms in the world's oceans. *Nature* **459**: 185–192.
- Arnosti, C., Steen, A.D., Ziervogel, K., Ghobrial, S., and Jeffrey, W.H. (2011) Latitudinal Gradients in Degradation of Marine Dissolved Organic Carbon. *PLoS ONE* **6**: e28900.
- Arrieta, J.M., Weinbauer, M.G., Lute, C., and Herndl, G.J. (2004) Response of bacterioplankton to iron fertilization in the Southern Ocean. *Limnology and Oceanography* **49**: 799–808.
- Assmy, P., Smetacek, V., Montresor, M., Klaas, C., Henjes, J., Strass, V.H., et al. (2013) Thick-shelled, grazer-protected diatoms decouple ocean carbon and silicon cycles in the iron-limited Antarctic Circumpolar Current. *Proceedings of the National Academy of Sciences* **110**: 20633–20638.
- Azam, F., Fenchel, T., Field, J. G., Grey, J. S., Meyer-Reil, L. A., and Thingstad, F. (1983). The ecological role of water-column microbes in the sea. *Mar. ecol. Prog. ser.*, **10**: 257-263.
- Azam, F. (1998) Microbial control of oceanic carbon flux: The Plot Thickens. *Science, New Series* **280**: 694–696.
- Azam, F. and Malfatti, F. (2007) Microbial structuring of marine ecosystems. *Nature Reviews Microbiology* **5**: 782–791.

-B-

- Bakker, D. C., Bozec, Y., Nightingale, P. D., Goldson, L., Messias, M. J., de Baar, H. J., et al. (2005). Iron and mixing affect biological carbon uptake in SOIREE and EisenEx, two Southern Ocean iron fertilisation experiments. *Deep Sea Research Part I: Oceanographic Research Papers* **52**: 1001-1019.
- Becker, J.W., Berube, P.M., Follett, C.L., Waterbury, J.B., Chisholm, S.W., DeLong, E.F., and Repeta, D.J. (2014) Closely related phytoplankton species produce similar suites of dissolved organic matter. *Frontiers in Microbiology* **5**: 111.
- Behringer, G., Ochsenkühn, M.A., Fei, C., Fanning, J., Koester, J.A., and Amin, S.A. (2018)

- Bacterial communities of diatoms display strong conservation across strains and time. *Frontiers in Microbiology* **9**: 659.
- Beier, S., Rivers, A.R., Moran, M.A., and Obernosterer, I. (2015) The transcriptional response of prokaryotes to phytoplankton-derived dissolved organic matter in seawater: The response of prokaryotes to DOM in seawater. *Environmental Microbiology* **17**: 3466–3480.
- Benner R. (2002) Chemical composition and reactivity. In *Biogeochemistry of Marine Dissolved Organic Matter*, ed. DA Hansell, CA Carlson. San Diego, CA: Elsevier, pp. 59–90.
- Benner, R., Pakulski, J.D., McCarthy, M., Hedges, J.I., and Hatcher, P.G. (1992) Bulk Chemical Characteristics of Dissolved Organic Matter in the Ocean. *Science, New Series* **255**: 1561–1564.
- Benner, R. and Strom, M. (1993) A critical evaluation of the analytical blank associated with DOC measurements by high-temperature catalytic oxidation. *Marine Chemistry* **41**: 153–160.
- Bertilsson, S., and Jones Jr, J. B. (2003) Supply of dissolved organic matter to aquatic ecosystems: autochthonous sources. In *Aquatic Ecosystems*. Academic Press, pp. 3-24.
- Bertrand, E.M., McCrow, J.P., Moustafa, A., Zheng, H., McQuaid, J.B., Delmont, T.O., et al. (2015) Phytoplankton–bacterial interactions mediate micronutrient colimitation at the coastal Antarctic sea ice edge. *Proceedings of the National Academy of Sciences* **112**: 9938–9943.
- Biddanda, B. and Benner, R. (1997) Major contribution from mesopelagic plankton to heterotrophic metabolism in the upper ocean. *Deep Sea Research Part I: Oceanographic Research Papers* **44**: 2069–2085.
- Biersmith, A. and Benner, R. (1998) Carbohydrates in phytoplankton and freshly produced dissolved organic matter. *Marine Chemistry* **63**: 131–144.
- Blain, S., Capparos, J., Guéneuguès, A., Obernosterer, I., and Oriol, L. (2014) Distributions and stoichiometry of dissolved nitrogen and phosphorus in the iron fertilized region near Kerguelen (Southern Ocean). *Biogeosciences Discussions* **11**: 9949–9977.
- Blain, S., Quéguiner, B., Armand, L., Belviso, S., Bombled, B., Bopp, L., et al. (2007) Effect of natural iron fertilization on carbon sequestration in the Southern Ocean. *Nature* **446**: 1070–1074.
- Blain, S., Sedwick, P. N., Griffiths, F. B., Quéguiner, B., Bucciarelli, E., Fiala, M., et al. (2002). Quantification of algal iron requirements in the Subantarctic Southern Ocean (Indian sector). *Deep Sea Research Part II: Topical Studies in Oceanography* **49**: 3255-3273.
- Blain, S., Tréguer, P., Belviso, S., Bucciarelli, E., Denis, M., Desabre, S., et al. (2001). A biogeochemical study of the island mass effect in the context of the iron hypothesis: Kerguelen Islands, Southern Ocean. *Deep Sea Research Part I: Oceanographic*

Research Papers **48**: 163-187.

- Blazewicz, S.J., Barnard, R.L., Daly, R.A., and Firestone, M.K. (2013) Evaluating rRNA as an indicator of microbial activity in environmental communities: limitations and uses. *The ISME Journal* **7**: 2061–2068.
- Boeuf, D., Cottrell, M.T., Kirchman, D.L., Lebaron, P., and Jeanthon, C. (2013) Summer community structure of aerobic anoxygenic phototrophic bacteria in the western Arctic Ocean. *FEMS Microbiology Ecology* **85**: 417–432.
- Botebol, H., Lesuisse, E., Šuták, R., Six, C., Lozano, J.-C., Schatt, P., et al. (2015) Central role for ferritin in the day/night regulation of iron homeostasis in marine phytoplankton. *Proceedings of the National Academy of Sciences* **112**: 14652–14657.
- Bowman, J.P., Mccammon, S.A., Brown, M.V., Nichols, D.S., and Mcmeekin, T.A. (1997) Diversity and association of psychrophilic bacteria in Antarctic sea ice. *Applied and Environmental Microbiology* **63**: 11.
- Bowman J.P. (2014) The Family *Cryomorphaceae*. In *The Prokaryotes*, eds. Rosenberg E., DeLong E.F., Lory S., Stackebrandt E., Thompson F.. Springer, Berlin, Heidelberg, pp. 539-550.
- Boyd, P.W., Jickells, T., Law, C.S., Blain, S., Boyle, E.A., Buesseler, K.O., et al. (2007) Mesoscale iron enrichment experiments 1993-2005: Synthesis and future directions. *Science, New Series* **315**: 612–617.
- Boyd, P.W., Watson, A.J., Law, C.S., Abraham, E.R., Trull, T., Murdoch, R., et al. (2000) A mesoscale phytoplankton bloom in the polar Southern Ocean stimulated by iron fertilization. *Nature* **407**: 695–702.
- Bray, J.R. and Curtis, J.T. (1957) An ordination of the upland forest communities of southern Wisconsin. *Ecological Monographs* **27**: 325–349.
- Brinkhoff, T., Giebel, H.-A., and Simon, M. (2008) Diversity, ecology, and genomics of the Roseobacter clade: a short overview. *Archives of Microbiology* **189**: 531–539.
- Brinkmeyer, R., Knittel, K., Jurgens, J., Weyland, H., Amann, R., and Helmke, E. (2003) Diversity and structure of bacterial communities in Arctic versus Antarctic pack ice. *Applied and Environmental Microbiology* **69**: 6610–6619.
- Britschgi, T.B. and Giovannoni, S.J. (1991) Phylogenetic analysis of a natural marine bacterioplankton population by rRNA gene cloning and sequencing. **57**: 7.
- Brown, M.V., Lauro, F.M., DeMaere, M.Z., Muir, L., Wilkins, D., Thomas, T., et al. (2012) Global biogeography of SAR11 marine bacteria. *Molecular Systems Biology* **8**: no. 1.
- Bucciarelli, E., Blain, S., and Tréguer, P. (2001). Iron and manganese in the wake of the Kerguelen Islands (Southern Ocean). *Marine Chemistry* **73**: 21-36.
- Buchan, A., Gonzalez, J.M., and Moran, M.A. (2005) Overview of the marine Roseobacter

lineage. *Applied and Environmental Microbiology* **71**: 5665–5677.

Buchan, A., LeCleir, G.R., Gulvik, C.A., and González, J.M. (2014) Master recyclers: features and functions of bacteria associated with phytoplankton blooms. *Nature Reviews Microbiology* **12**: 686–698.

Buesseler, K.O. (2004) The effects of iron fertilization on carbon sequestration in the Southern Ocean. *Science* **304**: 414–417.

Bunse, C. and Pinhassi, J. (2017) Marine bacterioplankton seasonal succession dynamics. *Trends in Microbiology* **25**: 494–505.

Buttigieg, P.L. and Ramette, A. (2014) A guide to statistical analysis in microbial ecology: a community-focused, living review of multivariate data analyses. *FEMS Microbiology Ecology* **90**: 543–550.

-C-

Callahan, B.J., McMurdie, P.J., Rosen, M.J., Han, A.W., Johnson, A.J.A., and Holmes, S.P. (2016) DADA2: High-resolution sample inference from Illumina amplicon data. *Nature Methods* **13**: 581–583.

Carlson CA. (2002) Production and removal processes. In *Biogeochemistry of Marine Dissolved Organic Matter*, ed. DA Hansell, CA Carlson. San Diego, CA: Elsevier, pp. 91–152.

Carlson, C.A., Morris, R., Parsons, R., Treusch, A.H., Giovannoni, S.J., and Vergin, K. (2009) Seasonal dynamics of SAR11 populations in the euphotic and mesopelagic zones of the northwestern Sargasso Sea. *The ISME Journal* **3**: 283–295.

Carlson, D.J., Brann, M.L., Mague, T.H., and Mayer, L.M. (1985) Molecular weight distribution of dissolved organic materials in seawater determined by ultrafiltration: a re-examination. *Marine Chemistry* **16**: 155–171.

Carlson, H.K., Clark, I.C., Blazewicz, S.J., Iavarone, A.T., and Coates, J.D. (2013) Fe(II) oxidation is an innate capability of nitrate-reducing bacteria that involves abiotic and biotic reactions. *Journal of Bacteriology* **195**: 3260–3268.

Chafee, M., Fernández-Guerra, A., Buttigieg, P.L., Gerdtts, G., Eren, A.M., Teeling, H., and Amann, R.I. (2018) Recurrent patterns of microdiversity in a temperate coastal marine environment. *The ISME Journal* **12**: 237–252.

Chaffron, S., Rehrauer, H., Pernthaler, J., and von Mering, C. (2010) A global network of coexisting microbes from environmental and whole-genome sequence data. *Genome Research* **20**: 947–959.

Chao, A. (1987) Estimating the population size for capture-recapture data with unequal

- catchability. *Biometrics* **43**: 783.
- Christian J.R, Anderson T.R. (2002) Modeling DOM biogeochemistry. In *Biogeochemistry of Marine Dissolved Organic Matter*, ed. DA Hansell, CA Carlson. San Diego, CA: Elsevier, pp. 717–747.
- Choi, S.B., Kim, J.G., Jung, M.Y., Kim, S.J., Min, U.G., Si, O.J., et al. (2016) Cultivation and biochemical characterization of heterotrophic bacteria associated with phytoplankton bloom in the Amundsen sea polynya, Antarctica. *Deep Sea Research Part II: Topical Studies in Oceanography* **123**: 126–134.
- Christaki, U., Lefèvre, D., Georges, C., Colombet, J., Catala, P., Courties, C., et al. (2014) Microbial food web dynamics during spring phytoplankton blooms in the naturally iron-fertilized Kerguelen area (Southern Ocean). *Biogeosciences* **11**: 6739–6753.
- Chun, H. and Keleş, S. (2010) Sparse partial least squares regression for simultaneous dimension reduction and variable selection. *Journal of the Royal Statistical Society: Series B (Statistical Methodology)* **72**: 3–25.
- Church, M.J., DeLong, E.F., Ducklow, H.W., Karner, M.B., Preston, C.M., and Karl, D.M. (2003) Abundance and distribution of planktonic *Archaea* and *Bacteria* in the waters west of the Antarctic Peninsula. *Limnology and Oceanography* **48**: 1893–1902.
- Church, M.J., Hutchins, D.A., and Ducklow, H.W. (2000) Limitation of bacterial growth by dissolved organic matter and iron in the Southern Ocean. *Applied and Environmental Microbiology* **66**: 455–466.
- Ciais, P., Sabine, C., Bala, G., Bopp, L., Brovkin, V., Canadell, J., et al. (2014) Carbon and other biogeochemical cycles. In *Climate Change 2013: The Physical Science Basis. Contribution of Working Group I to the Fifth Assessment Report of the Intergovernmental Panel on Climate Change*, Stocker, T.F., Qin, D., Plattner, G.-K., Tignor, M., Allen, S.K., Boschung, J., et al. (eds). Cambridge: Cambridge University Press, pp. 465–570.
- Cirri, E. and Pohnert, G. (2019) Algae–bacteria interactions that balance the planktonic microbiome. *New Phytologist* **223**: 100–106.
- Coale, K.H., Johnson, K.S., Chavez, F.P., Buesseler, K.O., Barber, R.T., Brzezinski, M.A., et al. (2004) Southern Ocean iron enrichment experiment: Carbon cycling in high- and low-Si waters. *Science, New Series* **304**: 408–414.
- Corilo, Y. E., ©PetroOrg Software, 2015, Florida State University, all rights reserved, <http://software.petroorg.com>
- Cottrell, M.T. and Kirchman, D.L. (2000) Natural assemblages of marine Proteobacteria and members of the Cytophaga-Flavobacter cluster consuming low- and high-molecular-weight dissolved organic matter. *Applied and Environmental Microbiology* **66**: 1692–1697.
- Cowie, R.O.M., Maas, E.W., and Ryan, K.G. (2011) Archaeal diversity revealed in Antarctic

sea ice. *Antarctic Science* **23**: 531–536.

- Croot, P. L., Andersson, K., Öztürk, M., and Turner, D. R. (2004). The distribution and speciation of iron along 6 E in the Southern Ocean. *Deep Sea Research Part II: Topical Studies in Oceanography* **51**: 2857-2879.
- Croot, P. L., Laan, P., Nishioka, J., Strass, V., Cisewski, B., Boye, M., et al. (2005). Spatial and temporal distribution of Fe (II) and H₂O₂ during EisenEx, an open ocean mesoscale iron enrichment. *Marine Chemistry* **95**: 65-88.
- Curson, A.R.J., Rogers, R., Todd, J.D., Brearley, C.A., and Johnston, A.W.B. (2008) Molecular genetic analysis of a dimethylsulfoniopropionate lyase that liberates the climate-changing gas dimethylsulfide in several marine α -proteobacteria and *Rhodobacter sphaeroides*. *Environmental Microbiology* **10**: 757–767.

-D-

- Dadaglio, L., Dinasquet, J., Obernosterer, I., and Joux, F. (2018) Differential responses of bacteria to diatom-derived dissolved organic matter in the Arctic Ocean. *Aquatic Microbial Ecology* **82**: 59–72.
- De Baar, H.J.W. (2005) Synthesis of iron fertilization experiments: From the Iron Age in the Age of Enlightenment. *Journal of Geophysical Research* **110**: C9.
- Deacon, G.E.R., 1933. A general account of the hydrology of the South Atlantic Ocean. *Discovery Reports* **7**: 171–238.
- Debeljak, P., Toulza, E., Beier, S., Blain, S., and Obernosterer, I. (2019) Microbial iron metabolism as revealed by gene expression profiles in contrasted Southern Ocean regimes. *Environmental Microbiology*.
- Del Giorgio, P. A., and J. J. Cole (2000) Bacterial energetics and growth efficiency. In *Microbial Ecology of the Oceans*, ed. D.L. Kirchman. Wiley-Liss, Inc, pp. 289–325.
- Delmont, T.O., Eren, A.M., Vineis, J.H., and Post, A.F. (2015) Genome reconstructions indicate the partitioning of ecological functions inside a phytoplankton bloom in the Amundsen Sea, Antarctica. *Frontiers in Microbiology* **6**: 1090.
- Delmont, T.O., Hammar, K.M., Ducklow, H.W., Yager, P.L., and Post, A.F. (2014) *Phaeocystis antarctica* blooms strongly influence bacterial community structures in the Amundsen Sea polynya. *Frontiers in Microbiology* **5**: 646.
- DeLong, E.F., Franks, D.G., and Alldredge, A.L. (1993) Phylogenetic diversity of aggregate-attached vs. free-living marine bacterial assemblages. *Limnology and Oceanography* **38**: 924–934.
- DeSantis, T.Z., Hugenholtz, P., Larsen, N., Rojas, M., Brodie, E.L., Keller, K., et al. (2006) Greengenes, a Chimera-Checked 16S rRNA Gene Database and Workbench

Compatible with ARB. *Applied and Environmental Microbiology* **72**: 5069–5072.

- Dinasquet, J., Landa, M., and Obernosterer, I. (2019) High contribution of Pelagibacterales to bacterial community composition and activity in spring blooms off Kerguelen Island (Southern Ocean). *BioRxiv*, 633925.
- Dinasquet, J., Richert, I., Logares, R., Yager, P., Bertilsson, S., and Riemann, L. (2017) Mixing of water masses caused by a drifting iceberg affects bacterial activity, community composition and substrate utilization capability in the Southern Ocean: Iceberg influence on bacterioplankton. *Environmental Microbiology* **19**: 2453–2467.
- Dittmar, T. and Stubbins, A. (2014) Dissolved organic matter in aquatic systems. In, *Treatise on Geochemistry*. Elsevier, pp. 125–156.
- Duce, R. A., and Tindale, N. W. (1991). Atmospheric transport of iron and its deposition in the ocean. *Limnology and Oceanography* **36**: 1715-1726.
- Ducklow, H.W., Fraser, W., Karl, D.M., Quetin, L.B., Ross, R.M., Smith, R.C., et al. (2006) Water-column processes in the West Antarctic Peninsula and the Ross Sea: Interannual variations and foodweb structure. *Deep Sea Research Part II: Topical Studies in Oceanography* **53**: 834–852.
- Dunker, A. K., Brown, C. J., Lawson, J. D., Iakoucheva, L. M., and Obradović, Z. (2002). Intrinsic disorder and protein function. *Biochemistry* **41**: 6573-6582.
- Dupont, C.L., Rusch, D.B., Yooseph, S., Lombardo, M.J., Alexander Richter, R., Valas, R., et al. (2012) Genomic insights to SAR86, an abundant and uncultivated marine bacterial lineage. *The ISME Journal* **6**: 1186–1199.
- Durham, B.P., Sharma, S., Luo, H., Smith, C.B., Amin, S.A., Bender, S.J., et al. (2015) Cryptic carbon and sulfur cycling between surface ocean plankton. *Proceedings of the National Academy of Sciences* **112**: 453–457.

-E-

- Edgar, R.C. (2016) UNOISE2: Improved error-correction for Illumina 16S and ITS amplicon sequencing. *BioRxiv*, 081257.
- Edgar, R.C. (2013) UPARSE: highly accurate OTU sequences from microbial amplicon reads. *Nature Methods* **10**: 996–998.
- Emerson, S., and Hedges, J. (2008) *Chemical oceanography and the marine carbon cycle*. Cambridge University Press.
- Eren, A. M., Esen, Ö. C., Quince, C., Vineis, J. H., Morrison, H. G., Sogin, M. L., et al. (2015) Anvi'o: an advanced analysis and visualization platform for 'omics data. *PeerJ*, **3**: e1319.

Eren, A.M., Morrison, H.G., Lescault, P.J., Reveillaud, J., Vineis, J.H., and Sogin, M.L. (2015) Minimum entropy decomposition: Unsupervised oligotyping for sensitive partitioning of high-throughput marker gene sequences. *The ISME Journal* **9**: 968–979.

-F-

Falkowski, P.G., Barber, R.T., and Smetacek, V. (1998) Biogeochemical controls and feedbacks on ocean primary production. *Science, New Series* **281**: 200–206.

Falkowski, P.G., Fenchel, T., and Delong, E.F. (2008) The microbial engines that drive Earth's biogeochemical cycles. *Science* **320**: 1034–1039.

Fandino, L., Riemann, L., Steward, G., and Azam, F. (2005) Population dynamics of Cytophaga-Flavobacteria during marine phytoplankton blooms analyzed by real-time quantitative PCR. *Aquatic Microbial Ecology* **40**: 251–257.

Farneti, R., Delworth, T.L., Rosati, A.J., Griffies, S.M., and Zeng, F. (2010) The role of mesoscale eddies in the rectification of the Southern Ocean response to climate change. *Journal of Physical Oceanography* **40**: 1539–1557.

Faust, K. and Raes, J. (2012) Microbial interactions: from networks to models. *Nature Reviews Microbiology* **10**: 538–550.

Fernández-Gómez, B., Richter, M., Schüler, M., Pinhassi, J., Acinas, S.G., González, J.M., and Pedrós-Alió, C. (2013) Ecology of marine Bacteroidetes: a comparative genomics approach. *The ISME Journal* **7**: 1026–1037.

Field, K.G., Gordon, D., Wright, T., Rappe, M., Urbach, E., Vergin, K., and Giovannoni, S.J. (1997) Diversity and depth-specific distribution of SAR11 cluster rRNA genes from marine planktonic bacteria. *Applied and Environmental Microbiology* **63**: 8.

Fourquez, M., Beier, S., Jongmans, E., Hunter, R., and Obernosterer, I. (2016) Uptake of leucine, chitin, and iron by prokaryotic groups during spring phytoplankton blooms induced by natural iron fertilization off Kerguelen Island (Southern Ocean). *Frontiers in Marine Science* **3**: 256.

Fourquez, M., Bressac, M., Deppeler, S.L., Ellwood, M., Obernosterer, I., Trull, T., et al. (Submitted) Microbial Competition for Fe can Influence the Fate of Carbon in the Subpolar Southern Ocean

Fourquez, M., Obernosterer, I., Davies, D.M., Trull, T.W., and Blain, S. (2015) Microbial iron uptake in the naturally fertilized waters in the vicinity of the Kerguelen Islands: phytoplankton–bacteria interactions. *Biogeosciences* **12**: 1893–1906.

Fuentes, S., Arroyo, J.I., Rodríguez-Marconi, S., Masotti, I., Alarcón-Schumacher, T., Polz, M.F., et al. (2019) Summer phyto- and bacterioplankton communities during low and high productivity scenarios in the Western Antarctic Peninsula. *Polar Biology* **42**: 159–

- Fuhrman, J.A., Cram, J.A., and Needham, D.M. (2015) Marine microbial community dynamics and their ecological interpretation. *Nature Reviews Microbiology* **13**: 133–146.
- Fuhrman, J.A., Hewson, I., Schwalbach, M.S., Steele, J.A., Brown, M.V., and Naeem, S. (2006) Annually reoccurring bacterial communities are predictable from ocean conditions. *Proceedings of the National Academy of Sciences* **103**: 13104–13109.

-G-

- Garcia-Martinez, J. and Rodriguez-Valera, F. (2000) Microdiversity of uncultured marine prokaryotes: the SAR11 cluster and the marine Archaea of Group I. *Molecular Ecology* **9**: 935–948.
- Gärdes, A., Iversen, M.H., Grossart, H.-P., Passow, U., and Ullrich, M.S. (2011) Diatom-associated bacteria are required for aggregation of *Thalassiosira weissflogii*. *The ISME Journal* **5**: 436–445.
- Gasol, J.M. and Kirchman, D.L. eds. (2018) Microbial ecology of the oceans, third edition. Hoboken, NJ: John Wiley & Sons/Blackwell.
- Geider, R. J., La Roche, J., Greene, R. M., and Olaizola, M. (1993) Response of the photosynthetic apparatus of *Phaeodactylum tricornutum* (Bacillariophyceae) to nitrate, phosphate, or iron starvation 1. *Journal of Phycology* **29**: 755-766.
- Gent, P.R. (2016) Effects of southern hemisphere wind changes on the Meridional Overturning Circulation in ocean models. *Annual Review of Marine Science* **8**: 79–94.
- Gentile, G., Giuliano, L., D’Auria, G., Smedile, F., Azzaro, M., De Domenico, M., and Yakimov, M.M. (2006) Study of bacterial communities in Antarctic coastal waters by a combination of 16S rRNA and 16S rDNA sequencing. *Environmental Microbiology* **8**: 2150–2161.
- Ghiglione, J.F., Galand, P.E., Pommier, T., Pedros-Alio, C., Maas, E.W., Bakker, K., et al. (2012) Pole-to-pole biogeography of surface and deep marine bacterial communities. *Proceedings of the National Academy of Sciences* **109**: 17633–17638.
- Ghiglione, J.F. and Murray, A.E. (2012) Pronounced summer to winter differences and higher wintertime richness in coastal Antarctic marine bacterioplankton: Temporal variation in Southern Ocean coastal bacterioplankton. *Environmental Microbiology* **14**: 617–629.
- Giebel, H.-A., Brinkhoff, T., Zwisler, W., Selje, N., and Simon, M. (2009) Distribution of *Roseobacter* RCA and SAR11 lineages and distinct bacterial communities from the subtropics to the Southern Ocean. *Environmental Microbiology* **11**: 2164–2178.
- Giebel, H.-A., Kalhoefer, D., Gahl-Janssen, R., Choo, Y.-J., Lee, K., Cho, J.-C., et al. (2013)

- Planktomarina temperata gen. nov., sp. nov., belonging to the globally distributed RCA cluster of the marine Roseobacter clade, isolated from the German Wadden Sea. *International journal of systematic and evolutionary microbiology* **63**: 4207–4217.
- Giebel, H.-A., Kalhoefer, D., Lemke, A., Thole, S., Gahl-Janssen, R., Simon, M., and Brinkhoff, T. (2011) Distribution of Roseobacter RCA and SAR11 lineages in the North Sea and characteristics of an abundant RCA isolate. *The ISME Journal* **5**: 8–19.
- Gilbert, J.A., Steele, J.A., Caporaso, J.G., Steinbrück, L., Reeder, J., Temperton, B., et al. (2012) Defining seasonal marine microbial community dynamics. *The ISME Journal* **6**: 298–308.
- Giovannoni, S.J., Britschgi, T. B., Moyer, C. L., and Field, K. G. (1990). Genetic diversity in Sargasso Sea bacterioplankton. *Nature* **345**: 60.
- Giovannoni, S.J. (2017) SAR11 Bacteria: The most abundant plankton in the oceans. *Annual Review of Marine Science* **9**: 231–255.
- Giovannoni, S. J., and M. S. Rappé. (2000) Evolution, diversity, and molecular ecology of marine prokaryotes. In *Microbial ecology of the oceans*, ed. D. L. E. Kirchman, Wiley-Liss, New York, NY, pp. 47–84.
- Giovannoni, S.J., Tripp, H.J., Givan, S., Podar, M., Vergin, K.L., Baptista, D., et al. (2005) Genome Streamlining in a Cosmopolitan Oceanic Bacterium. *Science, New Series* **309**: 1242–1245.
- Gonzalez, J.M., Fernandez-Gomez, B., Fernandez-Guerra, A., Gomez-Consarnau, L., Sanchez, O., Coll-Llado, M., et al. (2008) Genome analysis of the proteorhodopsin-containing marine bacterium Polaribacter sp. MED152 (Flavobacteria). *Proceedings of the National Academy of Sciences* **105**: 8724–8729.
- Gosink, J. J., Woese, C. R., and Staley, J. T. (1998). Polaribacter gen. nov., with three new species, *P. irgensii* sp. nov., *P. franzmannii* sp. nov. and *P. filamentus* sp. nov., gas vacuolate polar marine bacteria of the Cytophaga-Flavobacterium-Bacteroides group and reclassification of ‘Flectobacillus glomeratus’ as *Polaribacter glomeratus* comb. nov. *International Journal of Systematic and Evolutionary Microbiology* **48**: 223-235.
- Gower, J. C. (1966). Some distance properties of latent root and vector methods used in multivariate analysis. *Biometrika* **53**: 325-338.
- Grzyski, J.J., Carter, B.J., DeLong, E.F., Feldman, R.A., Ghadiri, A., and Murray, A.E. (2006) Comparative genomics of DNA fragments from six Antarctic marine planktonic bacteria. *Applied and Environmental Microbiology* **72**: 1532–1541.
- Grzyski, J.J., Riesenfeld, C.S., Williams, T.J., Dussaq, A.M., Ducklow, H., Erickson, M., et al. (2012) A metagenomic assessment of winter and summer bacterioplankton from Antarctica Peninsula coastal surface waters. *The ISME Journal* **6**: 1901–1915.
- Guindon, S. and Gascuel, O. (2003) A simple, fast, and accurate algorithm to estimate large phylogenies by maximum likelihood. *Systematic Biology* **52**: 696–704.

- Hansell, D.A. 2002. DOC in the global ocean carbon cycle. In *Biogeochemistry of Marine Dissolved Organic Matter*, ed. Hansell, D.A., Carlson, C.A. San Diego, CA: Elsevier, pp. 685–715.
- Hansell, D.A. (2013) Recalcitrant dissolved organic carbon fractions. *Annual Review of Marine Science* **5**: 421–445.
- Hansell, D.A. and Carlson, C.A. (1998) Deep-ocean gradients in the concentration of dissolved organic carbon. *Nature* **395**: 263–266.
- Hansell, D. A., Carlson, C. A., Repeta, D. J., and Schlitzer, R. (2009). Dissolved organic matter in the ocean: New insights stimulated by a controversy. *Oceanography*, **22**: 202-211.
- Hansman, R.L., Dittmar, T., and Herndl, G.J. (2015) Conservation of dissolved organic matter molecular composition during mixing of the deep water masses of the northeast Atlantic Ocean. *Marine Chemistry* **177**: 288–297.
- Hanson, C.A., Fuhrman, J.A., Horner-Devine, M.C., and Martiny, J.B.H. (2012) Beyond biogeographic patterns: processes shaping the microbial landscape. *Nature Reviews Microbiology* **10**: 497–506.
- Hedges, J. I., Keil, R. G., & Benner, R. (1997). What happens to terrestrial organic matter in the ocean?. *Organic geochemistry* **27**: 195-212.
- Hedges, J.I. (1992) Global biogeochemical cycles: progress and problems. *Marine Chemistry* **39**: 67–93.
- Hill, M. O. (1973) Diversity and evenness: a unifying notation and its consequences. *Ecology* **54**: 427-432.
- Hogle, S.L., Brahmsha, B., and Barbeau, K.A. (2017) Direct heme uptake by phytoplankton-associated *Roseobacter* Bacteria. *MSystems* **2**: e00124-16.
- Hollibaugh, J., Lovejoy, C., and Murray, A. (2007) Microbiology in polar oceans. *Oceanography* **20**: 140–145.
- Hollibaugh, J.T., Bano, N., and Ducklow, H.W. (2002) Widespread distribution in polar oceans of a 16S rRNA gene sequence with affinity to Nitrosospira-like ammonia-oxidizing bacteria. *Applied and Environmental Microbiology* **68**: 1478–1484.
- Hu, P., Dubinsky, E.A., Probst, A.J., Wang, J., Sieber, C.M.K., Tom, L.M., et al. (2017) Simulation of *Deepwater Horizon* oil plume reveals substrate specialization within a complex community of hydrocarbon degraders. *Proceedings of the National Academy of Sciences* **114**: 7432–7437.

-J-

- Ide, J., Ohashi, M., Takahashi, K., Sugiyama, Y., Piirainen, S., Kortelainen, P., et al. (2017) Spatial variations in the molecular diversity of dissolved organic matter in water moving through a boreal forest in eastern Finland. *Scientific Reports* **7**: 42102.
- Iudicone, D., Rodgers, K.B., Stendardo, I., Aumont, O., Madec, G., Bopp, L., et al. (2011) Water masses as a unifying framework for understanding the Southern Ocean carbon cycle. *Biogeosciences* **8**: 1031–1052.

-J-

- Jamieson, R.E., Rogers, A.D., Billett, D.S.M., Smale, D.A., and Pearce, D.A. (2012) Patterns of marine bacterioplankton biodiversity in the surface waters of the Scotia Arc, Southern Ocean. *FEMS Microbiology Ecology* **80**: 452–468.
- Jiao, N., Herndl, G.J., Hansell, D.A., Benner, R., Kattner, G., Wilhelm, S.W., et al. (2010) Microbial production of recalcitrant dissolved organic matter: long-term carbon storage in the global ocean. *Nature Reviews Microbiology* **8**: 593–599.
- Jickells, T. D., An, Z. S., Andersen, K. K., Baker, A. R., Bergametti, G., Brooks, N., et al. (2005) Global iron connections between desert dust, ocean biogeochemistry, and climate. *Science* **308**: 67–71.
- Johnson, W.M., Kido Soule, M.C., and Kujawinski, E.B. (2016) Evidence for quorum sensing and differential metabolite production by a marine bacterium in response to DMSP. *The ISME Journal* **10**: 2304–2316.

-K-

- Kaiser, K. and Benner, R. (2008) Major bacterial contribution to the ocean reservoir of detrital organic carbon and nitrogen. *Limnology and Oceanography* **53**: 99–112.
- Katoh, K., Rozewicki, J., and Yamada, K.D. (2017) MAFFT online service: multiple sequence alignment, interactive sequence choice and visualization. *Briefings in Bioinformatics*: *bbx108*.
- Kellerman, A.M., Dittmar, T., Kothawala, D.N., and Tranvik, L.J. (2014) Chemodiversity of dissolved organic matter in lakes driven by climate and hydrology. *Nature Communications* **5**: 3804.
- Kendall, M. G. (1943) *Advanced theory of statistics Vol-I*. Charles Griffin: London.

- Khatiwala, S., Primeau, F., and Hall, T. (2009) Reconstruction of the history of anthropogenic CO₂ concentrations in the ocean. *Nature* **462**: 346–349.
- Kim, H., Park, A.K., Lee, J.H., Kim, H.-W., and Shin, S.C. (2018) Complete genome sequence of *Colwellia hornerae* PAMC 20917, a cold-active enzyme-producing bacterium isolated from the Arctic Ocean sediment. *Marine Genomics* **41**: 54–56.
- Kim, J.-G., Park, S.-J., Quan, Z.-X., Jung, M.-Y., Cha, I.-T., Kim, S.-J., et al. (2014) Unveiling abundance and distribution of planktonic *Bacteria* and *Archaea* in a polynya in Amundsen Sea, Antarctica: Prokaryotic communities in Antarctic polynya. *Environmental Microbiology* **16**: 1566–1578.
- Kim, S., Kramer, R.W., and Hatcher, P.G. (2003) Graphical Method for Analysis of Ultrahigh-Resolution Broadband Mass Spectra of Natural Organic Matter, the Van Krevelen Diagram. *Analytical Chemistry* **75**: 5336–5344.
- Kimes, N.E., López-Pérez, M., Ausó, E., Ghai, R., and Rodriguez-Valera, F. (2014) RNA sequencing provides evidence for functional variability between naturally co-existing *Alteromonas macleodii* lineages. *BMC Genomics* **15**: 938.
- Kirchman, D.L. (2002) The ecology of Cytophaga–Flavobacteria in aquatic environments. *FEMS Microbiology Ecology* **39**: 91–100.
- Kirchman, D.L., Yu, L., and Cottrell, M.T. (2003) Diversity and abundance of uncultured Cytophaga-like bacteria in the Delaware estuary. *Applied and Environmental Microbiology* **69**: 6587–6596.
- Klindworth, A., Mann, A.J., Huang, S., Wichels, A., Quast, C., Waldmann, J., et al. (2014) Diversity and activity of marine bacterioplankton during a diatom bloom in the North Sea assessed by total RNA and pyrotag sequencing. *Marine Genomics* **18**: 185–192.
- Koch, B.P. and Dittmar, T. (2006) From mass to structure: an aromaticity index for high-resolution mass data of natural organic matter. *Rapid Communications in Mass Spectrometry* **20**: 926–932.
- Koch, B.P. and Dittmar, T. (2016) From mass to structure: an aromaticity index for high-resolution mass data of natural organic matter. *Rapid Communications in Mass Spectrometry* **30**: 250–250.
- Koh, E.Y., Atamna-Ismaeel, N., Martin, A., Cowie, R.O.M., Beja, O., Davy, S.K., et al. (2010) Proteorhodopsin-bearing bacteria in Antarctic sea ice. *Applied and Environmental Microbiology* **76**: 5918–5925.
- Koh, E.Y., Phua, W., and Ryan, K.G. (2011) Aerobic anoxygenic phototrophic bacteria in Antarctic sea ice and seawater: Aerobic anoxygenic phototrophic. *Environmental Microbiology Reports* **3**: 710–716.
- Korb, R. E., Whitehouse, M. J., and Ward, P. (2004). SeaWiFS in the Southern Ocean: spatial and temporal variability in phytoplankton biomass around South Georgia. *Deep Sea*

Kreutzer, M.F., Kage, H., and Nett, M. (2012) Structure and biosynthetic assembly of cupriachelin, a photoreactive siderophore from the bioplastic roducer *Cupriavidus necator* H16. *Journal of the American Chemical Society* **134**: 5415–5422.

Kreutzer, M.F. and Nett, M. (2012) Genomics-driven discovery of taiwachelin, a lipopeptide siderophore from *Cupriavidus taiwanensis*. *Organic & Biomolecular Chemistry* **10**: 9338.

Kujawinski, E. B., Hatcher, P. G., and Freitas, M. A. (2002) High-resolution Fourier transform ion cyclotron resonance mass spectrometry of humic and fulvic acids: improvements and comparisons. *Analytical chemistry* **74**: 413-419.

Kujawinski, E.B. (2011) The impact of microbial metabolism on marine dissolved organic matter. *Annual Review of Marine Science* **3**: 567–599.

-L-

La Roche, J., Boyd, P. W., McKay, R. M. L., & Geider, R. J. (1996). Flavodoxin as an *in situ* marker for iron stress in phytoplankton. *Nature* **382**: 802.

Laghdass, M., Catala, P., Caparros, J., Oriol, L., Lebaron, P., and Obernosterer, I. (2012) High contribution of SAR11 to microbial activity in the North West Mediterranean Sea. *Microbial ecology* **63**: 324-333.

Lambert, S., Tragin, M., Lozano, J.-C., Ghiglione, J.-F., Vaulot, D., Bouget, F.-Y., and Galand, P.E. (2019) Rhythmicity of coastal marine picoeukaryotes, bacteria and archaea despite irregular environmental perturbations. *The ISME Journal* **13**: 388–401.

Lami, R., Ghiglione, J., Desdevises, Y., West, N., and Lebaron, P. (2009) Annual patterns of presence and activity of marine bacteria monitored by 16S rDNA–16S rRNA fingerprints in the coastal NW Mediterranean Sea. *Aquatic Microbial Ecology* **54**: 199–210.

Lamy, D., Obernosterer, I., Laghdass, M., Artigas, F., Breton, E., Grattepanche, J., et al. (2009) Temporal changes of major bacterial groups and bacterial heterotrophic activity during a *Phaeocystis globosa* bloom in the eastern English Channel. *Aquatic Microbial Ecology* **58**: 95–107.

Landa, M., Blain, S., Christaki, U., Monchy, S., and Obernosterer, I. (2016) Shifts in bacterial community composition associated with increased carbon cycling in a mosaic of phytoplankton blooms. *The ISME Journal* **10**: 39–50.

Landa, M., Blain, S., Harmand, J., Monchy, S., Rapaport, A., and Obernosterer, I. (2018) Major changes in the composition of a Southern Ocean bacterial community in response to diatom-derived dissolved organic matter. *FEMS Microbiology Ecology* **94**: fiy034.

- Landa, M., Burns, A.S., Durham, B.P., Esson, K., Nowinski, B., Sharma, S., et al. (2019) Sulfur metabolites that facilitate oceanic phytoplankton–bacteria carbon flux. *The ISME Journal*.
- Landa, M., Burns, A.S., Roth, S.J., and Moran, M.A. (2017) Bacterial transcriptome remodeling during sequential co-culture with a marine dinoflagellate and diatom. *The ISME Journal* **11**: 2677–2690.
- Landa, M., Cottrell, M.T., Kirchman, D.L., Kaiser, K., Medeiros, P.M., Tremblay, L., et al. (2014) Phylogenetic and structural response of heterotrophic bacteria to dissolved organic matter of different chemical composition in a continuous culture study: Bacterial diversity and dissolved organic matter. *Environmental Microbiology* **16**: 1668–1681.
- Lasbleiz, M., Leblanc, K., Armand, L.K., Christaki, U., Georges, C., Obernosterer, I., and Quéguiner, B. (2016) Composition of diatom communities and their contribution to plankton biomass in the naturally iron-fertilized region of Kerguelen in the Southern Ocean. *FEMS Microbiology Ecology* **92**: fw171.
- Lauro, F.M., McDougald, D., Thomas, T., Williams, T.J., Egan, S., Rice, S., et al. (2009) The genomic basis of trophic strategy in marine bacteria. *Proceedings of the National Academy of Sciences* **106**: 15527–15533.
- Lê Cao, K. A., Rossouw, D., Robert-Granié, C., & Besse, P. (2008). A sparse PLS for variable selection when integrating omics data. *Statistical applications in genetics and molecular biology* **7**: no. 1.
- Le Quéré, C., Rodenbeck, C., Buitenhuis, E.T., Conway, T.J., Langenfelds, R., Gomez, A., et al. (2007) Saturation of the Southern Ocean CO₂ sink due to recent climate change. *Science* **316**: 1735–1738.
- Lechtenfeld, O.J., Kattner, G., Flerus, R., McCallister, S.L., Schmitt-Kopplin, P., and Koch, B.P. (2014) Molecular transformation and degradation of refractory dissolved organic matter in the Atlantic and Southern Ocean. *Geochimica et Cosmochimica Acta* **126**: 321–337.
- Lefèvre, D., Guigue, C., Obernosterer, I. (2008) The metabolic balance during a phytoplankton bloom induced by natural iron fertilization in the Southern Ocean (Kerguelen Plateau). *Deep Sea Research, Part II* **55**: 766-776.
- Legendre, P. and Gallagher, E.D. (2001) Ecologically meaningful transformations for ordination of species data. *Oecologia* **129**: 271–280.
- Legendre, P., and Legendre, L. F. (2012) *Numerical ecology* (Vol. 24). Elsevier.
- Lennon, J.T. and Jones, S.E. (2011) Microbial seed banks: the ecological and evolutionary implications of dormancy. *Nature Reviews Microbiology* **9**: 119–130.
- Letourneau, M.L. and Medeiros, P.M. (2019) Dissolved organic matter composition in a marsh-dominated estuary: Response to seasonal forcing and to the passage of a hurricane.

- Li, D.X., Zhang, H., Chen, X.H., Xie, Z.X., Zhang, Y., Zhang, S.F., et al. (2018) Metaproteomics reveals major microbial players and their metabolic activities during the blooming period of a marine dinoflagellate *Prorocentrum donghaiense*: Microbial metaproteome during a dinoflagellate bloom. *Environmental Microbiology* **20**: 632–644.
- Lima-Mendez, G., Faust, K., Henry, N., Decelle, J., Colin, S., Carcillo, F., et al. (2015) Determinants of community structure in the global plankton interactome. *Science* **348**: 1262073–1262073.
- Lindh, M.V., Sjöstedt, J., Andersson, A.F., Baltar, F., Hugerth, L.W., Lundin, D., et al. (2015) Disentangling seasonal bacterioplankton population dynamics by high-frequency sampling: High-resolution temporal dynamics of marine bacteria. *Environmental Microbiology* **17**: 2459–2476.
- Lindström, E.S. and Langenheder, S. (2012) Local and regional factors influencing bacterial community assembly: Bacterial community assembly. *Environmental Microbiology Reports* **4**: 1–9.
- Lo Giudice, A., Caruso, C., Mangano, S., Bruni, V., De Domenico, M., and Michaud, L. (2012) Marine Bacterioplankton Diversity and Community Composition in an Antarctic Coastal Environment. *Microbial Ecology* **63**: 210–223.
- Longnecker, K., Kido Soule, M.C., and Kujawinski, E.B. (2015) Dissolved organic matter produced by *Thalassiosira pseudonana*. *Marine Chemistry* **168**: 114–123.
- López-García, P., López-López, A., Moreira, D., and Rodríguez-Valera, F. (2001). Diversity of free-living prokaryotes from a deep-sea site at the Antarctic Polar Front. *FEMS Microbiology Ecology* **36**: 193-202.
- Lucas, J., Wichels, A., Teeling, H., Chafee, M., Scharfe, M., and Gerdtts, G. (2015) Annual dynamics of North Sea bacterioplankton: seasonal variability superimposes short-term variation. *FEMS Microbiology Ecology* **91**: fiv099.
- Lumpkin, R., and Speer, K. (2007) Global ocean meridional overturning. *Journal of Physical Oceanography* **37**: 2550-2562.
- Luo, H. and Moran, M.A. (2014) Evolutionary ecology of the marine *Roseobacter* Clade. *Microbiology and Molecular Biology Reviews* **78**: 573–587.
- Luo, H., Swan, B.K., Stepanauskas, R., Hughes, A.L., and Moran, M.A. (2014) Evolutionary analysis of a streamlined lineage of surface ocean *Roseobacters*. *The ISME Journal* **8**: 1428–1439.
- Luria, C., Ducklow, H., and Amaral-Zettler, L. (2014) Marine bacterial, archaeal and eukaryotic diversity and community structure on the continental shelf of the western Antarctic Peninsula. *Aquatic Microbial Ecology* **73**: 107–121.

- Luria, C.M., Amaral-Zettler, L.A., Ducklow, H.W., Repeta, D.J., Rhyne, A.L., and Rich, J.J. (2017) Seasonal Shifts in Bacterial Community Responses to Phytoplankton-Derived Dissolved Organic Matter in the Western Antarctic Peninsula. *Frontiers in Microbiology* **8**: 2117.
- Luria, C.M., Amaral-Zettler, L.A., Ducklow, H.W., and Rich, J.J. (2016) Seasonal Succession of Free-Living Bacterial Communities in Coastal Waters of the Western Antarctic Peninsula. *Frontiers in Microbiology* **7**: 1731.

-M-

- Malviya, S., Scalco, E., Audic, S., Vincent, F., Veluchamy, A., Poulain, J., et al. (2016) Insights into global diatom distribution and diversity in the world's ocean. *Proceedings of the National Academy of Sciences* **113**: E1516–E1525.
- Manganelli, M., Malfatti, F., Samo, T.J., Mitchell, B.G., Wang, H., and Azam, F. (2009) Major role of microbes in carbon fluxes during austral winter in the southern Drake Passage. *PLoS ONE* **4**: e6941.
- Mann, D.G. (1999) The species concept in diatoms. *Phycologia* **38**: 437–495.
- Marchetti, A., Parker, M.S., Moccia, L.P., Lin, E.O., Arrieta, A.L., Ribalet, F., et al. (2009) Ferritin is used for iron storage in bloom-forming marine pennate diatoms. *Nature* **457**: 467–470.
- Margalef, R. (1958) Temporal and spatial heterogeneity in phytoplankton. In *Perspectives in marine biology*. Berkeley and Los Angeles: Univ. Calif. Press, pp. 323-350.
- Marie, D., Simon, N., Guillou, L., Partensky, F., and Vaulot, D. (2000) Flow cytometry analysis of marine picoplankton. In *In Living Color*. Springer, Berlin, Heidelberg, pp. 421-454.
- Marinov, I., Gnanadesikan, A., Toggweiler, J.R., and Sarmiento, J.L. (2006) The Southern Ocean biogeochemical divide. *Nature* **441**: 964–967.
- Marshall, J. and Speer, K. (2012) Closure of the meridional overturning circulation through Southern Ocean upwelling. *Nature Geoscience* **5**: 171–180.
- Martin, J.H. (1990) Glacial-interglacial CO₂ change: The Iron Hypothesis. *Paleoceanography* **5**: 1–13.
- McBride, M.J. (2001) Bacterial Gliding Motility: Multiple Mechanisms for Cell Movement over Surfaces. *Annual Review of Microbiology* **55**: 49–75.
- McMurdie, P.J. and Holmes, S. (2013) phyloseq: An R package for reproducible interactive analysis and graphics of microbiome census data. *PLoS ONE* **8**: e61217.
- Medeiros, P.M., Seidel, M., Gifford, S.M., Ballantyne, F., Dittmar, T., Whitman, W.B., and

- Moran, M.A. (2017) Microbially-mediated transformations of estuarine dissolved organic matter. *Frontiers in Marine Science* **4**: 69.
- Medeiros, P.M., Seidel, M., Ward, N.D., Carpenter, E.J., Gomes, H.R., Niggemann, J., et al. (2015) Fate of the Amazon River dissolved organic matter in the tropical Atlantic Ocean: DOM in the Amazon river-ocean continuum. *Global Biogeochemical Cycles* **29**: 677–690.
- Méthé, B.A., Nelson, K.E., Deming, J.W., Momen, B., Melamud, E., Zhang, X., et al. (2005) The psychrophilic lifestyle as revealed by the genome sequence of *Colwellia psychrerythraea* 34H through genomic and proteomic analyses. *Proceedings of the National Academy of Sciences* **102**: 10913–10918.
- Metzl, N., Tilbrook, B., and Poisson, A. (1999) The annual fCO₂ cycle and the air-sea CO₂ flux in the sub-Antarctic Ocean. *Tellus B: Chemical and Physical Meteorology* **51**: 849-861.
- Moore, J.K. and Abbott, M.R. (2000) Phytoplankton chlorophyll distributions and primary production in the Southern Ocean. *Journal of Geophysical Research: Oceans* **105**: 28709–28722.
- Moore, J. K., and Abbott, M. R. (2002) Surface chlorophyll concentrations in relation to the Antarctic Polar Front: seasonal and spatial patterns from satellite observations. *Journal of Marine Systems* **37**: 69-86.
- Moore, J.K., Abbott, M.R., and Richman, J.G. (1999) Location and dynamics of the Antarctic Polar Front from satellite sea surface temperature data. *Journal of Geophysical Research: Oceans* **104**: 3059–3073.
- Moore, J.K., Doney, S.C., Glover, D.M., and Fung, I.Y. (2001) Iron cycling and nutrient-limitation patterns in surface waters of the World Ocean. *Deep Sea Research Part II: Topical Studies in Oceanography* **49**: 463–507.
- Mopper, K., Stubbins, A., Ritchie, J. D., Bialk, H. M., and Hatcher, P. G. (2007). Advanced instrumental approaches for characterization of marine dissolved organic matter: extraction techniques, mass spectrometry, and nuclear magnetic resonance spectroscopy. *Chemical Reviews* **107**: 419-442.
- Moran, M.A., Belas, R., Schell, M.A., Gonzalez, J.M., Sun, F., Sun, S., et al. (2007) Ecological genomics of marine Roseobacters. *Applied and Environmental Microbiology* **73**: 4559–4569.
- Moran, M.A., Buchan, A., González, J.M., Heidelberg, J.F., Whitman, W.B., Kiene, R.P., et al. (2004) Genome sequence of *Silicibacter pomeroyi* reveals adaptations to the marine environment. *Nature* **432**: 910–913.
- Moran, M.A., González, J.M., and Kiene, R.P. (2003) Linking a bacterial taxon to sulfur cycling in the sea: Studies of the marine Roseobacter Group. *Geomicrobiology Journal* **20**: 375–388.
- Morel, F. M., Rueter, J. G., and Price, N. M. (1991) Iron nutrition of phytoplankton and its

possible importance in the ecology of ocean regions with high nutrient and low biomass. *Oceanography* **4**: 56-61.

Morris, R. M., Rappé, M. S., Connon, S. A., Vergin, K. L., Siebold, W. A., Carlson, C. A., et al. (2002). SAR11 clade dominates ocean surface bacterioplankton communities. *Nature*, **420**: 806.

Mou, X., Vila-Costa, M., Sun, S., Zhao, W., Sharma, S., and Moran, M.A. (2011) Metatranscriptomic signature of exogenous polyamine utilization by coastal bacterioplankton: Polyamine-transforming genes in marine bacterial communities. *Environmental Microbiology Reports* **3**: 798–806.

Movva, N. R., Nakamura, K., and Inouye, M. (1980). Gene structure of the OmpA protein, a major surface protein of *Escherichia coli* required for cell-cell interaction. *Journal of molecular biology* **143**: 317-328.

Murray, A.E. and Grzymalski, J.J. (2007) Diversity and genomics of Antarctic marine microorganisms. *Philosophical Transactions of the Royal Society B: Biological Sciences* **362**: 2259–2271.

Murray, A.E., Peng, V., Tyler, C., and Wagh, P. (2011) Marine bacterioplankton biomass, activity and community structure in the vicinity of Antarctic icebergs. *Deep Sea Research Part II: Topical Studies in Oceanography* **58**: 1407–1421.

Murray, A.E., Preston, C.M., Massana, R., Taylor, L.T., Blakis, A., Wu, K., and Delong, E.F. (1998) Seasonal and spatial variability of bacterial and archaeal assemblages in the coastal waters near Anvers Island, Antarctica. *Applied and Environmental Microbiology* **64**: 11.

Myklestad, S.M. (2000) Dissolved organic carbon from phytoplankton. In *Marine Chemistry*, ed. Wangersky, P.J.. Berlin, Heidelberg: Springer, pp. 111–148.

-N-

Nagata, T. (2000) Production mechanisms of dissolved organic matter. In *Microbial ecology of the oceans*, ed. DL Kirchman, New York: Wiley-Liss, pp. 121–52.

Nagata, T. (2008) Organic matter-bacteria interactions in seawater. *Microbial ecology of the oceans* **2**: 207-241.

Needham, D.M. and Fuhrman, J.A. (2016) Pronounced daily succession of phytoplankton, archaea and bacteria following a spring bloom. *Nature Microbiology* **1**: 16005.

Needham, D.M., Sachdeva, R., and Fuhrman, J.A. (2017) Ecological dynamics and co-occurrence among marine phytoplankton, bacteria and myoviruses shows microdiversity matters. *The ISME Journal* **11**: 1614–1629.

Nelson, D.M., Tréguer, P., Brzezinski, M.A., Leynaert, A., and Quéguiner, B. (1995)

Production and dissolution of biogenic silica in the ocean: Revised global estimates, comparison with regional data and relationship to biogenic sedimentation. *Global Biogeochemical Cycles* **9**: 359–372.

Neumann, A.M., Balmonte, J.P., Berger, M., Giebel, H.A., Arnosti, C., Voget, S., et al. (2015) Different utilization of alginate and other algal polysaccharides by marine *Alteromonas macleodii* ecotypes: Polysaccharide utilization by *A. macleodii*. *Environmental Microbiology* **17**: 3857–3868.

Newton, R.J., Griffin, L.E., Bowles, K.M., Meile, C., Gifford, S., Givens, C.E., et al. (2010) Genome characteristics of a generalist marine bacterial lineage. *The ISME Journal* **4**: 784–798.

Nikrad, M.P., Cottrell, M.T., and Kirchman, D.L. (2014) Uptake of dissolved organic carbon by gammaproteobacterial subgroups in coastal waters of the West Antarctic Peninsula. *Applied and Environmental Microbiology* **80**: 3362–3368.

-O-

Obernosterer, I., Catala, P., Lebaron, P., and West, N.J. (2011) Distinct bacterial groups contribute to carbon cycling during a naturally iron fertilized phytoplankton bloom in the Southern Ocean. *Limnology and Oceanography* **56**: 2391–2401.

Obernosterer, I., Christaki, U., Lefèvre, D., Catala, P., Van Wambeke, F., and Lebaron, P. (2008) Rapid bacterial mineralization of organic carbon produced during a phytoplankton bloom induced by natural iron fertilization in the Southern Ocean. *Deep Sea Research Part II: Topical Studies in Oceanography* **55**: 777–789.

Obernosterer, I., Fourquez, M., and Blain, S. (2015) Fe and C co-limitation of heterotrophic bacteria in the naturally fertilized region off the Kerguelen Islands. *Biogeosciences* **12**: 1983–1992.

Obernosterer, I., Lami, R., Larcher, M., Batailler, N., Catala, P., and Lebaron, P. (2010) Linkage between bacterial carbon processing and the structure of the active bacterial community at a coastal site in the NW Mediterranean Sea. *Microbial ecology* **59**: 428–435.

Ogawa, H. (2001) Production of refractory dissolved organic matter by bacteria. *Science* **292**: 917–920.

Ogawa, H., Fukuda, R., and Koike, I. (1999) Vertical distributions of dissolved organic carbon and nitrogen in the Southern Ocean. *Deep Sea Research Part I: Oceanographic Research Papers* **46**: 1809–1826.

Ogawa, H. and Ogura, N. (1992) Comparison of two methods for measuring dissolved organic carbon in sea water. *Nature* **356**: 696–698.

Oh, H.M., Kwon, K.K., Kang, I., Kang, S.G., Lee, J.H., Kim, S.J., and Cho, J.C. (2010)

- Complete genome sequence of “Candidatus Puniceispirillum marinum” IMCC1322, a representative of the SAR116 clade in the Alphaproteobacteria. *Journal of Bacteriology* **192**: 3240–3241.
- Oksanen J., Blanchet FG., Kindt R., Legendre P., Minchin PR., O'Hara RB., et al. (2015), vegan: Community ecology package. R package version 3.4.2.
- Oliver, J.L., Barber, R.T., Smith, W.O., and Ducklow, H.W. (2004) The heterotrophic bacterial response during the Southern Ocean Iron Experiment (SOFeX). *Limnology and Oceanography* **49**: 2129–2140.
- Orphan, V. J. (2009) Methods for unveiling cryptic microbial partnerships in nature. *Current opinion in microbiology* **12**: 231-237.
- Orsi, A.H., Johnson, G.C., and Bullister, J.L. (1999) Circulation, mixing, and production of Antarctic Bottom Water. *Progress in Oceanography* **43**: 55–109.
- Orsi, A.H., Whitworth, T., and Nowlin, W.D. (1995) On the meridional extent and fronts of the Antarctic Circumpolar Current. *Deep Sea Research Part I: Oceanographic Research Papers* **42**: 641–673.
- Orsi, W.D., Smith, J.M., Liu, S., Liu, Z., Sakamoto, C.M., Wilken, S., et al. (2016) Diverse, uncultivated bacteria and archaea underlying the cycling of dissolved protein in the ocean. *The ISME Journal* **10**: 2158–2173.
- Osterholz, H., Singer, G., Wemheuer, B., Daniel, R., Simon, M., Niggemann, J., and Dittmar, T. (2016) Deciphering associations between dissolved organic molecules and bacterial communities in a pelagic marine system. *The ISME Journal* **10**: 1717–1730.
- O’Sullivan, L.A., Fuller, K.E., Thomas, E.M., Turley, C.M., Fry, J.C., and Weightman, A.J. (2004) Distribution and culturability of the uncultivated ‘AGG58 cluster’ of the Bacteroidetes phylum in aquatic environments. *FEMS Microbiology Ecology* **47**: 359–370.

-P-

- Paerl, R.W., Bouget, F.-Y., Lozano, J.-C., Vergé, V., Schatt, P., Allen, E.E., et al. (2017) Use of plankton-derived vitamin B1 precursors, especially thiazole-related precursor, by key marine picoeukaryotic phytoplankton. *The ISME Journal* **11**: 753–765.
- Palenik, B., Brahamsha, B., Larimer, F. W., Land, M., Hauser, L., Chain, P., et al. (2003). The genome of a motile marine *Synechococcus*. *Nature*, **424**:1037.
- Palenik, B., Ren, Q., Dupont, C.L., Myers, G.S., Heidelberg, J.F., Badger, J.H., et al. (2006) Genome sequence of *Synechococcus* CC9311: Insights into adaptation to a coastal environment. *Proceedings of the National Academy of Sciences* **103**: 13555–13559.

- Parada, A.E., Needham, D.M., and Fuhrman, J.A. (2016) Every base matters: assessing small subunit rRNA primers for marine microbiomes with mock communities, time series and global field samples: Primers for marine microbiome studies. *Environmental Microbiology* **18**: 1403–1414.
- Pinhassi, J., Sala, M.M., Havskum, H., Peters, F., Guadayol, O. s., Malits, A., and Marrase, C. (2004) Changes in bacterioplankton composition under different phytoplankton regimens. *Applied and Environmental Microbiology* **70**: 6753–6766.
- Piquet, A.M.-T., Bolhuis, H., Meredith, M.P., and Buma, A.G.J. (2011) Shifts in coastal Antarctic marine microbial communities during and after melt water-related surface stratification: Melt water and Antarctic marine microorganisms. *FEMS Microbiology Ecology* **76**: 413–427.
- Planquette, H., Statham, P.J., Fones, G.R., Charette, M.A., Moore, C.M., Salter, I., et al. (2007) Dissolved iron in the vicinity of the Crozet Islands, Southern Ocean. *Deep Sea Research Part II: Topical Studies in Oceanography* **54**: 1999–2019.
- Pollard, R.T., Lucas, M.I., and Read, J.F. (2002) Physical controls on biogeochemical zonation in the Southern Ocean. *Deep Sea Research Part II: Topical Studies in Oceanography* **49**: 3289–3305.

-Q-

- Quast, C., Pruesse, E., Yilmaz, P., Gerken, J., Schweer, T., Yarza, P., et al. (2012) The SILVA ribosomal RNA gene database project: improved data processing and web-based tools. *Nucleic Acids Research* **41**: D590–D596.
- Quéguiner, B. (2013) Iron fertilization and the structure of planktonic communities in high nutrient regions of the Southern Ocean. *Deep Sea Research Part II: Topical Studies in Oceanography* **90**: 43–54.

-R-

- Rappé, M.S., Connon, S.A., Vergin, K.L., and Giovannoni, S.J. (2002) Cultivation of the ubiquitous SAR11 marine bacterioplankton clade. *Nature* **418**: 630–633.
- Rembauville, M., Briggs, N., Ardyna, M., Uitz, J., Catala, P., Penkerch, C., et al. (2017) Plankton assemblage estimated with BGC-Argo floats in the Southern Ocean: Implications for seasonal successions and particle export. *Journal of Geophysical Research: Oceans* **122**: 8278–8292.
- Riedel, T., and Dittmar, T. (2014). A method detection limit for the analysis of natural organic matter via Fourier transform ion cyclotron resonance mass spectrometry. *Analytical chemistry* **86**: 8376-8382.

- Riemann, L., Steward, G.F., and Azam, F. (2000) Dynamics of bacterial community composition and activity during a mesocosm alatom bloom. *Applied and Environmental Microbiology* **66**: 11.
- Rinta-Kanto, J.M., Sun, S., Sharma, S., Kiene, R.P., and Moran, M.A. (2012) Bacterial community transcription patterns during a marine phytoplankton bloom: Phytoplankton bloom metatranscriptome. *Environmental Microbiology* **14**: 228–239.
- Robinson, C., and Williams, P. L. B. (2005) Respiration and its measurement in surface marine waters. In *Respiration in aquatic ecosystems*, ed. Del Giorgio, P. and P. J. le B. Williams. Oxford University Press, pp. 147-180.
- Rogge, A., Vogts, A., Voss, M., Jürgens, K., Jost, G., and Labrenz, M. (2017) Success of chemolithoautotrophic SUP05 and *Sulfurimonas* GD17 cells in pelagic Baltic Sea redox zones is facilitated by their lifestyles as *K*- and *r*-strategists: SUP05 and *Sulfurimonas* in sulfidic redox zones. *Environmental Microbiology* **19**: 2495–2506.
- Rohart, F., Gautier, B., Singh, A., and Lê Cao, K.A. (2017) mixOmics: An R package for ‘omics feature selection and multiple data integration. *PLOS Computational Biology* **13**: e1005752.
- Rossel, P.E., Vähätalo, A.V., Witt, M., and Dittmar, T. (2013) Molecular composition of dissolved organic matter from a wetland plant (*Juncus effusus*) after photochemical and microbial decomposition (1.25 yr): Common features with deep sea dissolved organic matter. *Organic Geochemistry* **60**: 62–71.
- Roth, V.N., Dittmar, T., Gaupp, R., and Gleixner, G. (2015) The Molecular composition of dissolved organic matter in forest soils as a function of pH and temperature. *PLOS ONE* **10**: e0119188.
- Rozema, P.D., Biggs, T., Sprong, P.A.A., Buma, A.G.J., Venables, H.J., Evans, C., et al. (2017) Summer microbial community composition governed by upper-ocean stratification and nutrient availability in northern Marguerite Bay, Antarctica. *Deep Sea Research Part II: Topical Studies in Oceanography* **139**: 151–166.
- Ruan, Q., Dutta, D., Schwalbach, M.S., Steele, J.A., Fuhrman, J.A., and Sun, F. (2006) Local similarity analysis reveals unique associations among marine bacterioplankton species and environmental factors. *Bioinformatics* **22**: 2532–2538.

-S-

- Sallée, J.-B., Llorc, J., Tagliabue, A., and Lévy, M. (2015) Characterization of distinct bloom phenology regimes in the Southern Ocean. *ICES Journal of Marine Science: Journal du Conseil* **72**: 1985–1998.
- Sander, S. G., and Koschinsky, A. (2011) Metal flux from hydrothermal vents increased by organic complexation. *Nature Geoscience* **4**: 145-150.

- Šantl-Temkiv, T., Finster, K., Dittmar, T., Hansen, B.M., Thyrhaug, R., Nielsen, N.W., and Karlson, U.G. (2013) Hailstones: A Window into the Microbial and Chemical Inventory of a Storm Cloud. *PLoS ONE* **8**: e53550.
- Sarmiento, H. and Gasol, J.M. (2012) Use of phytoplankton-derived dissolved organic carbon by different types of bacterioplankton: Use of phytoplankton-derived DOC by bacterioplankton. *Environmental Microbiology* **14**: 2348–2360.
- Sarmiento, H., Morana, C., and Gasol, J.M. (2016) Bacterioplankton niche partitioning in the use of phytoplankton-derived dissolved organic carbon: quantity is more important than quality. *The ISME Journal* **10**: 2582–2592.
- Sarmiento, H., Romera-Castillo, C., Lindh, M., Pinhassi, J., Sala, M.M., Gasol, J.M., et al. (2013) Phytoplankton species-specific release of dissolved free amino acids and their selective consumption by bacteria. *Limnology and Oceanography* **58**: 1123–1135.
- Sarmiento, J.L., Hughes, T.M.C., Stouffer, R.J., and Manabe, S. (1998) Simulated response of the ocean carbon cycle to anthropogenic climate warming. *Nature* **393**: 245–249.
- Sarmiento, J. L., Gruber, N., Brzezinski, M. A., and Dunne, J. P. (2004a) High-latitude controls of thermocline nutrients and low latitude biological productivity. *Nature* **427**: 56.
- Sarmiento, J. L., Slater, R., Barber, R., Bopp, L., Doney, S. C., Hirst, A. C., et al. (2004b) Response of ocean ecosystems to climate warming. *Global Biogeochemical Cycles* **18**: no. 3.
- Savory, J. J., Kaiser, N. K., McKenna, A. M., Xian, F., Blakney, G. T., Rodgers, R. P., et al. (2011) Parts-per-billion Fourier transform ion cyclotron resonance mass measurement accuracy with a “walking” calibration equation. *Analytical chemistry* **83**: 1732-1736.
- Sedwick, P. N., Blain, S., Quéguiner, B., Griffiths, F. B., Fiala, M., Bucciarelli, E., et al. (2002) Resource limitation of phytoplankton growth in the Crozet Basin, Subantarctic Southern Ocean. *Deep Sea Research Part II: Topical Studies in Oceanography* **49**: 3327-3349.
- Segev, E., Wyche, T.P., Kim, K.H., Petersen, J., Ellebrandt, C., Vlamakis, H., et al. (2016) Dynamic metabolic exchange governs a marine algal-bacterial interaction. *eLife* **5**: e17473.
- Seidel, M., Beck, M., Riedel, T., Waska, H., Suryaputra, I.G.N.A., Schnetger, B., et al. (2014) Biogeochemistry of dissolved organic matter in an anoxic intertidal creek bank. *Geochimica et Cosmochimica Acta* **140**: 418–434.
- Selje, N., Simon, M., and Brinkhoff, T. (2004) A newly discovered Roseobacter cluster in temperate and polar oceans. *Nature* **427**: 445–448.
- Seymour, J.R., Amin, S.A., Raina, J.B., and Stocker, R. (2017) Zooming in on the phycosphere: the ecological interface for phytoplankton–bacteria relationships. *Nature Microbiology* **2**: 17075.

- Shah, V., Chang, B.X., and Morris, R.M. (2017) Cultivation of a chemoautotroph from the SUP05 clade of marine bacteria that produces nitrite and consumes ammonium. *The ISME Journal* **11**: 263–271.
- Sheik, C.S., Jain, S., and Dick, G.J. (2014) Metabolic flexibility of enigmatic SAR324 revealed through metagenomics and metatranscriptomics: Disentangling the ecophysiological role of SAR324. *Environmental Microbiology* **16**: 304–317.
- Silipo, A. and Molinaro, A. (2010) The diversity of the core oligosaccharide in lipopolysaccharides. In *Endotoxins: Structure, Function and Recognition*, eds. Wang, X. and Quinn, P.J.. Dordrecht: Springer Netherlands, pp. 69–99.
- Simó, R. (2001) Production of atmospheric sulfur by oceanic plankton: biogeochemical, ecological and evolutionary links. *Trends in Ecology & Evolution* **16**: 287–294.
- Simon, M., Glöckner, F., and Amann, R. (1999) Different community structure and temperature optima of heterotrophic picoplankton in various regions of the Southern Ocean. *Aquatic Microbial Ecology* **18**: 275–284.
- Singh, S.K., Kotakonda, A., Kapardar, R.K., Kankipati, H.K., Sreenivasa Rao, P., Sankaranarayanan, P.M., et al. (2015) Response of bacterioplankton to iron fertilization of the Southern Ocean, Antarctica. *Frontiers in Microbiology* **6**: 863.
- Sloyan, B. M., and Rintoul, S. R. (2001) The Southern Ocean limb of the global deep overturning circulation. *Journal of Physical Oceanography* **31**: 143-173.
- Smetacek, V., Assmy, P., and Henjes, J. (2004) The role of grazing in structuring Southern Ocean pelagic ecosystems and biogeochemical cycles. *Antarctic Science* **16**: 541–558.
- Smith, D. C., and Azam, F. (1992). A simple, economical method for measuring bacterial protein synthesis rates in seawater using 3H-leucine. *Mar. Microb. Food Webs*, **6**: 107-114.
- Sokolov, S. and Rintoul, S.R. (2002) Structure of Southern Ocean fronts at 140 E. *Journal of Marine Systems* **37**: 151-184.
- Sowell, S.M., Wilhelm, L.J., Norbeck, A.D., Lipton, M.S., Nicora, C.D., Barofsky, D.F., et al. (2009) Transport functions dominate the SAR11 metaproteome at low-nutrient extremes in the Sargasso Sea. *The ISME Journal* **3**: 93–105.
- Speer, K., Rintoul, S.R., and Sloyan, B. (2000) The diabatic Deacon cell. *Journal of Physical Oceanography* **30**: 3212–3222.
- Staley, J.T. and Gosink, J.J. (1999) Poles Apart: Biodiversity and biogeography of sea ice bacteria. *Annual Review of Microbiology* **53**: 189–215.
- Staley, J. T., and Konopka, A. (1985). Measurement of *in situ* activities of nonphotosynthetic microorganisms in aquatic and terrestrial habitats. *Annual review of microbiology*, **39**: 321-346.

- Stanish, L.F., O'Neill, S.P., Gonzalez, A., Legg, T.M., Knelman, J., McKnight, D.M., et al. (2013) Bacteria and diatom co-occurrence patterns in microbial mats from polar desert streams: Diatom: bacteria co-occurrence in Dry Valley streams. *Environmental Microbiology* **15**: 1115–1131.
- Stewart, E.J. (2012) Growing unculturable bacteria. *Journal of Bacteriology* **194**: 4151–4160.
- Straza, T.R.A., Ducklow, H.W., Murray, A.E., and Kirchman, D.L. (2010) Abundance and single-cell activity of bacterial groups in Antarctic coastal waters. *Limnology and Oceanography* **55**: 2526–2536.
- Suzuki, M., Nakagawa, Y., Harayama, S., and Yamamoto, S. (2001) Phylogenetic analysis and taxonomic study of marine Cytophaga-like bacteria: proposal for *Tenacibaculum* gen. nov. with *Tenacibaculum maritimum* comb. nov. and *Tenacibaculum ovolyticum* comb. nov., and description of *Tenacibaculum mesophilum* sp. nov. and *Tenacibaculum amyolyticum* sp. nov. *International journal of systematic and evolutionary microbiology* **51**: 1639–1652.
- Suzuki, M.T. and Beja, O. (2007) An elusive marine photosynthetic bacterium is finally unveiled. *Proceedings of the National Academy of Sciences* **104**: 2561–2562.
- Swan, B.K., Martinez-Garcia, M., Preston, C.M., Sczyrba, A., Woyke, T., Lamy, D., et al. (2011) Potential for chemolithoautotrophy among ubiquitous bacteria lineages in the dark ocean. *Science* **333**: 1296–1300.
- Swan, B.K., Tupper, B., Sczyrba, A., Lauro, F.M., Martinez-Garcia, M., Gonzalez, J.M., et al. (2013) Prevalent genome streamlining and latitudinal divergence of planktonic bacteria in the surface ocean. *Proceedings of the National Academy of Sciences* **110**: 11463–11468.

-T-

- Tada, Y., Makabe, R., Kasamatsu-Takazawa, N., Taniguchi, A., and Hamasaki, K. (2013) Growth and distribution patterns of *Roseobacter/Rhodobacter*, SAR11, and *Bacteroidetes* lineages in the Southern Ocean. *Polar Biology* **36**: 691–704.
- Tada, Y., Nakaya, R., Goto, S., Yamashita, Y., and Suzuki, K. (2017) Distinct bacterial community and diversity shifts after phytoplankton-derived dissolved organic matter addition in a coastal environment. *Journal of Experimental Marine Biology and Ecology* **495**: 119–128.
- Tada, Y., Taniguchi, A., Nagao, I., Miki, T., Uematsu, M., Tsuda, A., and Hamasaki, K. (2011) Differing growth responses of major phylogenetic groups of marine bacteria to natural phytoplankton blooms in the western North Pacific Ocean. *Applied and Environmental Microbiology* **77**: 4055–4065.
- Taylor, J.D., Cottingham, S.D., Billinge, J., and Cunliffe, M. (2014) Seasonal microbial

- community dynamics correlate with phytoplankton-derived polysaccharides in surface coastal waters. *The ISME Journal* **8**: 245–248.
- Teeling, H., Fuchs, B.M., Becher, D., Klockow, C., Gardebrecht, A., Bennke, C.M., et al. (2012) Substrate-controlled succession of marine bacterioplankton populations induced by a phytoplankton bloom. *Science* **336**: 608–611.
- Teeling, H., Fuchs, B.M., Bennke, C.M., Krüger, K., Chafee, M., Kappelmann, L., et al. (2016) Recurring patterns in bacterioplankton dynamics during coastal spring algae blooms. *eLife* **5**: e11888.
- Thiele, S., Fuchs, B.M., Ramaiah, N., and Amann, R. (2012) Microbial community response during the iron fertilization experiment LOHAFEX. *Applied and Environmental Microbiology* **78**: 8803–8812.
- Thompson, A.W., Foster, R.A., Krupke, A., Carter, B.J., Musat, N., Vaultot, D., et al. (2012) Unicellular Cyanobacterium symbiotic with a single-celled eukaryotic alga. *Science* **337**: 1546–1550.
- Thornton, D.C.O. (2014) Dissolved organic matter (DOM) release by phytoplankton in the contemporary and future ocean. *European Journal of Phycology* **49**: 20–46.
- Tikhonov, M., Leach, R.W., and Wingreen, N.S. (2015) Interpreting 16S metagenomic data without clustering to achieve sub-OTU resolution. *The ISME Journal* **9**: 68–80.
- Timmermans, K.R., van der Wagt, B., and de Baar, H.J.W. (2004) Growth rates, half-saturation constants, and silicate, nitrate, and phosphate depletion in relation to iron availability of four large, open-ocean diatoms from the Southern Ocean. *Limnology and Oceanography* **49**: 2141–2151.
- Topping, J., Heywood, J., Ward, P., and Zubkov, M. (2006) Bacterioplankton composition in the Scotia Sea, Antarctica, during the austral summer of 2003. *Aquatic Microbial Ecology* **45**: 229–235.
- Trull, T., Rintoul, S.R., Hadfield, M., and Abraham, E.R. (2001) Circulation and seasonal evolution of polar waters south of Australia: implications for iron fertilization of the Southern Ocean. *Deep Sea Research Part II: Topical Studies in Oceanography* **48**: 2439–2466.

-U-

- Uitz, J., Claustre, H., Griffiths, F.B., Ras, J., Garcia, N., and Sandroni, V. (2009) A phytoplankton class-specific primary production model applied to the Kerguelen Islands region (Southern Ocean). *Deep Sea Research Part I: Oceanographic Research Papers* **56**: 541–560.
- Ussher, S. J., Achterberg, E. P., and Worsfold, P. J. (2004) Marine biogeochemistry of

iron. *Environmental Chemistry* **1**: 67-80.

-V-

Van Tol, H.M., Amin, S.A., and Armbrust, E.V. (2017) Ubiquitous marine bacterium inhibits diatom cell division. *The ISME Journal* **11**: 31–42.

Vartoukian, S.R., Palmer, R.M., and Wade, W.G. (2010) Strategies for culture of ‘unculturable’ bacteria. *FEMS Microbiology Letters* **309**: 1-7.

Vorobev, A., Sharma, S., Yu, M., Lee, J., Washington, B.J., Whitman, W.B., et al. (2018) Identifying labile DOM components in a coastal ocean through depleted bacterial transcripts and chemical signals: Labile DOM in a coastal ocean. *Environmental Microbiology* **20**: 3012–3030.

-W-

Wagner-Döbler, I. and Biebl, H. (2006) Environmental biology of the marine *Roseobacter* lineage. *Annual Review of Microbiology* **60**: 255–280.

Weber, T.S. and Deutsch, C. (2010) Ocean nutrient ratios governed by plankton biogeography. *Nature* **467**: 550–554.

Weinstein, J.N., Myers, T., Buolamwini, J., Raghavan, K., Van Osdol, W., Licht, J., et al. (1994) Predictive statistics and artificial intelligence in the U.S. National Cancer Institute’s drug discovery program for cancer and AIDS. *Stem Cells* **12**: 13–22.

Weinstein, J.N., Myers, T.G., O’Connor, P.M., Friend, S.H., Fornace, A.J., Kohn, K.W., et al. (1997) An information-intensive approach to the molecular pharmacology of cancer. *Science* **275**: 343–349.

West, N.J., Obernosterer, I., Zemb, O., and Lebaron, P. (2008) Major differences of bacterial diversity and activity inside and outside of a natural iron-fertilized phytoplankton bloom in the Southern Ocean. *Environmental Microbiology* **10**: 738–756.

Whitworth, T. (1980) Zonation and geostrophic flow of the Antarctic Circumpolar Current at Drake Passage. *Deep Sea Research Part A. Oceanographic Research Papers* **27**: 497-507.

Whitworth, T. and Nowlin, W.D. (1987) Water masses and currents of the Southern Ocean at the Greenwich Meridian. *Journal of Geophysical Research* **92**: 6462.

Wilkins, D., Lauro, F.M., Williams, T.J., Demaere, M.Z., Brown, M.V., Hoffman, J.M., et al. (2013a) Biogeographic partitioning of Southern Ocean microorganisms revealed by metagenomics: Biogeography of Southern Ocean microorganisms. *Environmental*

Microbiology **15**: 1318–1333.

Wilkins, D., van Sebille, E., Rintoul, S.R., Lauro, F.M., and Cavicchioli, R. (2013b) Advection shapes Southern Ocean microbial assemblages independent of distance and environment effects. *Nature Communications* **4**: 2457.

Wilkins, D., Yau, S., Williams, T.J., Allen, M.A., Brown, M.V., DeMaere, M.Z., et al. (2013c) Key microbial drivers in Antarctic aquatic environments. *FEMS Microbiology Reviews* **37**: 303–335.

Williams, P. L. (1975) Biological and chemical aspects of dissolved organic materials in seawater. In *Chemical oceanography*, (J. P. Riley and G. Skirrow, Eds.). Academic Press, New York, pp. 301-363.

Williams, T.J., Long, E., Evans, F., DeMaere, M.Z., Lauro, F.M., Raftery, M.J., et al. (2012) A metaproteomic assessment of winter and summer bacterioplankton from Antarctic Peninsula coastal surface waters. *The ISME Journal* **6**: 1883–1900.

Williams, T.J., Wilkins, D., Long, E., Evans, F., DeMaere, M.Z., Raftery, M.J., and Cavicchioli, R. (2013) The role of planktonic *Flavobacteria* in processing algal organic matter in coastal East Antarctica revealed using metagenomics and metaproteomics: Metaproteomics of marine Antarctic *Flavobacteria*. *Environmental Microbiology* **15**: 1302–1317.

Wold, H. (1966) Estimation of principal components and related models by iterative least squares. In *Multivariate analysis*. Wiley, krishnaiah, p.r. (ed.). Academic Press, New York, pp. 391-420.

Wold, S., Sjöström, M., and Eriksson, L. (2001) PLS-regression: a basic tool of chemometrics. *Chemometrics and Intelligent Laboratory Systems* **58**: 109–130.

Wu, X., Wu, L., Liu, Y., Zhang, P., Li, Q., Zhou, J., et al. (2018) Microbial interactions with dissolved organic matter drive carbon dynamics and community succession. *Frontiers in Microbiology* **9**: 1234.

Wu, Z., Rodgers, R. P., and Marshall, A. G. (2004) Two-and three-dimensional van Krevelen diagrams: a graphical analysis complementary to the Kendrick mass plot for sorting elemental compositions of complex organic mixtures based on ultrahigh-resolution broadband Fourier transform ion cyclotron resonance mass measurements. *Analytical chemistry* **76**: 2511-2516.

-X-

Xia, L.C., Ai, D., Cram, J., Fuhrman, J.A., and Sun, F. (2013) Efficient statistical significance approximation for local similarity analysis of high-throughput time series data. *Bioinformatics* **29**: 230–237.

Xing, P., Hahnke, R.L., Unfried, F., Markert, S., Huang, S., Barbeyron, T., et al. (2015) Niches of two polysaccharide-degrading *Polaribacter* isolates from the North Sea during a spring diatom bloom. *The ISME Journal* **9**: 1410–1422.

-Y-

Yooseph, S., Neelson, K.H., Rusch, D.B., McCrow, J.P., Dupont, C.L., Kim, M., et al. (2010) Genomic and functional adaptation in surface ocean planktonic prokaryotes. *Nature* **468**: 60–66.

-Z-

Zancarini, A., Echenique-Subiabre, I., Debroas, D., Taïb, N., Quiblier, C., and Humbert, J.-F. (2017) Deciphering biodiversity and interactions between bacteria and microeukaryotes within epilithic biofilms from the Loue River, France. *Scientific Reports* **7**: 4344.

Zehr, J.P. (2015) How single cells work together. *Science* **349**: 1163–1164.

Zeng, Y.-X., Yu, Y., Qiao, Z.-Y., Jin, H.-Y., and Li, H.-R. (2014) Diversity of bacterioplankton in coastal seawaters of Fildes Peninsula, King George Island, Antarctica. *Archives of Microbiology* **196**: 137–147.

Zhang, C., Dang, H., Azam, F., Benner, R., Legendre, L., Passow, U., et al. (2018) Evolving paradigms in biological carbon cycling in the ocean. *National Science Review* **5**: 481–499.

Zhou, J., Song, X., Zhang, C.-Y., Chen, G.-F., Lao, Y.-M., Jin, H., and Cai, Z.-H. (2018) Distribution Patterns of Microbial Community Structure Along a 7000-Mile Latitudinal Transect from the Mediterranean Sea Across the Atlantic Ocean to the Brazilian Coastal Sea. *Microbial Ecology* **76**: 592–609.

APPENDICES



Yan Liu

Appendix. 1

Microbial diversity and activity in the Southern Ocean

(Table 2 of Introduction)

Study Regions	Methods	Notes	Reference
Agulhas/Benguela Boundary	FISH	Different community structure and temperature optima of heterotrophic prokaryotes in various regions	Simon et al., 1999
Agulhas/Benguela Boundary	DGGE and FISH	The global distribution of RCA cluster	Selje et al., 2004
Agulhas/Benguela Boundary	DGGE	Distinct bacterial communities in oceanic regions and the distribution of SAR11 and Roseobacter clades in pelagic marine systems	Giebel et al., 2009
Amundsen Sea	454 pyrosequencing	Different environmental conditions and selection mechanisms controlling surface and deep ocean community structure and diversity	Ghiglione et al., 2012
Amundsen Sea	454 pyrosequencing	The overall vertical trends in the composition of bacterial community in the polynya centre, which were distinct from those of the sea ice stations	Kim et al., 2014
Antarctic Peninsula	Specific primer cloning	The microdiversity of SAR11 and archaeal marine Group I at depths	García-Martínez and Rodríguez-Valera, 2000
Antarctic Peninsula	FISH	Bacterial diversity and communities in Antarctic pack ice; Alphaproteobacteria, Gammaproteobacteria and cytophaga-Flavobacterium were dominant groups	Brinkmeyer et al., 2003

APPENDIX 1

Antarctic Peninsula	FISH	Planktonic Crenarchaeota and bacteria were both temporally and spatially variable in the WAP	Church et al., 2003
Antarctic Peninsula	Genomics	Genomes from six Antarctic planktonic bacteria indicated their cold adaptation in the permanently subzero waters	Grzymiski et al., 2006
Antarctic Peninsula	Genomics	Flavobacteria species, for example Polaribacter, and Gammaproterobacteria dominated in Antarctic cold waters	Murray and Grzymiski, 2007
Antarctic Peninsula	FISH	Abundance and single-cell activity of bacterial groups; The fractions of SAR11, Polaribacter, and Ant4D3 that were active differed from each other and varied among substrates	Straza et al., 2010
Antarctic Peninsula	DGGE and 16S rRNA clone library	A shift of bacterial groups from Alphaproteobacteria and Gammaproteobacteria to Cytophaga-Flavobacterium-Bacteroides during and after summertime melt water stratification	Piquet et al., 2011
Antarctic Peninsula	DGGE, CE-SSCP and tag pyrosequencing	A strong seasonal pattern with higher richness in winter and a clear influence of phytoplankton bloom events on bacterial community structure and diversity	Ghiglione and Murray, 2012
Antarctic Peninsula	Metagenomics	First study using metagenomics to identify seasonal shifts in Southern Ocean communities, highlighting the role of chemolithoautotrophic microorganisms in fixing CO ₂ in winter	Grzymiski et al., 2012
Antarctic Peninsula	Metaproteomics	A metaproteomic assessment of winter and summer bacteria in coastal surface waters	Williams et al., 2012
Antarctic Peninsula	Metagenomics	Global biogeography of SAR11	Brown et al., 2012
Antarctic Peninsula	454 pyrosequencing	The spatial variability in microbial community composition is relatively low (i.e., no significant north–south differences in community structure)	Luria et al., 2014

APPENDIX 1

Antarctic Peninsula	454 pyrosequencing	Similar patterns of bacterial communities between two coves in surface waters	Zeng et al., 2014
Antarctic Peninsula	DGGE and 16S rRNA gene amplicon sequencing	The shift of bacterial community composition governed by meltwater-related surface stratification and nutrient availability	Rozema et al., 2016
Antarctic Peninsula	16S rRNA gene amplicon sequencing	Clearly demonstrated the temporal relationship between phytoplankton blooms and seasonal succession in bacterial growth and community composition	Luria et al., 2016
Antarctic Peninsula	Metagenomics and metatranscriptomics	Similar bacterial community composition during two contrasting summer periods (Feb. and Mar.); Major bacterial groups did not show variation in C-assimilation between distinct Chlorophyll <i>a</i> periods, while they were more active in N-assimilation at higher Chlorophyll <i>a</i> level	Alcamán-Arias et al., 2018
Antarctic Peninsula	16S rRNA gene amplicon sequencing	Bacterial communities during low and high productivity scenarios in two consecutive summers	Fuentes et al., 2019
(near) Antarctic Peninsula	DGGE	Significant shifts in bacterial and archaeal communities on spatial and temporal scales	Murray et al., 1998
(near) Antarctic Peninsula	DGGE	Widespread distribution in polar oceans of the ammonia oxidizing bacteria	Hollibaugh et al., 2002
Atlantic Sector	T-RFLP	Bacterial abundance and production increased after iron fertilization, while no major changes of bacterial community composition in response to Fe fertilization	Arrieta et al., 2004
Atlantic Sector	DGGE	Distinct bacterial communities in oceanic regions and the distribution of SAR11 and Roseobacter clades in pelagic marine systems	Giebel et al. 2009

APPENDIX 1

Atlantic Sector	454 pyrosequencing and CARD-FISH	Algal exudates and decaying algal biomass resulted in a dynamic bacterial succession of distinct genera	Thiele et al., 2012
Atlantic Sector	16S rRNA clone library	This study identified three unique phylogenetic clusters which were not detected in any other iron fertilization studies. These clusters had different relative abundances in response to iron addition	Singh et al., 2015
Australian Sector	FISH and DGGE	Flavobacteria was significantly higher in PFZ and AAZ water samples than STZ and SAZ waters	Abell and Bowman, 2005a
Australian Sector	FISH and DGGE	Colonization and community dynamics of Flavobacteria on diatom detritus based on Southern Ocean seawater	Abell and Bowman, 2005b
Australian Sector	Metagenomics	Biogeographic partitioning of the Southern Ocean	Wilkins et al., 2013
Australian Sector	Metagenomics and metaproteomics	The role of Flavobacteria in processing algal organic matter in coastal east Antarctica	Williams et al., 2013
Australian Sector	Tag pyrosequencing technology	Distinct taxonomic profiles in different water masses; Advection shaped the composition of prokaryotic communities independent of distance and environmental selection	Wilkins et al., 2013
Drake Passage	16S rRNA gene clone library sequencing	Diversity of free-living prokaryotes from a deep-sea site (3000 m) at the Antarctic Polar Front	López-García et al., 2001
Drake Passage	DGGE	Bacteria were abundant and active in the mesopelagic layer, and could mediate significant carbon flux	Manganelli et al., 2009
Indian sector	FISH	Growth and distribution patterns of Roseobacter/Rhodobacter, SAR11, and Bacteroidetes along two transects	Tada et al., 2013

APPENDIX 1

Kerguelen plateau	CE-SSCP fingerprinting and 16S clone library	16S rDNA and 16S rRNA reveal contrasting bacterial diversity and activity inside and outside of a natural iron-fertilized phytoplankton bloom	West et al., 2008
Kerguelen plateau	MICRO-CARD-FISH	Distinct bacterial groups contribute to carbon cycling during a natural iron-fertilized phytoplankton bloom	Obernosterer et al., 2011
Kerguelen plateau	DGGE, CE-SSCP and tag pyrosequencing	A strong seasonal pattern with higher richness in winter and a clear influence of phytoplankton bloom events on bacterial community structure and diversity	Ghiglione and Murray, 2012
Kerguelen plateau	454 pyrosequencing	Different environmental conditions and selection mechanisms controlling surface and deep ocean community structure and diversity	Ghiglione et al., 2012
Kerguelen plateau	454 pyrosequencing	Different bloom stations formed distinct bacterial communities and DOM shaped bacterial communities	Landa et al., 2016
Kerguelen plateau	16S rRNA gene amplicon sequencing	High contribution of SAR11 to bacterial community composition and activity in spring blooms	Dinasquet et al., 2019
Ross Sea	DGGE	Widespread distribution in polar oceans of the ammonia oxidizing bacteria	Hollibaugh et al., 2002
Ross sea	16S rDNA and rRNA clone library	16S rDNA and 16S rRNA showed the evident divergences between bacterial diversity and activity at each site	Gentile et al., 2006
Ross Sea	16S amplicon sequencing	The first findings of aerobic anoxygenic phototrophs (AAnPs) in Antarctic sea ice and seawater	Koh et al., 2011
Ross sea	FISH	Bacteroidetes was equally dominant with the Actinobacteria and Gammaproteobacteria during the decay of sea ice	Lo Giudice et al., 2012
Ross Sea	454 pyrosequencing	Different environmental conditions and selection mechanisms controlling surface and deep ocean community structure and diversity	Ghiglione et al., 2012

APPENDIX 1

(near) Ross Sea	16S rRNA gene clone library	Archaeal diversity in Antarctic sea ice	Cowie et al., 2011
(near) Ross Sea	16S rDNA and rRNA amplicon sequencing	Proteorhodopsin-containing bacteria in Antarctic sea ice, generating from genomic DNA and cDNA transcripts of Alphaterobacteria, Gammaproteobacteria and Flavobacteria	Koh et al., 2010
Scotia Sea	Specific primer cloning	The diversity of both SAR11 and archaeal marine Group I showed significant shifts from deep samples to some surface clones	García-Martínez and Rodríguez-Valera, 2000
Scotia Sea	CARD-FISH	Bacterial community composition along eight zig-zag transects	Topping et al., 2006
Scotia Sea	16S rRNA gene clone library	Bacterial biomass, activity and community structure in the vicinity of Antarctic icebergs	Murray et al., 2010
Scotia Sea	FISH, 16S rRNA clone library	Bacterial communities in seven spatially separated samples	Jamieson et al. 2012
Scotia Sea	Metagenomics	Global biogeography of SAR11	Brown et al., 2012
Weddell Sea	DGGE and FISH	The global distribution of RCA cluster	Selje et al., 2004
Weddell Sea	Primers specific cloning	The diversity of both SAR11 and archaeal marine Group I showed significant shifts from deep samples to some surface clones	García-Martínez and Rodríguez-Valera, 2000
Weddell Sea	16S rRNA gene clone library	Bacterial biomass, activity and community structure in the vicinity of Antarctic icebergs	Murray et al., 2010
Weddell Sea	Metagenomics	Global biogeography of SAR11	Brown et al., 2012

Note studies located in several regions.

Appendix. 2

Prokaryotic diversity and activity in contrasting productivity regimes in late summer in the Kerguelen region (Southern Ocean)

--Master thesis

Sorbonne Université

Faculty of Sciences

Laboratoire d'Océanographie Microbienne (LOMIC), Observatoire Océanologique de Banyuls
(OOB)



PROKARYOTIC DIVERSITY AND ACTIVITY IN CONTRASTING PRODUCTIVITY REGIMES IN LATE SUMMER IN THE KERGUELEN REGION (SOUTHERN OCEAN)

Alejandra Elisa Hernández Magaña – 20170502

Promotor: Ingrid Obernosterer

Supervisor: Ingrid Obernosterer



Master thesis submitted to Ghent University for the partial fulfillment of the requirements for the
degree of **Master of Science in Marine Biological Resources (IMBRSea)**

Academic year: 2018-2019

'No data can be taken out of this work without prior approval of the thesis promoter'.

'I hereby confirm that I have independently composed this Master thesis and that no other than the indicated aid and sources have been used. This work has not been presented to any other examination board.'

[June 3, 2019]

[Signature]

A handwritten signature in black ink, appearing to be 'S. J. G.', written over the [Signature] label.

“La chance ne sourit qu'aux esprits bien prepares”.

- Louis Pasteur.

A mis ancestros, mis contemporáneos y a los que vienen...

Dedication / Dedicatoria

A mi madre, mi padre y mis hermanos, gracias por su amor incondicional y su enorme apoyo, a pesar de la distancia. Ustedes siempre serán mi inspiración para continuar.

A mi familia del lado Hernández y Magaña, por sus valores y ganas de siempre salir adelante.

A mis amigos que son la familia que uno elige, por que cada uno de ustedes ha dejado algo en mi, y si los nombrara a todos, tendría la familia más grande y bonita del mundo.

A mi México (lindo y querido), por que siempre habrá más cosas únicas y hermosas que adversidades... por que la ciencia crezca, tanto como la diversidad biológica y cultural que tenemos...

A mi *alma mater* la UNAM... donde han nacido una gran parte de mis oportunidades, donde he aprendido tanto de la vida, y no solo de la biología...

To my international friends (in and out of the Uni) that were with me during this 2-years journey (so called IMBRsea), even if we share a couple of weeks or months (in Oviedo, Ghent, Napoli or Banyuls...). Thanks for sharing all your culture, ideas, knowledge, languages, delicious food, and love, I hope you received the same from me.

Grazie mille ai miei amici del laboratorio a Napoli (Maila, Alex, Cecilia) et merci beaucoup à mes amis du laboratoire – bureau en Banyuls (Nawal, Cléliita and Guigui) for doing every day of work more enjoyable (funny) and less hard.

Thanks to my supervisor Ingrid Obernosterer, to give me the opportunity to join the LOMIC and be part of MOBYDICK project. Thanks for the guidance and support.

Very thanks to Yan Liu for sharing with me all your bioinformatics knowledge and patience.

To all the ones interested in read this thesis, as passionate as me by the fact that such a small beings (prokaryotes) can modify processes in a planetary scale... never stop to be amazed.

Table of contents

Executive Summary	I
Abstract	II
1. Introduction & Aims	1
1.1. Prokaryotic diversity and its role in the oceans	1
1.2. Southern Ocean and MOBYDICK Project	2
2. Material and Methods	3
2.1. Nucleic acids extraction	4
2.2. Data analysis	5
2.3. Statistical analysis	6
3. Results	7
3.1. Environmental conditions	7
3.2. Prokaryotic community distribution	9
3.3. Prokaryotic Diversity	11
3.4. Prokaryotic community composition	12
3.5. Taxa contributing to the difference between on and off plateau	17
4. Discussion	20
4.1. Prokaryotic community distribution	20
4.2. Prokaryotic Diversity	21
4.3. Taxa contributing to the difference <i>on</i> and <i>off plateau</i>.	22
5. Conclusion	23
6. Acknowledgements	24
7. References	25
8. Supplementary information	29

Executive Summary

Characterizing the prokaryotic diversity in the global ocean is still a challenge to address, especially to understand its relationship with the ecosystemic processes. The Southern Ocean (SO) is the most extended high-nutrient low-chlorophyll (HNLC) region in the global ocean, in which the biological productivity is limited by iron, however, in the vicinity of the Kerguelen Islands, an annual bloom takes place due to natural iron fertilization, being natural laboratory to understand the nutrient cycling in the SO. The present Master Thesis is part of the large multidisciplinary project MOBYDICK that aims to better understand the biological carbon pump considering end-to-end marine food webs, and linking biodiversity to biogeochemical fluxes in this region.

An oceanographic cruise was carried out in late Austral summer in 2018 to the Kerguelen region, where contrasting ecosystems were sampled at all trophic levels (from prokaryotes to top predators). In this framework, the main aim of this Master Thesis is to describe the composition of the total and active free-living and particle-attached prokaryotic community at contrasting sites, via next generation sequencing (Illumina) of the 16S rRNA gene.

It is provided a detailed description of the prokaryotic communities in the free-living and particle-attached size fractions. The prokaryotic communities showed to be constrained by the depth layer along the water column, especially for the free living fraction. In the case of the particle attached fraction, the connectivity between the depth layers in the water column is higher due to particle sinking. Above the surface mixed layer (SML), the prokaryotic communities showed to be different at the Stations off (M1, M3, M4) and on the plateau (M2), highlighting lower diversity on the plateau, and different composition of the community, predominantly by Flavobacteriales contributing with 50% of the relative abundance on the plateau. The alpha diversity for the particle attached fraction did not differ among sites, however, the overall alpha diversity of this size fraction was lower than that for the free living.

The most abundant members of the community that significantly contributed to the difference between sites, were mainly *Aurantvirga* and *Ulvibacter* on the plateau, and *Formosa* off plateau, normally associated to diatom-dominated blooms due to their metabolic capabilities to utilize polymers in high nutrient-conditions. Compared to the abundant groups, other groups such as Cellvibrionales and SAR11 showed contribution to the differences among contrasting ecosystems with relatively lower abundance in the community composition.

Abstract

In the Kerguelen Region (Southern Ocean), there are two contrasting regimes in terms of productivity and carbon export: an iron fertilized area which produces annual blooms on the plateau, and high-nutrient-low-chlorophyll (HNLC) off the plateau. The total (DNA) and active (RNA) free-living and particle-attached prokaryotic communities, were described during the late Austral summer. Depth was a constraining factor, especially for free living prokaryotic communities. Above the surface mixed layer, prokaryotic communities on and off the plateau were different (ANOSIM $p < 0.05$) with an overall lower diversity on plateau in comparison to off plateau. The community was dominated by Flavobacteriales on plateau (>50% relative abundance). The particle attached fraction showed lower alpha diversity compared to the free living one, in all sites. Main taxa contributing to the differences between regimes (SIMPER $p < 0.05$) belongs to Flavobacteriales such as *Aurantvirga* and *Ulvibacter* on plateau, and *Formosa* off plateau. Cellvibrionales and SAR11 also contributed to the differences between the two contrasting regimes. Overall, community composition changed among stations at both fractions, being more diverse in the free living one. Dominant groups as Flavobacteriales, could reflect the advantage over other community members, probably due to their polymer degradation capabilities.

1. Introduction & Aims

1.1 Prokaryotic diversity in the oceans

Microorganisms play a key role in several global processes, such as the maintenance of ecosystem functioning, or the biogeochemical cycling of nutrients (Falkowski *et al.*, 2008). Prokaryotes are especially abundant in the ocean and it is estimated that the majority remain unknown, due to the difficulties in obtaining culturable strains (Hugenholtz, 2002; Curtis *et al.*, 2006). In the last few decades, the majority of studies regarding microbial diversity have been conducted on PCR-based and culture-independent methods (Biers *et al.*, 2009; Yooseph *et al.*, 2010).

Nowadays, the use of culture-independent high-throughput sequencing of 16S rRNA genes has facilitated studies which explore the microbial composition and dynamics in several environments (Kim *et al.*, 2017). Next generation sequencing (NGS), has particularly become an extremely useful tool in order to describe with high resolution the microbial biodiversity (López-Pérez *et al.*, 2016).

Aiming to complete the general understanding of the prokaryotic diversity in the global ocean and its contribution as key players in different regions, major sampling and analysis efforts have taken place in the last decades (Rusch *et al.*, 2007; Sunagawa *et al.*, 2015; Salazar *et al.*, 2016; Mestre *et al.*, 2018). The high latitudes regions, however, especially the Southern Ocean, have been less studied due to the logistic difficulties of working there, but are of increasing interest due to their ecological importance and susceptibility in the frame of the global change (Biers *et al.*, 2009; Wilkins *et al.*, 2013).

1.2. Southern Ocean and MOBYDICK cruise

The Southern Ocean is a key area to understand the global carbon cycle, due to several processes taking place there, including the permanent upwelling around Antarctica which transports refractory dissolved organic matter (DOM) to the surface, and concurrent low primary production due to iron limitation (Wilkins *et al.*, 2013b). The Southern Ocean, has been characterized as the largest HNLC region within the global ocean (Landa *et al.*, 2018) and several studies in the area have revealed that the low biological productivity, despite the availability of nutrients, is principally determined by the impact of iron limitation on phytoplankton growth (Blain *et al.*, 2008; Singh *et al.*, 2015)

These conditions generate unique physico-chemical properties that enable high levels of microbial primary production to occur, which consequently impacts prokaryotic diversity and adapts their metabolisms (Wilkins *et al.*, 2013; Landa *et al.*, 2016, 2018). It has been studied the response of prokaryotic communities in the Southern Ocean to iron fertilization experiments, mainly through bulk parameters (Arrieta *et al.*, 2004), and in some cases also focusing in the composition of the communities (Thiele *et al.*, 2012; Singh *et al.*, 2015). These studies did not show differences before

and after the iron fertilization, however, differences in bacterial abundance, production and also succession in the prokaryotic communities have been observed in relation to phytoplankton blooms induced by natural iron fertilization (West *et al.*, 2008; Landa *et al.*, 2016; Liu *et al.*, 2019).

The Kerguelen Plateau, in the Indian sector of the Southern Ocean, is registered as a site where an annual massive phytoplankton bloom takes place due to natural iron fertilization processes (Armand *et al.*, 2008; Blain *et al.*, 2008; Mongin *et al.*, 2008; Jouandet *et al.*, 2014). The phytoplankton bloom induced by iron fertilization in this region can last for months a difference to the blooms induced by mesoscale iron fertilization, who typically last a few weeks (West *et al.*, 2008).

In the context of the carbon limited conditions in the Southern Ocean, the DOM and exudates produced by the phytoplankton during the bloom, might act as a selective pressure, affecting the prokaryotic abundance, activity and shaping the community composition (Singh *et al.*, 2015; Landa *et al.*, 2018; Liu *et al.*, 2019). It is suggested that the most adapted members to use the available organic matter or algal polymers will dominate, occupying the series of ecological niches provided by the availability of different algal products (Teeling *et al.*, 2012; Singh *et al.*, 2015; Liu *et al.*, 2019).

One of the current challenges in this frame, is to understand how the prokaryotic diversity is involved with the turnover of the organic carbon available (Landa *et al.*, 2016), and the consequent interactions with higher trophic levels. The present Master Thesis is part of the large multidisciplinary project MOBYDICK – Marine Ecosystem Biodiversity and Dynamics of Carbon around Kerguelen: an integrated view (2017-2022). The main objective of MOBYDICK is to better understand the biological carbon pump by (i) considering end-to-end marine food webs, and (ii) linking biodiversity to biogeochemical fluxes. To address this objective, an oceanographic cruise was carried out from February 18 to March 27 2018 to the Kerguelen region, where contrasting ecosystems were sampled at all trophic levels (from prokaryotes to top predators).

The principal objective of this Master thesis project is to describe the diversity of the total and active, free-living (<0.8 μm) and particle-attached (>0.8 μm) prokaryotic community at sites characterized by contrasting conditions in terms of productivity and carbon export. We also aimed to describe the prokaryotic community composition and to determine the members of the community that contribute to the differences between sites.

In comparison to previous studies carried out in the region of the Kerguelen Plateau, the MOBYDICK-cruise took place during the late Austral summer. The observations reported here, therefore, refer to the post-bloom phase, while the onset, peak and declining phases of early spring phytoplankton blooms had been investigated previously (KEOPS1&2).

2. Material and Methods

The oceanographic cruise MOBYDICK was carried out aboard the R/V Marion Dufresne from February 18 to March 27, 2018. This period corresponds to the end of the Austral summer in the Kerguelen region. Based on previous cruises four sampling sites with contrasted productivity regimes were selected. Station M2 is located above the Kerguelen Plateau (overall depth 520m), and characterized by higher Chlorophyll *a* (Chl *a*) concentrations than off of the plateau, where the other stations were located (M1, M3 and M4) (Figure 1). Three repeated samplings with around 10 days of interval took place at Station M2, two samplings at M4 and M3 and one single sampling at M1 (see Table 1 in Results Section).

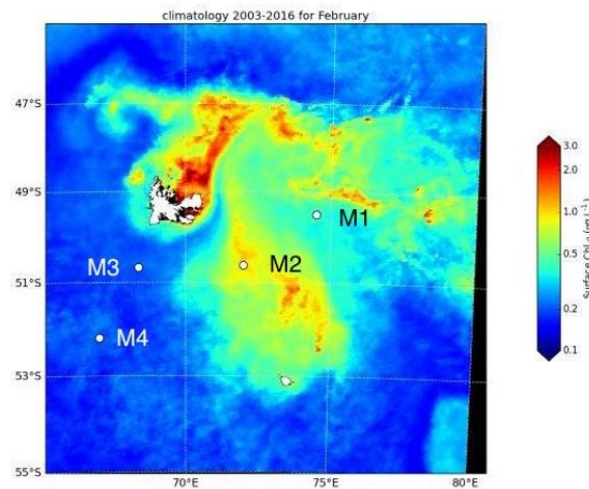


Figure 1. Sampling sites of the MOBYDICK Cruise southeast of Kerguelen Island (in white). Colour code represents mean chlorophyll concentrations derived from satellite ocean colour (climatological mean of 2003-2016 for February). Courtesy S. Blain.

Environmental parameters were collected throughout the water column and water samples for prokaryotic community composition were collected at four depths (10 m, 60 m, 125 m and 300 m) with 12 L Niskin bottles on a rosette equipped with a conductivity temperature depth sensor (CTD, model Seabird SBE9+). The depths for prokaryotic community composition were chosen according to the onboard CTD depth profiles with the aim to sample at the top and the base of the surface mixed layer (SML), the intermediate layer, and deep waters.

For the analysis of prokaryotic community composition the seawater samples were passed through a 60 µm nylon mesh and then 6 L of each sample were sequentially filtered through 0.8 µm pore-size polycarbonate membranes (47 mm diameter, Nuclepore, Whatman, Sigma Aldrich, St Louis, MO) and cells were concentrated on 0.22 µm cartridge (Sterivex™ Millipore, EMD, Billerica, MA), retrieving the particle attached (>0.8 µm) and free living fraction (<0.8 µm) respectively. The filters and cartridges were stored at -80° C until the DNA and RNA extraction.

Chl *a* concentrations were determined by High Performance Liquid Chromatography (HPLC), following the method of (Ras *et al.*, 2008) adapted from Van Heukelem & Thomas (2001). Abundances of heterotrophic and autotrophic prokaryotes and pico- and nano-eukaryotes were measured by Flow Cytometry (FACSAria II Becton Dickinson) analysed on a BD FACS Canto.

2.1. Nucleic acids extraction

To further understand the link between prokaryotic diversity, community structure and ecosystem functioning, it is important to associate microbial identity with their potential metabolic state. The ribosomal RNA (rRNA) abundance data has been suggested as an index of potential activity of microbial cells in order to identify the active members in microbial communities (Blazewicz *et al.*, 2013).

DNA and RNA extraction was performed simultaneously from the 0.8 and 0.2µm fractions, from the Sterivex™ cartridges and polycarbonate membranes respectively, using the AllPrep Kit (Qiagen, Hilden, Germany) with the following modifications based on Liu *et al.* (2019). The filter units were thawed and closed with a sterile pipette tip end at the outflow, 425 µl lysis buffer were added per sample (40mM EDTA, 50mM Tris and 0.75 M sucrose) and three freeze-thaw cycles were performed with liquid nitrogen and a water bath at 65°C. Subsequently, 25µl of freshly prepared lysozyme solution were added (2 mg ml⁻¹ final concentration), the filter units were placed in a rotary mixer and incubated at 37°C during 45 minutes, and then 8µl of proteinase K solution (0.2 mg ml⁻¹ final concentration) and sodium dodecyl sulfate (SDS) (1%) were added and maintained at 55°C with gentle agitation every 10 min for 2 hrs.

To protect the RNA, 10 µl of β-mercaptoethanol was added to 1 ml of RLT plus buffer provided by the kit, 1550 µl of this solution were added to each filter unit and mixed by inversion. The lysate was recovered by using a sterile 5 ml syringe and loaded in three additions onto the DNA columns by centrifuging at 10 000g for 30 s. DNA and RNA purifications were performed following the manufacturer's guidelines (Qiagen, Germany) in which RNA was treated with DNase to avoid contamination after first wash step.

The Invitrogen™ SuperScript™ VILO™ cDNA Synthesis Kit (Thermo Fisher Scientific Inc. Carlsbad, CA USA) was utilized to generate cDNA from the RNA extracts. Previous to the reverse transcription, purity of the RNA extracts was checked by PCR test with general primer sets 341F (5'-CCTACGGGNGGCWGCAG) and 805R (5'-GACTACHVGGGTATCTAATCC) for the prokaryotic 16S rRNA gene, followed by the examination of amplification products on 1% agarose electrophoresis.

PCR was performed using the primers 515F-Y (5'-GTGYCAGCMGCCGCGG TAA) and 926R (5'-CCGYCAATTYMTTTRAGTTT) that encompasses the V4 and V5 hypervariable regions of the 16S rDNA (Parada *et al.*, 2016), from the DNA and cDNA extracted previously. Triplicate 10 µl reaction mixtures contained 2 µg DNA, 5 µl KAPA2G Fast HotStart ReadyMix, 0.2 µM forward

primer and 0.2 μ M reverse primer. Polymeric chain reaction (PCR) amplification was performed under the following conditions: an initial denaturation step of 95°C for 3 min, followed by 30 cycles of denaturation at 95°C for 45 s, annealing at 50°C for 45 s, and extension at 68°C for 1:03 min. s, and a final elongation step at 68°C for 5 min.

The presence of amplification products was confirmed by 1% agarose electrophoresis and triplicates were pooled. Once pooled, the PCR products were purified by gel-filtration through Sephadex G-50 Super Fine resin (Amersham Biosciences, Uppsala, Sweden). The dry resin was deposited in a 45 μ l column charger, removed the excess with a scraper, placed the MultiScreen HV plate upside down on the charger and turned over together to obtain the plate wells filled with the resin. To the dry resin were added 300 μ l of ultrapure water and incubated per 3 hr at room temperature. The MultiScreen HV plate was placed on a standard 96 well microtiter plate and centrifuged at 910 g for 5 min to remove the water and compact the mini-columns. The samples were deposited in the mini-columns and the MultiScreen HV plate was placed on a standard 96 polypropylene plate and centrifuge per 5 min at 910 g. Then the purified samples were recovered for sequencing.

The 16S rRNA gene amplicons were sequenced via next generation sequencing (Illumina MiSeq 2 \times 250 bp chemistry on one flow-cell) at the platform GeT-PlaGe Genotoul (Toulouse, France). Mock community DNA (LGC standards, UK) was used as a standard for subsequent analyses and considered as a DNA sample for all treatments. In total, 128 samples (64 DNA and 64 cDNA) were sequenced. After the sequencing two samples were discarded, one due to low quality in the sequencing and the other due to the low number of reads.

2.2. Data analysis

The samples obtained in the sequencing run were demultiplexed at the platform GeT-PlaGe Genotoul (Toulouse, France). A total of 5 847 892 sequences were obtained. Processing sequences was conducted with the dada2 package for R version 1.10.1 (Callahan et al., 2016a), following the pipeline by Callahan *et al.*, (2016b). Primers were trimmed and the sequences were filtered based on their quality using filterAndTrim() in dada2 (maxEE=2, truncQ=2). Forward reads with a length of 245 bp, reverse reads with a length of 210 pb, and in total 4 253 969 reads were kept after quality filtering.

Amplicon sequence variants (ASVs) were inferred through the high resolution DADA2 method, resolving variants that differ by as little as one nucleotide (Callahan et al., 2016a; Callahan, McMurdie, & Holmes, 2017). This method relies on a parameterized model of substitution errors to distinguish sequencing errors from real biological variation (Callahan et al., 2016b). The generation of the ASVs does not depend on the fixation of arbitrary thresholds, contrary to the Operational Taxonomic Units (OTUs) which are clusters of reads that differs by less than a fixed dissimilarity threshold (usually 1 or 3%).

Error rates were estimated from the data, and inference of the sequence variants was made from the pooled sequences from all the samples. The 1 059 953 unique forward sequences and 1 619 348 reverse unique sequences were pooled to determine the sequence variants, then the forward and reverse sequences were merged and chimeras were removed. From this we obtained 54 491 unique ASVs. Taxonomy was assigned comparing the ASVs obtained against the SILVA database release 132 (Quast *et al.*, 2013). This database was cleaned, removing the ASVs recognized as Chloroplasts, Mitochondria and Eukaryotes using command `prune_taxa()` by Phyloseq R package version 1.26.1 (McMurdie & Holmes, 2013). The abundance table of the ASVs per sample was built with DADA2 and then combined with the taxonomy into a phyloseq-class object for further analysis.

From the 5 847 892 reads we obtained a total 18 699 ASVs for the 126 samples. The number of reads per sample varied between 3926 and 56840. The dataset was randomly subsampled to the lowest number of reads (3926) per sample with `rarefy_even_depth()` by Phyloseq, with the aim to enable comparisons between samples. After the subsampling 16664 ASVs remained in the dataset.

2.3. Statistical analysis

Taking into account the hydrological conditions in the study area and the stratification along the water column, we first aimed to explore the distribution patterns of the prokaryotic communities. We therefore applied Non-Metric Multidimensional Scaling (NMD), an ordination based on a dissimilarity matrix. In our case the Bray-Curtis dissimilarity matrix of the community structure was used, *i.e.*, occurrence and relative abundance of ASVs per sample.

The statistical analysis were performed in R 3.5.2 version, Bray–Curtis dissimilarity matrices were generated via `vegdist()` function based on the community structure. NMDS ordinations were generated based on Bray–Curtis dissimilarity using `metaMDS()` function in the package Vegan (Oksanen *et al.*, 2019).

Diversity indices were calculated with phyloseq command `estimate_richness()`. Analysis of similarity (ANOSIM) `anosim()` was performed to test significant differences in microbial communities between sampling depths and among sites in the surface mixed layer.

The contribution of individual species (ASVs) to the average Bray-Curtis dissimilarity between groups was obtained using similarity percentage analysis (SIMPER) `simper()`. The ASVs with a relative abundance lower than 1% in at least one sample were discarded prior the SIMPER analysis. Once the ASVs with a significant contribution to the dissimilarity between groups were obtained, the ASVs with a relative abundance higher than 5% in at least one sample were selected to plot them in a heatmap, with the package `pheatmap` version 1.0.12 for R (Kolde, 2019).

3. Results

3.1. Environmental conditions

During late Austral summer, the water column was stratified at the four sites with mixed layer depths ranging between 27m at Station M1 to up to 87m at Station M4 (Table 1). The Chl *a* concentrations at Station M2 varied from 0.28 mg m⁻³ in the surface mixed layer (SML) during the first visit to 0.62 mg m⁻³ during the third visit. Chl *a* dropped at about 150m depth to concentrations below 0.09 mg m⁻³ (Fig. 2).

Table 1. Environmental variables in surface waters (10m and 60m depth) during the study.

Site & visit	Depth (m)	Date	Long, Lat	SML (m)	Temp (°C)	Sal	Chl <i>a</i> (mg m ⁻³)	Het Prok (cells ml ⁻¹)	PicoNano (cells ml ⁻¹)
M1_1	10	09/03/2018	74.9011, -49.8498	27	5.08	33.89	0.31	6.06E+05	8.04E+03
	60				4.89	33.89	0.36	6.19E+05	8.01E+03
M2_1	10	26/02/2018	72.0007, -50.6163	62	5.21	33.86	0.28	1.15E+06	2.77E+03
	60				5.08	33.87	0.29	1.18E+06	3.19E+03
M2_2	10	06/03/2018	72.0181, -50.6278	61	5.24	33.86	0.32	8.37E+05	3.77E+03
	60				5.24	33.86	0.33	7.94E+05	3.49E+03
M2_3	10	16/03/2018	72.002, -50.6167	68	5.18	33.86	0.58	6.65E+05	8.13E+03
	60				5.07	33.86	0.62	7.08E+05	8.41E+03
M3_2	10	04/03/2018	68.0579, -50.6826	65	5.6	33.82	0.19	6.96E+05	3.72E+03
	60				5.6	33.82	0.19	6.65E+05	3.59E+03
M3_3	10	19/03/2018	68.0523, -50.7001	79	5.32	33.81	0.14	4.46E+05	1.49E+03
	60				5.32	33.81	0.14	4.45E+05	1.52E+03
M4_2	10	01/03/2018	67.1998, -52.6004	49	4.5	33.85	0.18	5.52E+05	3.18E+03
	60				4.48	33.85	0.18	5.50E+05	3.16E+03
M4_3	10	12/03/2018	67.207, -52.6019	87	4.47	33.85	0.21	5.01E+05	3.70E+03
	60				4.46	33.85	0.21	5.06E+05	3.76E+03

Depth refers to the sampling depth for the prokaryotic community analysis. SML, Surface mixed layer depth, Chl *a*, chlorophyll *a*; Het Prok, Heterotrophic prokaryotes; PicoNano, Pico-Nanophytoplankton.

In the case of Stations M3 and M4, Chl *a* concentrations were similar between visits, with higher concentrations in the upper 100 m depth (~0.2 mg m⁻³) (Fig. 2, M3, M4). Station M1 was visited only once during the cruise and the Chl *a* concentration is slightly higher than at the other off plateau sites (maximum ~0.39 mg m⁻³ at 75 m depth) (Fig. 2 M1).

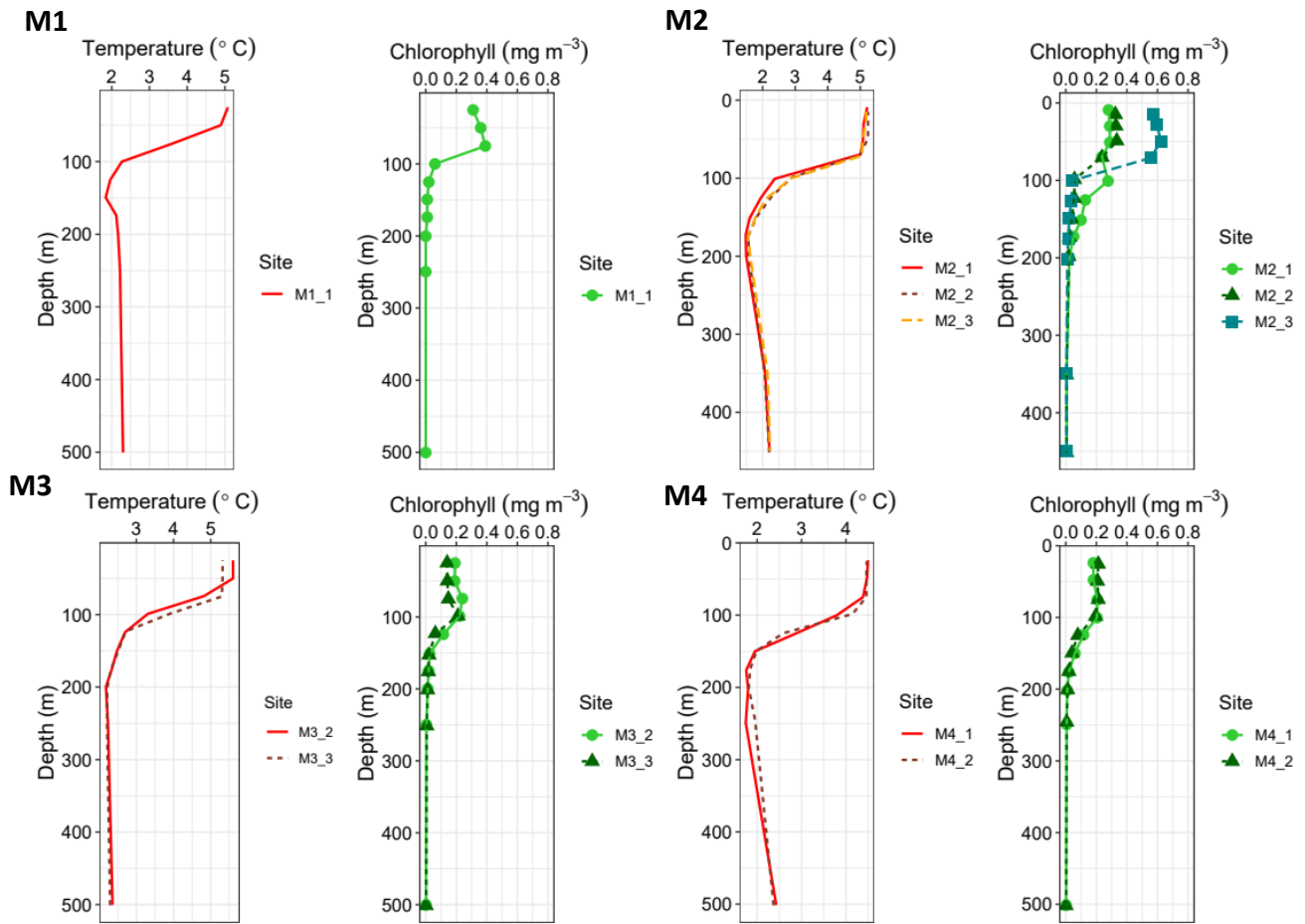


Figure 2. Vertical profiles of temperature and Chl *a* at the four sampling sites (M1, M2, M3 and M4). First visit: continued line and circle; second visit: dashed line and triangle; third visit (only for M2) long-dashed line and square.

Heterotrophic prokaryotic abundance was highest in surface waters at Station M2 during the first visit, and the abundance decreased by almost 2-fold two weeks later. At the off plateau sites, similar prokaryotic abundances were observed in surface waters.

Concentrations of Chl *a* and the abundance of heterotrophic prokaryotes were higher at Station M2 as compared to the off plateau sites.

3.2. Prokaryotic community distribution

A total of 126 samples were used to characterize the total (DNA) and the potentially active (RNA) prokaryotic community composition in the free living and in the particle attached fraction. 16 664 ASVs were obtained 13 044 ASVs for the free-living fraction and 10 993 ASVs for the particle-attached fraction; 7373 ASVs were shared between these fractions.

In surface waters (10m and 60m), the observed number of ASVs for the free living communities varied from 252 to 405 ASVs at Station M2, while this number was overall higher at the other sites (408 to 503 ASVs). In the particle attached communities, the number of ASVs was substantially lower and similar among sites (208 to 255 ASVs). At 125m depth for the free living community the number of ASVs ranged from 521 to 668, and for 300 m depth it varied from 657 to 865 ASVs.

According to the NMDS ordination, based on the community structure, the free-living prokaryotic communities, both total and active, were clustered by depth layer (Fig. 3). The communities of the deeper waters (300m) were distinct from the ones at 125m and from the communities at 10m and 60m depth. Except for Station M1, the 60m was at the base or well within the SML. The samples from the different depth layers were significantly different (DNA ANOSIM $R=0.71$, RNA $R=0.79$, $p<0.01$, Fig.3.A and B respectively). In the case of the particle-attached fraction of the total and active prokaryotic communities, the clusters by depth are less pronounced, although there is a gradient in the ordination where the cluster of the surface samples are followed by 125m and then by 300m depth (Fig. 3. C and D). The depth groups for both total (DNA) and active (RNA) communities are consistent.

In the surface mixed layer, the free-living prokaryotic communities are different between the sites on and off the plateau (Figure 4). For the free-living fraction, the difference is more pronounced than for the particle-attached fraction. The clusters per site for total (DNA) and active (RNA) communities have similar patterns.

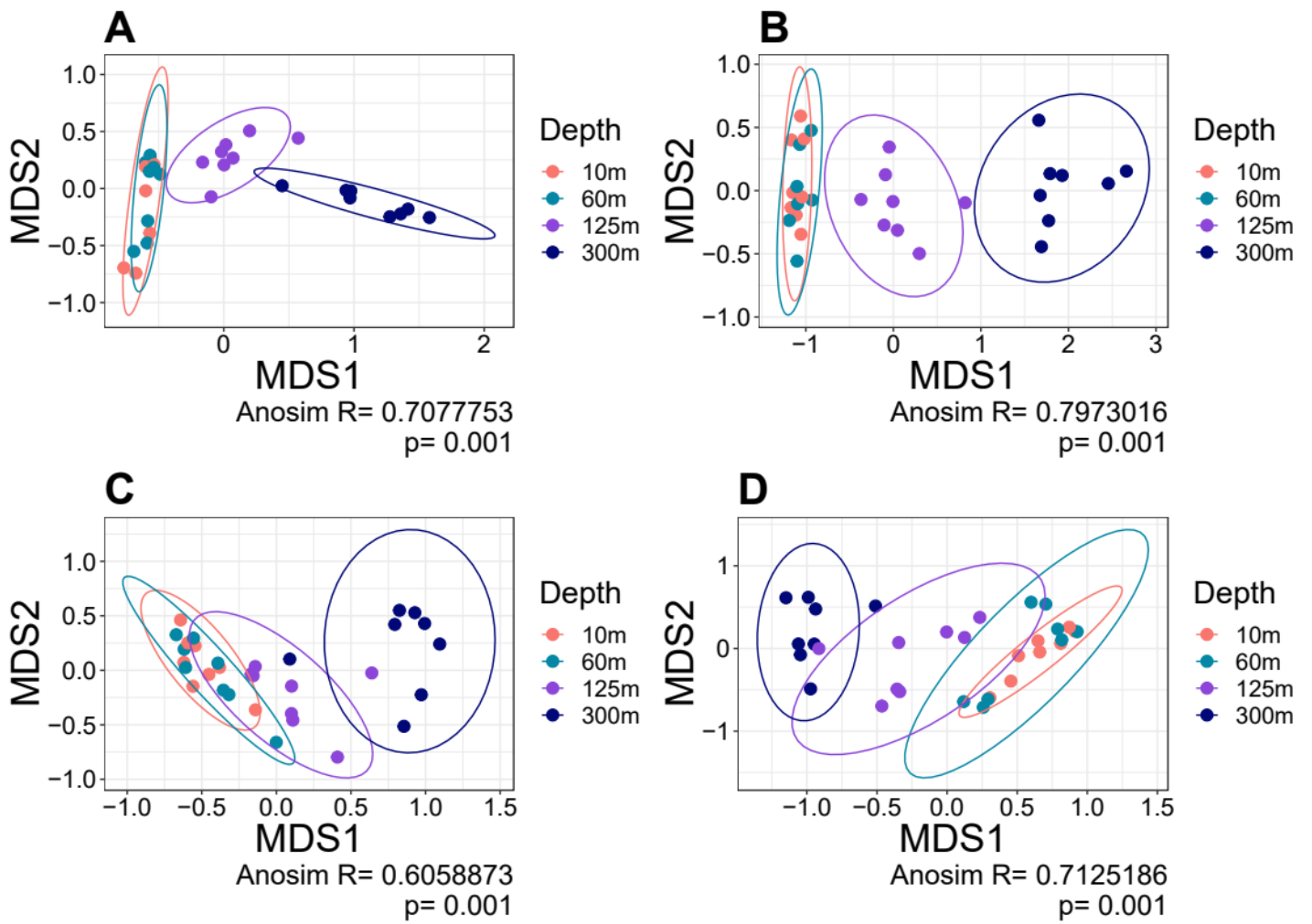


Figure 3. Non-Metric Multidimensional Scaling of prokaryotic communities from all depth layers based on Bray-Curtis Dissimilarity. A) total free-living community (DNA), B) active free-living community (RNA), C) total particle-attached community, D) active particle-attached community.

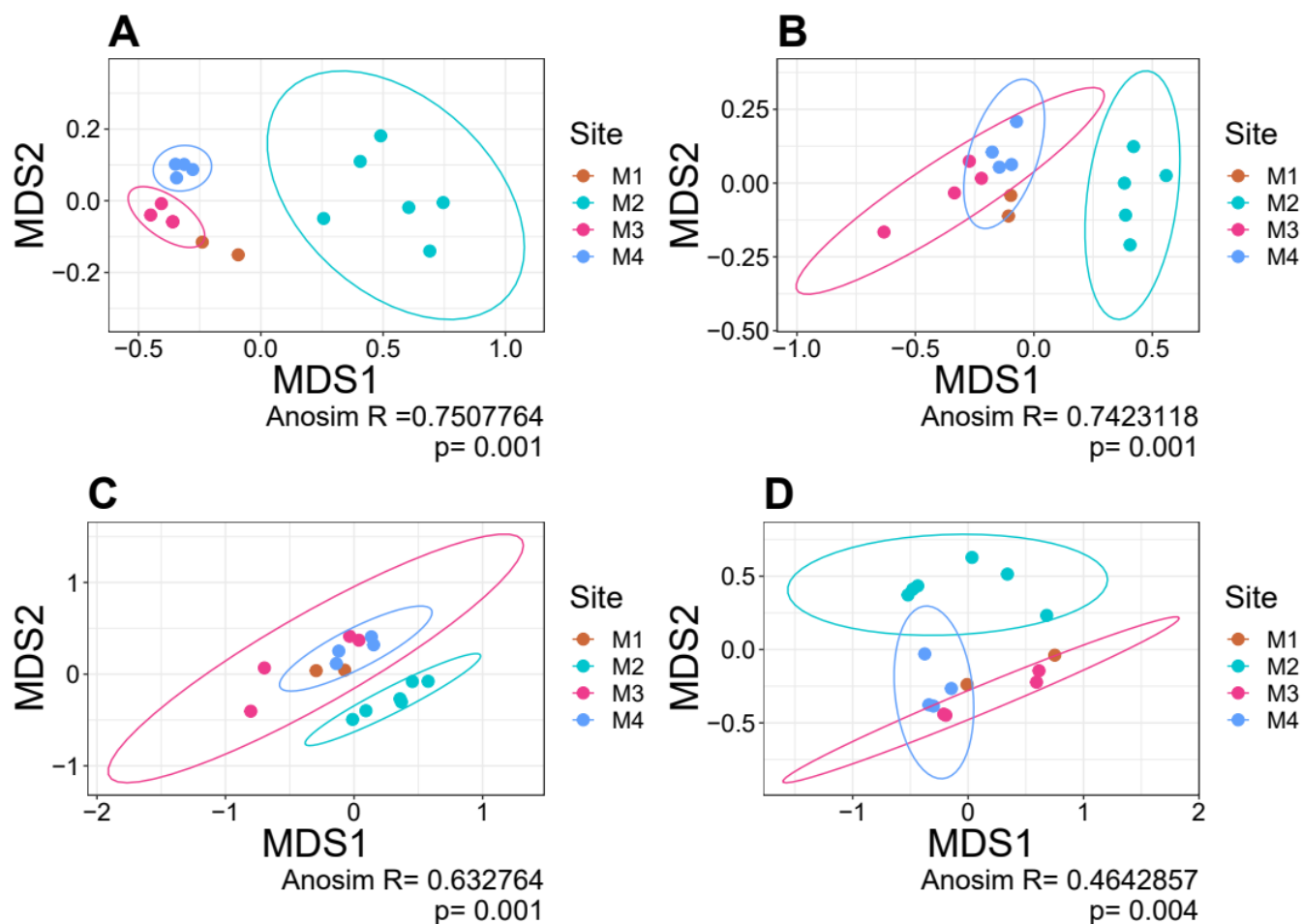


Figure 4. Non-Metric Multidimensional Scaling of prokaryotic communities from surface waters (10m and 60m) based on Bray-Curtis Dissimilarity. A) total free-living community (DNA), B) active free-living community C) total particle-attached community, D) active particle-attached community.

3.3. Prokaryotic Diversity

To estimate differences in the prokaryotic diversity among sites, we used different indices. Regarding the Shannon diversity index, the free-living communities on the plateau were less diverse than the communities at the sites off the plateau (Fig. 5). In contrast, in the case of the particle-attached fraction the overall difference among sites on and off plateau was less pronounced, especially due to the variability in the diversity in M3. A remarkable difference is that the free-living communities are more diverse than the particle-attached. A similar pattern was also observed for the observed richness and Inverse Simpson (Supplementary information, Fig.S1 and S2).

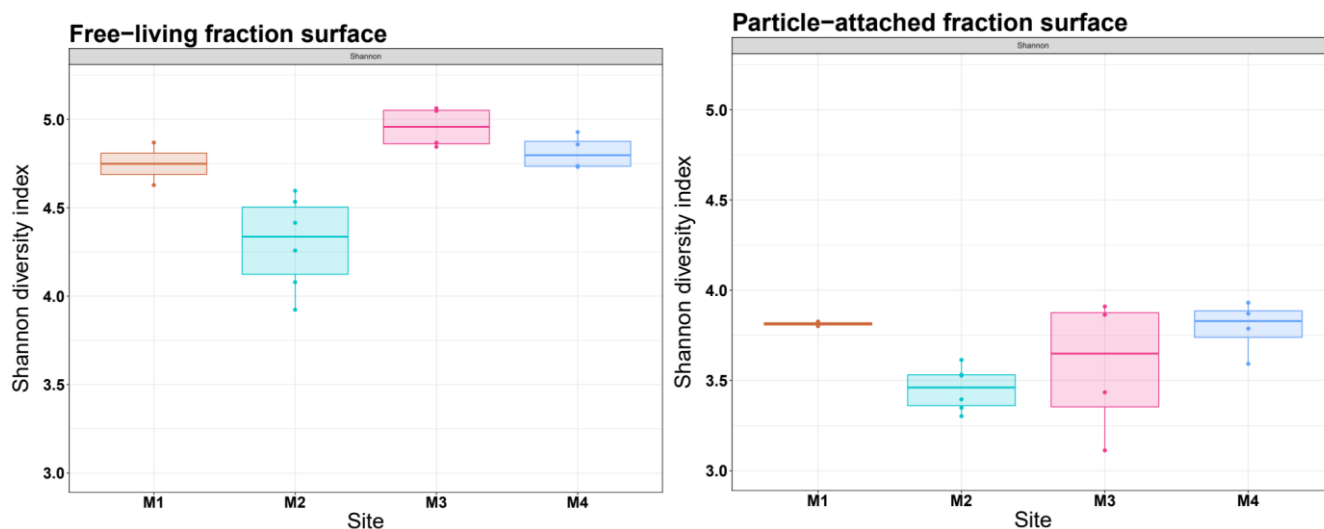


Figure 5. Shannon diversity index for the prokaryotic communities in the surface among sites. Left panel: total free-living fraction. Right panel: total particle-attached fraction.

3.4. Prokaryotic community composition

In order to identify the prokaryotic taxa, the ASVs were compared against the SILVA database release 132 at the highest taxonomic level possible (Quast *et al.*, 2013). The ASVs with the same taxonomy at the order level were pooled for the illustration of the relative abundance in the samples.

The free-living communities in surface waters were dominated by members of the orders Flavobacteriales, Rhodobacterales, Pelagibacterales (SAR11) and Cellvibrionales, which were distributed in a different way at Station M2 in comparison to the other sites (Fig. 6). In particular, at Station M2 the Flavobacteriales contributed to around 50% of the community composition, whereas in the off plateau stations the relative abundance of the Flavobacteriales amounts to around 30%. A more detailed view of the relative contribution of different Flavobacteriales groups (at the family and order level) for the free living fraction at Stations M2 and M3 is provided in Fig. 8. On the contrary, the relative contribution of SAR11 was between 2 to 10% at Station M2 meanwhile it accounted for up to 25% at the off plateau sites. Rhodobacterales had relatively homogeneous distribution between sites (between ~12 and 15% at all stations except for M1 ~20%). Cellvibrionales were abundant at Station M2, but did not reach the 5% for Station M3. On the contrary, SAR86 was abundant at Station M3, but not at Station M2.

Alteromonadales, Verrucomicrobiales, Kordiimonadales and Chitinophagales had low abundances at Station M2 (1.5 – 2% each), and their relative abundances were > 5% at Station M3. By contrast, SAR 406, Thiotricales and Parvibaculales were present at Station M3, but with really low relative abundances (<1.5%) at Station M2.

Regarding the particle attached communities in surface waters, not only differences between M2 and the off plateau sites, but also among the off plateau sites were observed. Flavobacteriales, Pseudomonadales, Rhodobacteriales and Cellvibrionales were among the most abundant groups (Figure 7). Flavobacteriales contributed with up to 50% to the total relative abundance at Station M2, and this group had variable contributions at the off plateau sites. Rhodobacteriales accounted for up to 40% during the first visit at Station M3, while its contribution was always around 10% at Station M2. A more detailed view of the relative contribution of different Flavobacteriales groups (at the family and order level) for the particle attached fraction at Stations M2 and M3 is provided in Fig. 9. Pseudomonadales are present and highly abundant during the second visit to M3, while during the third visit they were not detectable any more. Verrucomicrobiales had relative abundances of roughly 5% regardless of the site. Chitinophagales was present only at Station M2, however, it was among the top 5% only during the third visit at 10 m depth.

In contrast to the free-living fraction, SAR11 had low relative abundances in the particle-attached fraction at all sites. The other marked difference among free living and particle attached communities was the high abundance of Pseudomonadales, mainly at Station M3_2_60m (Fig. 7).

Because of the overall similarity of the community composition at Stations M1, M3 and M4, especially for the free-living fraction, Station M3 was chosen as an off plateau site for a further detailed comparison with Station M2 on the plateau.

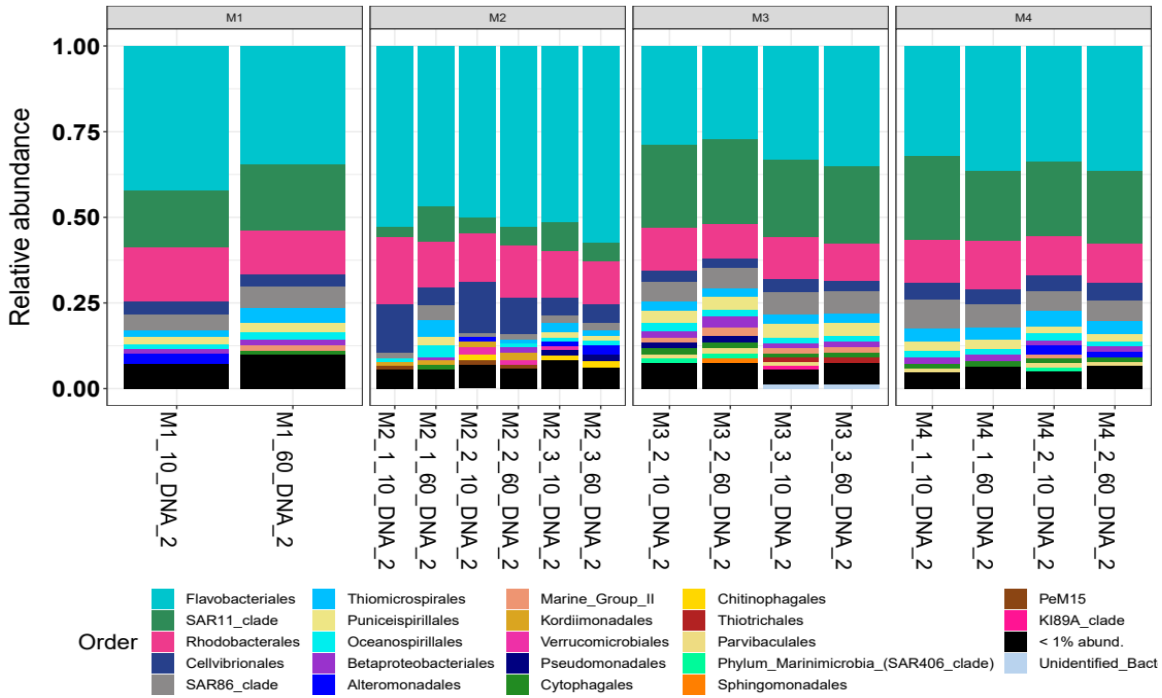


Figure 6. Relative abundance of free living taxa grouped at order level, in surface waters (Site names are composed by the Station identifier (M1, M2, M3 or M4), number of visit and depth, for instance, M2_2_10m refers to the site M2, second visit, 10m depth).

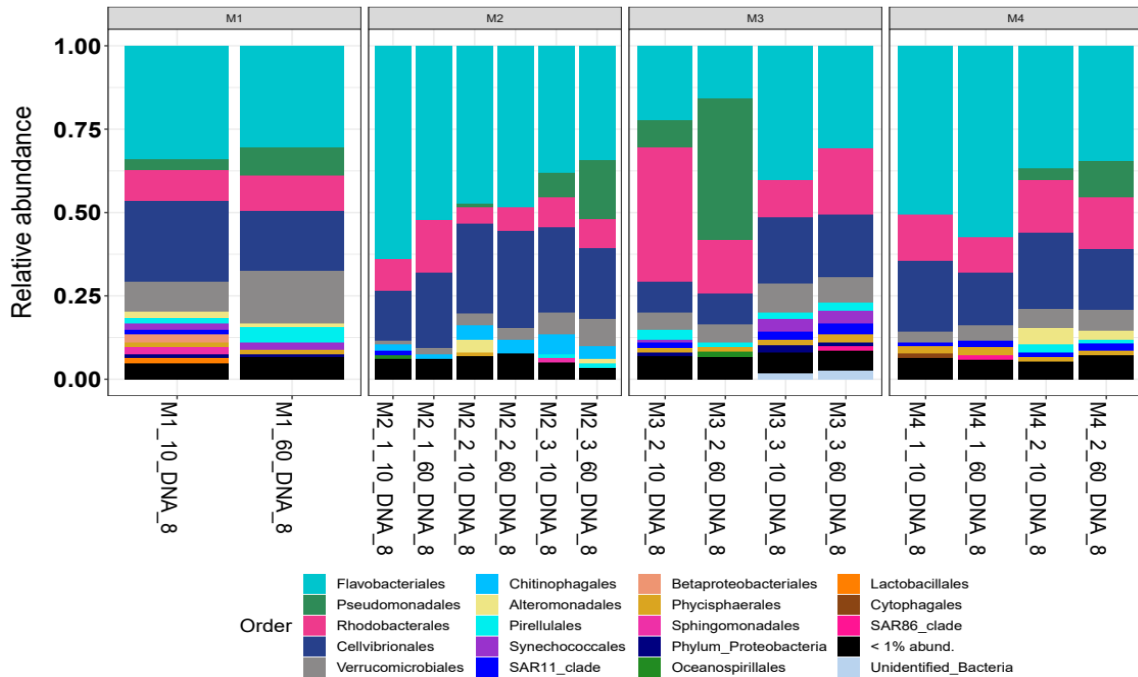


Figure 7. Relative abundance of particle attached taxa grouped at the order level in the surface waters (Site names are composed by the Station identifier (M1, M2, M3 or M4), number of visit and depth, for instance, M2_2_10m refers to the site M2, second visit, 10m depth).

Free living total Flavobacteriales surface

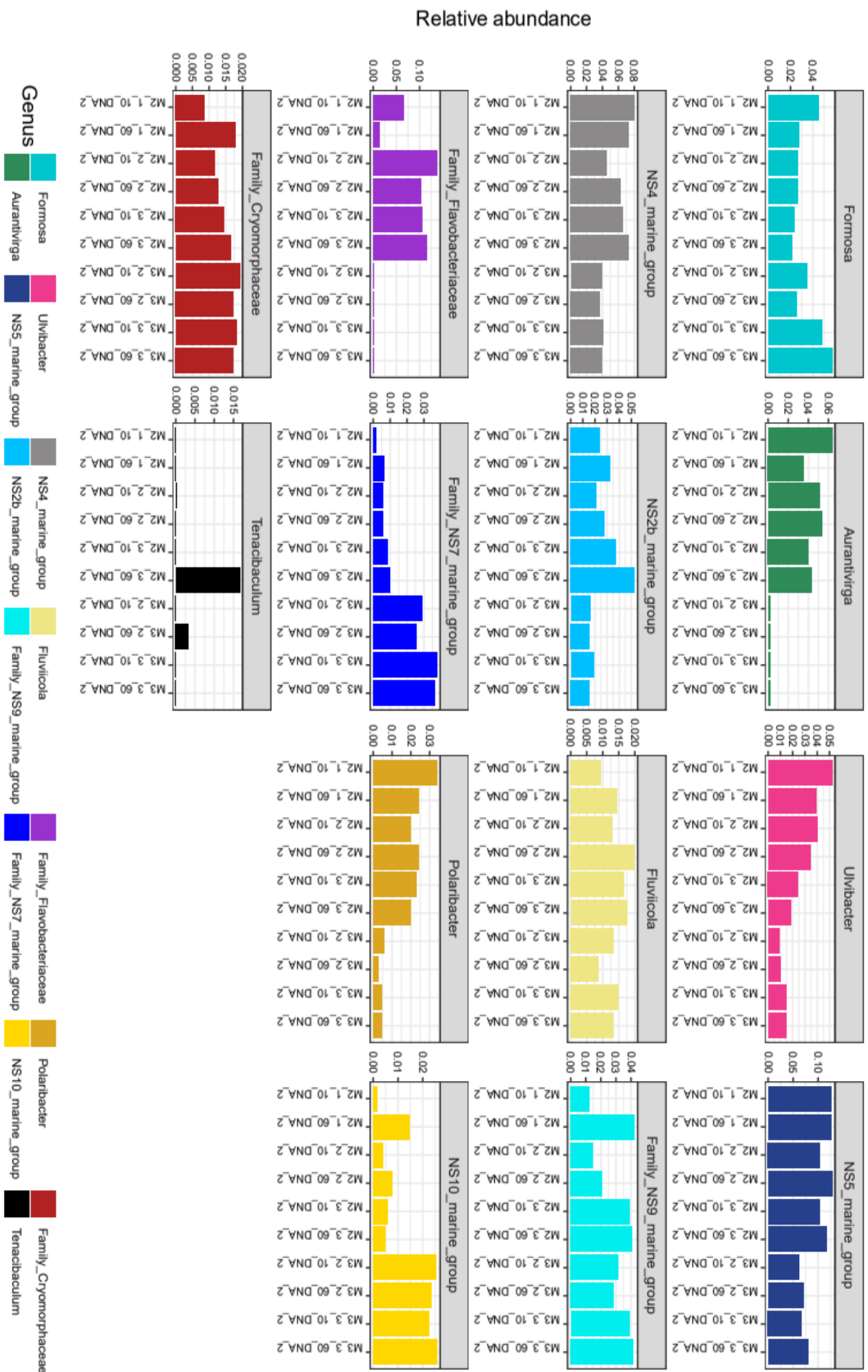


Figure 8. Detail relative abundance higher level identified of Order Flavobacteriales, free living total community (DNA), Stations M2 and M3. Notice the difference of scales.

Attached Flavobacteriales surface

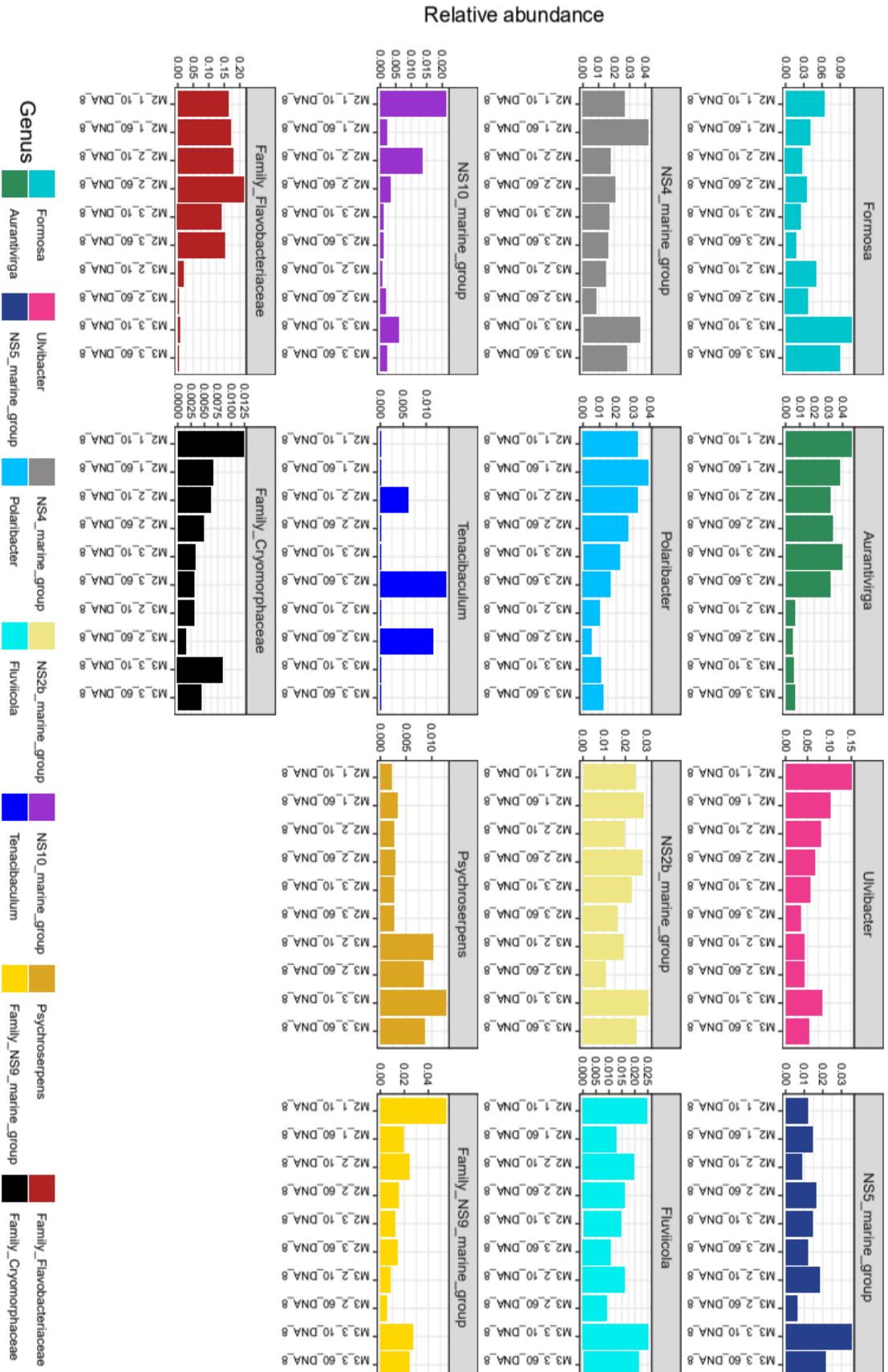


Figure 9. Detail relative abundance higher level identified of Order Flavobacteriales, particle attached total community (DNA), Stations M2 and M3. Notice the difference of scales.

3.5. Taxa contributing to the difference between on and off plateau

We then aimed to identify the ASVs that are contributing to the difference in the community composition in surface waters between on and off plateau sites. We performed a Simper analysis (permutations = 999) and then selected the ASVs contributing significantly ($p < 0.05$) to the difference between Stations M2 and M3 at 10m and 60m depth. In order to simplify the visualization of the information, the most abundant ASVs were considered. We chose ASVs with a relative abundance $> 5\%$ in at least one sample (Table 2). This analysis was applied separately to the total (DNA) and active (RNA) free-living and particle-attached communities (Figs. 10 and 11).

Table 2. Overview of ASVs contributing to the difference between community composition in the surface mixed layer at Station M2 and M3.

	No. ASVs $p < 0.05$, $> 1\%$ rel. abundance	Total contribution to dissimilarity	No. ASVs $p < 0.05$, $> 5\%$ rel. abundance	Total contribution to dissimilarity
Total free living	51	0.78	10	0.39
Active free living	42	0.61	8	0.14
Total particle attached	43	0.52	9	0.38
Active particle attached	34	0.35	6	0.19

In the free-living fraction, 10 highly abundant ASVs ($> 5\%$ relative abundance) contributed significantly to the differences between M2 and M3, explaining together up to 39% of the difference. Considering all ASVs ($> 1\%$ relative abundance; 51 ASVs) that contributed significantly to the differences between sites up to 78% can be explained (Table 2). In contrast, for the potentially active community (RNA), the contribution of the ASVs to the difference between sites was overall much lower, ranging from 61% for the free-living community (ASVs $> 1\%$ relative abundance; 42 ASVs) to 35% for the particle-attached community (ASVs $> 5\%$ relative abundance; 6 ASVs).

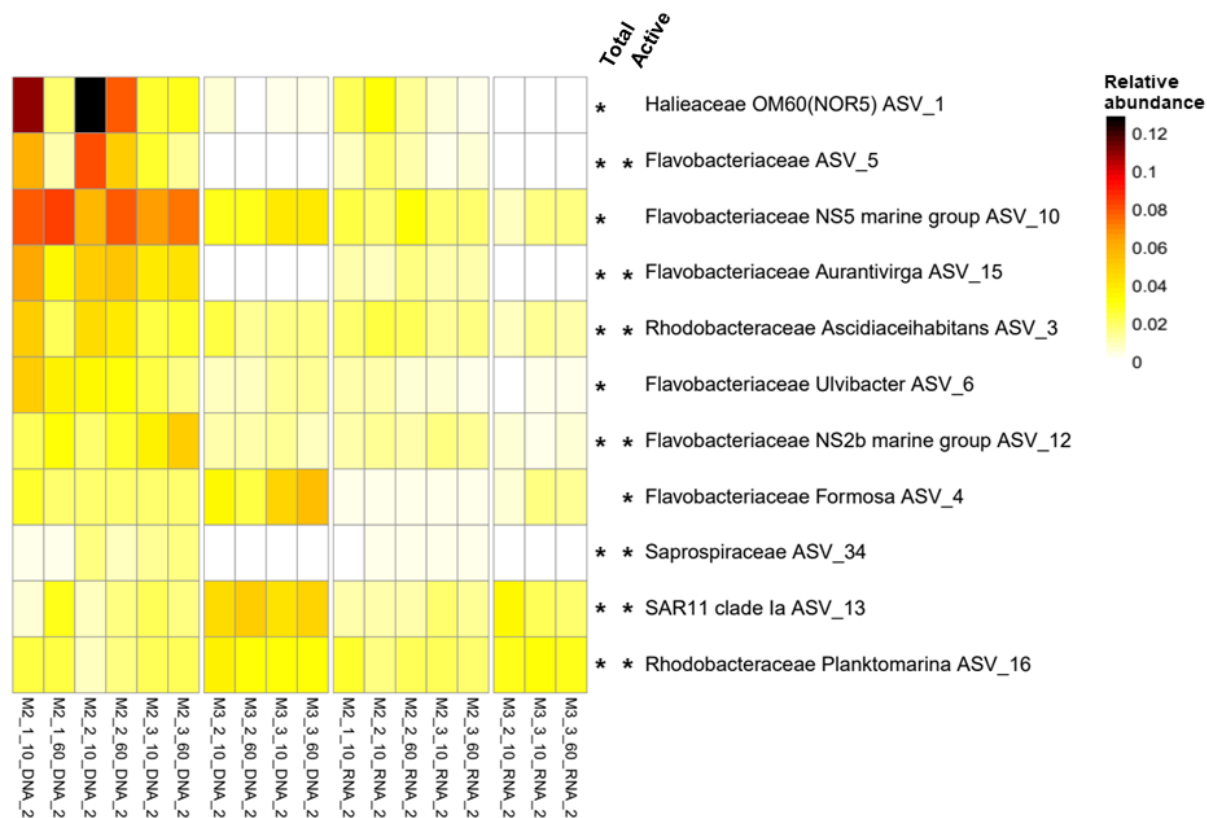


Figure 10. Relative abundance of ASVs in the free-living fraction at stations M2 and M3 at 10m depth. * ASVs contribute significantly ($p < 0.05$) to the dissimilarity between sites M2-M3 (SIMPER analysis), either for the total (DNA) or potentially active (RNA) community. Only the ASVs with relative abundance $> 5\%$ in at least one of the samples are shown. Note that the ASVs that contribute to the difference among sites are not always the same for the total and the active communities.

Among the ASVs contributing to the difference between Stations M2 and M3, for the total free living community, the most abundant one is ASV_1 belonging to Cellvibrionales from the Family Halieaceae and the genus OM60(NOR5).

Five ASVs identified as Flavobacteriaceae contributed further to the difference between sites, and four of them (ASV_5, ASV_10 NS5 Marine group, ASV 16 Aurantivirga and ASV_6 Ulvibacter) were more abundant at Station M2 than at Station M3. ASV_12, belonging to NS2b marine group, was more abundant at Station M3 (Fig. 10). SAR11 and Planktomarina also contributed to the difference between sites and both were more abundant at Station M3.

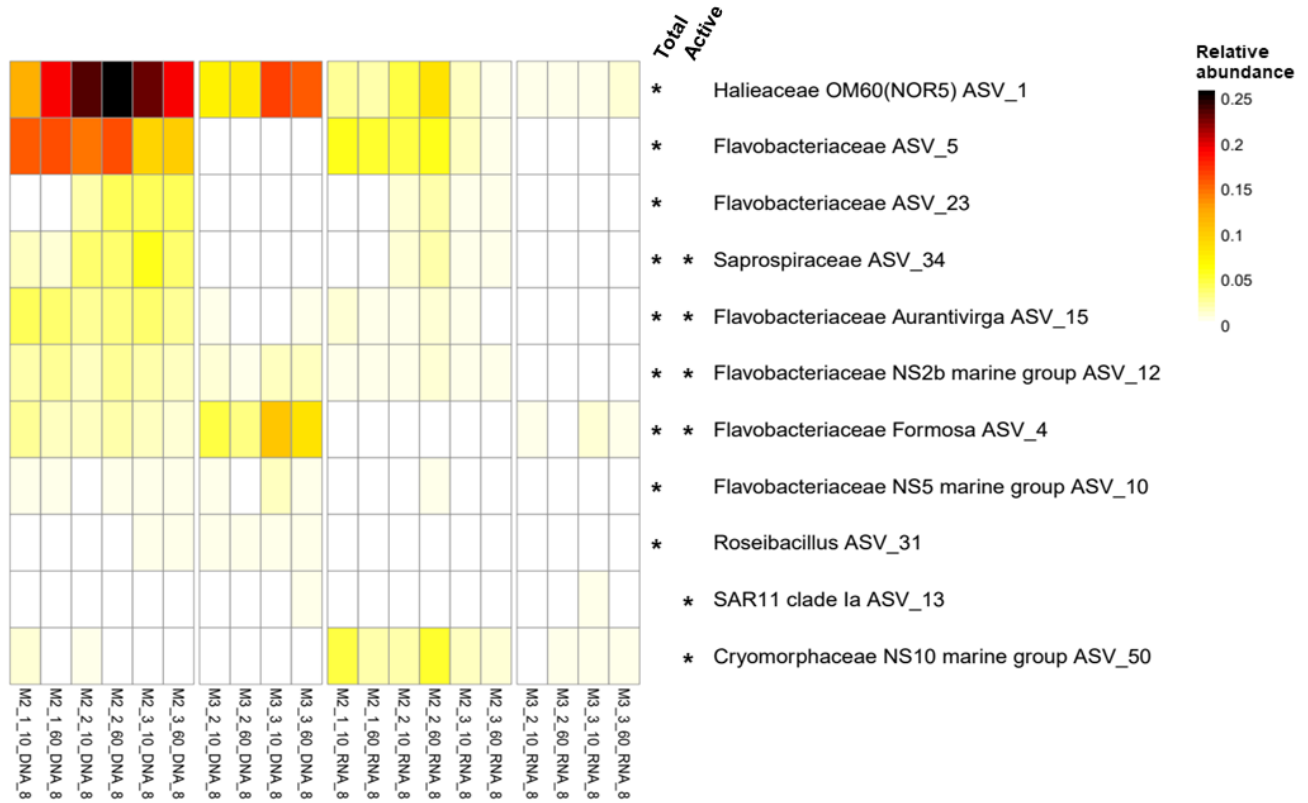


Figure 11. Relative abundance of ASVs in the particle attached fraction at stations M2 and M3 at 10m depth. * ASVs contribute significantly ($p < 0.05$) to the dissimilarity between sites M2-M3 (SIMPER analysis), either for the total (DNA) or potentially active (RNA) community. Only the ASVs with relative abundance $> 5\%$ in at least one of the samples are shown. Note that the ASVs that contribute to the difference among sites are not always the same for the total and the active communities.

Regarding the active free living community, there are 8 ASVs contributing significantly to the difference between sites (Fig. 10). All 8 ASVs were also identified as significantly different for the total community, except for Formosa belonging to Flavobacteria, an ASV that was more abundant at Station M3 than M2.

In the case of the particle attached fraction, ASV_1 Haliaceae OM60(NOR5) contributed to the dissimilarity between sites, and this was the most abundant group, especially at Station M2. Six ASVs identified as part of the family Flavobacteriaceae contributed to the dissimilarity to the total community. Only 3 of them were significantly different also for the active community (Aurantivirga, NS2b marine group and Formosa) (Figure 12).

4. Discussion

In the region east of the Kerguelen Islands annual spring phytoplankton blooms occur due to natural iron fertilization of the surface waters. According to observations and models based on satellite-derived chlorophyll-a (Chl *a*) the bloom above the Kerguelen plateau starts in early November, reaching its maximum by mid-December. At this time point, concentrations of Chl *a* are roughly 2.5 mg m⁻³ in *on-plateau* surface waters as compared to 1.1 mg m⁻³ in *off-plateau* waters, and they decrease to less than 0.5 mg m⁻³ by February (Mongin et al., 2008). The MOBYDICK cruise was conducted during the late Austral summer. The maximum concentration of Chl *a* in the SML was measured at the site M2 (0.62 mg m⁻³) that is below the normal bloom concentrations, corresponding to post-bloom conditions.

4.1. Prokaryotic community distribution

Distribution of prokaryotic communities in the environment is influenced by the environmental parameters, especially in aquatic ecosystems. The characteristics defining water masses, can be associated to horizontal and vertical distribution of the organisms. Stratification and mixing processes have shown to be related to changes in the diversity in the water column (Gallagher *et al.*, 2004; Frank *et al.*, 2016). Free living total and potentially active communities show a differential distribution according to the depth (Fig 3 A and B). The communities in the deep waters are different from the ones at 125 m depth and the ones in 10 and 60 m depth.

Several factors can constrain the vertical distribution of the microorganisms in the water column. One of them is the vertical dispersion limitation of the small size particles (as picoplankton), due to the slow sinking velocity and the physical barrier that the stratification of the water column supposes. Due to this fact, the picoplankton was not considered as an important contributor to the carbon export in the deep-water layers (Michaels and Silver, 1988), however, nowadays there is recognized as well the role of the microorganisms associated to bigger particles, with consequently higher sinking rates (Farnelid *et al.*, 2019).

In the case of MOBYDICK, we distinguished between the free living prokaryotes (<0.8 μm) and the particle attached ones (>0.8 μm). The large size of the particles facilitates the sinking process by itself, then, the response is a vertical connectivity of the microorganisms from the surface to the deeper layers. Similar to the findings in the study of Mestre and collaborators (2018), for the MOBYDICK cruise the free-living communities are more isolated vertically than the larger size fractions, which showed highest similarity through the water column (Fig. 3 C and D).

Considering that the nature of the particles in attached fraction can be diverse, either organic matter, faecal pellets, or alive organisms, like phyto- and zooplankton, then the implications of the high connectivity along the water column are beyond the microbial composition of the community, but the ecological and trophic interactions (Boeuf *et al.*, 2019).

The communities on plateau sites were different from the ones off plateau, in the SML during the post bloom conditions. This was also observed in previous studies during the peak and declining phases of early spring phytoplankton blooms (West *et al.*, 2008; Landa *et al.*, 2016)

4.2. Prokaryotic Diversity

The study of prokaryotic diversity and community composition is of importance for a better understanding of function and dynamics of the microbial communities (Kim *et al.*, 2017). A first approach to explore the diversity of the communities is to know the measures of alpha diversity, as the observed richness, and indices as Shannon that takes into account the occurrence and the evenness of the observed taxa. If comparing the Shannon diversity among sites for the free living fraction in the SML, M2 shows less diversity than the sites off plateau (Fig. 5).

Low diversity in high productivity regions can be associated to the predominance of few taxa in the community composition, either due to strategies of fast nutrient utilization, but also potentially influenced by direct interactions with members of the phytoplankton community (Zhou *et al.*, 2018). A reduction of bacterial richness has been shown in bloom areas in temperate regions of the ocean, dominated by only a few, probably most competitive bacterial groups (Wemheuer *et al.*, 2014). In the present study, the free living fraction at Station M2 on the plateau was dominated by Flavobacteriales, contributing to more than 50% of the total community composition, followed by Rhodobacteriales and Cellvibrionales, whereas at the stations off plateau, Flavobacteria (~30%) and SAR11 (~25%) had similar relative abundances (Fig. 6). Some groups of Bacteroidetes as Flavobacteriales, are presumed to be fast-growers, utilizing highly complex organic matter first, dominating over other groups (Teeling *et al.*, 2012).

In the present study the measures of alpha diversity for the particle attached fraction are not different among sites on and off plateau (fig. 5). These communities were mainly dominated by Flavobacteriales, Rhodobacteriales and Cellvibrionales, but with variation within samples of the same sites, not allowing to detect a clear pattern to differentiate between on and off plateau Stations (Fig. 7 M3 and M4).

Particle attached communities, showed lower alpha diversity than the free living communities at all the stations, regardless their location with respect to the plateau. The debate about the comparison between particle attached and free living prokaryotes is controversial, while several studies show higher diversity, abundance and higher specific metabolic activity in the particle attached fraction than in the free living counterpart (Zhang *et al.*, 2007; Ortega-Retuerta *et al.*, 2013; Rieck *et al.*, 2015) others do not find significant differences (Bachmann *et al.*, 2018).

The differences between the free living and particle attached communities are related to their differences in lifestyle and metabolic capabilities, consequently, the particle attached communities assemblage is influenced by the composition, origin and quality of the particles (Zhang *et al.*, 2007; Ortega-Retuerta *et al.*, 2013; Rieck *et al.*, 2015). The nature of the particle composition should be

examined in further research to better understand the particle attached communities. With respect to the MOBYDICK-project, these analyses are currently in progress.

4.3. Taxa contributing to the difference *on and off plateau*.

For the free living fraction, the differences in the surface layers between on and off plateau are consistent with differences in the diversity indices and with the community composition. In an attempt to elucidate better the ecological meaning of this differences, we can focus on the taxa that contribute with the main differences among on and off plateau.

At the level of ASV, the most abundant one, in M2, and consequently contributing to the difference between M2 and M3 is the ASV1 (group OM60(NOR5) from the Cellvibrionales. This oligotrophic marine gammaproteobacterial group (OM), had higher relative abundance at Station M2 (plateau), mainly during the first visit. This group has a cosmopolitan distribution in marine surface waters, and it can reach high seasonal abundances especially in coastal environments, where it also co-occurs with algal blooms (Yan *et al.*, 2009). Recently, by metatranscriptomics analysis, it was found that Cellvibrionales had high contribution to the expression of genes for the uptake of siderophore-bound iron (Debeljak *et al.*). This can suggest the importance of this group in this iron fertilized area of the Southern Ocean.

The order Flavobacteriales dominated the whole community in the surface waters (Fig. 6 and 7), however, going in to the deeper taxonomic level identified (Fig. 8 and 9), there are differences at the genus level between on and off plateau sites.

Marine genera of Flavobacteriales have been reported as major component of the microbial communities in the ocean pelagic zone, strongly coupled to phytoplanktonic primary production (Bowman, J. P., 2006). Some members of the Flavobacteriales are more abundant at the site M2, such as *Aurantivirga*, NS5 and *Ulvibacter*, while off plateau the genus *Formosa* is more abundant, either for the free living or for the particle attached fraction. Recently, the enzymatic capability of the degradation of biopolymers such as proteins and polysaccharides by some marine Bacteroidetes, more specifically Flavobacteriia have been described through metagenomics and proteomics methods (Xing *et al.*, 2015).

The genus *Formosa* also from Flavobacteriales had higher relative abundances at the site M3. This genus has been observed in marine environments rich in organic matter, such as aggregates of particulate organic matter or associated to diatoms-dominated blooms. A particularity of this genus is the capability of degradation of algal polysaccharides and the production of some toxic secondary metabolites, that can potentially kill various algal species (Mann *et al.*, 2013; Williams *et al.*, 2013).

In the Southern Ocean, specifically in the Kerguelen region, Flavobacteriales from the groups NS5, *Ulvibacter* and NS9 were shown to have positive correlations with major diatom species such as

Thalassionema nitzschoides and *Chaetoceros curvisetus* (Liu *et al.*, 2019). Previous surveys found some species of *Chaetoceros* dominant above the Kerguelen plateau (Landa *et al.*, 2016). Also, *Fragilariopsis kerguelensis* was strongly positively correlated with several flavobacterial groups such as NS5, NS9 and NS10. The occurrence of the diatoms species at the sites visited during the present study could explain the predominance of the prokaryotic groups on and off plateau.

Despite the post bloom conditions during late summer for MOBYDICK cruise, the influence of the diatom blooms and related succession, can still shape the prokaryotic communities. So far, it is known that the phytoplanktonic community during the cruise was dominated in relative abundance by *Fragilariopsis* and in biomass by *Corethron*, these analyses are currently in progress. As part of the main objectives in the MOBYDICK project, it is aimed to bring together the relevant information of different work packages to study the end to end carbon cycle.

5. Conclusion

The present work provides a detailed description of the prokaryotic communities in the free- living and particle-attached size fractions during late summer in the vicinity of the Kerguelen Islands (Southern Ocean). Using Illumina sequencing of the 16S rRNA gene, a total of 16 664 ASVs were obtained, and the distribution, diversity and most abundant groups of the prokaryotic community were described. The prokaryotic communities showed to be constrained by the depth layer along the water column, especially for the free living fraction. In the case of the particle attached fraction, the differences among depths layers is significant, but the pattern is less marked in the spatial ordination (NMDS), suggesting connectivity between the depth layers in the water column due to particle sinking. Further studies are needed to investigate the nature of the particles associated to the particle attached size fraction.

In the SML, the prokaryotic communities showed to be different at the Stations off (M1, M3, M4) and on the plateau (M2), as revealed by differences in the diversity (lower diversity determined on the plateau) and the composition of the community (clear predominance of Flavobacteriales on the plateau). The alpha diversity for the particle attached fraction did not differ among sites, however, the overall alpha diversity of this size fraction was lower than for the free living.

The predominant prokaryotic taxa were mainly genus of Flavobacteria, normally associated to diatom-dominated blooms probably due to their metabolic capabilities to utilize polymers in high nutrient-conditions. Other groups such as Cellvibrios and SAR11 were shown do contribute to the differences among sites in the surface and being important the community composition on and off plateau. Future research is needed to understand the relationship between the prokaryotic communities and the phytoplankton assemblages, as well as other trophic levels, to better understand the ecosystemic role of the prokaryotic diversity in the Southern Ocean and its temporal variability.

6. Acknowledgements

We thank the principal investigator of the MOBYDICK project B. Quéguiner and the Chief Scientist Ingrid Obernosterer, as well as all the cruise members of the R/V Marion Dufresne for all the work on board, including sampling and environmental parameters measurements. Especial thanks to Pavla Debeljak for the sample collection for the prokaryotic diversity analysis. Thanks to Philippe Catala for flow cytometry analysis of heterotrophic prokaryotes and piconano-eukaryotes. Thanks to the SAPIGH analytical platform at the Observatoire d'océanologie de Villefranche-sur-mer LOV, where the analyses by HPLC to determine Chlorophyll a were performed. Many thanks to Yan Liu for the invaluable guidance with the lab work and the bioinformatics. Thanks to Coco Koeder and Angel Rain for their comments to improve this manuscript. Especial thanks to Ingrid Obernosterer for the opportunity to participate in the MOBYDICK project, and for all the guidance, feedback and support that made possible this master thesis.

This work was supported by the French Research program of the INSU-CNRS LEFE-CYBER (Les enveloppes fluides et l'environnement –Cycles biogéochimiques, environnement et ressources), the French ANR (Agence Nationale de la Recherche, ANR-17-CEO-0013-02), and the French Oceanographic Fleet (Flotte Océanographique Française, FOF). The MOBYDICK cruise has the following DOI: <https://doi.org/10.17600/18000403>

7. References

- Armand, LK, Cornet-Barthaux, V, Mosseri, J, and Quéguiner, B (2008). Late summer diatom biomass and community structure on and around the naturally iron-fertilised Kerguelen Plateau in the Southern Ocean. *Deep Sea Res Part II Top Stud Oceanogr* 55, 653–676.
- Arrieta, JM, Weinbauer, MG, Lute, C, and Herndl, GJ (2004). Response of bacterioplankton to iron fertilization in the Southern Ocean. *Limnol Oceanogr* 49, 799–808.
- Bachmann, J, Heimbach, T, Hassenrück, C, Kopprio, GA, Iversen, MH, Grossart, HP, and Gärdes, A (2018). Environmental Drivers of Free-Living vs. Particle-Attached Bacterial Community Composition in the Mauritania Upwelling System. *Front Microbiol* 9.
- Biers, EJ, Sun, S, and Howard, EC (2009). Prokaryotic Genomes and Diversity in Surface Ocean Waters: Interrogating the Global Ocean Sampling Metagenome. *Appl Environ Microbiol* 75, 2221–2229.
- Blain, S, Sarthou, G, and Laan, P (2008). Distribution of dissolved iron during the natural iron-fertilization experiment KEOPS (Kerguelen Plateau, Southern Ocean). *Deep Sea Res Part II Top Stud Oceanogr* 55, 594–605.
- Boeuf, D, Edwards, BR, Eppley, JM, Hu, SK, Poff, KE, Romano, AE, Caron, DA, Karl, DM, and DeLong, EF (2019). Biological composition and microbial dynamics of sinking particulate organic matter at abyssal depths in the oligotrophic open ocean. *Proc Natl Acad Sci*, 201903080.
- Bowman, J. P. (2006). (12) The Marine Clade of the Family Flavobacteriaceae: The Genera *Aequorivita*, *Arenibacter*, *Cellulophaga*, *Croceibacter*, *Formosa*, *Gelidibacter*, *Gillisia*, *Maribacter*, *Mesonina*, *Muricauda*, *Polaribacter*, *Psychroflexus*, *Psychroserpens*, *Robiginitalea*, *Salegentibacter*, *Tenacibaculum*, *Ulvibacter*, *Vitellibacter* and *Zobellia* | Request PDF. Available at: https://www.researchgate.net/publication/279614645_The_Marine_Clade_of_the_Family_Flavobacteriaceae_The_Genera_Aequorivita_Arenibacter_Cellulophaga_Croceibacter_Formosa_Gelidibacter_Gillisia_Maribacter_Mesonina_Muricauda_Polaribacter_Psychroflexus_Psyc. Accessed June 3, 2019.
- Curtis, TP, Head, IM, Lunn, M, Woodcock, S, Schloss, PD, and Sloan, WT (2006). What is the extent of prokaryotic diversity? *Philos Trans R Soc B Biol Sci* 361, 2023–2037.
- Debeljak, P, Toulza, E, Beier, S, Blain, S, and Obernosterer, I Microbial iron metabolism as revealed by gene expression profiles in contrasted Southern Ocean regimes. *Environ Microbiol* 0.
- Falkowski, PG, Fenchel, T, and DeLong, EF (2008). The Microbial Engines That Drive Earth's Biogeochemical Cycles. *Science* 320, 1034–1039.

- Farnelid, H, Turk-Kubo, K, Ploug, H, Ossolinski, JE, Collins, JR, Mooy, BASV, and Zehr, JP (2019). Diverse diazotrophs are present on sinking particles in the North Pacific Subtropical Gyre. *ISME J* 13, 170.
- Frank, AH, Garcia, JAL, Herndl, GJ, and Reinthaler, T (2016). Connectivity between surface and deep waters determines prokaryotic diversity in the North Atlantic Deep Water. *Environ Microbiol* 18, 2052–2063.
- Gallagher, JM, Carton, MW, Eardly, DF, and Patching, JW (2004). Spatio-temporal variability and diversity of water column prokaryotic communities in the eastern North Atlantic. *FEMS Microbiol Ecol* 47, 249–262.
- Hugenholtz, P (2002). Exploring prokaryotic diversity in the genomic era. *Genome Biol* 3, reviews0003.1-reviews0003.8.
- Jouandet, M-P, Jackson, GA, Carlotti, F, Picheral, M, Stemmann, L, and Blain, S (2014). Rapid formation of large aggregates during the spring bloom of Kerguelen Island: observations and model comparisons. *Biogeosciences* 11, 4393–4406.
- Landa, M, Blain, S, Christaki, U, Monchy, S, and Obernosterer, I (2016). Shifts in bacterial community composition associated with increased carbon cycling in a mosaic of phytoplankton blooms. *ISME J* 10, 39–50.
- Landa, M, Blain, S, Harmand, J, Monchy, S, Rapaport, A, and Obernosterer, I (2018). Major changes in the composition of a Southern Ocean bacterial community in response to diatom-derived dissolved organic matter. *FEMS Microbiol Ecol* 94.
- Liu, Y, Debeljak, P, Rembauville, M, Blain, S, and Obernosterer, I (2019). Diatoms shape the biogeography of heterotrophic prokaryotes in early spring in the Southern Ocean. *Environ Microbiol* 21, 1452–1465.
- López-Pérez, M, Kimes, NE, Haro-Moreno, JM, and Rodriguez-Valera, F (2016). Not All Particles Are Equal: The Selective Enrichment of Particle-Associated Bacteria from the Mediterranean Sea. *Front Microbiol* 7.
- Mann, AJ et al. (2013). The Genome of the Alga-Associated Marine Flavobacterium *Formosa agariphila* KMM 3901^T Reveals a Broad Potential for Degradation of Algal Polysaccharides. *Appl Environ Microbiol* 79, 6813–6822.
- Mestre, M, Ruiz-González, C, Logares, R, Duarte, CM, Gasol, JM, and Sala, MM (2018). Sinking particles promote vertical connectivity in the ocean microbiome. *Proc Natl Acad Sci* 115, E6799–E6807.
- Michaels, AF, and Silver, MW (1988). Primary production, sinking fluxes and the microbial food web. *Deep Sea Res Part Oceanogr Res Pap* 35, 473–490.

Mongin, M, Molina, E, and Trull, TW (2008). Seasonality and scale of the Kerguelen plateau phytoplankton bloom: A remote sensing and modeling analysis of the influence of natural iron fertilization in the Southern Ocean. *Deep Sea Res Part II Top Stud Oceanogr* 55, 880–892.

Oksanen, F. J., Guillaume Blanchet, Michael Friendly, Roeland Kindt, Pierre Legendre, Dan McGlinn, Peter R. Minchin, R. B. O'Hara, Gavin L. Simpson, Peter Solymos, M. Henry H. Stevens, Eduard Szoecs and Helene Wagner (2019). *vegan: Community Ecology Package*. R package version 2.5-4. <https://CRAN.R-project.org/package=vegan>

Ortega-Retuerta, E, Joux, F, Jeffrey, WH, and Ghiglione, JF (2013). Spatial variability of particle-attached and free-living bacterial diversity in surface waters from the Mackenzie River to the Beaufort Sea (Canadian Arctic). *Biogeosciences* 10, 2747–2759.

Quast, C., Pruesse, E., Yilmaz, P., Gerken, J., Schweer, T., Yarza, P., ... & Glöckner, F. O. (2013). The SILVA ribosomal RNA gene database project: improved data processing and web-based tools. *Nucleic acids research*, 41(D1), D590-D596.

R Core Team (2019). *R: A language and environment for statistical computing*. R Foundation for Statistical Computing, Vienna, Austria. URL <https://www.R-project.org/>.

Raivo Kolde (2019). *pheatmap: Pretty Heatmaps*. R package version 1.0.12. <https://CRAN.R-project.org/package=pheatmap>

Ras, J, Claustre, H, and Uitz, J (2008). Spatial variability of phytoplankton pigment distributions in the Subtropical South Pacific Ocean: comparison between in situ and predicted data. 17.

Rieck, A, Herlemann, DPR, Jürgens, K, and Grossart, H-P (2015). Particle-Associated Differ from Free-Living Bacteria in Surface Waters of the Baltic Sea. *Front Microbiol* 6.

Rusch, DB et al. (2007). The Sorcerer II Global Ocean Sampling Expedition: Northwest Atlantic through Eastern Tropical Pacific. *PLOS Biol* 5, e77.

Salazar, G, Cornejo-Castillo, FM, Benítez-Barrios, V, Fraile-Nuez, E, Álvarez-Salgado, XA, Duarte, CM, Gasol, JM, and Acinas, SG (2016). Global diversity and biogeography of deep-sea pelagic prokaryotes. *ISME J* 10, 596–608.

Singh, SK, Kotakonda, A, Kapardar, RK, Kankipati, HK, Sreenivasa Rao, P, Sankaranarayanan, PM, Vetaikorumagan, SR, Gundlapally, SR, Nagappa, R, and Shivaji, S (2015). Response of bacterioplankton to iron fertilization of the Southern Ocean, Antarctica. *Front Microbiol* 6.

Sunagawa, S et al. (2015). Structure and function of the global ocean microbiome. *Science* 348, 1261359–1261359.

Teeling, H et al. (2012). Substrate-Controlled Succession of Marine Bacterioplankton Populations Induced by a Phytoplankton Bloom. *Science* 336, 608–611.

Thiele, S, Fuchs, BM, Ramaiah, N, and Amann, R (2012). Microbial Community Response during the Iron Fertilization Experiment LOHAFEX. *Appl Environ Microbiol* 78, 8803–8812.

- Van Heukelem, L, and Thomas, CS (2001). Computer-assisted high-performance liquid chromatography method development with applications to the isolation and analysis of phytoplankton pigments. *J Chromatogr A* 910, 31–49.
- Wemheuer, B, Güllert, S, Billerbeck, S, Giebel, H-A, Voget, S, Simon, M, and Daniel, R (2014). Impact of a phytoplankton bloom on the diversity of the active bacterial community in the southern North Sea as revealed by metatranscriptomic approaches. *FEMS Microbiol Ecol* 87, 378–389.
- West, NJ, Obernosterer, I, Zemb, O, and Lebaron, P (2008). Major differences of bacterial diversity and activity inside and outside of a natural iron-fertilized phytoplankton bloom in the Southern Ocean. *Environ Microbiol* 10, 738–756.
- Wilkins, D, Yau, S, Williams, TJ, Allen, MA, Brown, MV, DeMaere, MZ, Lauro, FM, and Cavicchioli, R (2013). Key microbial drivers in Antarctic aquatic environments. *FEMS Microbiol Rev* 37, 303–335.
- Williams, TJ, Wilkins, D, Long, E, Evans, F, DeMaere, MZ, Raftery, MJ, and Cavicchioli, R (2013). The role of planktonic *Flavobacteria* in processing algal organic matter in coastal East Antarctica revealed using metagenomics and metaproteomics: Metaproteomics of marine Antarctic *Flavobacteria*. *Environ Microbiol* 15, 1302–1317.
- Xing, P et al. (2015). Niches of two polysaccharide-degrading *Polaribacter* isolates from the North Sea during a spring diatom bloom. *ISME J* 9, 1410–1422.
- Yan, S, Fuchs, BM, Lenk, S, Harder, J, Wulf, J, Jiao, N-Z, and Amann, R (2009). Biogeography and phylogeny of the NOR5/OM60 clade of Gammaproteobacteria. *Syst Appl Microbiol* 32, 124–139.
- Yooseph, S et al. (2010). Genomic and functional adaptation in surface ocean planktonic prokaryotes. *Nature* 468, 60–66.
- Zhang, R, Liu, B, Lau, SCK, Ki, J-S, and Qian, P-Y (2007). Particle-attached and free-living bacterial communities in a contrasting marine environment: Victoria Harbor, Hong Kong. *FEMS Microbiol Ecol* 61, 496–508.
- Zhou, J, Richlen, ML, Sehein, TR, Kulis, DM, Anderson, DM, and Cai, Z (2018). Microbial Community Structure and Associations During a Marine Dinoflagellate Bloom. *Front Microbiol* 9.

8. Supplementary information

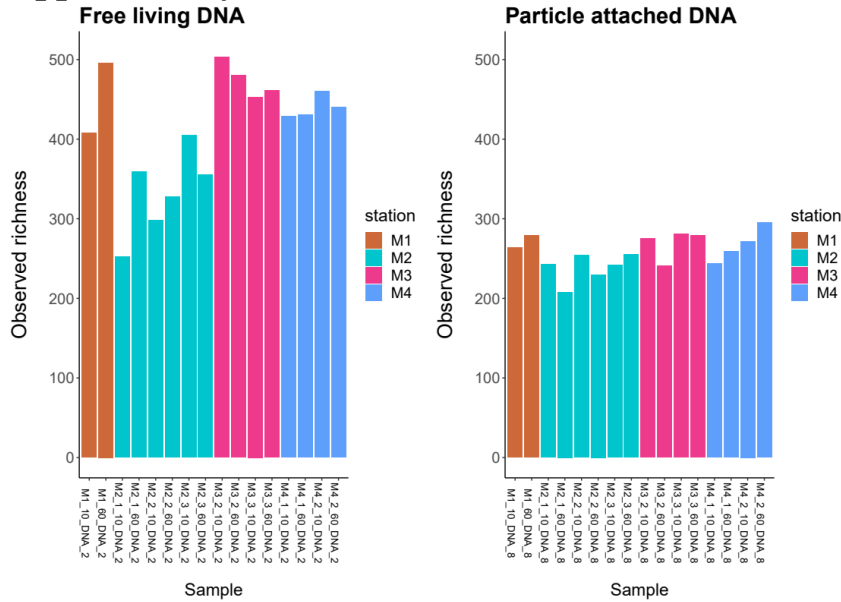


Fig. S1. Observed richness (ASVs number) in the surface mixed layer.

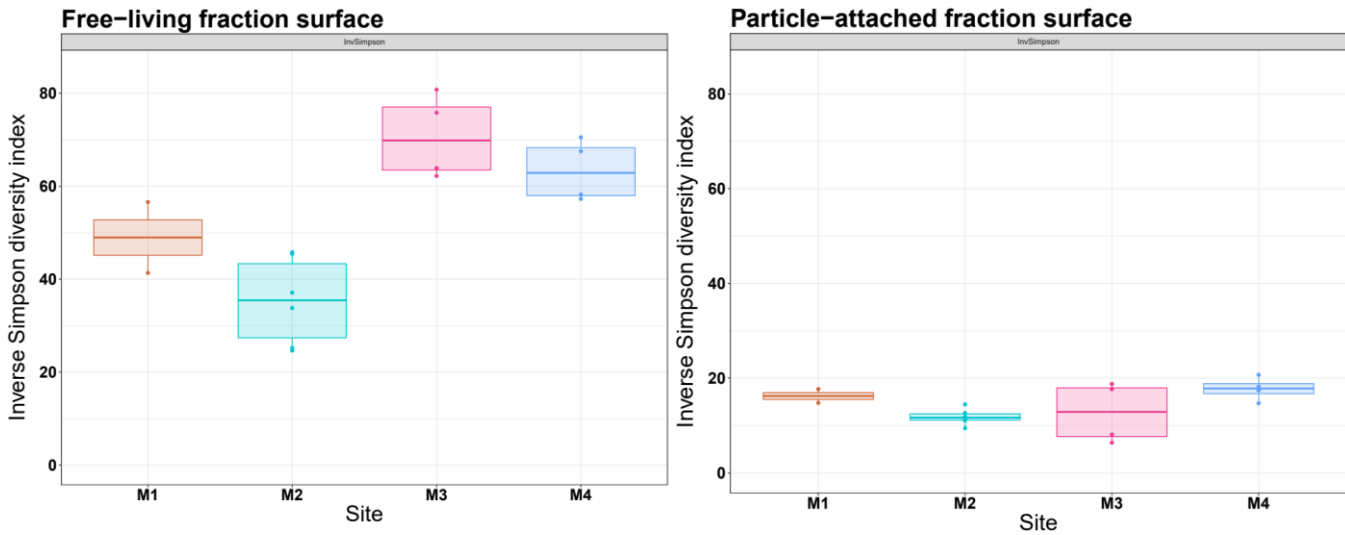


Fig. S2. Inverse Simpson diversity index in surface (10 and 60m) for free-living (left) and particle-attached (right) prokaryotic communities.

The raw data of this work (sequences of 16S DNA amplicon) are in the Laboratoire d'Océanographie Microbienne (LOMIC), Observatoire Océanologique de Banyuls (OOB). UPMC/CNRS UMR 7621. Contact person: Ingrid Obernosterer ingrid.obernosterer@obs-banyuls.fr

Avenue du Fontaulé 66650 Banyuls sur mer,

France. Tel : (33) 04 68 88 73 53. <http://lomic.obs-banyuls.fr>

List of communications

- **Yan Liu**, Stéphane Blain, Olivier Crispi, Mathieu Rembauville, Ingrid Obernosterer
IMBER Meeting Jun. 2019, Brest: Seasonal dynamics of prokaryotes and their associations with diatoms in the Southern Ocean (Talk given by Ingrid Obernosterer)
- **Yan Liu**, Stéphane Blain, Olivier Crispi, Mathieu Rembauville, Ingrid Obernosterer
InterLab Meeting May 2019, Barcelona: Diatom-prokaryote associations during spring blooms in the Southern Ocean unveiled by a Remote Access Sampler (Talk)
- **Yan Liu**, Pavla Debeljak, Mathieu Rembauville, Stéphane Blain, Ingrid Obernosterer
LOMIC Meeting Jun. 2018, Banyuls sur mer: Are diatoms drivers of prokaryotic community composition in the Southern Ocean (Talk)
- **Yan Liu**, Pavla Debeljak, Mathieu Rembauville, Stephane Blain, Ingrid Obernosterer
SOCLIM Annual Meeting Oct. 2018, Paris: Diatoms shape the biogeography of heterotrophic bacteria in the Southern Ocean (Talk)